UNIVERSITÀ DEGLI STUDI DI TRIESTE

XXXIII CICLO DEL DOTTORATO DI RICERCA IN AMBIENTE E VITA

Istituto Nazionale di Oceanografia e di Geofisica Sperimentale - OGS

MARINE MICROBES AND ORGANIC MATTER: THE INTERPLAY DRIVING THE OCEANS' BIOGEOCHEMICAL ENGINE

Settore scientifico-disciplinare: **Bio/07**

DOTTORANDO
DOTT. VINCENZO MANNA

COORDINATORE
PROF. GIORGIO ALBERTI

SUPERVISORE DI TESI
DOTT.SSA PAOLA DEL NEGRO

CO-SUPERVISORE DI TESI
DOTT. MAURO CELUSSI

ANNO ACCADEMICO 2019/2020

Marine Microbes and Organic Matter

The Interplay Driving The Oceans' Biogeochemical Engine

We have become tinkerers of microbial evolution
and we don't understand what we are doing.

Paul G. Falkowski

Abstract

All the heterotrophic life in the ocean, from bacteria to whales, is sustained by organic matter turnover. This ”currency of life” exists in countless physical and chemical arrangements, spanning from small dissolved molecules to big sinking macroaggregates. Organic matter consumption, remineralization and production processes are essentially carried out by microbes. Photoautotrophic microbes are responsible for half of the Earth's carbon fixation, being the major organic matter source in the ocean. Marine heterotrophic microbes (*Bacteria* and *Archaea*) mediate organic matter turnover, effectively regulating carbon and energy fluxes in the ocean. Although developing over very small spatial and temporal scales, the interplay between marine microbes and organic matter is of pivotal importance for global biogeochemical dynamics. The overarching aim of this thesis was to investigate this interplay, and its biogeochemical consequences, encompassing different environmental forcing as well as spatial and temporal scales. The first Chapter was aimed to investigate how long-term environmental changes affect microbe-mediated organic matter processing. A monthly planktonic biogeochemical time series was analysed with a time-oriented machine learning approach. A prolonged salinity anomaly resulted to cause of profound biogeochemical changes in the study area, limiting microbe-mediated organic matter turnover for several years. In Chapter 2 the effect of a transient environmental perturbation, an exceptional cold event, on the metabolism of planktonic microbes was investigated. A high-frequency sampling during and after the event was coupled with experimental temperature manipulations; their outcomes demonstrated that during these phenomena microbial metabolic rates are at their lower thermal limit. Microbial growth was impaired even when the event ceased, highlighting how ecosystemic consequences of extreme weather phenomena extend beyond their duration. The third Chapter was focused on microscale interactions between Antarctic heterotrophic microbes and particulate organic matter. Microcosms experiment were carried out incubating natural free-living communities with phytodetritus. Outcomes from this research have highlighted that particulate matter composition substantially shapes the associated microbial community and thus its metabolic capabilities. Finally, in Chapter 4 organic matter degradation modes were investigated with respect to microbial lifestyle (i.e., free-living vs. particle-attached). Several Antarctic bacterial isolates were screened for their degradative potential when growing exposed to particles or in particle-free media. Production and activity of exoenzymes were finely tuned according to growth conditions and that the presence of particles enhanced the release of cell-free enzymes. The work done in this thesis furthers the current understanding of the biogeochemical implications of the marine microbes-organic matter interplay. By evaluating the consequences of regional perturbations, this thesis provides sound ecological and methodological frameworks to assess the effects of present and future changes on microbe-mediated organic matter turnover. Additionally, specific microbial assemblages, and thus degradation modes, could be associ-

ated with particulate matter composition, linking the microscale interactions between microbes and organic matter to global biogeochemical dynamics.

Riassunto

Tutte le forme di vita eterotrofa negli oceani, dai batteri alle balene, dipendono dalla sostanza organica. Questa ”valuta” della vita è presente in una miriade di strutture chimiche e fisiche, dalle piccole molecole disciolte ai grandi aggregati che sedimentano lungo la colonna d'acqua. I processi di consumo, produzione e remineralizzazione della sostanza organica sono essenzialmente a carico degli organismi unicellulari. Insieme, eucarioti e procarioti fototrofi fissano circa la metà della CO_2 su scala globale, rappresentando la prinicipale fonte di sostanza organica negli oceani. Questa vasta riserva di materia organica è processata, in maniera quasi esclusiva, dal batterioplancton (*Bacteria* e *Archaea*) eterotrofo. Sebbene la maggior parte delle interazioni tra questi e la sostanza organica avvengano su scale spaziali e temporali estremamente ridotte, questi processi regolano i flussi globali di carbonio ed energia, risultando di fondamentale importanza per la biogeochimica degli oceani. In quest'ottica, lo scopo principale di questo lavoro è di esaminare come questa interazione evolva a seguito di perturbazioni ambientali e quali siano gli effetti, a diverse scale temporali e spaziali, sulle dinamiche biogeochmiche. Il primo Capitolo si propone di analizzare gli effetti che i cambiamenti ambientali a lungo termine possono avere sul processamento della sostanza organica da parte del batterioplancton eterotrofo. A questo scopo, una serie temporale di dati biogeochimici è stata analizzata con l'ausilio del *machine learning* per evidenziare il ruolo dei fattori ambientali nel determinare i cambiamenti osservati nei tassi di utilizzo della materia organica. Una prolungata siccità ha pesantemente influenzato la biogeochmica dell'area di studio, limitando il processamento microbico della sostanza organica per alcuni anni. Nel Capitolo 2 sono stati investigati gli effetti di un evento meteorologico estremo sui tassi di degradazione e produzione di materia organica a carico di procarioti eterotrofi. Grazie ad un campionamento effettuato durante e dopo l'evento, combinato con esperimenti di manipolazione della temperatura, questo capitolo mostra come le temperature eccezionalmente basse raggiunte durante l'evento abbiano rappresentato un limite termico per il metabolismo microbico. La crescita microbica è risultata limitata anche dopo la fine dell'evento, dimostrando che le conseguenze biogeochmice di eventi estremi perdurano oltre la durata degli stessi. Il lavoro descritto nel terzo Capitolo era mirato ad analizzare le interazioni di microscala tra le comunità microbiche e la materia organica particellata. A questo scopo, esperimenti di incubazione in microcosmi sono stati effettuati con comunità microbiche naturali antartiche e fitodetrito. I risultati di questi esperimenti hanno dimostrato che la composizione della materia organica particellata influenza la comunità microbica associata, selezionando per specifici *taxa* microbici e quindi specifiche modalità di degradazione. Nel quarto Capitolo, una serie di esperimenti con isolati batterici antartici e fitodetrito sono stati messi a punto con lo scopo di indagare la relazione tra modalità di degradazione enzimatica e la presenza o assenza di sostanza organica particellata. La produzione e l'attività di esoenzimi è risultata finemente regolata dalle condizioni di crescita, con una spiccata produzione di esoenzimi liberi in pre-

senza di particolato detritale. Il lavoro presentato in questa testi avanza le attuali conoscenze sulle implicazioni biogeochmiche delle interazioni tra i procarioti marini e la materia organica. Esaminando le consequenze di perturbazioni ecosistemiche, a breve e lungo termine, sul metabolismo microbico, questa tesi fornisce una solida base ecologica e metodologica per migliorare l'analisi e l'interpretazione ecologica di cambiamenti presenti e futuri. In questo lavoro inoltre, specifiche comunità microbiche, e di conseguenza specifici schemi di degradazione, sono stati associati alla composizione del particellato organico, collegando le interazioni di microscala con le dinamiche biogeochmiche globali.

Contents

1

Introduction

1.1. Organic matter biogeochemistry

1.1.1. Organic matter in the marine environment

Organic matter (OM) in the ocean exists as a size continuum, spanning from nanometres to metres in size (Verdugo et al., 2004). This range is operationally fractionated into particulate and dissolved organic matter (POM and DOM, respectively). The distribution of these size fractions is highly skewed towards the lower end (i.e., nanometres) of this range. POM, including living and non-living components of sinking and suspended particles, contribute less than 2% to the global organic carbon (OC) reservoir (Gardner et al., 2006). The submicron size range (i.e., 1µm – 1nm) is occupied by small particles, gels, and colloids, which, despite their abundance in seawater, are difficult to quantify and characterize (Verdugo et al., 2004). Below the micrometre threshold, further separation occurs. Macromolecules, microgels and other high molecular weight (HMW) organic compounds are separated from the truly dissolved, low molecular weight (LMW) molecules by ultrafiltration methods (Benner and Amon, 2015). These two fractions account for ~22 and ~77%, respectively, of the total OC standing stock (Benner and Amon, 2015).

Even though all heterotrophic life in ocean is sustained by organic matter, most of this "currency of life" is in a dissolved state and thus inaccessible to the vast majority of consumers. Although several eukaryotes can utilize DOM to partially meet their metabolic requirements (First and Hollibaugh, 2009; Flynn et al., 2013; Michelou et al., 2007), the magnitude of DOM removal by marine prokaryotes is far greater. Indeed, marine bacterioplankton catalyses the OM transformation from the dissolved, unavailable state to the particulate, exploitable one (Azam and Malfatti, 2007). Over the cascade of biochemical events underlining OM processing, some of the intermediate products accumulate for various reasons (e.g., chemical or physical properties slowing down degradation mechanisms; Dittmar, 2015). This results in the build-up of OM pools, such as DOM, over time scales spanning from hours to thousands of years (Hansell, 2013 and references therein). The pivotal importance of DOM for microbial life is in sharp contrast with its accumulation over such long time scales. This contradiction is partially explained by DOM reactivity classes (Carlson and Hansell, 2015). On very short time scales (i.e., minutes to days), marine microbes produce and utilize DOM defined as "labile", the fraction of DOM serving as a bridge between production and respiration. This fraction does not accumulate, and its occurrence is constrained by system productivity (Dittmar and Arnosti, 2018). Over longer time scales (i.e., seasonal to decadal), the excess microbial production coupled with external carbon inputs leads to net accumulation of "semi-labile" DOM (Carlson and Hansell, 2015). "Refractory" DOM is the fraction that accumulates over longer time scales (i.e., decades to millennia), making up most of the DOM pool (Hansell, 2013). Its recalcitrance to degradation can be interpreted as the results of proteins, lipids and polysaccharides transformation or selective degradation, which make refractory DOM difficult to metabolize (Hertkorn et al., 2006).

1.1.2. Sources

Approximately 50% of the global net photosynthesis is carried out by photoautotrophic microbes in the euphotic layer of the ocean (Field et al., 1998). This photosynthetically produced OC is then used to fuel phytoplankton biosynthetic pathways. However, fluctuations in environmental (e.g., temperature, salinity, pH, irradiance, inorganic nutrients availability etc.) as well as biological factors (community composition, physiological state of the cells, grazing pressure etc.) may lead to the uncoupling between photosynthesis and cell growth, ultimately resulting in extracellular release of the photosynthate (Myklestad, 2005). Except for phytoplankton blooms, the OC fixed by phytoplankton rarely accumulates, being rather continuously turned over by mortality processes (Strom, 2008) or contributing to the POM inventory.

In addition to photoautotrophic processes in the sunlit layer of the ocean, members of *Bacteria* and *Archaea* domains are able to fix CO_2 using the reduction potential derived from the oxidation of reduced inorganic compounds. These chemoautotrophic processes have been demonstrated to occur in all kind of environments, from hydrothermal vents (Jannasch and Mottl, 1985) to hypoxic and anoxic ocean waters (Walsh et al., 2009) as well as in oxygenated deep waters (Hansman et al., 2009). Chemoautotrophic processes may represent a consistent fraction of the exported production in the dark ocean (15-53%, Reinthaler et al., 2010). Dissolved inorganic carbon (DIC) fixation is not an inherently autotrophic (i.e., photo- or chemo-) pathway, but heterotrophs can incorporate CO_2 too trough carboxylation reactions. These pathways are implicated in the synthesis of lipids, nucleotides, and amino acids, as well as in anaplerosis (Alonso-Sáez et al., 2010). Anaplerotic reactions form intermediates of metabolic pathways and are thus important in compensating metabolic imbalance in oligotrophic conditions (Palovaara et al., 2014) or in fuelling higher metabolic rates following pulses of labile OM (Baltar et al., 2016). A recent meta-analysis of DIC fixation rates (Baltar and Herndl, 2019) highlighted the non-negligible contribution of these metabolic pathways to oceanic primary production rates. Considering non-photosynthetic DIC fixation rates, primary production estimates may be between 5 and 22% higher, underlining how chemoautotrophy may be a substantial source of autochthonous OM in certain systems.

Mesozooplankton grazing on phytoplankton remove 10 to 40% of the primary production in marine systems (Calbet, 2001), passing energy and nutrients to higher trophic levels according to the “classical” marine food web scheme (Cushing, 1989). However, this transfer is not efficient, and leaks occur at its very first step, the prey handling. Using tracers (^{14}C) Lampert, 1978 demonstrated that during the feeding process, a consistent fraction of the phytoplankton OC is released as DOC, as a consequence of a process defined as “sloppy feeding”. The amount of DOC released through this leak varies between 16 and 70% of the grazed carbon, according to the prey size (Møller et al., 2003; Saba et al., 2011). Moreover, through the excretion of undigested material as faecal pellets, mesozooplankton contributes to POM fluxes. In open ocean, picophytoplankton (0.2-2 um in size) is the main photoautotrophic player, yet, due to its reduced size, is not effectively grazed by mesozooplankton (Calbet and Landry, 1999). This planktonic fraction is efficiently grazed by microzooplankton (i.e., <200 um) which remove an estimated 60-70% of the daily oceanic primary production

(Calbet and Landry, 1999). Through sloppy feeding, micrograzers release up to 40% of the prey OC in a dissolved form (Nagata, 2000).

Viruses are considered the most abundant predators in the marine environment (Breitbart, 2012). They control the abundance and production rates of the microbial plankton, effectively shaping micro- and macronutrients biogeochemistry in the sea (Middelboe, 2010). Through lytic infection, viral progeny is produced following host cell lysis, resulting in the release of cytoplasmic content as DOM. This process is termed viral shunt (Wilhelm and Suttle, 1999). The resulting DOM is readily utilized by prokaryotic cells, meeting between 10 and 40% of their carbon demand (Middelboe, 2010; Suttle, 2007). While the net effect of grazing is the transfer of OM to higher trophic levels, the DOM produced through viral shunt is exclusively processed by microbes. This "priming effect" feeds a loop in which the activity of non-infected bacteria is enhanced by the viral shunt-derived DOM, ultimately boosting OM remineralization rates (Bonilla-Findji et al., 2009; Fuhrman, 1999; Suttle, 2007; Weinbauer et al., 2011).

Despite representing a minor fraction of the OC reservoir, sinking and suspended particles represents significant hot spot of microbial metabolism in all aquatic environments (Grossart and Simon, 1993). The abundance and activity of microbes associated with particles, virtually hosted by all particles, may exceed that of the surrounding water by orders of magnitude (Smith et al., 1995; Arnosti, 2011). In this scenario microbial extracellular enzymes are of fundamental importance in POM hydrolysis (Arnosti, 2011), solubilizing it to DOM. Solubilization and uptake rates are often decoupled on particles (Smith et al., 1992), leading to the release of a DOM-rich plume, the volume of which can be up to 100 fold the one of the original particle (Kiørboe et al., 2001), representing a substantial DOM input for water column microbes.

1.1.3. Sinks

Despite the ocean-wide primary production range varies over two orders of magnitude (Behrenfeld and Falkowski, 1997), DOM concentrations show a remarkably small variability throughout the ocean (Hansell et al., 2009). Considering that photosynthesis-derived DOM brings a substantial contribution to the global OM inventory, the offset between its concentration and primary production indicates the existence of several removal processes.

As the major OM source is represented by either photo- or chemoautotrophy (see section 1.1.2), the main OM sink is respiration. Through this process, an electrochemical potential is generated from the flow of electrons, from reduced compounds through a membrane transport system, to an electron acceptor (Carlson et al., 2007). This energy is then collected and stored in adenosine-5'-triphosphate (ATP) molecule. The hydrolysis of the high-energy phosphate bonds of the ATP molecules is then used to fuel cell metabolism. On an ecosystem level, respiration represents one of the largest components of the marine carbon budget. Although all microbes (except obligated fermenters) carry out respiration, prokaryotes represent the most abundant organisms in the sea (Whitman et al., 1998). Much of the oceanic organic carbon is thus respired by bacterioplankton and archaeaplankton, effectively controlling OM biogeochemistry in the ocean (Carlson et al., 2007 and references therein).

The ocean is a three-dimensional environment, highly structured by physical factors (i.e., temperature, salinity, density, light penetration, pressure); consequently, different biogeochemical dynamics develop in different physico-chemical compartments of the ocean. The starting point of OM biogeochemical cycle is the sunlit ocean where photosynthetic organisms reduce CO_2 into organic molecules. Roughly half of the primary production is consumed by the phytoplankton themselves to meet their energy requirements, reintroducing CO_2 into the environment through the oxidation of organic molecules (Falkowski et al., 1998). Primary producers are consumed by herbivores, kicking off the OM trophic transfer along the marine food web (Cushing, 1989). However, as described in section 1.1.2, this transfer is not efficient, and a variable fraction of this newly produced OM is enlisted into the DOM pool. Other mechanisms, like viral lysis or physiological DOM excretion, contribute to build up the DOM pool, which in the end accounts for ~50% of the oceanic primary production (Field et al., 1998). This enormous organic carbon reservoir serves as a substrate for the metabolism of heterotrophic microbes (Dittmar and Stubbins, 2013). Indeed, within the microbial loop, heterotrophic bacterioplankton shuffle OM from the dissolved to the particulate pool, making these packages of food available to be transferred to higher trophic levels (Azam et al., 1983; Cole and Pace, 1995; Pomeroy et al., 2007). Nonetheless, OM degradation leads to the release of inorganic nutrients, such as phosphate and ammonia, as well as CO_2 to the water column, continuously feeding the surface OM cycling (Goldman and Dennett, 2000).

Since some organic matter is not readily remineralized in the euphotic ocean, these surface cycles are not “leak-proof”. In the sunlit ocean, one of the DOM removal mechanisms is linked to photochemical transformation. Chromophores embedded in HMW DOM can absorb the UV radiation, generating LMW compounds, enhancing the DOM uptake and remineralization by heterotrophic prokaryotes (Anderson and Williams, 1999). A by-product of these photochemical reactions is the release of labile phosphorous- and nitrogen-containing compounds, further enhancing microbial production (Moran, 2000). Although photochemical transformation may represent a significant direct, as well as indirect, DOM sinks, the spatial extent of these processes is constrained by the depth of the euphotic layer of the ocean.

In addition to the aforementioned processes, HMW DOM (i.e., macromolecules and microgels) may spontaneously assemble into bigger structures. These are called self-assembled microgels (Verdugo, 2012) and are complex matrices formed by cross-linked polymers. Following changes in chemical (i.e., pH, salinity) or physical (i.e., temperature) conditions, these gels may further aggregate into dense particles and sink. Although theoretically this process may represent a consistent DOM removal mechanism, fluxes of DOM to self-assembled microgels are not yet quantified (Carlson and Hansell, 2015). A fraction of this pool sinks towards the ocean bottom as POM, carrying nutrients and carbon from surface to ocean depths. This vertical flux of organic carbon is the underlining principle of the biological carbon pump. Being a pump and not a cycle means that the net effect of POM sinking is the removal, rather than the recycling, of carbon, which can be sequestered from the oceanic and atmospheric reservoirs potentially for thousands of years (Dittmar and Arnosti, 2018). However, the efficiency of this process is rather low as a variable fraction between 1 and 6%

reaches the ocean floor and an even less quantity, ~0.3%, escapes further degradation in marine sediments and is effectively sequestered (Dunne et al., 2007; Sundquist and Visser, 2003). Particles resulting from the aggregation of HMW OM (i.e., marine snow) sink more slowly or even stay suspended in the water column, whereas faecal pellets or phytodetritus, generally heavier, sink directly through the water column (Dittmar and Arnosti, 2018 and references therein). As not all heterotrophic microbes possess the metabolic capability to face all the OM moieties, DOM degradation is a selective process. This enzymatic fractionation of OM (Smith et al., 1992), is one of the main reasons why refractory DOM accumulates over time in the ocean. The ensemble of these processes has been conceptualized as the microbial carbon pump (Jiao et al., 2011). Through this process, microbial activity "pumps" OM from the labile pool to the refractory one, which may represent an effective carbon sink due to its recalcitrance to degradation (Jiao et al., 2010).

All living organisms in the ocean contribute to OM shuffling from one pool to another. Yet, the main mechanisms through which this shuffling is achieved (i.e., production and respiration) are carried out by unicellular organisms (Falkowski et al., 1998). Albeit occurring at micrometre scale, these processes shape global OM fluxes, regulating the Earth's biogeochemical homeostasis (Carlson et al., 2007; Stocker, 2012).

1.1.4. Marine microbes shall not live by carbon alone

Microbial production and consumption of marine DOM drive major fluxes of carbon in the surface and deep ocean; yet the biochemical reactions that drive these fluxes are not dependent on carbon alone. Indeed, the metabolic pathways underlining OM production and consumption are heavily dependent on both macro- (i.e., nitrogen – N and phosphorous – P) and micronutrients (e.g., iron, cobalt, nickel, and zinc; Moran et al., 2016), linking several biogeochemical cycles. On a global scale, primary production is highly heterogenous, with large areas of low productivity and small areas of high primary production. Vast expanses of the global ocean are oligotrophic, with low concentrations of inorganic essential nutrients (Fe, N and P ions, Morel et al., 2007). Productivity hotspots occur in coastal and upwelling zones, were the continuous nutrient inputs derived either from terrestrial runoff or from ingression of deep nutrient-rich waters, foster primary production (van Dongen-Vogels et al., 2012). Within the DOM pool, molecules such as proteins, nucleic acids, vitamins, and secondary metabolites contain N and P, as well as other micronutrients (Keil and Kirchman, 1993; Björkman and Karl, 2003; Sañudo-Wilhelmy et al., 2012). Due to their importance for global primary production, and their significant presence, two additional sub-pools are identified within the DOM one, accounting for dissolved organic nitrogen (DON) and dissolved organic phosphorous (DOP).

A considerable fraction of the total nitrogen pool in natural waters is often associated with DON (Berman and Bronk, 2003). The LMW portion of the DON pool is made up of urea and dissolved amino acids (~5-10%) whereas the HMW fraction (~30%) is mostly composed by hydrolysable amino acids and humic substances (Sipler and Bronk, 2015). DON can be produced by several organisms (i.e., phytoplankton, N_2 fixers, bacteria, zooplankton) within the water column. Phytoplankton can be a significant source of DON in aquatic environments either by active release or exudation or

as indirect consequence of viral lysis and/or zooplankton sloppy feeding (reviewed by Bronk and Steinberg, 2008). N_2 fixers can be a significant source of N in marine systems either directly, releasing amino acids, DON or ammonium, or indirectly, through remineralization of DON by associated bacteria (Mulholland, 2007; Sheridan et al., 2002). Bacteria contribute to DON release in several ways. The hydrolytic degradation of POM as well as of HMW OM may release DON in the environment (Smith et al., 1992; Grossart and Simon, 1998). Also, passive diffusion trough membranes, active excretion of amino acids or other N-containing compounds may contribute to the DON pool (Azam and Malfatti, 2007). Finally, viral lysis of prokaryotic and eukaryotic cells substantially contributes to the DON pool (Brussaard, 2004; Suttle, 2005). While some phytoplankton species can uptake and utilized DON sources such as urea, (Bronk et al., 2007), prokaryotic degradation accounts for the major N flux from the DON pool (Berman and Bronk, 2003). Using proteolytic enzymes, microbes break down HMW DON to its LMW constituent molecules, making N-compounds more accessible to other organisms. Bacterial degradation of DON followed by the uptake of the resulting products from phytoplankton has been extensively demonstrated (Berman et al., 1999; Palenik and Henson, 1997). However, proteolytic enzymes occur on autotrophic cell surfaces as well, accounting for an estimated 20% of DON turnover in open ocean and coastal environments (Mulholland et al., 1998; Mulholland, 2003). Most of the remineralized DON ends up in the dissolved inorganic nitrogen pool as ammonia (NH_4^+; Sipler and Bronk, 2015), fuelling regenerated primary production.

P is increasingly considered to be the major limiting nutrient for both phytoplankton and bacteria in the ocean (Dyhrman et al., 2007). While inorganic P is generally considered the most bioavailable form of P, its concentration is rarely above 3 µM in the surface ocean (Karl and Björkman, 2015). Thus, its importance for microbial life, coupled with its global scarcity indicates the existence of highly specific and sensitive P-handling mechanisms for most marine microbes. The uptake of inorganic P and its consequent incorporation into one of the many P-containing intracellular compounds starts DOP production. About 25% of the oceanic DOP pool is composed by HMW molecules, such as nucleic acids, phospholipids, and other compounds abundant in microbial cells (Kolowith et al., 2001). Since it is energetically expensive to degrade these molecules to retrieve inorganic P, marine microbes have evolved the ability to directly utilize DOP compounds as metabolic precursors (e.g., Rittenberg and Hespell, 1975; Ruby et al., 1985; Wanner, 1993). The importance of P for microbial life is underlined by the fact that pathways for DOP degradation or assimilation are found in both autotrophic and heterotrophic microbes (White et al., 2010). Controlled experiments have demonstrated that labile DOP remineralization rates were in excess respect to bacterial inorganic P demand, and thus prokaryotic-mediated DOP remineralization may represent a significant source of inorganic P for primary producers (White et al., 2012). These findings suggest that the major processes driving inorganic P turnover may cycle mostly on a local, rather than oceanic, scale.

1.2. Microbe-mediated organic matter processing

1.2.1. Mechanisms

Given the wide array of its sources, OM reservoir is made up by thousands of compounds, differing for chemical formulas, size and reactivity to biotic and abiotic transformations (Hansell, 2013; Riedel and Dittmar, 2014). Measurement of OM characteristics such as age, molecular size, ad microbial growth on selected organic substrates have led to development of a "size-reactivity continuum" theory (Benner and Amon, 2015 and references therein). According to this idea, HMW OM is generally younger and more biologically reactive than the LMW fraction and is thus preferentially used by heterotrophic microbes.

Direct uptake of molecules by heterotrophic prokaryotes is constrained by the size of cell-wall porins, limiting the effective uptake size to 600 Da (Weiss et al., 1991). Therefore, the selectivity towards HMW molecules comes at the price of a supplemental step, the external hydrolysis of target molecules, carried out by means of extracellular enzymes. Extracellular enzymes can be either cell-associated or cell-free (Chróst, 1990; Baltar et al., 2010). Cell-associated ectoenzymes are bound to the outer cell-wall or localized in the periplasmic space. The synthesis and utilization of cell-bound enzymes represent a cost-effective strategy for microbes. The hydrolysis site is indeed localized in the immediate surroundings of (or even inside) the cell, reducing the amount of hydrolysis product lost by diffusion. The drawback of this strategy is that microbes must be physically near the target molecules as OM distribution in the sea is patchy (Allison et al., 2012). Cell-free enzymes may originate from active secretion, changes in cell physiology and grazing or viral lysis (see Baltar, 2018 for a review). Given the coarse OM distribution in the ocean, releasing enzymes into the water column may not seem a very effective strategy. Indeed, the hydrolysis can happen further away from the enzyme-producing cell, resulting in the loss of the hydrolysate which can be eventually taken up by other cells. However, the strategy of releasing enzymes into the environment become efficient when the OM source is in particulate form and within a defined distance from the enzyme producing cells (Vetter et al., 1998; Vetter and Deming, 1999). The analysis of the cost-benefit ratio of these two enzyme producing strategies have led to the development of the paradigm that free-living microbes preferentially use cell-bound enzymes to cope with the patchy OM distribution in the sea, whereas particle-associated cells, due to their proximity to OM sources mainly rely on cell-free enzymes.

This paradigm has been recently challenged by the discovery of an alternative uptake mechanisms of HMW OM. This consists in the hydrolysis of polysaccharides bounded on the outer cell membrane and subsequent transport of large fragments into the periplasmic space, with little or no release of hydrolysis products (Cuskin et al., 2015; Reintjes et al., 2017). Firstly discovered in intestinal bacteria, this uptake mechanism revealed to be widespread across the surface ocean, changing previous conceptions on the interactions among members of microbial communities during HMW OM processing (Arnosti et al., 2018). The production of extracellular enzymes by at least a fraction of the microbial community initiates degradation of HMW molecules. However, the hydrolysis carried out by ectoenzymes is intrinsically external, mean-

ing that a fraction of the hydrolysis products will be inevitably lost, favouring cells that do not invest in ectoenzymes production (Folse and Allison, 2012; Mislan et al., 2014). This scenario delineates two macro categories of microbes: sharing (i.e., enzyme producers) and cheating (i.e., non-producers) (Allison, 2005; Kaiser et al., 2015). The discovery of an alternative HMW OM uptake mechanism put out a third player, the selfish microbe (Cuskin et al., 2015) so termed as bacteria using this mechanism do not share hydrolysis product with other organisms. Consequently, when selfish uptake is dominant, OM flux can be reduced towards both sharing and cheating bacteria, driving microbial community dynamics in the ocean (Arnosti et al., 2018). Moreover, selfish uptake in the ocean may be taxa-substrate specific (Reintjes et al., 2017), suggesting that the selective uptake of HMW OM may plays a key role in shaping the OM size-reactivity continuum (Benner and Amon, 2015).

Enzymatic degradation of HMW OM supply heterotrophic microbes with organic molecules, which are further used to fuel their metabolism and growth. The heterotrophic carbon production (HCP) is the ensemble of those biochemical reactions catalysing the incorporation of DOM into bacterial biomass. HCP is one of the most important microbial processes in the ocean as it represents the underlying principle of the microbial loop (Ducklow, 2000). Through this process indeed, DOM is recovered and transformed into particulate food, initiating bacterivory-based food webs. Extracellular enzymes represent the initial step of microbial HMW OM remineralization, regulating the functioning of the marine carbon cycle (Arnosti, 2011).

1.2.2. Drivers

Since OM utilization processes by heterotrophic prokaryotes are affected by a plethora of different environmental and biotic controls, it is extremely complex to investigate and quantify the effect of each driver on microbial metabolic rates. Nonetheless, factors such as temperature, substrate availability and chemical composition as well as the structure of the microbial community have been considered as the main controlling factors driving microbial metabolic patterns in the ocean.

Temperature affects the rates of all biochemical processes on Earth and is regarded as an ever present, interactive factor, ultimately modulating heterotrophic microbes resource requirements (Morán et al., 2017). Higher (or lower) thermal energy will translate into a higher (or lower) kinetic energy of biomolecules, determining an increase (or a decrease) in cellular processes rates and thus activity (Boscolo-Galazzo et al., 2018). However, the stimulating or repressing effect of temperature does not go on indefinitely. Both organisms and metabolic reactions have an optimal temperature threshold, beyond which the metabolic efficiency of the cell is impaired, resulting in a decrease in growth efficiency (Hall and Cotner, 2007). Although this principle could be confidently applied in most of the cases, the experimental work of Wiebe and colleagues (Wiebe et al., 1993) demonstrated that there are some exceptions to this mechanism. Indeed, by comparing the growth rates of marine bacterial isolates from subtropical to polar environments, they found a consistent reduction of bacterial growth rates when temperature approached the lower end of their growth optimum, regardless of substrate concentration. Noteworthy, this effect was less evident in bacteria isolated from polar environments, which were able to overcome the temper-

ature effect when higher substrate concentration was supplied. Pomeroy and Wiebe, 2001 extensively reviewed the topic of co-limitation by the temperature-substrate interaction, concluding that this effect is enhanced in temperate water bodies during winter when water temperature is near the lower end of the optimal growth range. However, this interactive effect is present as well when temperature approaches the upper limit of the optimal growth range, although in this case substrate concentration and quality (i.e., macromolecular composition) plays a preponderant role in the reduction of growth efficiency (Apple et al., 2006). Cumulative evidence also suggest that temperature may exert a differential control on different OM-degradation modes. Depending on OM state (i.e., dissolved or particulate), on the taxonomical identity of microbial taxa and on environmental conditions, OM degradation can be carried out using either cell-free or cell-bound extracellular enzymes (Baltar, 2018, see also Section 1.1.3). Albeit there are few studies focusing on the control on activity and fate of cell-free exoenzymes, observational, as well as experimental, studies have found a consistent inverse relationship between temperature and the activity of cell-free exoenzymes (Baltar et al., 2016; Baltar et al., 2017). All these evidences highlight temperature as the main factor driving the activity and the relative importance of cell-free exoenzymes, indicating that the warmer the temperature, the lower the proportion of cell-free exoenzyme hydrolysis. Therefore, temperature is the main driving factor of microbial metabolism, controlling both the rates and modes of OM processing in the ocean.

The stability and size of OM pools in the ocean depend on the inflows and outflows in and out these pools. Shifting elements between pools, microbes have a leading role in controlling OM fluxes. Yet, OM quality, intended as the suitability to degradation of organic molecules, is the upstream driving force of these fluxes. The number and characteristics of all the different compounds making up the DOM pool are largely unknown. In the last years, novel analytical approaches reveal the presence of potentially millions different structural low-molecular mass feature in the bulk DOM (Osterholz et al., 2015; Zark et al., 2017). Although the full picture behind this enormous diversity is far from being fully portrayed, recent experiments have shown that marine organisms actively secrete molecular pools as diverse as DOM, even if grown on a single OM source (Koch et al., 2014; Lechtenfeld et al., 2015). Carbohydrates, proteins and lipids made up an estimated 20-40% of the bulk DOM (Pakulski and Benner, 1994), representing a significant OM source for heterotrophic microbes. In the past decades, numerous studies focused on dose-response experiments have shown how simple sugars and dissolved amino acids may meet a substantial portion of the bacterial carbon demand across a wide array of environments (see Church, 2008 for a review). However, these labile compounds represent a rough 1% of the DOM pool. Albeit a large fraction of bacterial metabolism may be supported by the consumption of labile substrates, other substrate pools must be necessary to fuel the remaining fraction of metabolic demand. In this regard, polysaccharides have received significant attention in the last few years, as two thirds of oceanic DOM are made up by these compounds (Lin and Guo, 2015). Most of this carbohydrate inventory is primary producers-derived, either as cell constituent or as excreted OM (Thornton, 2014; Becker et al., 2020). The biological origin of polysaccharides translates into a high degree of complexity, as both the amount and the diversity of algal-derived polysaccharides changes accord-

ing to microalgae growth phase and environmental conditions (see Mühlenbruch et al., 2018 for a review). Two important trade-offs underline polysaccharides utilization by heterotrophic microbes. Since bacterial porins allow the passage of molecules only below 600 Da (Weiss et al., 1991), the primary utilization of polysaccharides, and of HMW-OM in general, implies an upstream enzymatic degradation of the target molecules; the first trade-off is thus the ability to produce extracellular enzymes to access this OM pool. However, hydrolytic enzymes are selective with respect to the structure of their target substrate, implying that, due to genetic constrains (i.e., presence/absence of genes encoding for a specific enzyme), a prokaryotic cell is able to use only a define set of OM sources (Dittmar and Arnosti, 2018). To overcome these constrains, enzyme production and activity may be coordinated within a microbial assemblage, becoming a community effort. One possible scenario was envisioned by Reintjes et al., 2019), who, through incubation experiments, demonstrated that initial OM degradation carried out by fast responsive taxa may produce hydrolysis products which in the end fuel the growth of scavenger (i.e., non-enzyme producing) taxa. However, these dynamics were not conserved for all the investigated substrates and was also different among different sampling locations, highlighting the role of different microbial communities in shaping OM fluxes.

Biogeographical patterns in marine microbial communities have recently received the attention of the scientific community thanks to sampling expeditions such as Tara Oceans and Malaspina (Duarte, 2015; Sunagawa et al., 2015), finally coupling functional information (i.e., metagenomic and metatranscriptomic) with taxonomy. From these and many other studies, marine microbial biogeographical pattern emerged, showing differences in community composition with depth, latitude and distance from the coast (e.g., Wietz et al., 2010; Arnosti et al., 2011; Zinger et al., 2011). These differences in microbial communities are paralleled by their modes of OM utilization. As an example, the rates and patterns of exoenzymatic OM degradation show strong latitudinal gradients. Higher latitude communities show a narrow spectrum of substrate degradation potential when compared to lower latitude environments (Arnosti et al., 2011). A similar narrowing enzymatic array has been shown to exist from surface to the deep ocean (Steen et al., 2012; Balmonte et al., 2018), as well as with increasing distance from the coast (D'Ambrosio et al., 2014). Further investigations of the difference in functional pattern between surface and mesopelagic communities have highlighted a greater functional potential in the latter ones (Shi et al., 2011; Letscher et al., 2015; Sunagawa et al., 2015). These differences are thought to be related to OM diversity already processed by surface communities and in transit towards the oceans' interior, where different, and more specialized, strategies are required to exploit this source of energy. The emergence of these biogeographical gradients demonstrates that the rates at which OM is processed, as well as its fate, is a function of both OM structure and microbial community capabilities. An even stronger link was established by the work of Teeling et al., 2012 and Teeling et al., 2016, who demonstrated a very sharp bacterioplankton succession in response to the onset, development and decay of a phytoplankton bloom in the North Sea. In the same framework (i.e., a phytoplankton bloom in the North Sea), Reintjes et al., 2020 showed that not only different assemblages exhibit different OM degradation patterns, but also that the modes (i.e., selfish uptake or external hydrolysis, see Section 1.1.3) with which algal-derived

polysaccharides are degraded change accordingly, linking the identity and function of microbial assemblages with OM fate and fluxes in the ocean.

1.3. With small microbes come global dynamics

1.3.1. Microscale interactions

Although the ocean may appear as a homogeneous expanse of well mixed planktonic organisms and solutes, the life of a planktonic microbe is defined by processes and dynamics developing within a fraction of a drop of water. At microscopic scale indeed, seawater presents an utterly complex architecture made up by microniches developing around the OM continuum. Marine microbes interact with a wide array of OM physical shapes, such as gels, colloids, living and dead cells, marine snow etc. (Long and Azam, 2001). Copious colonization of these structures by heterotrophic microbes lead to a chemical and physical alteration of these microenvironments, creating additional patchiness in the microscale realm (Azam and Malfatti, 2007). For example, POM degradation trough extracellular enzymes leads to a DOM leakage from the primary POM source to the surrounding water column (Kiørboe et al., 2001), forming a DOM gradient around the particle (Stocker, 2012). The DOM plume can then be exploited by non-particle associated microbes in the surrounding water column, increasing bacterial production up to one order of magnitude (Stocker et al., 2008).

Many of the processes regarded as OM sources (e.g., grazing, excretion, exudation, etc. see Section 1.1.2) contribute to create patchiness in the ocean; among these, zooplankton is a considerable source of microscale patches. DOM diffusing from either living or dead zooplankton has been predicted to fuel the microbial food web (Tang et al., 2014). Also, trough the incomplete feeding upon preys (i.e., sloppy feeding), zooplankton generate DOM patches providing valuable resources for nearby heterotrophic microbes (Møller et al., 2003). Finally, faecal pellets excreted by zooplankton are shown to support hotspots of microbial metabolism and abundance on the pellets themselves and in the surrounding seawater (Thor et al., 2003; Köster and Paffenhöfer, 2013). DOM-rich patches are also generated by the action of marine viruses. When the viral infection results in the lysis of the host's cell, the intracellular OM is released in seawater, generating OM hotspots for heterotrophic microbes. Although the size of these patches is dependent on the size and identity of the lysed organisms, these DOM micro patches can last for several minutes (Stocker, 2012). Given the conspicuous amount of viral infections across the global ocean (10^{23} per second; Suttle, 2007), viral derived OM patches may represent a significant OM source for marine bacteria.

The larger end of the OM continuum size spectrum is represented by suspended and sinking organic particles, comprised of living and dead protist cells, individual zooplankton as well as their faecal pellets and coagulated microbial exudates (Simon et al., 2002; Tang et al., 2014; Jenkins et al., 2015). These particles are enriched in organic and inorganic molecules, resulting in nutrients concentration several order of magnitudes higher than the surrounding seawater (Prgzelin and Alldredge, 1983). Organic particles are thus a microbes' equivalent of oases into a desert (Seymour and

Stocker, 2018). These nutrients hotspots are readily colonized by microbes which use cell-bound and cell-free exoenzymes to degrade and consume the particle-associated organic material (Smith et al., 1992). Abundance of particle-associated microbes exceed the background cell concentration by up to 10000-fold, enhancing colonization and growth of other microbes and attracting bacterivorous organisms (Grossart and Ploug, 2000). The particle-associated microbial communities are typically distinct from the free-living counterpart, often enriched in specific groups, tightly linked to the quality of the particles (Salazar et al., 2015; Bižić-Ionescu et al., 2015). Experimental and observational studies with phenotypic and meta-omics approaches have demonstrated that also the functional capabilities of particle-attached microbes are substantially different from that of free-living communities. Metabolic rates of particle-associated microbes are higher than those measured in the surrounding seawater (Thor et al., 2003), with a marked difference in terms of OM degradation expressed by the two communities, both in terms of pattern (i.e., exoenzymes suite; Martinez et al., 1996) and modes (i.e., cell-free and cell-bound exoenzymes; Karner and Herndl, 1992). Furthermore, genes associate with a "social" behaviour, like quorum sensing, motility, adhesion and antibiotic resistance are often highly represented and upregulated in particle-associated microbes (Ganesh et al., 2014; Satinsky et al., 2014; Jatt et al., 2015). These differences demonstrate, unequivocally, that, however small, organic particles represent peculiar microhabitats where complex ecological interactions develop and where the very engine of biogeochemical cycles resides (Long and Azam, 2001; Azam and Malfatti, 2007).

1.3.2. Biogeochemical implications

Chemical physical and biological processes, occurring at spatial scales of micrometres and time periods of fractions of seconds to minutes, shape the behaviour and ecology of marine microbes (Seymour and Stocker, 2018). Despite these processes are extremely localized if compared to the vast, turbulent ocean, their outcomes accumulate over larger scales, influencing ocean productivity, biogeochemistry and ecology (Azam, 1998; Stocker, 2012).

Primary producers regulate food web productivity and carbon cycle functioning and efficiency; factors regulating their growth have therefore a significant footprint on marine biogeochemical dynamics. Perhaps the most important factor controlling phytoplankton productivity is the availability of inorganic nutrient inputs. While this topic is generally addressed with a large-scale perspective (i.e., oceanic circulation, freshwater inputs etc.) they are often finely tuned by microscale processes. Among these processes, the interactions occurring between heterotrophic microbes and individual phytoplankton cells are the most notable example (Seymour et al., 2017). The phycosphere is the planktonic equivalent of the rizosphere, localized around the roots of land plants (Raaijmakers et al., 2009). The conspicuous release of DOM by phytoplankton cells leads to the formation of a chemical gradient around the cells, representing a nutrient-rich microenvironment readily exploited by heterotrophic microbes (Mitchell et al., 1985). Capitalization of nutrients in the phycosphere substantially affects the growth of the surrounding microbes, especially the motile ones, as they can quickly reach these OM hotspots (Bowen et al., 1993). However, the relationship between heterotrophic bacteria in phytoplankton developing in the phycosphere

is not a one way one. Phytoplankton can indeed benefit from the localized inorganic nutrient remineralization carried out by bacteria in the phycosphere (Grossart et al., 2005), from the delivery of vitamins (e.g., B12, Amin et al., 2012) and iron (Amin et al., 2009), all provided by bacteria to phytoplankton cells. By contrast, some microscale processes can also limit primary productivity. In certain conditions, bacteria may be more efficient in inorganic nutrients scavenging and utilization, outcompeting phytoplankton (Currie and Kalff, 1984). Among the phycosphere inhabitants, Furusawa et al., 2003 observed algicidal bacteria, capable to parasitize and even kill phytoplankton cells. These kind of microscale interactions are thus of paramount importance for the ecological interplay between marine bacteria and primary producers, shaping global primary productivity patterns.

At a global scale, OM fluxes shape and are shaped by microbial activities. Dwelling deeper, the interactions between microbes, and between them and the OM pool, fundamentally happen at microscale; yet they influence ocean basin-scale carbon fluxes (Azam, 1998). As illustrated in the previous section, DOM is essentially patchy in the pelagic environment. To use these DOM patches, heterotrophic microbes employ specific responses, such as chemotaxis. Experimental observations as well as modelling studies have shown that behavioural responses may increase bacterial DOM processing rates (Stocker et al., 2008). Due to the finite nature of these OM patches, the absolute amount of carbon "cycled" may remain the same despite an increase in its utilization rates (Stocker, 2012). However, if these DOM pulses are particularly nutritious or persisting for longer time periods, bacteria growing on these patches may present an increased growth efficiency, leading to a higher proportion of DOM converted into biomass and thus channelled to higher trophic levels (Stocker, 2012). The consequences of microscale interactions between marine microbes and OM on global biogeochemical dynamics are even more evident when considering POM-involving processes. POM sinking from the sunlit to the deep ocean represents the underlying principle of the biological carbon pump (see Section 1.1.4). The amount of carbon that reaches the seafloor, where it will be eventually removed from the oceanic and atmospheric reservoir is strongly governed by the rate at which this OM pool is turned over by particle-attached microbes (Giering et al., 2014). Colonization and subsequent degradation of organic particles are inherently microscale processes, involving specific metabolic and behavioural responses. Chemotactic, motile bacteria readily colonize organic particles, rapidly degrading them with a suite of ectohydrolytic enzymes (Kiørboe, 2001). These processes result not only in the assimilation of the particles' carbon but also in the formation of smaller particles, which sinks slower and may be consumed by microbes at that depth (Collins et al., 2015). Moreover, not all constituents of the particle's OM pool will be degraded at the same rate, due to the different enzymatic repertoires expressed by their associated microbial community. Consequently, particles' OM is enzymatically fractionated (Smith et al., 1992), affecting further colonization and degradation dynamics, ultimately impacting the amount of carbon recycled or buried. Overall, the rich suite of interactions between microbes and OM deeply regulate microscale carbon fluxes, ultimately affecting global biogeochemical dynamics.

1.4. Study areas

1.4.1. The northern Adriatic Sea

The northern Adriatic Sea (Fig. 1.1) is a shallow (average depth of 35m), landlocked temperate basin in the northernmost part of the Mediterranean Sea. On the western side of the basin, the Po river discharge can either originate a southward intense coastal current, or flow to the eastern Adriatic coast, generally sustaining cyclonic circulation; on the eastern side a weaker and warmer current flows along the coast coming from the southern Adriatic Sea (Poulain et al., 2001). Within this basin, water column stratification occurs from spring to mid-autumn, driven by freshwater inputs and surface heating; during winter, cold north-easterly wind cause cooling and intense water mixing, driving dense water formation (Gačić et al., 2001). All these features greatly affect the spatial and temporal dynamics of planktonic microbes, showing patterns very similar to typical temperate coastal environments, with exceptions determined by anomalous physical-chemical conditions (Celussi and Del Negro, 2012).

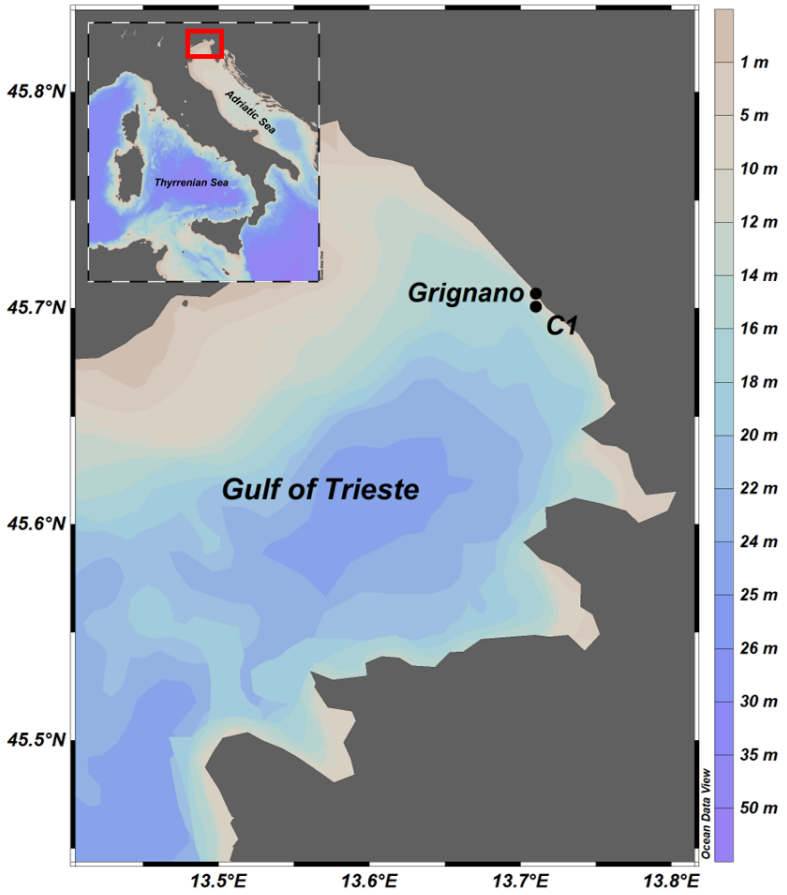

Figure 1.1: Map of the study area in the northern Adriatic Sea. Stations sampled for the activities describes in Chapter 2 (C1) and Chapter 3 (Grignano) are marked on the map.

The abundant freshwater inputs in the basin, and the consequent inflow of inorganic nutrients, sustain a high primary production, ascribing this basin among the most pro-

ductive areas of the Mediterranean Sea (Durrieu de Madron et al., 2011). Freshwater-triggered diatoms blooms develop in late winter, whereas prokaryotic biomass prevails over the other plankton during the nutrient-depleted summer, followed by a second short-lasting fall bloom (Fonda Umani et al., 2012 and references therein). While diatoms and nanoflagellates are the dominant components of phytoplankton through most of the year, cyanobacteria (*Synechococcus*) are the prevailing phototrophs in late summer (Fonda Umani et al., 2012). Both DOM and POM dynamics are peculiar in this basin. DOC dynamics are tightly linked with primary production, increasing from early spring to peak in late summer (De Vittor et al., 2008). This seasonal accumulation has been ascribed to both oceanographic and biological features. During summer, when the river outflow is at its minimum, the cyclonic circulation in the basin stalls, favouring OM accumulation (Puddu et al., 2000). The increase in DOC concentration may be also due to accumulation of refractory compounds or to an impaired microbe-mediated processing due to P-limitation (Puddu et al., 2003). This basin is also rich in POM and for this reason has received much attention since the 1980's, becoming a natural laboratory in which early studies on POM colonization and degradation have been carried out (Herndl and Peduzzi, 1988; Kaltenbock and Herndl, 1992; Rath et al., 1998). This high abundance of organic particles has been suggested to be due to the peculiar water mass circulation patterns as well as marked changes in temperature and nutrient concentration (Cozzi et al., 2004). For all the above mentioned reasons, in this basin the interactions between microbes and OM develop in a wide and often complex framework, making it an ideal setting to investigate the effect of environmental forcing on microbial-driven OM fluxes in the pelagic realm.

1.4.2. The Ross Sea

The Southern Ocean covers ~10% of the world's ocean (Rogers et al., 2020), yet it is responsible for the ventilation of the global ocean as well as for an approximate 10% drawdown of anthropogenic CO_2 emissions (Turner et al., 2009; Hauck et al., 2015). The Southern Ocean is considered a high nutrient-low chlorophyll system because of the limitation of primary producer growth by micronutrients such as iron (Strzepek et al., 2011; Boyd et al., 2012). Nonetheless, its coastal, shallower areas represent hotspots of primary production (Smetacek and Nicol, 2005). In these terms, the Ross Sea (Fig. 1.2) represents one of the most biologically active areas in the Southern Ocean, accounting for 1/3 of its total productivity (Smith et al., 2014; Smith et al., 2012). Primary producer biomass is dominated by either diatoms or *Phaeocystis* sp., depending on the stratification degree of the water column (Smith et al., 2014), and is heavily grazed by zooplankton and fishes, channelling carbon to the higher trophic levels (Deppeler and Davidson, 2017). Despite the heavy grazing pressure, up to 50% of the carbon fixed into biomass by primary producers is exported as POM in the mesopelagic system, accounting for up to 40% of the global POM export (Ducklow et al., 2001; Catalano et al., 2010). In the Ross Sea area, a considerable fraction of the surface-exported POM may be represented by intact and even healthy phytoplankton cells (DiTullio et al., 2000; Zoccarato et al., 2016). Agusti et al., 2015 found that phytodetrital POM is widespread at depth in the global ocean, unveiling a potentially overlooked OM source in the dark ocean. POM vertical flux, and thus the biological carbon pump efficiency, is largely dependent on the microscale processes exerted

byheterotrophic microbes (see section 1.4.2). While microbial community dynamics associated with marine snow have been object of many experimental and environmental studies (e.g. Bižić-Ionescu et al., 2015, Bižić-Ionescu et al., 2018; Fontanez et al., 2015; Datta et al., 2016; Pelve et al., 2017; Duret et al., 2019), there is a limited amount of information on microbial communities associated with phytodetrital POM (Bidle et al., 2002). The Ross Sea represent thus a natural laboratory where to study microbial dynamics underlying phytodetritus colonization and degradation patterns and its implications for OM biogeochemistry.

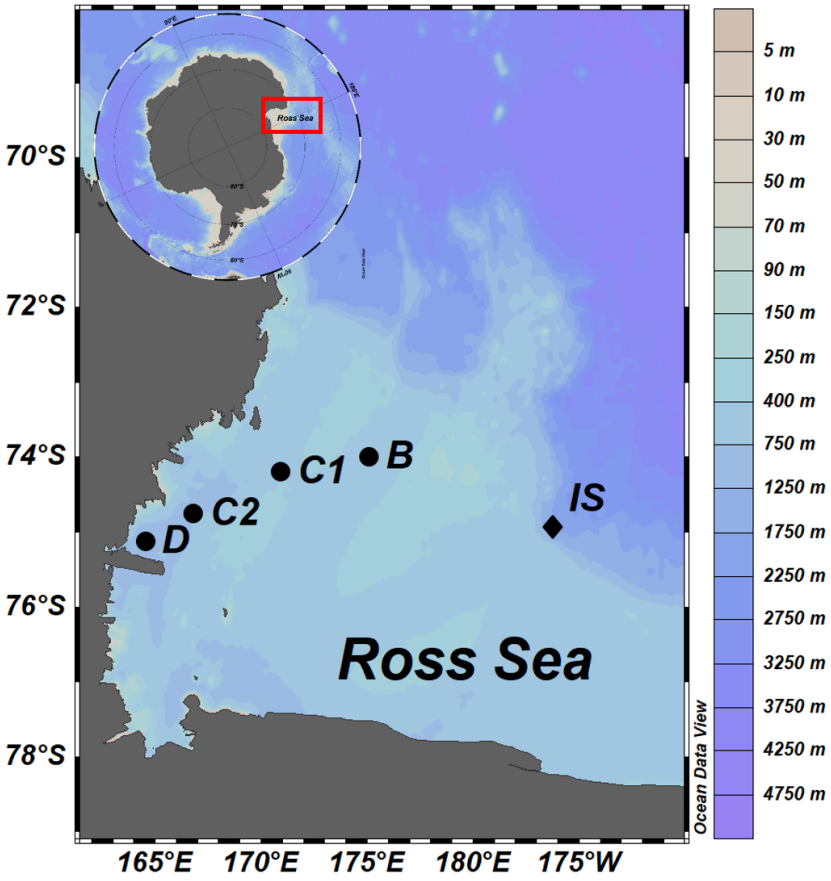

Figure 1.2: Map of the study area in the Southern Ocean. Stations marked by dots were sampled for the activities described in Chapter 4 and Chapter 5; the station marked by a diamond was sampled for the activities described in Chapter 5.

1.5. Thesis aims and structure

The major aim of this thesis was to investigate how the interplay between microbes and organic matter shapes, and in turn is shaped by, oceans' biogeochemical dynamics. To tackle this question, this thesis covers the marine microbes-organic matter interplay from two perspectives. A "top-down" approach was used to assess the effect of regional scale environmental perturbations on microbe-mediated organic matter processing. All the processes underlying this hub for ecosystems functioning are controlled by a plethora of environmental factors (see section 1.2.2). However

wide, background environmental fluctuations repeat themselves over different spatial scales (i.e., seasonal, decadal etc.) and biological processes synchronize with them. Yet, episodic environmental disturbances (i.e., storms, draught or flooding events etc.) may represent sources of extreme variability which pose unknown environmental constrains to microbe-mediated organic matter processing. Then, through a "bottom-up" approach, detailed investigations were aimed i) to resolve changes in microbial communities' structure and function when interacting with POM and ii) to link strategies of OM degradation with microbes' lifestyle. As detailed in section 1.3, the microscale interactions between microbes and POM influence global biogeochemical dynamics. Different microbial assemblages develop on POM as it sinks trough the water column, a recruitment that is heavily dependent on the environmental "seed" communities as well as on the POM features. The functional identity of POM-colonizing microbes will also define OM fluxes in the particles' surroundings. Indeed, the different foraging strategies highlighted in section 1.2.1 (i.e., the production of cell-bound and cell-free exoenzymes) may further shape POM-associated microbial assemblages, resulting in alterations in POM degradation efficiency and modes, ultimately affecting the rates at which carbon its cycled in marine systems. The conceptual scheme depicted in Figure 1.3 is aimed to aid an integrated understanding of the main processes investigated in this thesis as well as of their interrelationships.

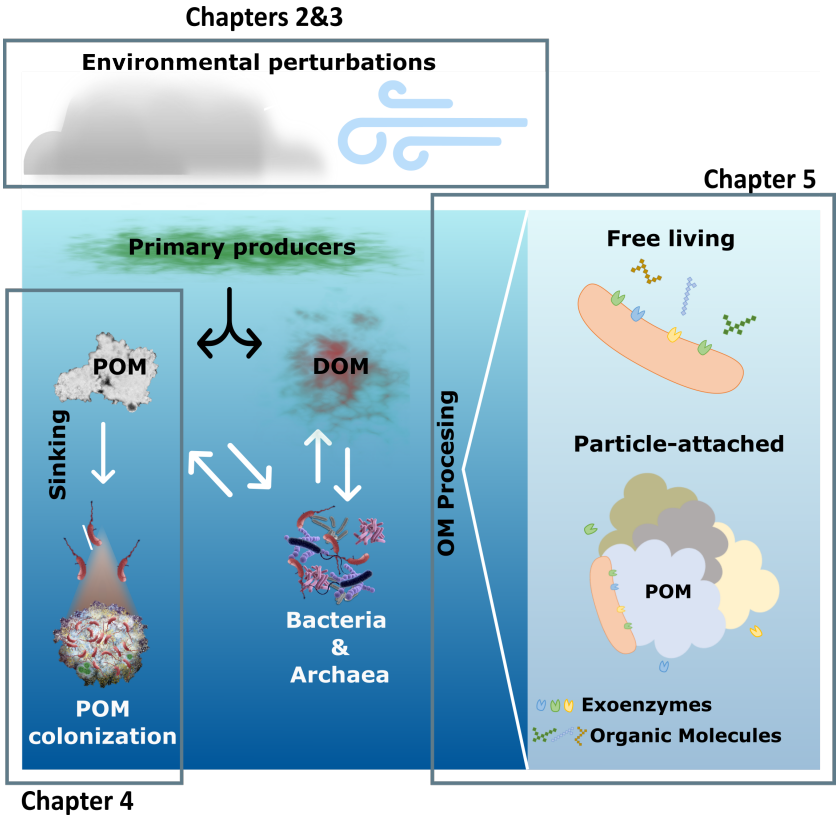

Figure 1.3: Conceptual scheme depicting the main metabolic and functional processes addressed in this thesis, with indication of the chapters in which specific processes are investigated. POM: particulate organic matter; DOM: dissolved organic matter; OM: organic matter. Redrawn from Reintjes et al., 2019; Zhang et al., 2015). Some of the images are courtesy of http://gingercreative.net.au/.

To illustrate the methods with which these aims were fulfilled as well as the main results achieved, four case studies are presented in this thesis. Each of them represents a published manuscript in which I contributed both to analytical work (i.e., experimental and/or data analysis) as well as to manuscript writing and editing.

- The first study was specifically aimed to investigate how long-term environmental changes affect microbe-mediated organic matter processing. For this work a monthly planktonic time series gathered in the Gulf of Trieste (northern Adriatic Sea) was analysed. Trough time-series analysis coupled with a machine learning approach, a prolonged salinity anomaly in the mid part of the series was identified. This resulted to be the driver of profound biogeochemical changes in the study area. Following this anomaly, microbial growth was limited by organic matter availability for several years, inducing cascading effects on the whole planktonic food web.
  Manna, V., De Vittor, C., Giani, M., Del Negro, P., Celussi, M., 2021. Long-term patterns and drivers of microbial organic matter utilization in the northernmost basin of the Mediterranean Sea. Marine Environmental Research, 164, 105245. https://doi.org/10.1016/j.marenvres.2020.105245

- The purpose of the second study case was to address the effect of an extreme cold event on the metabolism of planktonic microbes in the Gulf of Trieste (northern Adriatic Sea). Although these kinds of events are common in the area, their effect on microbe-organic matter interplay, and thus their biogeochemical consequences, are poorly studied. Combining a high frequency sampling during and after the event with temperature manipulation experiments, this chapter shows how the temperature drop induced by the event represented a lower thermal limit for resident heterotrophic microbes. This limitation lasted for a prolonged time frame, altering the functioning of local trophic webs.
  Manna, V., Fabbro, C., Cerino, F., Bazzaro, M., Del Negro, P., Celussi, M., 2019. Effect of an extreme cold event on the metabolism of planktonic microbes in the northernmost basin of the Mediterranean Sea. Estuarine, Coastal and Shelf Science, 225, 106252. https://doi.org/10.1016/j.ecss.2019.106252

- The third chapter is focused on microscale interactions between Antarctic heterotrophic microbes and POM. Microcosms experiment were carried out incubating natural free-living communities with phytodetrital POM, following changes in community composition as well as in metabolic activities. Outcomes from this work have highlighted that phytodetritus “taxonomy” (i.e., the composition of the phytoplankton community from which the detritus was generated) substantially shapes the associated microbial community and thus its metabolic capabilities. This chapter sheds light on the microscale dynamics regulating POM fate as it sinks trough the water column and thus the efficiency of the biological carbon pump.
  Manna, V., Malfatti, F., Banchi, E., Cerino, F., De Pascale, F., Franzo, A., Schiavon, R., Vezzi, A., Del Negro, P., Celussi, M., 2020. Prokaryotic response to phytodetritus-derived organic material in epi- and mesopelagic Antarctic waters. Frontiers in

Microbiology, 11:1242.
https://doi.org/10.3389/fmicb.2020.01242

- The fourth study case was developed to investigate organic matter degradation modes with respect to microbial lifestyle (i.e., free-living vs. particle-attached). To pursue this aim, several Antarctic bacterial isolates were screened for their degradative potential when growing in particle-free media and when exposed to phytodetrital POM. Results from these experiments showed that production and activity of exoenzymes were finely tuned according to growth conditions and that the presence of particles enhanced the release of cell-free enzymes. While confirming the current view on degradation modes of free-living vs. particle-attached microbes, this study provides precious insights on microscale interaction between microbes and POM at single strain level.
Manna, V., Del Negro, P., Celussi, M., 2019. Modulation of hydrolytic profiles of cell-bound and cell-free exoenzymes in Antarctic marine bacterial isolates. Advances in Oceanography and Limnology, 10, 32–43.
https://doi.org/10.4081/aiol.2019.8240

References

Agusti, S., González-Gordillo, J. I., Vaqué, D., Estrada, M., Cerezo, M. I., Salazar, G., Gasol, J. M., & Duarte, C. M. (2015). Ubiquitous healthy diatoms in the deep sea confirm deep carbon injection by the biological pump. *Nature Communications*, *6*(1), 7608. https://doi.org/10.1038/ncomms8608

Allison, S. D. (2005). Cheaters, diffusion and nutrients constrain decomposition by microbial enzymes in spatially structured environments. *Ecology Letters*, *8*(6), 626–635. https://doi.org/10.1111/j.1461-0248.2005.00756.x

Allison, S. D., Chao, Y., Farrara, J. D., Hatosy, S., & Martiny, A. C. (2012). Fine-scale temporal variation in marine extracellular enzymes of coastal southern california. *Frontiers in Microbiology*, *3*(AUG). https://doi.org/10.3389/fmicb.2012.00301

Alonso-Sáez, L., Galand, P. E., Casamayor, E. O., Pedrós-Alió, C., & Bertilsson, S. (2010). High bicarbonate assimilation in the dark by Arctic bacteria. *The ISME Journal*, *4*(12), 1581–1590. https://doi.org/10.1038/ismej.2010.69

Amin, S. A., Parker, M. S., & Armbrust, E. V. (2012). Interactions between Diatoms and Bacteria. *Microbiology and Molecular Biology Reviews*, *76*(3), 667–684. https://doi.org/10.1128/mmbr.00007-12

Amin, S. A., Green, D. H., Hart, M. C., Küpper, F. C., Sunda, W. G., & Carrano, C. J. (2009). Photolysis of iron-siderophore chelates promotes bacterial-algal mutualism. *Proceedings of the National Academy of Sciences of the United States of America*, *106*(40), 17071–17076. https://doi.org/10.1073/pnas.0905512106

Anderson, T. R., & Williams, P. J. (1999). A one-dimensional model of dissolved organic carbon cycling in the water column incorporating combined biological-photochemical decomposition. *Global Biogeochemical Cycles*, *13*(2), 337–349. https://doi.org/10.1029/1999GB900013

Apple, J. K., Del Giorgio, P. A., & Kemp, W. M. (2006). Temperature regulation of bacterial production, respiration, and growth efficiency in a temperate salt-marsh estuary. *Aquatic Microbial Ecology*, *43*(3), 243–254. https://doi.org/10.3354/ame043243

Arnosti, C., Reintjes, G., & Amann, R. (2018). A mechanistic microbial underpinning for the size-reactivity continuum of dissolved organic carbon degradation. *Marine Chemistry*, *206*, 93–99. https://doi.org/10.1016/j.marchem.2018.09.008

Arnosti, C. (2011). Microbial Extracellular Enzymes and the Marine Carbon Cycle. *Annual Review of Marine Science*, *3*(1), 401–425. https://doi.org/10.1146/annurev-marine-120709-142731

Arnosti, C., Steen, A. D., Ziervogel, K., Ghobrial, S., & Jeffrey, W. H. (2011). Latitudinal gradients in degradation of marine dissolved organic carbon. *PLoS ONE*, *6*(12), e28900. https://doi.org/10.1371/journal.pone.0028900

Azam, F., Fenchel, T., Field, J., Gray, J., Meyer-Reil, L., & Thingstad, F. (1983). The Ecological Role of Water-Column Microbes in the Sea. *Marine Ecology Progress Series*, *10*(3), 257–263. https://doi.org/10.3354/meps010257

Azam, F. (1998). Microbial control of oceanic carbon flux: The plot thickens. *Science*, *280*(5364), 694–696. https://doi.org/10.1126/science.280.5364.694

Azam, F., & Malfatti, F. (2007). Microbial structuring of marine ecosystems. *Nature Reviews Microbiology*, *5*(10), 782–791. https://doi.org/10.1038/nrmicro1747

Balmonte, J. P., Teske, A., & Arnosti, C. (2018). Structure and function of high Arctic pelagic, particle-associated and benthic bacterial communities. *Environmental Microbiology*, *20*(8), 2941–2954. https://doi.org/10.1111/1462-2920.14304

Baltar, F. (2018). Watch out for the "living dead : Cell-free enzymes and their fate. *Frontiers in Microbiology*, *8*(JAN), 2438. https://doi.org/10.3389/fmicb.2017.02438

Baltar, F., Arístegui, J., Gasol, J. M., Sintes, E., Van Aken, H. M., & Herndl, G. J. (2010). High dissolved extracellular enzymatic activity in the deep central Atlantic ocean. *Aquatic Microbial Ecology*, *58*(3), 287–302. https://doi.org/10.3354/ame01377

Baltar, F., & Herndl, G. J. (2019). Ideas and perspectives: Is dark carbon fixation relevant for oceanic primary production estimates? *Biogeosciences*, *16*(19), 3793–3799. https://doi.org/10.5194/bg-16-3793-2019

Baltar, F., Lundin, D., Palovaara, J., Lekunberri, I., Reinthaler, T., Herndl, G. J., & Pinhassi, J. (2016). Prokaryotic Responses to Ammonium and Organic Carbon Reveal Alternative CO2 Fixation Pathways and Importance of Alkaline Phosphatase in the Mesopelagic North Atlantic. *Frontiers in Microbiology*, *7*, 1670. https://doi.org/10.3389/fmicb.2016.01670

Baltar, F., Morán, X. A. G., & Lønborg, C. (2017). Warming and organic matter sources impact the proportion of dissolved to total activities in marine extracellular enzymatic rates. *Biogeochemistry*, *133*(3), 307–316. https://doi.org/10.1007/s10533-017-0334-9

Becker, S., Tebben, J., Coffinet, S., Wiltshire, K., Iversen, M. H., Harder, T., Hinrichs, K. U., & Hehemann, J. H. (2020). Laminarin is a major molecule in the marine carbon cycle. *Proceedings of the National Academy of Sciences of the United States of America*, *117*(12), 6599–6607. https://doi.org/10.1073/pnas.1917001117

Behrenfeld, M. J., & Falkowski, P. G. (1997). Photosynthetic rates derived from satellite-based chlorophyll concentration. *Limnology and Oceanography*, *42*(1), 1–20. https://doi.org/10.4319/lo.1997.42.1.0001

Benner, R., & Amon, R. M. (2015). The size-reactivity continuum of major bioelements in the Ocean. *Annual Review of Marine Science*, *7*(1), 185–205. https://doi.org/10.1146/annurev-marine-010213-135126

Berman, T., Béchemin, C., & Maestrini, S. Y. (1999). Release of ammonium and urea from dissolved organic nitrogen in aquatic ecosystems. *Aquatic Microbial Ecology*, *16*(3), 295–302. https://doi.org/10.3354/ame016295

Berman, T., & Bronk, D. A. (2003). Dissolved organic nitrogen: A dynamic participant in aquatic ecosystems. *Aquatic Microbial Ecology*, *31*(3), 279–305. https://doi.org/10.3354/ame031279

Bidle, K. D., Manganelli, M., & Azam, F. (2002). Regulation of Oceanic Silicon and Carbon Preservation by Temperature Control on Bacteria. *Science*, *298*(5600), 1980–1984. https://doi.org/10.1126/science.1076076

Bižić-Ionescu, M., Ionescu, D., & Grossart, H.-P. (2018). Organic Particles: Heterogeneous Hubs for Microbial Interactions in Aquatic Ecosystems. *Frontiers in Microbiology*, *9*, 2569. https://doi.org/10.3389/fmicb.2018.02569

Bižić-Ionescu, M., Zeder, M., Ionescu, D., Orlić, S., Fuchs, B. M., Grossart, H.-P., & Amann, R. (2015). Comparison of bacterial communities on limnic versus coastal marine particles reveals profound differences in colonization. *Environmental Mi-*

crobiology, *17*(10), 3500–3514. https://doi.org/https://doi.org/10.1111/1462-2920.12466

Björkman, K. M., & Karl, D. M. (2003). Bioavailability of dissolved organic phosphorus in the euphotic zone at Station ALOHA, North Pacific Subtropical Gyre. *Limnology and Oceanography*, *48*(3), 1049–1057. https://doi.org/10.4319/lo.2003.48.3.1049

Bonilla-Findji, O., Hernd, G. J., Gattuso, J. P., & Weinbauer, M. G. (2009). Viral and flagellate control of prokaryotic production and community structure in offshore mediterranean waters. *Applied and Environmental Microbiology*, *75*(14), 4801–4812. https://doi.org/10.1128/AEM.01376-08

Boscolo-Galazzo, F., Crichton, K. A., Barker, S., & Pearson, P. N. (2018). Temperature dependency of metabolic rates in the upper ocean: A positive feedback to global climate change? *Global and Planetary Change*, *170*, 201–212. https://doi.org/10.1016/j.gloplacha.2018.08.017

Bowen, J. D., Stolzenbach, K. D., & Chisholm, S. W. (1993). Simulating bacterial clustering around phytoplankton cells in a turbulent ocean. *Limnology and Oceanography*, *38*(1), 36–51. https://doi.org/10.4319/lo.1993.38.1.0036

Boyd, P. W., Arrigo, K. R., Strzepek, R., & van Dijken, G. L. (2012). Mapping phytoplankton iron utilization: Insights into Southern Ocean supply mechanisms. *Journal of Geophysical Research: Oceans*, *117*(C6). https://doi.org/https://doi.org/10.1029/2011JC007726

Breitbart, M. (2012). Marine viruses: Truth or dare. *Annual Review of Marine Science*, *4*(1), 425–448. https://doi.org/10.1146/annurev-marine-120709-142805

Bronk, D. A., See, J. H., Bradley, P., & Killberg, L. (2007). DON as a source of bioavailable nitrogen for phytoplankton. *Biogeosciences*, *4*(3), 283–296. https://doi.org/10.5194/bg-4-283-2007

Bronk, D. A., & Steinberg, D. K. (2008). Nitrogen Regeneration. *Nitrogen in the Marine Environment* (pp. 385–467). Elsevier. https://doi.org/10.1016/B978-0-12-372522-6.00008-6

Brussaard, C. P. (2004). Viral control of phytoplankton populations - A review. *Journal of Eukaryotic Microbiology*, *51*(2), 125–138. https://doi.org/10.1111/j.1550-7408.2004.tb00537.x

Calbet, A. (2001). Mesozooplankton grazing effect on primary production: A global comparative analysis in marine ecosystems. *Limnology and Oceanography*, *46*(7), 1824–1830. https://doi.org/10.4319/lo.2001.46.7.1824

Calbet, A., & Landry, M. R. (1999). Mesozooplankton influences on the microbial food web: Direct and indirect trophic interactions in the oligotrophic open ocean. *Limnology and Oceanography*, *44*(6), 1370–1380. https://doi.org/10.4319/lo.1999.44.6.1370

Carlson, C. A., del Giorgio, P. A., & Herndl, G. J. (2007). Microbes and the dissipation of energy and respiration: From cells to ecosystems. *Oceanography*, *20*(SPL.ISS. 2), 89–100. https://doi.org/10.5670/oceanog.2007.52

Carlson, C. A., & Hansell, D. A. (2015). DOM Sources, Sinks, Reactivity, and Budgets. In D. A. Hansell & C. A. B. T. B. o. M. D. O. M. (E. Carlson (Eds.), *Biogeochemistry of Marine Dissolved Organic Matter: Second Edition* (pp. 65–126). Academic Press. https://doi.org/10.1016/B978-0-12-405940-5.00003-0

Catalano, G., Budillon, G., La Ferla, R., Povero, P., Ravaioli, M., Saggiomo, V., Accornero, A., Azzaro, M., Carrada, G., Giglio, F., Langone, L., Mangoni, O., Misic, C., & Modigh, M. (2010). The Ross Sea. In L. Liu, K.-K. Atkinson, L. Quinones, & R. Talaue-McManus (Eds.), *Carbon and nutrient fluxes in continental margins: A global synthesis* (pp. 303–318). Springer.

Celussi, M., & Del Negro, P. (2012). Microbial degradation at a shallow coastal site: Long-term spectra and rates of exoenzymatic activities in the NE Adriatic Sea. *Estuarine, Coastal and Shelf Science*, *115*, 75–86. https://doi.org/10.1016/j.ecss.2012.02.002

Chróst, R. J. (1990). Microbial Ectoenzymes in Aquatic Environments. In T. D. Brock, J. Overbeck, & R. J. Chróst (Eds.), *Aquatic microbial ecology* (pp. 47–78). Springer New York. https://doi.org/10.1007/978-1-4612-3382-4_3

Church, M. J. (2008). Resource control of bacterial dynamics in the sea. *Microbial ecology of the oceans* (pp. 335–382). John Wiley & Sons, Ltd. https://doi.org/https://doi.org/10.1002/9780470281840.ch10

Cole, J. J., & Pace, M. L. (1995). Bacterial secondary production in oxic and anoxic freshwaters. *Limnology and Oceanography*, *40*(6), 1019–1027. https://doi.org/10.4319/lo.1995.40.6.1019

Collins, J. R., Edwards, B. R., Thamatrakoln, K., Ossolinski, J. E., Ditullio, G. R., Bidle, K. D., Doney, S. C., & Van Mooy, B. A. (2015). The multiple fates of sinking particles in the North Atlantic Ocean. *Global Biogeochemical Cycles*, *29*(9), 1471–1494. https://doi.org/10.1002/2014GB005037

Cozzi, S., Ivančić, I., Catalano, G., Djakovac, T., & Degobbis, D. (2004). Dynamics of the oceanographic properties during mucilage appearance in the Northern Adriatic Sea: Analysis of the 1997 event in comparison to earlier events. *Journal of Marine Systems*, *50*(3-4), 223–241. https://doi.org/10.1016/j.jmarsys.2004.01.007

Currie, D. J., & Kalff, J. (1984). A comparison of the abilities of freshwater algae and bacteria to acquire and retain phosphorus. *Limnology and Oceanography*, *29*(2), 298–310. https://doi.org/10.4319/lo.1984.29.2.0298

Cushing, D. H. (1989). A difference in structure between ecosystems in strongly stratified waters and in those that are only weakly stratified. *Journal of Plankton Research*, *11*(1), 1–13. https://doi.org/10.1093/plankt/11.1.1

Cuskin, F., Lowe, E. C., Temple, M. J., Zhu, Y., Cameron, E. A., Pudlo, N. A., Porter, N. T., Urs, K., Thompson, A. J., Cartmell, A., Rogowski, A., Hamilton, B. S., Chen, R., Tolbert, T. J., Piens, K., Bracke, D., Vervecken, W., Hakki, Z., Speciale, G., … Gilbert, H. J. (2015). Human gut Bacteroidetes can utilize yeast mannan through a selfish mechanism. *Nature*, *517*(7533), 165–169. https://doi.org/10.1038/nature13995

D'Ambrosio, L., Ziervogel, K., Macgregor, B., Teske, A., & Arnosti, C. (2014). Composition and enzymatic function of particle-associated and free-living bacteria: A coastal/offshore comparison. *ISME Journal*, *8*(11), 2167–2179. https://doi.org/10.1038/ismej.2014.67

Datta, M. S., Sliwerska, E., Gore, J., Polz, M. F., & Cordero, O. X. (2016). Microbial interactions lead to rapid micro-scale successions on model marine particles. *Nature Communications*, *7*(1), 11965. https://doi.org/10.1038/ncomms11965

De Vittor, C., Paoli, A., & Fonda Umani, S. (2008). Dissolved organic carbon variability in a shallow coastal marine system (Gulf of Trieste, northern Adriatic Sea). *Estuarine, Coastal and Shelf Science*, *78*(2), 280–290. https://doi.org/10.1016/j.ecss.2007.12.007

Deppeler, S. L., & Davidson, A. T. (2017). Southern ocean phytoplankton in a changing climate. *Frontiers in Marine Science*, *4*, 40. https://doi.org/10.3389/fmars.2017.00040

Dittmar, T., & Stubbins, A. (2013). Dissolved Organic Matter in Aquatic Systems. In H. D. Holland & K. K. B. T. T. o. G. (E. Turekian (Eds.), *Treatise on Geochemistry: Second Edition* (pp. 125–156). Elsevier. https://doi.org/10.1016/B978-0-08-095975-7.01010-X

Dittmar, T. (2015). Reasons Behind the Long-Term Stability of Dissolved Organic Matter. In D. A. Hansell & C. A. B. T. B. o. M. D. O. M. (E. Carlson (Eds.), *Biogeochemistry of Marine Dissolved Organic Matter: Second Edition* (pp. 369–388). Academic Press. https://doi.org/10.1016/B978-0-12-405940-5.00007-8

Dittmar, T., & Arnosti, C. (2018). An inseparable liason: Marine microbes and nonliving organic matter. In J. M. Gasol & D. L. Kirchman (Eds.), *Microbial ecology of the oceans* (Third, pp. 189–218). John Wiley & Sons, Inc.

DiTullio, G. R., Grebmeier, J. M., Arrigo, K. R., Lizotte, M. P., Robinson, D. H., Leventer, A., Barry, J. P., VanWoert, M. L., & Dunbar, R. B. (2000). Rapid and early export of Phaeocystis antarctica blooms in the Ross Sea, Antarctica. *Nature*, *404*(6778), 595–598. https://doi.org/10.1038/35007061

Duarte, C. M. (2015). Seafaring in the 21st century: The Malaspina 2010 circumnavigation expedition. *Limnology and Oceanography Bulletin*, *24*(1), 11–14. https://doi.org/10.1002/lob.10008

Ducklow, H. (2000). Bacterioplankton production and biomass in the oceans. *Microbial Ecology of the Oceans, 1st edition* (pp. 1–47). John Wiley & Sons, Inc.

Ducklow, H. W., Steinberg, D. K., & Buesseler, K. O. (2001). Upper ocean carbon export and the biological pump. *Oceanography*, *14*(SPL.ISS. 4), 50–58. https://doi.org/10.5670/oceanog.2001.06

Dunne, J. P., Sarmiento, J. L., & Gnanadesikan, A. (2007). A synthesis of global particle export from the surface ocean and cycling through the ocean interior and on the seafloor. *Global Biogeochemical Cycles*, *21*(4), n/a–n/a. https://doi.org/10.1029/2006GB002907

Duret, M. T., Lampitt, R. S., & Lam, P. (2019). Prokaryotic niche partitioning between suspended and sinking marine particles. *Environmental Microbiology Reports*, *11*(3), 386–400. https://doi.org/https://doi.org/10.1111/1758-2229.12692

Durrieu de Madron, X., Guieu, C., Sempéré, R., Conan, P., Cossa, D., D'Ortenzio, F., Estournel, C., Gazeau, F., Rabouille, C., Stemmann, L., Bonnet, S., Diaz, F., Koubbi, P., Radakovitch, O., Babin, M., Baklouti, M., Bancon-Montigny, C., Belviso, S., Bensoussan, N., … Verney, R. (2011). Marine ecosystems' responses to climatic and anthropogenic forcings in the Mediterranean. *Progress in Oceanography*, *91*(2), 97–166. https://doi.org/10.1016/j.pocean.2011.02.003

Dyhrman, S. T., Ammerman, J. W., & van Mooy, B. A. (2007). Microbes and the marine phosphorus cycle. *Oceanography*, *20*(SPL.ISS. 2), 110–116. https://doi.org/10.5670/oceanog.2007.54

Falkowski, P. G., Barber, R. T., & Smetacek, V. (1998). Biogeochemical controls and feedbacks on ocean primary production. *Science*, *281*(5374), 200–206. https://doi.org/10.1126/science.281.5374.200

Field, C. B., Behrenfeld, M. J., Randerson, J. T., & Falkowski, P. (1998). Primary production of the biosphere: Integrating terrestrial and oceanic components. *Science*, *281*(5374), 237–240. https://doi.org/10.1126/science.281.5374.237

First, M. R., & Hollibaugh, J. T. (2009). The model high molecular weight DOC compound, dextran, is ingested by the benthic ciliate Uronema marinum but does not supplement ciliate growth. *Aquatic Microbial Ecology*, *57*(1), 79–87. https://doi.org/10.3354/ame01338

Flynn, K. J., Stoecker, D. K., Mitra, A., Raven, J. A., Glibert, P. M., Hansen, P. J., Granéli, E., & Burkholder, J. M. (2013). Misuse of the phytoplankton-zooplankton dichotomy: The need to assign organisms as mixotrophs within plankton functional types. *Journal of Plankton Research*, *35*(1), 3–11. https://doi.org/10.1093/plankt/fbs062

Folse, H. J., & Allison, S. D. (2012). Cooperation, Competition, and Coalitions in Enzyme-Producing Microbes: Social Evolution and Nutrient Depolymerization Rates. *Frontiers in Microbiology*, *3*(SEP), 338. https://doi.org/10.3389/fmicb.2012.00338

Fonda Umani, S., Malfatti, F., & Del Negro, P. (2012). Carbon fluxes in the pelagic ecosystem of the Gulf of Trieste (Northern Adriatic Sea). *Estuarine, Coastal and Shelf Science*, *115*, 170–185. https://doi.org/10.1016/j.ecss.2012.04.006

Fontanez, K. M., Eppley, J. M., Samo, T. J., Karl, D. M., & DeLong, E. F. (2015). Microbial community structure and function on sinking particles in the North Pacific Subtropical Gyre. *Frontiers in Microbiology*, *6*, 469. https://doi.org/10.3389/fmicb.2015.00469

Fuhrman, J. A. (1999). Marine viruses and their biogeochemical and ecological effects. *Nature*, *399*(6736), 541–548. https://doi.org/10.1038/21119

Furusawa, G., Yoshikawa, T., Yasuda, A., & Sakata, T. (2003). Algicidal activity and gliding motility of Saprospira sp. SS98-5. *Canadian Journal of Microbiology*, *49*(2), 92–100. https://doi.org/10.1139/w03-017

Gačić, M., Poulain, P.-M., Zore-Armanda, M., & Barale, V. (2001). Overview. In B. Cushman-Roisin, M. Gačić, & P.-M. Poulain (Eds.), *Physical Oceanography of the Adriatic Sea. Past, Present and Future* (pp. 1–44). Kluwer Academic Publishers.

Ganesh, S., Parris, D. J., Delong, E. F., & Stewart, F. J. (2014). Metagenomic analysis of size-fractionated picoplankton in a marine oxygen minimum zone. *ISME Journal*, *8*(1), 187–211. https://doi.org/10.1038/ismej.2013.144

Gardner, W. D., Mishonov, A. V., & Richardson, M. J. (2006). Global POC concentrations from in-situ and satellite data. *Deep-Sea Research Part II: Topical Studies in Oceanography*, *53*(5-7), 718–740. https://doi.org/10.1016/j.dsr2.2006.01.029

Giering, S. L. C., Sanders, R., Lampitt, R. S., Anderson, T. R., Tamburini, C., Boutrif, M., Zubkov, M. V., Marsay, C. M., Henson, S. A., Saw, K., Cook, K., & Mayor, D. J. (2014). Reconciliation of the carbon budget in the ocean's twilight zone. *Nature*, *507*(7493), 480–483. https://doi.org/10.1038/nature13123

Goldman, J. C., & Dennett, M. R. (2000). Growth of marine bacteria in batch and continuous culture under carbon and nitrogen limitation. *Limnology and Oceanography*, *45*(4), 789–800. https://doi.org/10.4319/lo.2000.45.4.0789

Grossart, H. P., & Ploug, H. (2000). Bacterial production and growth efficiencies: Direct measurements on riverine aggregates. *Limnology and Oceanography*, *45*(2), 436–445. https://doi.org/10.4319/lo.2000.45.2.0436

Grossart, H. P., & Simon, M. (1998). Significance of limnetic organic aggregates (lake snow) for the sinking flux of particulate organic matter in a large lake. *Aquatic Microbial Ecology*, *15*(2), 115–125. https://doi.org/10.3354/ame015115

Grossart, H.-P., Levold, F., Allgaier, M., Simon, M., & Brinkhoff, T. (2005). Marine diatom species harbour distinct bacterial communities. *Environmental Microbiology*, *7*(6), 860–873. https://doi.org/https://doi.org/10.1111/j.1462-2920.2005.00759.x

Grossart, H.-P., & Simon, M. (1993). Limnetic macroscopic organic aggregates (lake snow): Occurrence, characteristics, and microbial dynamics in Lake Constance. *Limnology and Oceanography*, *38*(3), 532–546. https://doi.org/https://doi.org/10.4319/lo.1993.38.3.0532

Hall, E. K., & Cotner, J. B. (2007). Interactive effect of temperature and resources on carbon cycling by freshwater bacterioplankton communities. *Aquatic Microbial Ecology*, *49*(1), 35–45. https://doi.org/10.3354/ame01124

Hansell, D. A. (2013). Recalcitrant dissolved organic carbon fractions. *Annual Review of Marine Science*, *5*(1), 421–445. https://doi.org/10.1146/annurev-marine-120710-100757

Hansell, D. A., Carlson, C. A., Repeta, D. J., & Schlitzer, R. (2009). Dissolved organic matter in the ocean a controversy stim ulates new insights. *Oceanography*, *22*(SPL.ISS. 4), 202–211. https://doi.org/10.5670/oceanog.2009.109

Hansman, R. L., Griffin, S., Watson, J. T., Druffel, E. R., Ingalls, A. E., Pearson, A., & Aluwihare, L. I. (2009). The radiocarbon signature of microorganisms in the mesopelagic ocean. *Proceedings of the National Academy of Sciences of the United States of America*, *106*(16), 6513–6518. https://doi.org/10.1073/pnas.0810871106

Hauck, J., Völker, C., Wolf-Gladrow, D. A., Laufkötter, C., Vogt, M., Aumont, O., Bopp, L., Buitenhuis, E. T., Doney, S. C., Dunne, J., Gruber, N., Hashioka, T., John, J., Quéré, C. L., Lima, I. D., Nakano, H., Séférian, R., & Totterdell, I. (2015). On the Southern Ocean CO2 uptake and the role of the biological carbon pump in the 21st century. *Global Biogeochemical Cycles*, *29*(9), 1451–1470. https://doi.org/https://doi.org/10.1002/2015GB005140

Herndl, G. J., & Peduzzi, P. (1988). The Ecology of Amorphous Aggregations (Marine Snow) in the Northern Adriatic Sea: *Marine Ecology*, *9*(1), 79–90. https://doi.org/10.1111/j.1439-0485.1988.tb00199.x

Hertkorn, N., Benner, R., Frommberger, M., Schmitt-Kopplin, P., Witt, M., Kaiser, K., Kettrup, A., & Hedges, J. I. (2006). Characterization of a major refractory component of marine dissolved organic matter. *Geochimica et Cosmochimica Acta*, *70*(12), 2990–3010. https://doi.org/10.1016/j.gca.2006.03.021

Jannasch, H. W., & Mottl, M. J. (1985). Geomicrobiology of deep-sea hydrothermal vents. *Science*, *229*(4715), 717–725. https://doi.org/10.1126/science.229.4715.717

Jatt, A. N., Tang, K., Liu, J., Zhang, Z., & Zhang, X. H. (2015). Quorum sensing in marine snow and its possible influence on production of extracellular hydrolytic

enzymes in marine snow bacterium Pantoea ananatis B9. *FEMS Microbiology Ecology*, *91*(2), 1–13. https://doi.org/10.1093/femsec/fiu030

Jenkins, W. J., Smethie, W. M., Boyle, E. A., & Cutter, G. A. (2015). Water mass analysis for the U.S. GEOTRACES (GA03) North Atlantic sections. *Deep-Sea Research Part II: Topical Studies in Oceanography*, *116*, 6–20. https://doi.org/10.1016/j.dsr2.2014.11.018

Jiao, N., Herndl, G. J., Hansell, D. A., Benner, R., Kattner, G., Wilhelm, S. W., Kirchman, D. L., Weinbauer, M. G., Luo, T., Chen, F., & Azam, F. (2010). Microbial production of recalcitrant dissolved organic matter: Long-term carbon storage in the global ocean. *Nature Reviews Microbiology*, *8*(8), 593–599. https://doi.org/10.1038/nrmicro2386

Jiao, N., Herndl, G. J., Hansell, D. A., Benner, R., Kattner, G., Wilhelm, S. W., Kirchman, D. L., Weinbauer, M. G., Luo, T., Chen, F., & Azam, F. (2011). The microbial carbon pump and the oceanic recalcitrant dissolved organic matter pool. *Nature Reviews Microbiology*, *9*(7), 555. https://doi.org/10.1038/nrmicro2386-c5

Kaiser, C., Franklin, O., Richter, A., & Dieckmann, U. (2015). Social dynamics within decomposer communities lead to nitrogen retention and organic matter build-up in soils. *Nature Communications*, *6*(1), 8960. https://doi.org/10.1038/ncomms9960

Kaltenbock, E., & Herndl, G. J. (1992). Ecology of amorphous aggregations (marine snow) in the northern Adriatic Sea. IV. Dissolved nutrients and the autotrophic community associated with marine snow. *Marine Ecology Progress Series*, *87*(1-2), 147–159. https://doi.org/10.3354/meps087147

Karl, D. M., & Björkman, K. M. (2015). Dynamics of Dissolved Organic Phosphorus. In D. A. Hansell & C. A. B. T. B. o. M. D. O. M. (E. Carlson (Eds.), *Biogeochemistry of Marine Dissolved Organic Matter: Second Edition* (pp. 233–334). Academic Press. https://doi.org/10.1016/B978-0-12-405940-5.00005-4

Karner, M., & Herndl, G. J. (1992). Extracellular enzymatic activity and secondary production in free-living and marine-snow-associated bacteria. *Marine Biology*, *113*(2), 341–347. https://doi.org/10.1007/BF00347289

Keil, R. G., & Kirchman, D. L. (1993). Dissolved combined amino acids: Chemical form and utilization by marine bacteria. *Limnology and Oceanography*, *38*(6), 1256–1270. https://doi.org/10.4319/lo.1993.38.6.1256

Kiørboe, T., Ploug, H., & Thygesen, U. H. (2001). Fluid motion and solute distribution around sinking aggregates. I. Small-scale fluxes and heterogeneity of nutrients in the pelagic environment. *Marine Ecology Progress Series*, *211*, 1–13. https://doi.org/10.3354/meps211001

Kiørboe, T. (2001). Formation and fate of marine snow: Small-scale processes with large- scale implications. *Scientia Marina*, *65*(S2), 57–71. https://doi.org/10.3989/scimar.2001.65s257

Koch, B. P., Kattner, G., Witt, M., & Passow, U. (2014). Molecular insights into the microbial formation of marine dissolved organic matter: Recalcitrant or labile? *Biogeosciences*, *11*(15), 4173–4190. https://doi.org/10.5194/bg-11-4173-2014

Kolowith, L. C., Ingall, E. D., & Benner, R. (2001). Composition and cycling of marine organic phosphorus. *Limnology and Oceanography*, *46*(2), 309–320. https://doi.org/10.4319/lo.2001.46.2.0309

Köster, M., & Paffenhöfer, G. A. (2013). Oxygen consumption of fecal pellets of doliolids (Tunicata, Thaliacea) and planktonic copepods (Crustacea, Copepoda). *Journal of Plankton Research*, *35*(2), 323–336. https://doi.org/10.1093/plankt/fbs092

Lampert, W. (1978). Release of dissolved organic carbon by grazing zooplankton. *Limnology and Oceanography*, *23*(4), 831–834. https://doi.org/10.4319/lo.1978.23.4.0831

Lechtenfeld, O. J., Hertkorn, N., Shen, Y., Witt, M., & Benner, R. (2015). Marine sequestration of carbon in bacterial metabolites. *Nature Communications*, *6*(1), 6711. https://doi.org/10.1038/ncomms7711

Letscher, R. T., Moore, J. K., Teng, Y. C., & Primeau, F. (2015). Variable C : N : P stoichiometry of dissolved organic matter cycling in the Community Earth System Model. *Biogeosciences*, *12*(1), 209–221. https://doi.org/10.5194/bg-12-209-2015

Lin, P., & Guo, L. (2015). Spatial and vertical variability of dissolved carbohydrate species in the northern Gulf of Mexico following the Deepwater Horizon oil spill, 2010-2011. *Marine Chemistry*, *174*, 13–25. https://doi.org/10.1016/j.marchem.2015.04.001

Long, R. A., & Azam, F. (2001). Microscale patchiness of bacterioplankton assemblage richness in seawater. *Aquatic Microbial Ecology*, *26*(2), 103–113. https://doi.org/10.3354/ame026103

Martinez, J., Smith, D. C., Steward, G. F., & Azam, F. (1996). Variability in ectohydrolytic enzyme activities of pelagic marine bacteria and its significance for substrate processing in the sea. *Aquatic Microbial Ecology*, *10*(3), 223–230. https://doi.org/10.3354/ame010223

Michelou, V. K., Cottrell, M. T., & Kirchman, D. L. (2007). Light-stimulated bacterial production and amino acid assimilation by cyanobacteria and other microbes in the North Atlantic Ocean. *Applied and Environmental Microbiology*, *73*(17), 5539–5546. https://doi.org/10.1128/AEM.00212-07

Middelboe, M. (2010). Microbial disease in the sea: Effects of viruses on carbon and nutrient cycling. In R. Ostfeld, F. Keesing, & V. Eviner (Eds.), *Infectious Disease Ecology: Effects of Ecosystems on Disease and of Disease on Ecosystems* (pp. 242–259). Princeton University Press.

Mislan, K. A., Stock, C. A., Dunne, J. P., & Sarmiento, J. L. (2014). Group behavior among model bacteria influences particulate carbon remineralization depths. *Journal of Marine Research*, *72*(3), 183–218. https://doi.org/10.1357/002224014814901985

Mitchell, J. G., Okubo, A., & Fuhrman, J. A. (1985). Microzones surrounding phytoplankton form the basis for a stratified marine microbial ecosystem. *Nature*, *316*(6023), 58–59. https://doi.org/10.1038/316058a0

Møller, E. F., Thor, P., & Nielsen, T. G. (2003). Production of DOC by Calanus finmarchicus, C. glacialis and C. hyperboreus through sloppy feeding and leakage from fecal pellets. *Marine Ecology Progress Series*, *262*, 185–191. https://doi.org/10.3354/meps262185

Moran, M. A. (2000). UV radiation effects on microbes and microbial processes. In D. L. Kirchman (Ed.), *Microbial Ecology of the Oceans* (pp. 201–228). John Wiley & Sons, Inc.

Moran, M. A., Kujawinski, E. B., Stubbins, A., Fatland, R., Aluwihare, L. I., Buchan, A., Crump, B. C., Dorrestein, P. C., Dyhrman, S. T., Hess, N. J., Howe, B., Longnecker, K., Medeiros, P. M., Niggemann, J., Obernosterer, I., Repeta, D. J., & Waldbauer, J. R. (2016). Deciphering ocean carbon in a changing world. *Proceedings of the National Academy of Sciences of the United States of America*, *113*(12), 3143–3151. https://doi.org/10.1073/pnas.1514645113

Morán, X. A. G., Gasol, J. M., Pernice, M. C., Mangot, J. F., Massana, R., Lara, E., Vaqué, D., & Duarte, C. M. (2017). Temperature regulation of marine heterotrophic prokaryotes increases latitudinally as a breach between bottom-up and top-down controls. *Global Change Biology*, *23*(9), 3956–3964. https://doi.org/10.1111/gcb.13730

Mühlenbruch, M., Grossart, H. P., Eigemann, F., & Voss, M. (2018). Mini-review: Phytoplankton-derived polysaccharides in the marine environment and their interactions with heterotrophic bacteria. *Environmental Microbiology*, *20*(8), 2671–2685. https://doi.org/10.1111/1462-2920.14302

Mulholland, M. R. (2007). The fate of nitrogen fixed by diazotrophs in the ocean. *Biogeosciences*, *4*(1), 37–51. https://doi.org/10.5194/bg-4-37-2007

Mulholland, M. R., Glibert, P. M., Berg, G. M., Van Heukelem, L., Pantoja, S., & Lee, C. (1998). Extracellular amino acid oxidation by microplankton: A cross-ecosystem comparison. *Aquatic Microbial Ecology*, *15*(2), 141–152. https://doi.org/10.3354/ame015141

Mulholland, P. (2003). Large-Scale Patterns in Dissolved Organic Carbon Concentration, Flux, and Sources. In S. E. G. Findlay & R. L. B. T. A. E. Sinsabaugh (Eds.), *Aquatic Ecosystems* (pp. 139–159). Academic Press. https://doi.org/10.1016/b978-012256371-3/50007-x

Myklestad, S. M. (2005). Dissolved Organic Carbon from Phytoplankton. In P. J. Wangersky (Ed.), *Marine Chemistry* (pp. 111–148). Springer-Verlag. https://doi.org/10.1007/10683826_5

Nagata, T. (2000). "Picopellets" Produced by Phagotrophic Nanoflagellates: Role in the Material Cycling within Marine Environments. In N. Handa, E. Tanoue, & T. Hama (Eds.), *Dynamics and Characterization of Marine Organic Matter* (pp. 241–256). Springer Netherlands. https://doi.org/10.1007/978-94-017-1319-1_12

Osterholz, H., Niggemann, J., Giebel, H. A., Simon, M., & Dittmar, T. (2015). Inefficient microbial production of refractory dissolved organic matter in the ocean. *Nature Communications*, *6*(1), 7422. https://doi.org/10.1038/ncomms8422

Pakulski, J. D., & Benner, R. (1994). Abundance and distribution of carbohydrates in the ocean. *Limnology and Oceanography*, *39*(4), 930–940. https://doi.org/10.4319/lo.1994.39.4.0930

Palenik, B., & Henson, S. E. (1997). The use of amides and other organic nitrogen sources by the phytoplankton Emiliania huxleyi. *Limnology and Oceanography*, *42*(7), 1544–1551. https://doi.org/10.4319/lo.1997.42.7.1544

Palovaara, J., Akram, N., Baltar, F., Bunse, C., Forsberg, J., Pedrós-Alió, C., González, J. M., & Pinhassi, J. (2014). Stimulation of growth by proteorhodopsin phototro-

phy involves regulation of central metabolic pathways in marine planktonic bacteria. *Proceedings of the National Academy of Sciences of the United States of America*, *111*(35), E3650–E3658. https://doi.org/10.1073/pnas.1402617111

Pelve, E. A., Fontanez, K. M., & DeLong, E. F. (2017). Bacterial Succession on Sinking Particles in the Ocean's Interior. *Frontiers in Microbiology*, *8*, 2269. https://doi.org/10.3389/fmicb.2017.02269

Pomeroy, L. R., le Williams, P. J., Azam, F., & Hobbie, J. E. (2007). The microbial loop. *Oceanography*, *20*(SPL.ISS. 2), 28–33. https://doi.org/10.5670/oceanog.2007.45

Pomeroy, L. R., & Wiebe, W. J. (2001). Temperature and substrates as interactive limiting factors for marine heterotrophic bacteria. *Aquatic Microbial Ecology*, *23*(2), 187–204. https://doi.org/10.3354/ame023187

Poulain, P.-M., Kourafalou, V. H., & Cushman-Roisin, B. (2001). Northern Adriatic Sea. In B. Cushman-Roisin, M. Gačić, & P.-M. Poulain (Eds.), *Physical Oceanography of the Adriatic Sea* (pp. 143–165). Kluwer Academic Publishers. https://doi.org/10.1007/978-94-015-9819-4_5

Prgzelin, B. B., & Alldredge, A. L. (1983). Primary production of marine snow during and after an upwelling event. *Limnology and Oceanography*, *28*(6), 1156–1167. https://doi.org/10.4319/lo.1983.28.6.1156

Puddu, A., Zoppini, A., Fazi, S., Rosati, M., Amalfitano, S., & Magaletti, E. (2003). Bacterial uptake of DOM released from P-limited phytoplankton. *FEMS Microbiology Ecology*, *46*(3), 257–268. https://doi.org/10.1016/S0168-6496(03)00197-1

Puddu, A., Zoppini, A., & Pettine, M. (2000). Dissolved organic matter and microbial food web interactions in the marine environment: The case of the Adriatic Sea. *International Journal of Environment and Pollution*, *13*(1), 473–494. https://doi.org/10.1504/ijep.2000.002331

Raaijmakers, J. M., Paulitz, T. C., Steinberg, C., Alabouvette, C., & Moënne-Loccoz, Y. (2009). The rhizosphere: A playground and battlefield for soilborne pathogens and beneficial microorganisms. *Plant and Soil*, *321*(1-2), 341–361. https://doi.org/10.1007/s11104-008-9568-6

Rath, J., Wu, K. Y., Herndl, G. J., & DeLong, E. F. (1998). High phylogenetic diversity in a marine-snow-associated bacterial assemblage. *Aquatic Microbial Ecology*, *14*(3), 261–269. https://doi.org/10.3354/ame014261

Reinthaler, T., van Aken, H. M., & Herndl, G. J. (2010). Major contribution of autotrophy to microbial carbon cycling in the deep North Atlantic's interior. *Deep-Sea Research Part II: Topical Studies in Oceanography*, *57*(16), 1572–1580. https://doi.org/10.1016/j.dsr2.2010.02.023

Reintjes, G., Arnosti, C., Fuchs, B., & Amann, R. (2019). Selfish, sharing and scavenging bacteria in the Atlantic Ocean: A biogeographical study of bacterial substrate utilisation. *The ISME Journal*, *13*(5), 1119–1132. https://doi.org/10.1038/s41396-018-0326-3

Reintjes, G., Arnosti, C., Fuchs, B. M., & Amann, R. (2017). An alternative polysaccharide uptake mechanism of marine bacteria. *The ISME Journal*, *11*(7), 1640–1650. https://doi.org/10.1038/ismej.2017.26

Reintjes, G., Fuchs, B. M., Scharfe, M., Wiltshire, K. H., Amann, R., & Arnosti, C. (2020). Short-term changes in polysaccharide utilization mechanisms of marine bacte-

rioplankton during a spring phytoplankton bloom. *Environmental Microbiology*, *22*(5), 1884–1900. https://doi.org/10.1111/1462-2920.14971

Riedel, T., & Dittmar, T. (2014). A Method Detection Limit for the Analysis of Natural Organic Matter via Fourier Transform Ion Cyclotron Resonance Mass Spectrometry. *Analytical Chemistry*, *86*(16), 8376–8382. https://doi.org/10.1021/ac501946m

Rittenberg, S. C., & Hespell, R. B. (1975). Energy efficiency of intraperiplasmic growth of Bdellovibrio bacteriovorus. *Journal of Bacteriology*, *121*(3), 1158–1165. https://doi.org/10.1128/jb.121.3.1158-1165.1975

Rogers, A., Frinault, B., Barnes, D., Bindoff, N., Downie, R., Ducklow, H., Friedlaender, A., Hart, T., Hill, S., Hofmann, E., Linse, K., McMahon, C., Murphy, E., Pakhomov, E., Reygondeau, G., Staniland, I., Wolf-Gladrow, D., & Wright, R. (2020). Antarctic Futures: An Assessment of Climate-Driven Changes in Ecosystem Structure, Function, and Service Provisioning in the Southern Ocean. *Annual Review of Marine Science*, *12*(1), 87–120. https://doi.org/10.1146/annurev-marine-010419-011028

Ruby, E. G., McCabe, J. B., & Barke, J. I. (1985). Uptake of intact nucleoside monophosphates by Bdellovibrio bacteriovorus 109J. *Journal of Bacteriology*, *163*(3), 1087–1094. https://doi.org/10.1128/jb.163.3.1087-1094.1985

Saba, G. K., Steinberg, D. K., & Bronk, D. A. (2011). The relative importance of sloppy feeding, excretion, and fecal pellet leaching in the release of dissolved carbon and nitrogen by Acartia tonsa copepods. *Journal of Experimental Marine Biology and Ecology*, *404*(1-2), 47–56. https://doi.org/10.1016/j.jembe.2011.04.013

Salazar, G., Cornejo-Castillo, F. M., Borrull, E., Díez-Vives, C., Lara, E., Vaqué, D., Arrieta, J. M., Duarte, C. M., Gasol, J. M., & Acinas, S. G. (2015). Particle-association lifestyle is a phylogenetically conserved trait in bathypelagic prokaryotes. *Molecular Ecology*, *24*(22), 5692–5706. https://doi.org/10.1111/mec.13419

Sañudo-Wilhelmy, S. A., Cutter, L. S., Durazo, R., Smail, E. A., Gómez-Consarnau, L., Webb, E. A., Prokopenko, M. G., Berelson, W. M., & Karl, D. M. (2012). Multiple B-vitamin depletion in large areas of the. *Proceedings of the National Academy of Sciences of the United States of America*, *109*(35), 14041–14045. https://doi.org/10.1073/pnas.1208755109

Satinsky, B. M., Crump, B. C., Smith, C. B., Sharma, S., Zielinski, B. L., Doherty, M., Meng, J., Sun, S., Medeiros, P. M., Paul, J. H., Coles, V. J., Yager, P. L., & Moran, M. A. (2014). Microspatial gene expression patterns in the Amazon River Plume. *Proceedings of the National Academy of Sciences of the United States of America*, *111*(30), 11085–11090. https://doi.org/10.1073/pnas.1402782111

Seymour, J. R., Amin, S. A., Raina, J. B., & Stocker, R. (2017). Zooming in on the phycosphere: The ecological interface for phytoplankton-bacteria relationships. *Nature Microbiology*, *2*(May). https://doi.org/10.1038/nmicrobiol.2017.65

Seymour, J. R., & Stocker, R. (2018). The ocean's microscale: A microbe's view of the sea. In J. M. Gasol & D. L. Kirchman (Eds.), *Microbial ecology of the oceans* (Third, pp. 289–344). John Wiley & Sons, Inc.

Sheridan, C. C., Steinberg, D. K., & Kling, G. W. (2002). The microbial and metazoan community associated with colonies of Trichodesmium spp.: A quantitative

survey. *Journal of Plankton Research*, *24*(9), 913–922. https://doi.org/10.1093/plankt/24.9.913

Shi, Y., Tyson, G. W., Eppley, J. M., & Delong, E. F. (2011). Integrated metatranscriptomic and metagenomic analyses of stratified microbial assemblages in the open ocean. *ISME Journal*, *5*(6), 999–1013. https://doi.org/10.1038/ismej.2010.189

Simon, M., Grossart, H. P., Schweitzer, B., & Ploug, H. (2002). Microbial ecology of organic aggregates in aquatic ecosystems. *Aquatic Microbial Ecology*, *28*(2), 175–211. https://doi.org/10.3354/ame028175

Sipler, R. E., & Bronk, D. A. (2015). Dynamics of Dissolved Organic Nitrogen. *Biogeochemistry of Marine Dissolved Organic Matter: Second Edition* (pp. 127–232). Elsevier. https://doi.org/10.1016/B978-0-12-405940-5.00004-2

Smetacek, V., & Nicol, S. (2005). Polar ocean ecosystems in a changing world. *Nature*, *437*(7057), 362–368. https://doi.org/10.1038/nature04161

Smith, D. C., Simon, M., Alldredge, A. L., & Azam, F. (1992). Intense hydrolytic enzyme activity on marine aggregates and implications for rapid particle dissolution. *Nature*, *359*(6391), 139–142. https://doi.org/10.1038/359139a0

Smith, D. C., Steward, G. F., Long, R. A., & Azam, F. (1995). Bacterial mediation of carbon fluxes during a diatom bloom in a mesocosm. *Deep-Sea Research Part II*, *42*(1), 75–97. https://doi.org/10.1016/0967-0645(95)00005-B

Smith, W. O., Ainley, D. G., Arrigo, K. R., & Dinniman, M. S. (2014). The Oceanography and Ecology of the Ross Sea. *Annual Review of Marine Science*, *6*(1), 469–487. https://doi.org/10.1146/annurev-marine-010213-135114

Smith, W. O., Sedwick, P. N., Arrigo, K. R., Ainley, D. G., & Orsi, A. H. (2012). The Ross Sea in a sea of change. *Oceanography*, *25*(3), 90–103. https://doi.org/10.5670/oceanog.2012.80

Steen, A. D., Ziervogel, K., Ghobrial, S., & Arnosti, C. (2012). Functional variation among polysaccharide-hydrolyzing microbial communities in the Gulf of Mexico. *Marine Chemistry*, *138-139*, 13–20. https://doi.org/10.1016/j.marchem.2012.06.001

Stocker, R. (2012). Marine microbes see a sea of gradients. *Science*, *338*(6107), 628–633. https://doi.org/10.1126/science.1208929

Stocker, R., Seymour, J. R., Samadani, A., Hunt, D. E., & Polz, M. F. (2008). Rapid chemotactic response enables marine bacteria to exploit ephemeral microscale nutrient patches. *Proceedings of the National Academy of Sciences of the United States of America*, *105*(11), 4209–4214. https://doi.org/10.1073/pnas.0709765105

Strom, S. L. (2008). Microbial ecology of ocean biogeochemistry: A community perspective. *Science*, *320*(5879), 1043–1045. https://doi.org/10.1126/science.1153527

Strzepek, R. F., Maldonado, M. T., Hunter, K. A., Frew, R. D., & Boyd, P. W. (2011). Adaptive strategies by Southern Ocean phytoplankton to lessen iron limitation: Uptake of organically complexed iron and reduced cellular iron requirements. *Limnology and Oceanography*, *56*(6), 1983–2002. https://doi.org/10.4319/lo.2011.56.6.1983

Sunagawa, S., Coelho, L. P., Chaffron, S., Kultima, J. R., Labadie, K., Salazar, G., Djahanschiri, B., Zeller, G., Mende, D. R., Alberti, A., Cornejo-Castillo, F. M., Costea, P. I.,

Cruaud, C., D'Ovidio, F., Engelen, S., Ferrera, I., Gasol, J. M., Guidi, L., Hildebrand, F., … Bork, P. (2015). Structure and function of the global ocean microbiome. *Science*, *348*(6237), 1261359. https://doi.org/10.1126/science.1261359

Sundquist, E. T., & Visser, K. (2003). The Geologic History of the Carbon Cycle. In H. D. Holland & K. K. B. T. T. o. G. Turekian (Eds.), *Treatise on Geochemistry* (pp. 425–472). Pergamon. https://doi.org/10.1016/B0-08-043751-6/08133-0

Suttle, C. A. (2005). Viruses in the sea. *Nature*, *437*(7057), 356–361. https://doi.org/10.1038/nature04160

Suttle, C. A. (2007). Marine viruses - Major players in the global ecosystem. *Nature Reviews Microbiology*, *5*(10), 801–812. https://doi.org/10.1038/nrmicro1750

Tang, K. W., Gladyshev, M. I., Dubovskaya, O. P., Kirillin, G., & Grossart, H. P. (2014). Zooplankton carcasses and non-predatory mortality in freshwater and inland sea environments. *Journal of Plankton Research*, *36*(3), 597–612. https://doi.org/10.1093/plankt/fbu014

Teeling, H., Fuchs, B. M., Becher, D., Klockow, C., Gardebrecht, A., Bennke, C. M., Kassabgy, M., Huang, S., Mann, A. J., Waldmann, J., Weber, M., Klindworth, A., Otto, A., Lange, J., Bernhardt, J., Reinsch, C., Hecker, M., Peplies, J., Bockelmann, F. D., … Amann, R. (2012). Substrate-controlled succession of marine bacterioplankton populations induced by a phytoplankton bloom. *Science*, *336*(6081), 608–611. https://doi.org/10.1126/science.1218344

Teeling, H., Fuchs, B. M., Bennke, C. M., Krüger, K., Chafee, M., Kappelmann, L., Reintjes, G., Waldmann, J., Quast, C., Glöckner, F. O., Lucas, J., Wichels, A., Gerdts, G., Wiltshire, K. H., & Amann, R. I. (2016). Recurring patterns in bacterioplankton dynamics during coastal spring algae blooms. *eLife*, *5*(APRIL2016), 1–31. https://doi.org/10.7554/eLife.11888

Thor, P., Dam, H. G., & Rogers, D. R. (2003). Fate of organic carbon released from decomposing copepod fecal pellets in relation to bacterial production and ectoenzymatic activity. *Aquatic Microbial Ecology*, *33*(3), 279–288. https://doi.org/10.3354/ame033279

Thornton, D. C. (2014). Dissolved organic matter (DOM) release by phytoplankton in the contemporary and future ocean. *European Journal of Phycology*, *49*(1), 20–46. https://doi.org/10.1080/09670262.2013.875596

Turner, J., Comiso, J. C., Marshall, G. J., Lachlan-Cope, T. A., Bracegirdle, T., Maksym, T., Meredith, M. P., Wang, Z., & Orr, A. (2009). Non-annular atmospheric circulation change induced by stratospheric ozone depletion and its role in the recent increase of Antarctic sea ice extent. *Geophysical Research Letters*, *36*(8). https://doi.org/10.1029/2009GL037524

van Dongen-Vogels, V., Seymour, J. R., Middleton, J. F., Mitchell, J. G., & Seuront, L. (2012). Shifts in picophytoplankton community structure influenced by changing upwelling conditions. *Estuarine, Coastal and Shelf Science*, *109*, 81–90. https://doi.org/10.1016/j.ecss.2012.05.026

Verdugo, P. (2012). Marine microgels. *Annual Review of Marine Science*, *4*(1), 375–400. https://doi.org/10.1146/annurev-marine-120709-142759

Verdugo, P., Alldredge, A. L., Azam, F., Kirchman, D. L., Passow, U., & Santschi, P. H. (2004). The oceanic gel phase: A bridge in the DOM-POM continuum. *Marine Chemistry*, *92*(1-4), 67–85. https://doi.org/10.1016/j.marchem.2004.06.017

Vetter, Y. A., & Deming, J. W. (1999). Growth rates of marine bacterial isolates on particulate organic substrates solubilized by freely released extracellular enzymes. *Microbial Ecology*, *37*(2), 86–94. https://doi.org/10.1007/s002489900133

Vetter, Y. A., Deming, J. W., Jumars, P. A., & Krieger-Brockett, B. B. (1998). A predictive model of bacterial foraging by means of freely released extracellular enzymes. *Microbial Ecology*, *36*(1), 75–92. https://doi.org/10.1007/s002489900095

Walsh, D. A., Zaikova, E., Howes, C. G., Song, Y. C., Wright, J. J., Tringe, S. G., Tortell, P. D., & Hallam, S. J. (2009). Metagenome of a versatile chemolithoautotroph from expanding oceanic dead zones. *Science*, *326*(5952), 578–582. https://doi.org/10.1126/science.1175309

Wanner, B. L. (1993). Gene regulation by phosphate in enteric bacteria. *Journal of Cellular Biochemistry*, *51*(1), 47–54. https://doi.org/10.1002/jcb.240510110

Weinbauer, M. G., Chen, F., & Wilhelm, S. W. (2011). Virus-mediated redistribution and partitioning of carbon in the global oceans. In N. Jiao, F. Azam, & S. Sanders (Eds.), *Microbial Carbon Pump in the Ocean.* (pp. 54–56). Science/AAAS.

Weiss, M. S., Abele, U., Weckesser, J., Welte, W., Schiltz, E., & Schulz, G. E. (1991). Molecular architecture and electrostatic properties of a bacterial porin. *Science*, *254*(5038), 1627–1630. https://doi.org/10.1126/science.1721242

White, A. E., Karl, D. M., Björkman, K. M., Beversdorf, L. J., & Leteliera, R. M. (2010). Production of organic matter by Trichodesmium IMS101 as a function of phosphorus source. *Limnology and Oceanography*, *55*(4), 1755–1767. https://doi.org/10.4319/lo.2010.55.4.1755

White, A., Watkins-Brandt, K., Engle, M., Burkhardt, B., & Paytan, A. (2012). Characterization of the rate and temperature sensitivities of bacterial remineralization of dissolved organic phosphorus compounds by natural populations. *Frontiers in Microbiology*, *3*, 276. https://doi.org/10.3389/fmicb.2012.00276

Whitman, W. B., Coleman, D. C., & Wiebe, W. J. (1998). Prokaryotes: The unseen majority. *Proceedings of the National Academy of Sciences of the United States of America*, *95*(12), 6578–6583. https://doi.org/10.1073/pnas.95.12.6578

Wiebe, W. J., Sheldon, W. M., & Pomeroy, L. R. (1993). Evidence for an enhanced substrate requirement by marine mesophilic bacterial isolates at minimal growth temperatures. *Microbial Ecology*, *25*(2), 151–159. https://doi.org/10.1007/BF00177192

Wietz, M., Gram, L., Jørgensen, B., & Schramm, A. (2010). Latitudinal patterns in the abundance of major marine bacterioplankton groups. *Aquatic Microbial Ecology*, *61*(2), 179–189. https://doi.org/10.3354/ame01443

Wilhelm, S. W., & Suttle, C. A. (1999). Viruses and nutrient cycles in the sea. *BioScience*, *49*(10), 781–788. https://doi.org/10.2307/1313569

Zark, M., Christoffers, J., & Dittmar, T. (2017). Molecular properties of deep-sea dissolved organic matter are predictable by the central limit theorem: Evidence from tandem FT-ICR-MS. *Marine Chemistry*, *191*, 9–15. https://doi.org/10.1016/j.marchem.2017.02.005

Zhang, C. L., Xie, W., Martin-Cuadrado, A.-B., & Rodriguez-Valera, F. (2015). Marine Group II Archaea, potentially important players in the global ocean carbon cycle. *Frontiers in Microbiology*, *6*, 1108. https://doi.org/10.3389/fmicb.2015.01108

Zinger, L., Amaral-Zettler, L. A., Fuhrman, J. A., Horner-Devine, M. C., Huse, S. M., Welch, D. B., Martiny, J. B., Sogin, M., Boetius, A., & Ramette, A. (2011). Global patterns of bacterial beta-diversity in seafloor and seawater ecosystems. *PLoS ONE*, *6*(9), e24570. https://doi.org/10.1371/journal.pone.0024570

Zoccarato, L., Pallavicini, A., Cerino, F., Fonda Umani, S., & Celussi, M. (2016). Water mass dynamics shape Ross Sea protist communities in mesopelagic and bathypelagic layers. *Progress in Oceanography*, *149*, 16–26. https://doi.org/10.1016/j.pocean.2016.10.003

2

Long-term patterns and drivers of microbial organic matter utilization in the northernmost basin of the Mediterranean Sea

This Chapter is adapted from: Manna, V., De Vittor, C., Giani, M., Del Negro, P., Celussi, M., 2021. Long-term patterns and drivers of microbial organic matter utilization in the northernmost basin of the Mediterranean Sea. Marine Environmental Research, 164, 105245. https://doi.org/10.1016/j.marenvres.2020.105245

2.1. Introduction

By producing, utilizing, and processing one of the largest organic matter (OM) pools on the Earth (Hansell et al., 2009), marine heterotrophic prokaryotes represent the gears spinning beneath the oceans' biogeochemical engine. With half of the global primary production occurring in the ocean (Field et al., 1998), photosynthetic microorganisms represent one of the major OM sources in marine environments. While most of the phytoplankton-derived OM ends up in dissolved form (DOM, Wagner et al., 2020), particulate OM (POM) may derive either from DOM aggregation or from plankton itself (reviewed by Kharbush et al., 2020). Prokaryotes may access both DOM and POM either by direct uptake of small enough molecules (<600 Da, Weiss et al., 1991) or by enzymatic breakdown of high molecular weight OM (Chróst, 1992). The uptake of these low molecular weight organic molecules and their subsequent incorporation into microbial biomass converts DOM into POM, which is then suitable for the consumption by higher trophic levels (Cole and Pace, 1995). Therefore, measuring the heterotrophic carbon production (HCP) under different conditions provides an estimation of both prokaryotic growth and of the rates at which OM is moved from one pool to another (Ducklow, 2000).

Organic matter in the marine environment exists in a wide array of physical (e.g., size fraction, Verdugo et al., 2004) and chemical (e.g., number of organic compounds, Riedel and Dittmar, 2014) forms. This diversity is enhanced in coastal areas, where the proximity to the land and the reduced water column depth determine soil- and seabed-derived OM inputs. Moreover, a collateral, freshwater-mediated, flux of inorganic nutrients may fuel OM production by phytoplankton, making coastal zones hot spots of microbial-mediated OM processing (Celussi et al., 2019). Marine heterotrophic prokaryotes rely, therefore, on a plethora of different OM arrangements to fuel their growth. Like many other features of marine plankton, metabolic rates are controlled by environmental drivers such as temperature, pH, salinity, and organic matter features (Arnosti, 2011; Morán et al., 2017; Pomeroy and Wiebe, 2001). These factors are inherently spatially and temporally variable in coastal areas, posing therefore a challenge to the disentanglement of their role in microbial OM processing rates.

The intrinsic variability of coastal areas reflects the internal biological forcing as well as the intense terrestrial, offshore, and atmospheric forcing affecting these boundary zones. Therefore, inadequate temporal and spatial sampling strategies may over- or underestimate the magnitude and the effects of extreme events and even miss them (Ribera d'Alcalà et al., 2004). Multiyear fixed observations are the key tool for carrying out a reliable estimation of plankton dynamics over time, as their analysis allows to distinguish recurrent patterns from exceptional events (Fuhrman et al., 2015) as time represents the ecosystem's path towards its actual state. Therefore, analysing the ecological processes from a temporal perspective allows to quantify, characterize, and compare the fluxes of energy, matter and information underlying the observed changes (Ribera d'Alcalà, 2019).

Here we used a 21-year-long (1999-2019) biogeochemical time series from the Gulf of Trieste (northern Adriatic Sea). We analysed monthly measurements of HCP, Chlorophyll *a*, particulate and dissolved organic carbon, as well as the abundance of

heterotrophic prokaryotes and *Synechococcus.* Long-term trends were extracted from the time series and clustered with a time-constrained algorithm, to identify coherent periods among the selected variables. The non-parametric, machine learning, random forest approach, was used to investigate the relative importance and the partial effect of environmental drivers and OM sources on the observed HCP rates over time. The primary goal of the time series analysis was to identify and describe HCP long-term dynamics, underlining microbial-mediated OM processing. Furthermore, we aimed to assess the importance of OM sources, as well as key environmental drivers, in determining HCP rates across the temporal spanning of the series.

2.2. Materials and methods

2.2.1. Study area and data

The The Gulf of Trieste is a land-locked, river-influenced, shallow (<25 m) embayment occupying the northernmost part of the Adriatic Sea. The main freshwater runoff comes from the Isonzo river outflow, in the north-western part of the Gulf, while freshwater sources along its eastern boundary are of torrential nature (Comici and Bussani, 2007). The river runoff in the area is widely variable, driving broad seasonal and interannual salinity fluctuations with values spanning between 28.5 (Kralj et al., 2019) and >38.4 (Raicich et al., 2013). Seawater temperature shows a broad seasonal variability, from winter minima below 4.3°C (Raicich et al., 2013) and summer maxima up to 28°C (Malačič et al., 2006). The area is under the influence of a strong wind regime, characterized by the alternance of south- and north-easterly winds (i.e., Scirocco and Bora, Stravisi, 1977). The strong short-term variability of this system is dotted by extreme events like heat waves, salinity anomalies and cold outbreaks which affect the functioning of the local pelagic ecosystem (Celussi and Del Negro, 2012; Lipizer et al., 2012; Mihanović et al., 2013). Despite its limited extension, the Gulf of Trieste experiences heavy environmental fluctuations, which drive the significant biological variability observed at different temporal resolutions. As the main source of organic and inorganic nutrients in the area is represented by freshwater inputs (Cozzi et al., 2020), their broad temporal variability induces changes in OM standing stocks and production/degradation rates. Previous studies on dissolved OM have highlighted the extreme temporal variability of this pool, showing that the concentration and bioavailability of the DOC pool changes greatly even on a daily scale (De Vittor et al., 2009; De Vittor et al., 2008). The extreme variability of the OM pool drives, together with environmental factors, changes in bacterioplankton community composition and metabolic rates over interannual, seasonal and even sub-daily time scales (Paoli et al., 2006; Tinta et al., 2015).

The dataset analysed in the present study consists of monthly records of HCP rates, heterotrophic prokaryotes (HP) and *Synechococcus* (SYN) abundance and biogeochemical variables including temperature, salinity, particulate and dissolved organic carbon (POC and DOC, respectively), particulate nitrogen (PN), and Chlorophyll *a* (Chl *a*). Samples were collected monthly, from January 1999 to December 2019 at 4 depths (~0.5, 5, 10 and 15 m) at the station C1 (45°42'2" N, 13°42'36" E), in the north-eastern part of the Gulf of Trieste, 200 m offshore. From 2002 to 2005, samples were

collected twice per month. Since 2006, C1 station is included in the Italian Long-Term Ecological Research (LTER) network, as part of the northern Adriatic LTER site. Details on sampling procedures are provided in Celussi and Del Negro, 2012.

2.2.2. Heterotrophic carbon production

HCP rates with the method of $_3$H-leucine (Leu) incorporation (Kirchman et al., 1985). Triplicate 1.7 mL subsamples and one control killed with 5% trichloroacetic acid – TCA – final concentration (f.c.) were amended with 20 nM radiotracer and incubated at *in situ* temperature in the dark for 1 h. The extraction of 3H-labelled proteins was carried out following the microcentrifugation method (Smith, 1992). After the addition of 1 mL of scintillation cocktail (Ultima Gold™ MV; Packard), activity was determined by a TRI-CARB 2900 TR Liquid Scintillation Analyzer. Carbon biomass production was then estimated using the conversion factor of 3.1 kg C mol^{-1} Leu incorporated, assuming a two-fold isotope dilution (Simon and Azam, 1989).

2.2.3. Heterotrophic prokaryiotes and *Synechococcus* abundance

HP and SYN abundance was estimated by epifluorescence microscopy following the protocol of Porter and Feig, 1980. Triplicate samples aliquots (50 mL) were fixed with dolomite-buffered formalin (prefiltered through 0.2 µm PES syringe filters, 2% f.c.) and filtered onto 0.2 µm black polycarbonate filters (Whatman) after being stained with 4'6 diamidino-2-phenylindole (DAPI, Sigma-Aldrich) at 1 µg mL^{-1} (f. c.) for 15 min in the dark. The filters were then mounted between layers of immersion oil (Type A, Cargille) and stored at −20°C until analysis. Samples were counted at 1000× magnification (Olympus BX60F5) under a UV (BP 330–385 nm, BA 420 nm) and a green (BP 480–550 nm, BA 590 nm) filter set for HP and SYN, respectively. A minimum of 300 cells were counted for each filter in at least 20 randomly selected fields.

2.2.4. Biogeochemical variables

Temperature and salinity were measured by means of multiparametric probes, either Idronaut Ocean Seven (models 401 and 316) or SBE 19plus SEACAT, calibrated every 6–12 months.

Chl *a* concentration was determined spectrofluorometrically according to Lorenzen and Jeffrey, 1980. Samples were filtered onto glass fibre filters (Whatman GF/F) and stored at -20/-80°C. Chl *a* extraction was carried out from the homogenate filter at 4 °C overnight in the dark, with 90% acetone. Chl *a* fluorescence was measured with a Perkin Elmer LS50B or Jasco FP-6500 spectrofluorometers at 450 nm excitation and 665 nm emission wavelengths. Calibration was made with pure Chl *a* from spinach (Sigma Aldrich). The coefficient of variation (CV) among triplicates was lower than 5%. Data quality was controlled by participating in the QUASIMEME intercalibration programme.

POC and PN were determined by high-temperature oxidation using an elemental analyser CHNS 2400 Perkin Elmer Elemental or (CHNO)-S Costech mod. ECS 4010 applying the methods performed by Pella and Colombo, 1973 and Sharp, 1974. Water samples (0.5 L) were filtered on 25-mm Whatman GF/F pre-combusted filters and

stored at −20°C. Prior to analysis, the filter was treated with HCl 1N to remove the carbonate, oven-dried at 60°C for 1 h and inserted in a tin capsule. Known amounts of standard acetanilide (C_8H_9NO—Carlo Erba; assay ≥99.5%) were used to calibrate the instrument. The relative standard deviations for three replicates of internal quality control sample replicates were lower than 10%. The accuracy of the method is verified periodically against the certified marine sediment reference material PACS-2 (National Research Council Canada).

Samples for DOC analyses were filtered on board, through precombusted (4 h at 480°C) and acidified (HCl 1N) Whatman GF/F glass fibre filters and stored at -20°C until analysis. Filtration was performed using a glass syringe and a filter holder in order to prevent atmospheric contamination. DOC was determined via HTCO method (Sugimura and Suzuki, 1988) using a Shimadzu TOC 5000A or a Shimadzu TOC VCSH analyser with a quartz combustion column filled with 1.2% Pt on silica pillows. For the analysis, 150 µL of acidified (pH <2) sample were injected into the instrument port. Carbon concentration was calculated from a 5-point standardisation curve carried out every day using potassium hydrogen phthalate as reference. Each concentration value was determined from a minimum of three injections, with a CV lower than 2%. Replicates of more samples have shown coefficients of variation comprised between 1.5 and 4%. The accuracy of the results is checked by periodic analysis of certified reference material (CRM-University of Miami) and is guaranteed by the excellent results obtained in the biannual participation to the international intercalibration exercises (Quasimeme Laboratory Performance Study).

2.2.5. Data analysis

Prior to analysis, data were quality checked, inspecting for the presence of outliers and anomalous data points. As data were collected twice per month between 2002 and 2005, observations were monthly averaged to obtain a single datapoint. Then, missing data (no more than 5 consecutive observations) were interpolated with a weighted moving average. We used the function *na_seadec* of the R package *imputeTs* (Moritz and Bartz-Beielstein, 2017) to remove the seasonal component from each univariate time series, through a 12-month smoothing window, prior to missing data imputation. We used this workflow to avoid interpolation biases due to the seasonal variability. After the imputation of missing observation, a dataset was created using depth integrated (trapezoid rule) HCP rates, organic matter sources (i.e., Chl *a*, POC and DOC) and HP and SYN abundances. From each time series, the long-term trend and the seasonal components were extracted with the locally estimated scatterplot smoothing (LOESS, *st*l package), using 12 observations as target frequency for seasonal extraction. LOESS smoothing fits simple models to localized subsets of the data to build up a function that describes the deterministic part of the variation in the data (Cleveland et al., 1990). Trends of surface salinity and temperature anomalies, calculated as the deviation from the time series mean, were extracted using a LOESS fit.

To identify patterns in the examined long-term trends, a time-constrained clustering (Legendre et al., 1985) was used. By chronologically constraining a clustering algorithm is it possible to identify coherent periods and major breakpoints in a time

series (Romagnan et al., 2015). The time constrained clustering was implemented with the function *chclust* from the package *rioja* (Juggins, 2020). Long-term trends were clustered using the CONISS clustering algorithm (Grimm, 1987), a variant of the Ward's minimum variance clustering. Microbial time series (i.e., HCP, HP and SYN) were analysed using from Bray-Curtis distance metric, suitable to reveal functional patterns over time. To investigate their role as structuring ecosystem drivers, OM time series (Chl *a*, DOC and POC) were analysed using the Euclidean metric. Clusters of coherent time periods were identified using the function *cutreeDynamic* (package *dynamicTreeCut*, Langfelder et al., 2007). This method allows to identify clusters based on their shape rather than on a fixed cut height, aiding the detection of nested clusters (Langfelder et al., 2007). Data were presented as annotated dendrograms and time series plots, created and visualized with the package *dendextend* (Galili, 2015) and *ggplot2* (Wickham, 2016), respectively.

We used Random Forest (RF) to test for the relative importance of selected features in determining HCP rates in our dataset. RF is a non-parametric, robust, machine learning tool, established on ensembles of regression (or classification) trees (Breiman, 2001). In each regression tree composing the forest, a subset of the data is randomly selected and is iteratively partitioned based on the strongest associated predictor. At each node (i.e., branch split in the tree), a random subset draw form the predictors pool is considered for partitioning. The bootstrapping of both data and explanatory variables minimizes problems associated with the presence of data outliers or artefacts, and with variable collinearity, also avoiding data overfitting (Pomati et al., 2020). This mechanism allows to extrapolate the importance of each feature, assessed by permuting a predictor across all the generated trees, and quantifying the changes in model's error rate. Permutation of the most important variables leads to a greater increase in model's error rates. By randomly selecting a subset of data at each iteration, the RF leaves an out-of-bag portion of the data on which the model performances are internally evaluated. This removes the need for the canonical train/test dataset split, increasing the number of observations available for model running. See also Thomas et al., 2018 for a more extensive explanation of RF. For our RF analysis we used the package *randomForest* (Liaw and Wiener, 2002), which implements the RF algorithm as formulated by Breiman, 2001. The forest was composed by 1000 trees and the number of random predictor variables selected at each split was set equal to 3. Model outputs were analysed using the package *DALEX* (Biecek, 2018). All the aforementioned data analysis workflow has been carried out with the R software v. 3.6.1 (R Core Team, 2019).

2.3. Results

2.3.1. Time series features

Descriptive statistics of the analysed time series is reported in Appendix Table A.1. Three coherent time periods were identified in the HCP time series by the time-constrained clustering (Fig. 2.1 a). Their underlying long-term structure consisted of two major cycles, spanning between 1999 and 2007 and between 2012 and 2019 (red and green clusters in Fig. 2.1 a, respectively). The cycles peaks (2005 and 2007 for the first cycle, 2014 for the second one, Fig. 2.1 a) were separated by a U-shaped

trendline (2008-2011, Fig. 2.1 a), which made up the third coherent time slot (blue cluster in Fig. 2.1 a). Given the observed pattern in HCP time series, we analysed Chl *a*, DOC and POC long-term trends to link the observed HCP dynamics with the onesunderlying major sources of OM at the study area. Remarkably, we identified

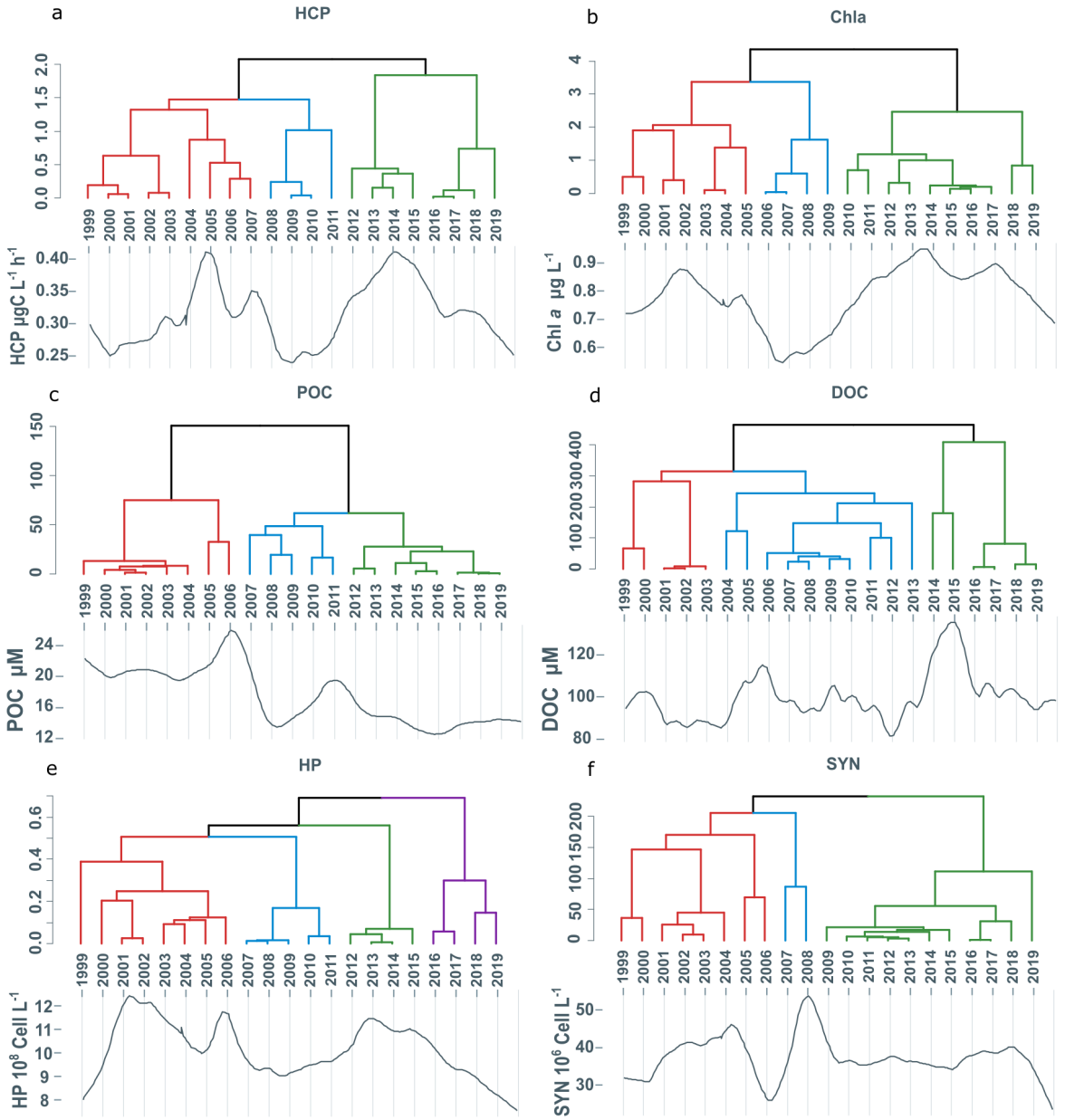

Figure 2.1: Time-constrained clustering of long-term trends extracted from the microbial and organic matter time series. The trends were extracted using the locally estimates scatterplot smoothing (LOESS). a) HCP - heterotrophic carbon production; b) Chl *a* - Chlorophyll *a* concentration; c) POC - Particulate organic carbon concentration; d) DOC - Dissolved organic carbon concentration; e) HP - Heterotrophic prokaryotes abundance; f) SYN – *Synechococcus* abundance. Units of measure are indicated on the corresponding panels. Note that Y-axes are differently scaled. Data were clustered in a time-constrained fashion using the CONISS algorithm (see Section 2.2.5). Cluster identified as different by the *cutreeDynamic* function (*dynamicTreeCut* package, see Section 2.2.5) are color-coded.

similar tripartite long-term structures (Fig. 2.1 b, c, and d). However, the break dates

defining the three periods showed some differences among the analysed variables.

The observed Chl *a* trend showed a similar long-term structure, with two major cycles connected by a period of trend minima (Fig. 2.1 b). The first cycle was shorter when compared to the HCP one, spanning from 1999 to 2005 (red cluster in Fig. 2.1 b). In the Chl *a* time series, the transition period occurred earlier (2006-2009, blue cluster in Fig. 2.1 b) although developing over the same time interval (~4 years). This led to a prolonged second cycle, developing over ~10 years (2010-2019, green cluster in Fig. 2.1 b). While sharing the same three-period clustering structure of HCP and Chl *a*, the latent long-term dynamic of POC was different (Fig. 2.1 c). Indeed, the long-term trend highlighted a less cyclical structure (Fig. *1* c), suggesting the existence of two different regimes (1999-2006 and 2012-2019, red and green clusters in Fig. 2.1 c, respectively). The first period was characterized by consistently higher POC values compared to the second one (Fig. 2.1 c). The two regimes were characterized by a sharp transition, spanning from 2007 to 2011 (blue cluster in Fig. 2.1 c). Time-constrained clustering analysis of DOC long-term trend (Fig. 2.1 d) revealed the absence of the cyclical structure observed for the other OM sources (Fig. 2.1 b, c). Indeed, the latent long-term structure of DOC time series highlighted the succession of three regimes, with an overall increasing trend over time. The length of the identified periods was notably uneven (Fig. 2.1 d). The first period was the shortest, with a span of ~5 years, followed by the longest middle time slot among the analysed time series, lasting about 10 years. The third period, identified between 2014 and 2019, was characterized by a remarkable peak between 2014 and 2015. In Fig. 2.1 d, the three periods are shown as red, blue, and green clusters, respectively.

The long-term dynamics of HCP, Chl *a*, and POC time series shared a similar, three period- underlying structure (Fig. 2.1 a-d). To explore how the "living" microbial compartment is affected and affects these dynamics, HP and SYN time series underwent the same analysis pipeline (Fig. 2.1 e-f). The long-term trend of HP time series showed a latent two cycles structure like that observed for the HCP series (Fig. 2.1 e and a, respectively). As seen in HCP time series, the first cycle (red cluster in Fig. 2.1 e) included a primary and a secondary peak, which in the HP time series occurred earlier in the series (2001-2002 and 2006, respectively, Fig. 2.1 e). The two cyclical structures were connected by a U-shaped transition period (blue cluster in Fig. 2.1 e), although the decrease in the trend component was milder than those observed for the other series (Fig. 2.1). Notably, the HP time series was the only one in which an additional coherent period was found by the clustering algorithm. This effectively broke the second cycle in two different parts: a peaking slot, between 2012 and 2015 (green cluster, Fig. 2.1 e) and a decreasing slot (2016-2019, purple cluster in Fig. 2.1 e). In the SYN time series, the first cluster identified a cyclic structure lasting from 1999 to 2006 (red cluster in Fig. 2.1 f), matching the first period identified for HP, HCP and POC (Fig. 2.1 e, a and c, respectively). The latest part of the series (green cluster in Fig. 2.1 f) did not show a cyclic pattern being instead characterized by a stable, almost linear, long-term trend, decreasing between 2018 and 2019 (Fig. 2.1 f). The transition period between the two long-term structures was the shortest among the investigated time series (2007-2008, blue cluster in Fig. 2.1 f). Noteworthy, the middle period in the SYN series was the only one characterized by a strongly increasing trend, peaking in 2008

(Fig. 2.1 f).

Noteworthy, the dynamic long-term structure characterising the analysed time series was reflected in their seasonal component. Indeed, except for DOC, all the time series showed a changing seasonal figure over time (Fig. 2.2). Overall, seasonal figures were stable over prolonged time periods at the beginning and at the end of the time series (Fig. 2.2), showing alternate states progressing toward the successive shape in the middle years of the series (i.e., the years centred around 2010, Fig. 2.2). This structure matched the one described for the long-term trends, identifying the middle period (the blue clusters in Fig. 2.1) as a transition phase between two regimes. HCP seasonal figure progressed from a marked July seasonal peak to a diffuse summer plateau, lasting from June to September (Fig. 2.2 a). Also, the winter peak progressively disappeared with time (Fig. 2.2 a). A similar result was highlighted by the Chl *a* seasonal plot (Fig. 2.2 b), showing the development of a seasonal minimum between February and March from 2007-2008 on. A forward shift in the seasonal maximum, from April to May, was evident from 2010 on (Fig. 2.2 b). This shift was coupled with an increased seasonal amplitude (i.e., the difference between maximum and minimum value). Moreover, while a progression preceded and followed the seasonal peak in the earlier part of the series, the May peak was reached with and followed by a steeper slope (Fig. 2.2 b). POC seasonality showed a neat change over the time-period considered. The seasonal peak localized between August and September in the early years of the series gradually shifted to May from 2007-2008 on (Fig. 2.2 c). As for Chl *a*, the seasonal amplitude increased during this shift and a similar winter seasonality changes was observed (Fig. 2.2 c). Remarkably, DOC seasonal figure did not show any changes over the length of the series, keeping the summer maxima-winter minima dynamic unaltered (Fig. 2.2 d). In the early years of the time series, HP and SYN were characterized by a unique and well-defined seasonal peak in September (Fig. 2.2 e-f). Over the years, both peaks shifted in time. The HP September peak gradually lost its importance until 2010, in favour of a new autumnal peak between October and November (Fig. 2.2 e). The *Synechococcus* peak was instead backward shifted, becoming a summer plateau lasting between June and August (Fig. 2.2 f). While the change in HP seasonal figure developed gradually year after year, SYN seasonality changed abruptly, over the course of just 4 years (Fig. 2.2 e-f).

To explore the role of physical variables in determining the observed long-term features in biological time series, we analysed surface temperature and salinity anomalies. On a yearly basis, temperature showed a rather flat linear trend, with few deviations from the time series mean (Fig. 2.3 a). The years between 1999 and 2006 were characterized by frequent negative temperature anomalies in the first half of the year (January to June, Fig. 2.3 c). Notably, these anomalies persisted throughout summer in 2006 (Fig. 2.1 c). Overall, the frequency of positive anomalies increased over time, although there was no discernible monthly pattern.

Surface salinity anomalies showed an increasing trend between 1999 and 2004 (Fig. 2.3 b). Salinity anomalies were well above the series mean until 2008 (Fig. 2.3 b). This high salinity anomaly was followed by an abrupt negative anomaly in 2009, peaking with the anomaly minimum reached in 2015 (Fig. 2.3 b). Subsequently, the anomaly trend steadily increased until the end of the series (Fig. 2.3 b). We used

ht!

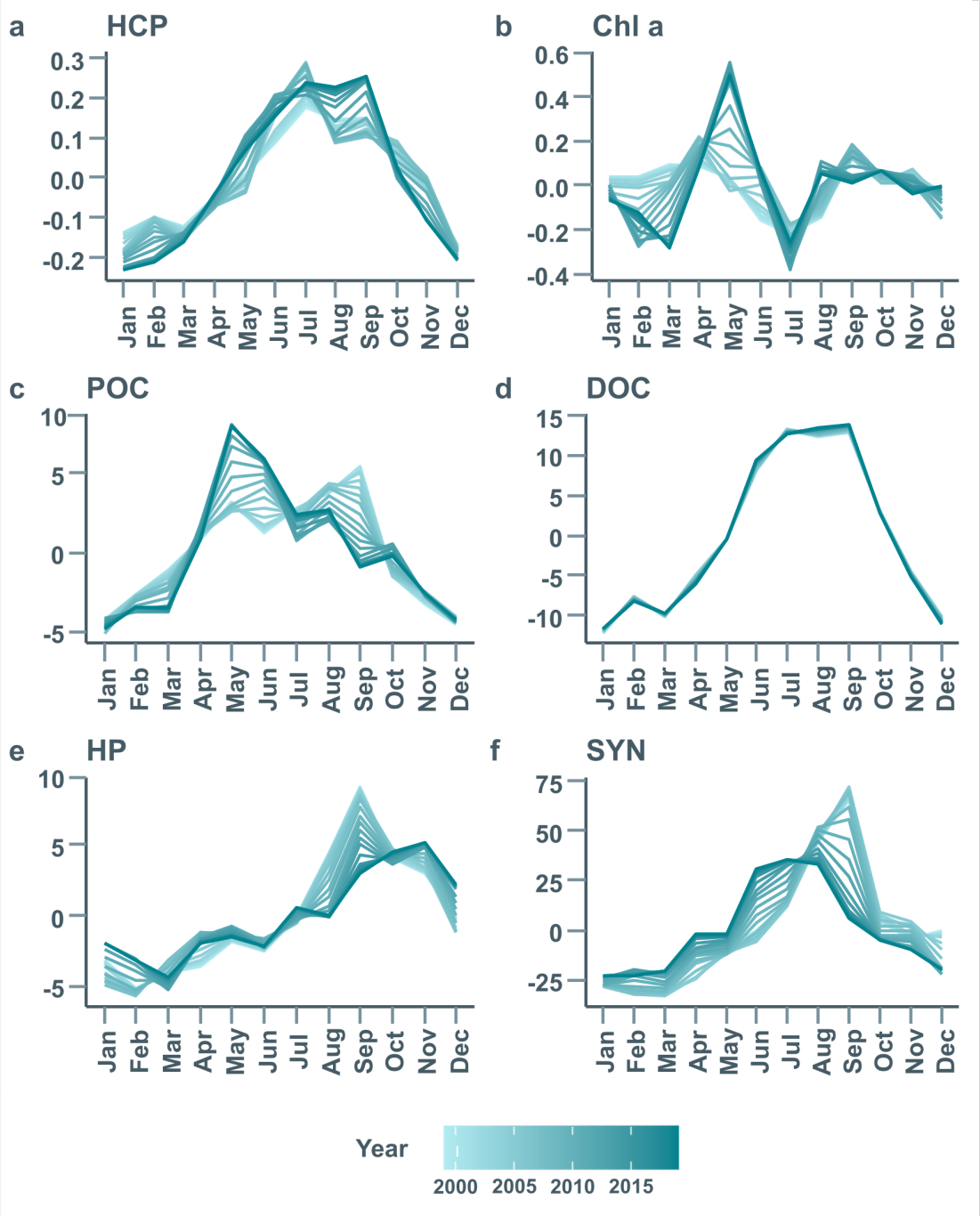

Figure 2.2: Seasonal figures obtained from the seasonal decomposition with locally estimated scatterplot smoothing (LOESS, see Section 2.2.5). Note that Y-axes are differentially scaled and unitless. a) HCP - Heterotrophic carbon production; b) Chl *a* - Chlorophyll *a* concentration; c) POC - Particulate organic carbon concentration; d) DOC - Dissolved organic carbon concentration; e) HP - Heterotrophic prokaryotes abundance; f) SYN – *Synechococcus* abundance.

the particulate C/N value as an indication of freshwater-derived organic matter, using a value of 7.8 to discern between marine (<7.8) or freshwater-derived (>7.8) organic matter (Giani et al., 2009). The lowest median C/N were found between 2005 and 2009 (Fig. 2.3 d) confirming the reduced freshwater input to the sampling station suggested by the salinity anomalies.

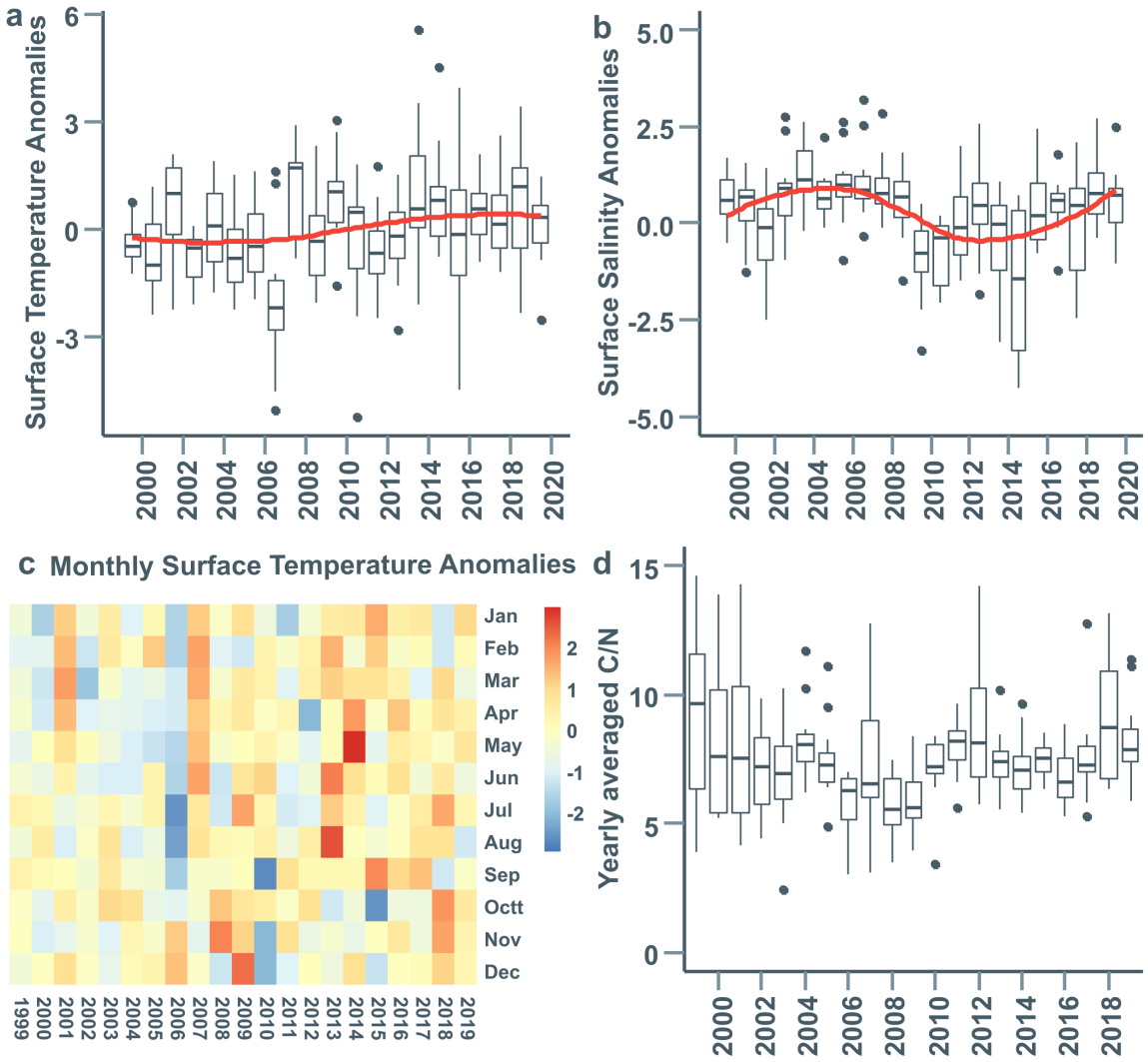

Figure 2.3: Box plots of surface temperature (a) and salinity (b) anomalies grouped by year. Trendlines are extracted using the locally estimated scatterplot smoothing (LOESS, see Section 2.2.5). c) Heatmap showing monthly surface temperature anomalies. d) Surface C/N ratios grouped by year.

2.3.2. Effect of environmental drivers on HCP rates

The RF approach allowed to rank the selected explanatory variable according to their contribution to predict HCP rates (see Section 2.2.5). Temperature and POC were identified as the most important variables (Fig. 2.4). The remaining variables (i.e., SYN, HP, Chl *a*, DOC, and salinity) had a similar contribution to the model, accounting for ~10% of the predictive power (Fig. 2.4). The computation of local fea-

tures importance from the RF model showed varying time-related patterns (Fig. 2.5). On a yearly basis (Fig. 2.5 a), oscillations of features importance were linked to the observed long-term patterns reported in Fig. 2.1.

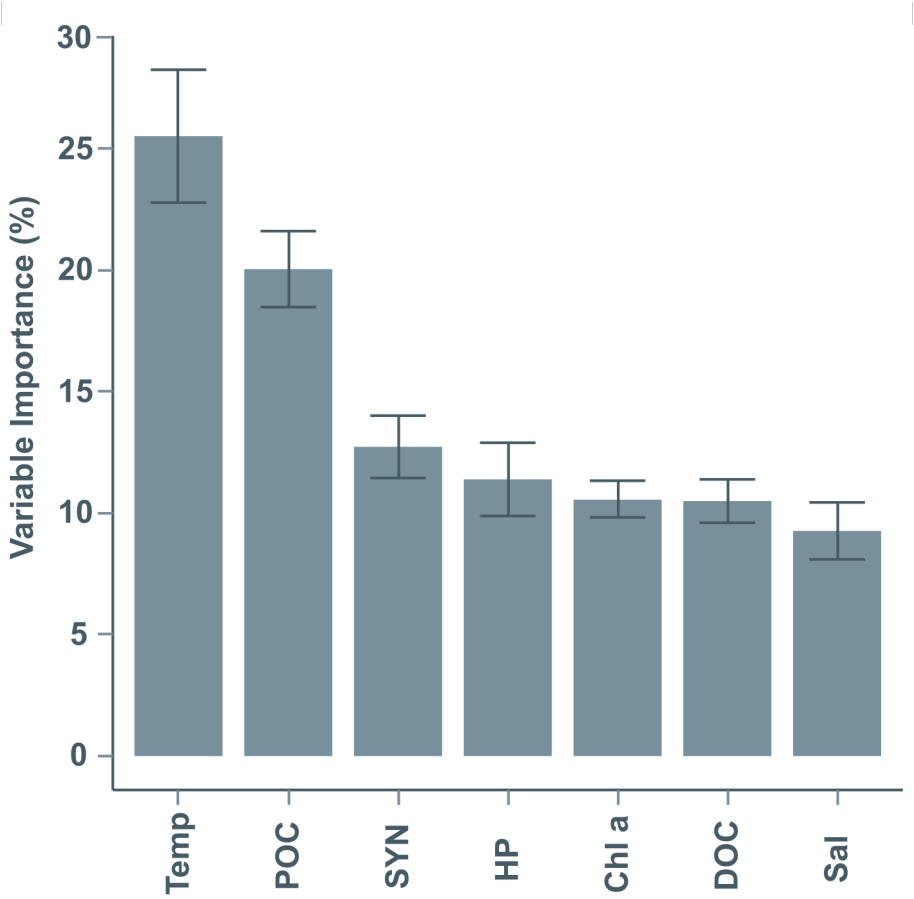

Figure 2.4: Random Forest ranking of HCP rates predictors. The importance reflects the change in the mean squared error of the model when the variable of interest is permuted. Error bars represent the standard deviation calculated over 999 permutations. Temp-Temperature; POC-Particulate organic carbon concentration; SYN-*Synechococcus* abundance; HP-Heterotrophic prokaryotes abundance; Chl *a*-Chlorophyll *a* concentration; DOC-Dissolved organic carbon concentration; Sal-Salinity.

Temperature and POC importance showed an anticorrelated pattern, with peaks of POC importance corresponding to drops in temperature ranking (Fig. 2.5 a). This pattern was conserved until 2006, when the two features started following the same trend. The transition between the two modes of variability was localized in 2007-2009, when temperature and POC showed a co-occurring peak. Remarkably, this switch matched with the transition period identified from the HCP long-term trend (Fig. 2.1). Subsequently, the ranking of both variables showed an increasing, albeit oscillating, trend (Fig. 2.5 a). SYN importance maxima were observed in 2006-2007, followed by an abrupt minimum in 2008 (Fig. 2.5 a), matching with the increasing long-term trend emerging from the time-constrained clustering (Fig. 2.1). Subsequently, a second period of higher relative importance developed between 2010 and 2012, although with a milder evolution (Fig. 2.5 a). Chl *a* was relatively less important in determining HCP rates in the first years of the series (1999-2006, Fig. 2.5 a). Following a peak in

2007, this feature importance was stable over time, with values slightly higher than the previous previous period (Fig. 2.5 a). This finding agrees with the increased Chl *a* concentration suggested by the long-term trend analysis (Fig. 2.1 b). Time-related feature importance dynamics highlighted an increase in salinity relative importance from 2002 to 2006 (Fig. 2.5 a), implicating a relevant effect of the positive anomalies during those years (Fig. 2.3 b and d) on HCP rates.

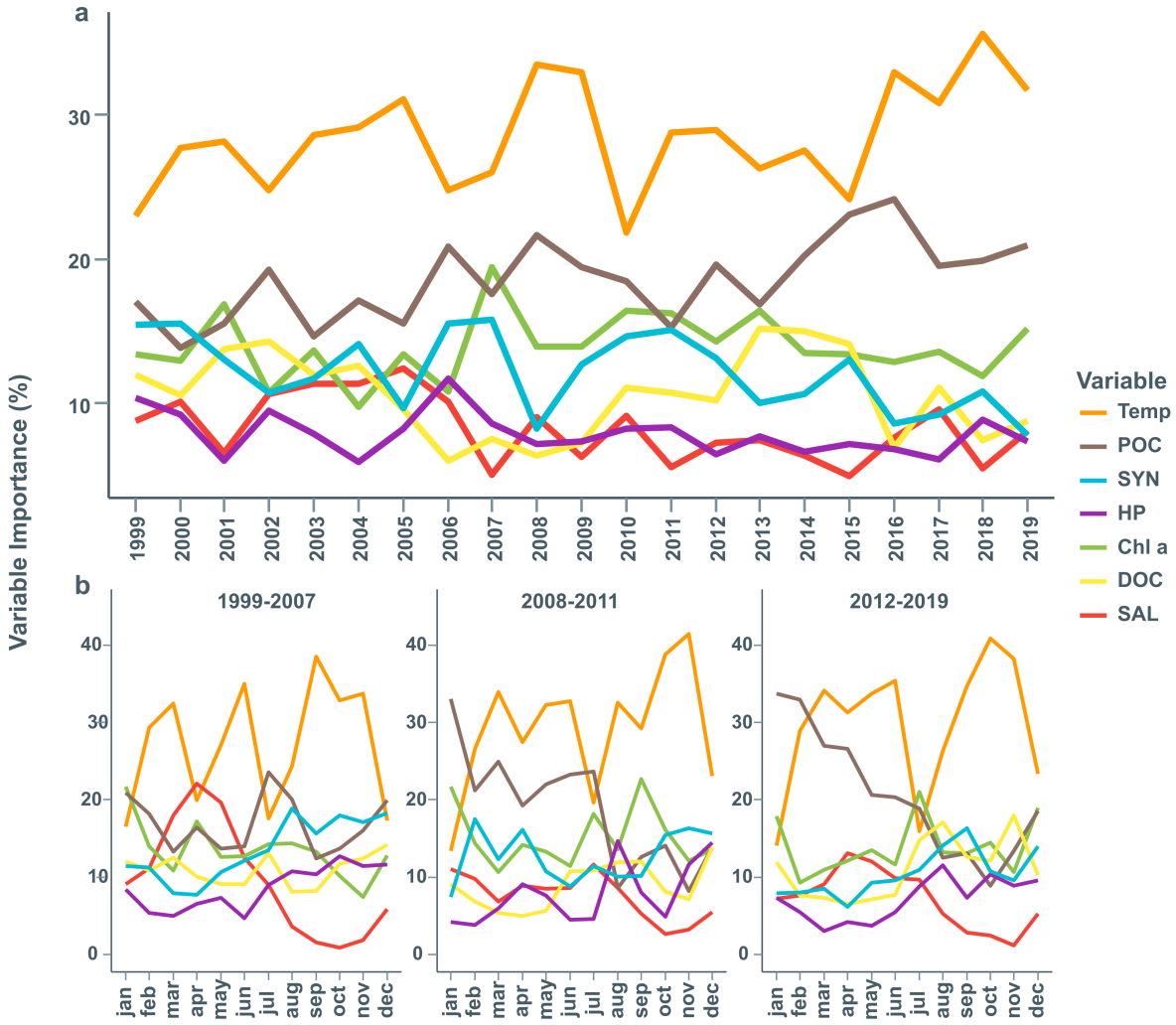

Figure 2.5: Time series of local feature importance extracted from the Random Forest model. a) year-aggregated features importance; b) monthly aggregated features importance. Each of the three panels in b) represents the indicated time slots, identified based on the time-constrained clustering showed in Fig. 2.1. See Section2.2.5 for details. Temp-Temperature; POC-Particulate organic carbon concentration; SYN-*Synechococcus* abundance; HP-Heterotrophic prokaryotes abundance; Chl *a*-Chlorophyll *a* concentration; DOC-Dissolved organic carbon concentration; Sal-Salinity.

2.4. Discussion

Our overarching aim was to disentangle the dynamics underlying the microbe-mediated processing of organic matter. To pursue this aim, we used a Random Forest approach, allowing us to model and thus explain the observed HCP rates as a function

of selected environmental drivers. The primary reason behind the use of Random Forest relies on its high performance and reliability in the estimation of variable importance. This was especially important as our goal was not to predict HCP rates in future scenarios but rather to investigate its drivers both at global and local (i.e., single observation) levels. With this algorithm, variable importance estimation is not biased by highly correlated predictors, leading to reliable and ecologically meaningful extraction of feature importance (Cutler et al., 2007). These features have been successfully exploited by other works on microbial aquatic time series (e.g., Pomati et al., 2020; Thomas et al., 2018), providing a sound benchmark on its performances on these kinds of data. Finally, Random Forest modelling is relatively easy to implement and analyse in open source programming environments (such as R or Phyton) when compared to other Machine Learning algorithms. We thus used this particular method aiming for (i) reproducibility of our analysis and (ii) to possibly boost its usage in the analysis of high dimensional datasets among aquatic microbial ecologist, as no cutting-edge expertise is necessary to implement this method.

With this approach, we were able to link the observed long-term HCP patterns with environmental drivers. We did this on an interannual scale (Fig. 2.5 a), to investigate environmental drivers of the HCP long-term trend, as well as on a seasonal scale (Fig. 2.5 b), to tease apart the factors shaping the changes of the annual cycle over time.

2.4.1. Main metabolic drivers: the role of temperature and POC

The most important variables contributing to the model were temperature and POC concentration, with relative importance substantially higher than that assigned to the other variables (Fig. 2.4). The temperature-substrate interplay has been regarded as a driver of microbial growth in both coastal and open-ocean ecosystems across the globe (Fuhrman et al., 2015; Giovannoni and Vergin, 2012; Lønborg et al., 2016; Šolić et al., 2019) and quantifying its influence is a central topic since the teenage of microbial ecology (Ducklow, 2000). The breakdown of variable importance at a local level (Fig. 2.5) showed that the relationship between POC and temperature changed over time. At interannual scales, POC long-term maxima correspond to temperature importance minima (e.g., 2002 and 2006, Fig. 2.1 c and Fig. 2.5 a), highlighting a reduced role of temperature influence at high substrate availability conditions, as shown by their anticorrelated pattern. From Fig. 2.5 a, an upward trend of temperature importance was evident since 2015, coupled with an increase in POC importance in 2016. Several studies report a temperature increase in the northern Adriatic Sea and in general in the Mediterranean Sea (Cozzi et al., 2020; Giani et al., 2012; Kralj et al., 2019; Pisano et al., 2020; Raicich and Colucci, 2019; Šolić et al., 2020; Šolić et al., 2019) , thus explaining the increase in temperature importance. Moreover, while we failed to discern an obvious trend, the frequency of positive anomalies at both interannual and seasonal scales increased since 2013-2014 (Fig. 2.3 a and c), in accordance with the random forest results (Fig. 2.5 a). The years between 2015 and 2016 were characterized by POC minima, determining the increase in POC importance in explaining HCP rates. This pattern would suggest that, under a reduced POC availability regime, the temperature increase may have enhanced the limiting effect of substrate on microbial metabolic rates (Apple et al., 2006; Celussi et al., 2019), determining a decline in HCP rates since 2015, as shown in Fig. 2.1 a.

The temperature-substrate swing was better represented by the seasonal importance during the period 1999-2007 (Fig. 2.5 b). Temperature was the most HCP contributing factor during winter (January-March, Fig. 2.1 b), while substrate availability, represented by Chl *a* and POC, increased, to the detriment of temperature, in early spring and summer (Fig. 2.5 b). This scheme suggests that temperature may have a greater effect on HCP rates in cold conditions, whereas during summer (i.e., July-August, Fig. 2.5 b) substrate availability exerts a greater influence due to the limited freshwater runoff supporting primary productivity. In other words, extreme cold events might have important consequences on the planktonic trophic webs of temperate coastal areas, by reducing the channelling of OM through plankton and diminishing the overall (secondary) productivity for periods much longer than the climatic events duration (Manna et al., 2019). The functioning of this scheme has been proposed for the northern Adriatic Sea (Celussi et al., 2019), and validated through experimental studies in other coastal environments (Arandia-Gorostidi et al., 2017; Huete-Stauffer et al., 2015), corroborating our findings. Seasonal variable importance patterns showed signal of change in these mechanisms in the last part of the time series (2012-2019, Fig. 2.5 b), pointing to an increased control exerted by substrate availability over temperature in winter. This pattern is likely explained by the increasing frequency of winter positive temperature anomalies over time (Fig. 2.3 c), which relieve the temperature control on metabolic rates, coupled with POC annual minima (Fig. 2.2 c) which determine a substrate shortage for heterotrophic microbes.

2.4.2. Time-related patterns of minor environmental drivers

The long-term features analysis revealed a shared underlying structure, made up of three periods of coherent observations with the years between 2006 and 2011 representing a transition period between two regimes (blue cluster in Fig. 2.1). The onset of this transition period was different according to the considered variable, with an overall one-year delay, displaying however a meaningful consequentiality. The beginning of this period was indeed observed at first in Chl *a* time series in 2006, followed by POC in 2007 and then by HCP in 2008 (Fig. 2.1 b, c, and a, respectively). Remarkably, the 2006-2011 time frame did not only represent a transition between long-term structures, but it also displayed different seasonal figures (Fig. 2.2). This highlights a scheme in which a prolonged draught period (see Section 2.4.2) limited phytoplankton biomass, determining a consequent decrease of autochthonous POC concentration, ultimately affecting microbial metabolic rates.

While the seasonal figures at the beginning and at the end of the time series were remarkably different, changes happened slowly through time, determining, at least partially, the observed delay in the transition period onset. Nonetheless, the observed delay may be due to the relatively low sampling frequency (i.e., one month), which prevented us to use a smoothing window shorter than 12 months (see Section 2.2.5) to extract the long-term trends. Therefore, the minimum time frame for a meaningful clustering was one year, contributing to the observed offset between variables.

Salinity

Surface salinity time series revealed that the years between 2002 and 2008 were characterized by positive salinity anomalies (Fig. 2.3 b), implying a prolonged period of reduced runoff at the study site. This was indeed the case for the entire northern Adriatic Sea, which, consequently to the draught event, experienced a reduction in river-brought inorganic nutrients up to half of those measured in years of typical discharge regimes (Cozzi and Giani, 2011). While the overall feature importance ranked salinity as the least contributing variable (Fig. 2.4), HCP rates were locally affected by freshwater dynamics. Noteworthy, we found the signature of the draught event in the interannual pattern of variable importance, linking the observed changes with the reduced freshwater inputs (Fig. 2.5 a). In the study area, OM pulses are mainly driven by freshwater inputs, either by direct advection of terrestrially derived organic matter or by delivering inorganic nutrients, fostering autochthonous organic matter production (Lipizer et al., 2012). However, river-advected OM is often enriched in complex, recalcitrant substrates (i.e., aromatic compounds, lignin, soil OM; Galy et al., 2007). Autochthonous OM, richer in labile molecules, is thus more suitable for degradation than river-advected one. This scheme would explain the generally low contribution of salinity to HCP rates despite the inverse association often found between these variable and microbial metabolic rates in freshwater-influenced Mediterranean coastal reas (Celussi and Del Negro, 2012; Celussi et al., 2019; Zaccone and Caruso, 2019).

Chlorophyll *a*

The occurrence of this low river discharge period was remarkably consistent with the Chl *a* trend showed in Fig. 2.1 b. The transition period identified by the time-constrained cluster analysis (blue cluster in Fig. 2.1 b) gathered the years affected by the draught event, linking the river-borne inorganic nutrient flux and the resident photosynthetic biomass. Several time series analyses of both Chl *a* and phytoplankton community (e.g. Bernardi Aubry et al., 2012; Cabrini et al., 2012; Mozetič et al., 2010) have shown a general oligotrophication of the northern Adriatic Sea (until 2007-2009) driven by the reduction of freshwater inputs. Our results show that this oligotrophication period was followed by an increasing Chl *a* trend peaking and then plateauing from 2013 to 2016 (Fig. 2.1 b), as also evidenced by Cozzi et al., 2020 for the same area. This second phase was characterized by a remarkable shift in Chl *a* seasonal cycle, a feature explaining the changes in HCP seasonal variable importance pattern over the three periods (Fig. 2.5 b). This was indeed characterized by a progressive loss of the late-winter Chl *a* – Salinity-driven time frame, representing the signature of the early-spring bloom, well matching with the seasonal shift depicted in Fig. 2.2 b. The observed changes in Chl *a* long-term dynamics and in their effect on HCP rates may be likely explained by a shift in phytoplankton community composition (and thus the autochthonous OM features) of over time. A recent analysis of the Gulf of Trieste phytoplankton community time series (2010-2017, Cerino et al., 2019) pointed out a shift in the resident phytoplankton community, coupled with the reduction in size of the bloom-forming species. This shift was coupled with the appearance of a phytoplankton maximum in May and the loss of the early-spring, diatom-dominated, bloom previously characterizing the area (Cabrini et al., 2012), thus corroborating our hypotheses.

Particulate organic carbon

POC time series closely followed the seasonality shift observed for Chl *a* (Fig. 2.2 c) suggesting that POC in the area is tightly linked to Chl *a* dynamics and thus predominantly phytoplankton derived. This agrees with the significant relationships between Chl *a* and POC observed in the northern Adriatic Sea byGiani et al., 2005. The appearance of smaller phytoplankton taxa would thus explain the observed long-trend POC regimes (Fig. 2.1 c). Higher POC values (1999-2006, Fig. 2.1 c) corresponded to bigger phytoplankton species (e.g., *Pseudo-nitzschia* spp. and large *Chaetoceros* spp., Cerino et al., 2019) whereas a shift towards smaller phytoplankton representatives (e.g., small *Chaeotoceros* spp. and *Cyclotella* spp., Cerino et al., 2019) brought to a reduced POC concentration (2012-2019, Fig. 2.1 c). The autochthonous origin of POM was suggested also by its yearly median C/N, which, despite the wide variability observed for some years (i.e., 1999, 2002, 2012 and 2018, Fig. 2.3 d), ranged between 5 and 10. These values are comparable with those reported for the northern Adriatic Sea (5.4-8.2; Giani et al., 2005; Giani et al., 2003), suggesting a low contribution of river-advected POM (Faganeli et al., 1988; Giani et al., 2009). Taken together, these results imply that autochthonous POM and thus phytoplankton itself, represents the major source of particulate OM in the study area, a conclusion supported by the low overall contribution of salinity in determining the observed HCP rates (Fig. 2.4). It is therefore plausible that land-derived particles settle in the 'close' proximity of the river deltas and do not pronouncedly contribute to the POC pool at our study site. Furthermore, the outcome of POC as the second most contributing variable (Fig. 2.4) strongly suggests that particle-attached microbes may play a major role in OM processing in the Gulf of Trieste. This agrees with the strong positive association between POC and OM degradation rates previously reported by Celussi and Del Negro, 2012 for the study area. In coastal environments indeed, particle attached microbes are generally more metabolically active than their free-living counterpart (Crump et al., 1998; Smith et al., 2013). On a global scale, more than 70% of the POM is consumed by prokaryotes, highlighting their pivotal role in coastal, as well as oceanic, marine carbon cycling (Giering et al., 2014).

Dissolved organic carbon

Even though heterotrophic life in the ocean is fuelled by organic matter, most of this organic carbon reservoir is in a dissolved form (Hansell et al., 2009). The transformation from the dissolved pool to the particulate one is mostly mediated by the microbial loop (Azam and Malfatti, 2007). HCP is the metabolic process catalysing this transformation and thus, theoretically, heavily dependent on DOM. Yet, our results highlighted that DOC contribution in determining the observed HCP rates was unexpectedly low (Fig. 2.4). Moreover, while no seasonal shift was detected over the DOC time series (Fig. 2.2 d), some local importance patterns were highlighted by the random forest (Fig. 2.5). DOC contribution was higher between 2001 and 2003 covering the years affected by mucilage events (Fonda Umani et al., 2007). Mucilage formation is a process relying on the increasing gelling capacity of OM (Azam et al., 1999). Within the mucus matrix, OM production, degradation and remineralization rates are greatly enhanced compared to the surrounding water column, representing an additional source of labile OM for planktonic microbes (Del Negro et al., 2005; Fonda Umani et al., 2007;

Herndl, 1992). Thus, the observed increase in DOC importance concomitantly to these events may be due to these processes.

The interannual peak observed between 2013 and 2015 was coupled with an increase in DOC seasonal importance over summer months (2012-2019, Fig. 2.5 b). The DOC pattern was coupled with a maximum in long-term HCP trend as well as with its seasonal shift over time (Fig 2.1 a and 2.2 a). These results hint to a reliance of heterotrophic microbial processes on the dissolved OM pool beside that on the particulate one, as also suggested by the declining long-term POC trend in those years (Fig. 2.1 c). This dynamic would also explain the prolonged HCP seasonal peak trough spring and summer (Fig. 2.1 a) established in the last part of the series, which would initiate with POC degradation to be then sustained by bioavailable DOC (BDOC), as also highlighted by the seasonal variable importance pattern for the period 2012-2019 (Fig. 2.5 b).

A previous study on the DOC temporal dynamics in the study area failed to find a significant association between DOC concentration and phytoplankton biomass or salinity (De Vittor et al., 2008). Nevertheless, summer increase in DOC concentration during the stratification period has been already reported in the Gulf of Trieste as well as in other coastal and semi-enclosed marine areas, where it has been ascribed to (i) decoupling between primary production and bacterial carbon demand and (ii) to the accumulation of exudates above the seasonal pycnocline (Lipizer et al., 2012 and references therein). The overall seasonal evolution may be abruptly altered by intense episodic disturbances, such as strong dilutions due to floods and wind storms (Lipizer et al., 2012), causing short-term fluctuations in DOC concentration, similar to or even larger than seasonal variability (De Vittor et al., 2008). Our results suggest that the dimension of the DOC pool is potentially untouched by long-term changes (Fig. 2.2 d) and that DOC dynamics evolve on separate scales of variability driven by microbial activity, seasonal stratification and oceanographic constrains. Combined, these factors allow the progressive accumulation of DOC, decoupling the temporal variability of particulate and dissolved OM. Previous experiments (De Vittor et al., 2009) showed that BDOC is a highly variable, but minor, fraction of DOC therefore we suppose that the amount of BDOC utilized by bacterial activity may be too small, in comparison with the accumulating refractory DOC, to be detectable on the monthly time scale.

Synechococcus

Synechococcus abundance was ranked as the third contributing variable to the observed HCP rates (Fig. 2.4). In the northern Adriatic Sea, where *Prochlorococcus* cells are only occasionally present (Celussi et al., 2015 and references therein), *Synechococcus* may represent a consistent contributor to the total phytoplankton biomass (Bernardi Aubry et al., 2006), accounting for 40 to 60% to the total primary production (Magazzù et al., 1989; Vadrucci et al., 2005). The SYN-derived OM thus represents a non-negligible source of substrate for the heterotrophic OM processing. The increasing long-term trend of *Synechococcus* during the Chl *a* minimum (2007-2008, Fig. 2.1 f) following the reduced freshwater inputs, may be due to its reduced size, as smaller cells easily outcompete bigger ones in nutrient-limiting conditions (Moutin et al., 2002).

The increased interannual SYN importance observed between 2006 and 2011 (Fig. 2.5 a) suggests that heterotrophic processes may have been fuelled by *Synechococcus*-derived OM following the low river discharge period, which was likely the cause of the observed delay between the Chl *a* and HCP long-term decrease (Fig. 2.1 a and b). This hypothesis is supported by the findings of Beg Paklar et al., 2020 who observed an enhanced contribution of the microbial food web to OM cycling under high salinity-induced oligotrophy. The intimate physical association between *Synechococcus* and heterotrophic bacteria have been observed in coastal, offshore, and even Antarctic waters (Malfatti F and Azam F, 2009), suggesting that the tight metabolic coupling between these organisms may be a fundamental biogeochemical driver on a global scale. Over the three periods identified in the HCP series, the seasonal importance pattern of SYN changed during the HCP transition period, replacing the Chl *a* peak characterizing the first period (Fig. 2.5 b), further suggesting that SYN-derived OM represented the main organic substrate for the heterotrophic picoplankton between 2008 and 2011. Nevertheless, we cannot rule out that the general relationship between SYN and HCP could be due to the active leucine uptake performed by *Synechococcus* itself (Paoli et al., 2008) or that *Synechococcus* can better thrive under these environmental forcing. However, the differentiation of the importance of SYN on the HCP over the three periods strongly suggests a reliance of heterotrophic production on picocyanobacterial-OM in oligotrophic conditions.

2.4.3. Draught implications for microbial growth

The occurrence of a temperature-substrate co-limitation may be assessed from the deviation of the Arrhenius' linear response of microbial growth to temperature (Arrhenius, 1889; Pomeroy and Wiebe, 2001). By comparing the Arrhenius' response for each of the three periods identified in the HCP time series (Fig. 2.6), a non-linear response of microbial growth to temperature during the transition period (identified in blue in Fig. 2.6 and in Fig. 2.1) becomes evident. The non-linear response in the upper-left part of the Arrhenius' plot (Fig. 2.6) is due to the response of the microbial community to limiting resources rather than to a thermal stress, as demonstrated by Apple et al., 2006 in a river-influenced coastal area. The substrate-driven HCP limitation has been highlighted on regional (Celussi et al., 2019; Šolić et al., 2017) as well as on global scales (see López-Urrutia and Morán, 2007 for coastal ecosystems; Lønborg et al., 2016 for open ocean) using either inorganic or organic nutrients. This result, taken together with the above discussed findings, demonstrate that between 2008 and 2011 microbial-mediated OM processing was limited by substrate availability. Albeit transient limitation of microbial OM processing has been demonstrated to occur following intense wind outbreaks in the Gulf of Trieste (Manna et al., 2019), to the best of our knowledge this is the first time that an interannual limitation of microbial growth is reported in the northern Mediterranean Sea. The trophodynamic scheme developed by Fonda Umani et al., 2012 for the northern Adriatic Sea demonstrated that this trophic network is heavily dependent on the energy deriving from heterotrophic bacterioplankton. Thus, a prolonged period of limited microbial OM reworking may have had cascading effects on the entire planktonic trophic network for several years, impairing the productivity of the whole ecosystem.

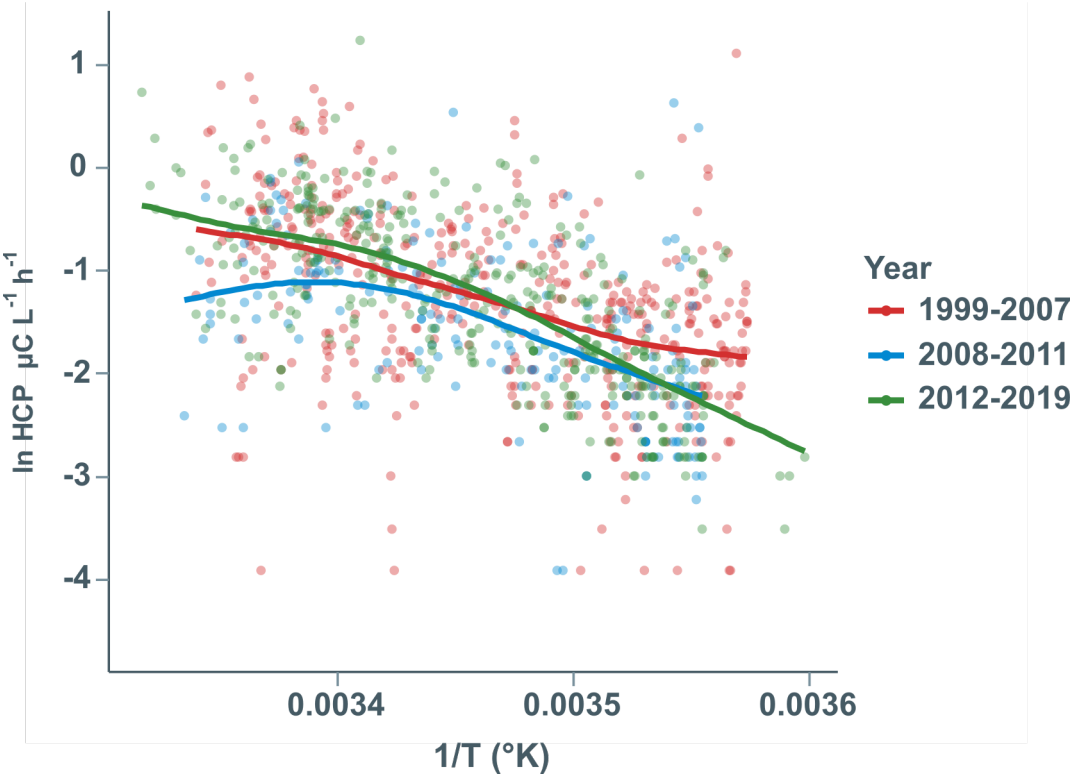

Figure 2.6: Arrhenius plot of the natural logarithm of the heterotrophic carbon production (ln HCP) against the inverse absolute temperature (1/T). Fit lines for each of the three-period highlighted in legend are extracted with locally estimated scatterplot smoothing (LOESS, see Section 2.2.5).

2.5. Conclusions

The analysis of a 21-year-long time series allowed us to investigate time-related patterns underlying the evolution of the "inseparable liaison" between microbes and organic matter (DDittmar and Arnosti, 2018). By means of canonical time series analysis coupled with a machine learning approach, we were able to tease apart, in a temporal fashion, long-term environmental drivers of microbial growth. Microbe-mediated organic matter processing in the northernmost part of the Mediterranean Sea is essentially driven by temperature and OM availability, with a heavier reliance on the particulate pool. The tight coupling between POC and Chl *a* dynamics indicated that primary producers-derived POC is the most important OM source for resident heterotrophic microbes, establishing a strong connection with land-derived freshwater inputs and HCP rates. A multi-year draught event between 2002 and 2008 heavily modified these biogeochemical links, determining a reduction of primary producers' biomass impacting both quantitatively and qualitatively OM standing stocks. Teasing apart HCP drivers in a temporal fashion, we demonstrated that *Synechococcus*-derived OM fuelled heterotrophic metabolism during the low Chl *a* period and that the high salinity anomaly induced substantial shifts in HCP drivers on both interannual and seasonal scales, leading to a multi-year limitation of microbial growth. Here we demonstrate that transient regional processes have significant consequences on plankton dynamics, potentially affecting the entire ecosystem productivity. These consequences extend beyond the duration of the processes themselves, leading to long-term, eventually abrupt, biogeochemical shifts. With this study, we provide an updated insight on the long-term biogeochemical dynamics of one of the most productive areas of the Mediterranean Sea.

The sound results of the Random Forest model were ecologically meaningful and contributed remarkably to validate our initial hypothesis. Therefore, we believe that, with the increasing amount of data gathered by multiannual observation, the approach used in this study will provide a better understanding of long-term ecosystem dynamics. As time is the main axis along which the ecosystems move (Ribera d'Alcalà, 2019), understanding the past may help to explain present and future changes.

Acknowledgements

The authors would like to thank the personnel of ARPA and of the Miramare MPA for providing the vessels and the crews for sampling activities. Data for this study have been collected thanks to the support of the Regione Friuli Venezia Giulia and of the programs INTERREG Italy-Slovenia 2 and 3. We highly acknowledge the work of all scientists that have been working in microbial ecology and biogeochemistry at our institute over the years and contributed to the dataset construction: M. Borin Dolfin, C. Comici, E. Crevatin, F. De Prà, C. Falconi, A.A. Gallina, A. Karuza, M. Kralj, C. Larato, A. Paoli, P. Ramani, F. Relitti, F. Tamberlich, A. Valeri, under the supervision of PIs S. Fonda Umani and C. Solidoro.

References

Apple, J. K., Del Giorgio, P. A., & Kemp, W. M. (2006). Temperature regulation of bacterial production, respiration, and growth efficiency in a temperate salt-marsh estuary. *Aquatic Microbial Ecology*, *43*(3), 243–254. https://doi.org/10.3354/ame043243

Arandia-Gorostidi, N., Huete-Stauffer, T. M., Alonso-Sáez, L., & G. Morán, X. A. (2017). Testing the metabolic theory of ecology with marine bacteria: Different temperature sensitivity of major phylogenetic groups during the spring phytoplankton bloom. *Environmental Microbiology*, *19*(11), 4493–4505. https://doi.org/https://doi.org/10.1111/1462-2920.13898

Arnosti, C. (2011). Microbial Extracellular Enzymes and the Marine Carbon Cycle. *Annual Review of Marine Science*, *3*(1), 401–425. https://doi.org/10.1146/annurev-marine-120709-142731

Arrhenius, S. (1889). Über die Reaktionsgeschwindigkeit bei der Inversion von Rohrzucker durch Säuren. *Zeitschrift für Physikalische Chemie*, *4U*(1). https://doi.org/10.1515/zpch-1889-0416

Azam, F., Umani, S. F., & Funari, E. (1999). Significance of bacteria in the mucilage phenomenon in the northern adriatic sea. *Annali dell'Istituto superiore di sanita*, *35 3*, 411–9.

Azam, F., & Malfatti, F. (2007). Microbial structuring of marine ecosystems. *Nature Reviews Microbiology*, *5*(10), 782–791. https://doi.org/10.1038/nrmicro1747

Beg Paklar, G., Vilibić, I., Grbec, B., Matić, F., Mihanović, H., Džoić, T., Šantić, D., Šestanović, S., Šolić, M., Ivatek-Šahdan, S., & Kušpilić, G. (2020). Record-breaking salinities in the middle adriatic during summer 2017 and concurrent changes in the microbial food web. *Progress in Oceanography*, *185*, 102345. https://doi.org/https://doi.org/10.1016/j.pocean.2020.102345

Bernardi Aubry, F., Acri, F., Bastianini, M., Pugnetti, A., & Socal, G. (2006). Picophytoplankton contribution to phytoplankton community structure in the gulf of venice (nw adriatic sea). *International Review of Hydrobiology*, *91*(1), 51–70. https://doi.org/https://doi.org/10.1002/iroh.200410787

Bernardi Aubry, F., Cossarini, G., Acri, F., Bastianini, M., Bianchi, F., Camatti, E., De Lazzari, A., Pugnetti, A., Solidoro, C., & Socal, G. (2012). Plankton communities in the northern Adriatic Sea: Patterns and changes over the last 30 years. *Estuarine, Coastal and Shelf Science*, *115*, 125–137. https://doi.org/10.1016/j.ecss.2012.03.011

Biecek, P. (2018). Dalex: Explainers for complex predictive models in r. *Journal of Machine Learning Research*, *19*(84), 1–5. http://jmlr.org/papers/v19/18-416.html

Breiman, L. (2001). Random Forests. *Machine Learning*, *45*(1), 5–32. https://doi.org/10.1023/A:1010933404324

Cabrini, M., Fornasaro, D., Cossarini, G., Lipizer, M., & Virgilio, D. (2012). Phytoplankton temporal changes in a coastal northern Adriatic site during the last 25 years. *Estuarine, Coastal and Shelf Science*, *115*, 113–124. https://doi.org/10.1016/j.ecss.2012.07.007

Celussi, M., Gallina, A. A., Ras, J., Giani, M., & Del Negro, P. (2015). Effect of sunlight on prokaryotic organic carbon uptake and dynamics of pigments relevant to

photoheterotrophy in the Adriatic Sea. *Aquatic Microbial Ecology*, *74*(3), 235–249. https://www.int-res.com/abstracts/ame/v74/n3/p235-249/

Celussi, M., & Del Negro, P. (2012). Microbial degradation at a shallow coastal site: Long-term spectra and rates of exoenzymatic activities in the NE Adriatic Sea. *Estuarine, Coastal and Shelf Science*, *115*, 75–86. https://doi.org/10.1016/j.ecss.2012.02.002

Celussi, M., Zoccarato, L., Bernardi Aubry, F., Bastianini, M., Casotti, R., Balestra, C., Giani, M., & Del Negro, P. (2019). Links between microbial processing of organic matter and the thermohaline and productivity features of a temperate river-influenced mediterranean coastal area. *Estuarine, Coastal and Shelf Science*, *228*, 106378. https://doi.org/https://doi.org/10.1016/j.ecss.2019.106378

Cerino, F., Fornasaro, D., Kralj, M., Giani, M., & Cabrini, M. (2019). Phytoplankton temporal dynamics in the coastal waters of the north-eastern adriatic sea (mediterranean sea) from 2010 to 2017. *Nature Conservation*, *34*, 343–372. https://doi.org/10.3897/natureconservation.34.30720

Chróst, R. J. (1992). Significance of bacterial ectoenzymes in aquatic environments. *Hydrobiologia*, *243-244*(1), 61–70. https://doi.org/10.1007/BF00007020

Cleveland, R. B., Cleveland, W. S., McRae, J. E., & Terpenning, I. (1990). Stl: A seasonal-trend decomposition. *Journal of official statistics*, *6*(1), 3–73.

Cole, J. J., & Pace, M. L. (1995). Bacterial secondary production in oxic and anoxic freshwaters. *Limnology and Oceanography*, *40*(6), 1019–1027. https://doi.org/10.4319/lo.1995.40.6.1019

Comici, C., & Bussani, A. (2007). Analysis of the River Isonzo discharge (1998-2005). *Bollettino di Geofisica Teorica ed Applicata*, *48*, 435–454.

Cozzi, S., Cabrini, M., Kralj, M., De Vittor, C., Celio, M., & Giani, M. (2020). Climatic and anthropogenic impacts on environmental conditions and phytoplankton community in the gulf of trieste (northern adriatic sea). *Water*, *12*(9), 2652. https://doi.org/10.3390/w12092652

Cozzi, S., & Giani, M. (2011). River water and nutrient discharges in the Northern Adriatic Sea: Current importance and long term changes. *Continental Shelf Research*, *31*(18), 1881–1893. https://doi.org/10.1016/j.csr.2011.08.010

Crump, B. C., Baross, J. A., & Simenstad, C. A. (1998). Dominance of particle-attached bacteria in the Columbia River estuary, USA. *Aquatic Microbial Ecology*, *14*(1), 7–18. https://www.int-res.com/abstracts/ame/v14/n1/p7-18/

Cutler, D. R., Edwards Jr., T. C., Beard, K. H., Cutler, A., Hess, K. T., Gibson, J., & Lawler, J. J. (2007). Random forests for classification in ecology. *Ecology*, *88*(11), 2783–2792. https://doi.org/https://doi.org/10.1890/07-0539.1

De Vittor, C., Larato, C., & Umani, S. F. (2009). The application of a plug-flow reactor to measure the biodegradable dissolved organic carbon (bdoc) in seawater. *Bioresource Technology*, *100*(23), 5721–5728. https://doi.org/https://doi.org/10.1016/j.biortech.2009.06.056

De Vittor, C., Paoli, A., & Fonda Umani, S. (2008). Dissolved organic carbon variability in a shallow coastal marine system (Gulf of Trieste, northern Adriatic Sea). *Estuarine, Coastal and Shelf Science*, *78*(2), 280–290. https://doi.org/10.1016/j.ecss.2007.12.007

Del Negro, P., Crevatin, E., Larato, C., Ferrari, C., Totti, C., Pompei, M., Giani, M., Berto, D., & Fonda Umani, S. (2005). Mucilage microcosms. *Science of The Total Environment*, *353*(1), 258–269. https://doi.org/https://doi.org/10.1016/j.scitotenv.2005.09.018

Dittmar, T., & Arnosti, C. (2018). An inseparable liason: Marine microbes and nonliving organic matter. In J. M. Gasol & D. L. Kirchman (Eds.), *Microbial ecology of the oceans* (Third, pp. 189–218). John Wiley & Sons, Inc.

Ducklow, H. (2000). Bacterioplankton production and biomass in the oceans. *Microbial Ecology of the Oceans, 1st edition* (pp. 1–47). John Wiley & Sons, Inc.

Faganeli, J., Malej, A., Pezdic, J., & Malacic, V. (1988). C: N: P ratios and stable c-isotopic ratios as indicators of sources of organic-matter in the gulf of trieste (northern adriatic). *Oceanologica Acta*, *11*(4), 377–382.

Field, C. B., Behrenfeld, M. J., Randerson, J. T., & Falkowski, P. (1998). Primary production of the biosphere: Integrating terrestrial and oceanic components. *Science*, *281*(5374), 237–240. https://doi.org/10.1126/science.281.5374.237

Fonda Umani, S., Del Negro, P., Larato, C., De Vittor, C., Cabrini, M., Celio, M., Falconi, C., Tamberlich, F., & Azam, F. (2007). Major inter-annual variations in microbial dynamics in the Gulf of Trieste (northern Adriatic Sea) and their ecosystem implications. *Aquatic Microbial Ecology*, *46*(2), 163–175. https://www.int-res.com/abstracts/ame/v46/n2/p163-175/

Fonda Umani, S., Malfatti, F., & Del Negro, P. (2012). Carbon fluxes in the pelagic ecosystem of the Gulf of Trieste (Northern Adriatic Sea). *Estuarine, Coastal and Shelf Science*, *115*, 170–185. https://doi.org/10.1016/j.ecss.2012.04.006

Fuhrman, J. A., Cram, J. A., & Needham, D. M. (2015). Marine microbial community dynamics and their ecological interpretation. *Nature Reviews Microbiology*, *13*(3), 133–146. https://doi.org/10.1038/nrmicro3417

Galili, T. (2015). Dendextend: An R package for visualizing, adjusting and comparing trees of hierarchical clustering. *Bioinformatics*, *31*(22), 3718–3720. https://doi.org/10.1093/bioinformatics/btv428

Galy, V., France-Lanord, C., Beyssac, O., Faure, P., Kudrass, H., & Palhol, F. (2007). Efficient organic carbon burial in the Bengal fan sustained by the Himalayan erosional system. *Nature*, *450*(7168), 407–410. https://doi.org/10.1038/nature06273

Giani, M., Berto, D., Rampazzo, F., Savelli, F., Alvisi, F., Giordano, P., Ravaioli, M., & Frascari, F. (2009). Origin of sedimentary organic matter in the north-western adriatic sea. *Estuarine, Coastal and Shelf Science*, *84*(4), 573–583. https://doi.org/https://doi.org/10.1016/j.ecss.2009.07.031

Giani, M., Djakovac, T., Degobbis, D., Cozzi, S., Solidoro, C., & Fonda Umani, S. (2012). Recent changes in the marine ecosystems of the northern Adriatic Sea. *Estuarine, Coastal and Shelf Science*, *115*, 1–13. https://doi.org/10.1016/j.ecss.2012.08.023

Giani, M., Savelli, F., Berto, D., Zangrando, V., Ćosović, B., & Vojvodić, V. (2005). Temporal dynamics of dissolved and particulate organic carbon in the northern adriatic sea in relation to the mucilage events. *Science of The Total Environment*, *353*(1), 126–138. https://doi.org/https://doi.org/10.1016/j.scitotenv.2005.09.062

Giani, M., Savelli, F., & Boldrin, A. (2003). Temporal variability of particulate organic carbon, nitrogen and phosphorus in the northern adriatic sea. In B. Kronvang (Ed.), *The interactions between sediments and water* (pp. 319–325). Springer Netherlands.

Giering, S. L. C., Sanders, R., Lampitt, R. S., Anderson, T. R., Tamburini, C., Boutrif, M., Zubkov, M. V., Marsay, C. M., Henson, S. A., Saw, K., Cook, K., & Mayor, D. J. (2014). Reconciliation of the carbon budget in the ocean's twilight zone. *Nature*, *507*(7493), 480–483. https://doi.org/10.1038/nature13123

Giovannoni, S. J., & Vergin, K. L. (2012). Seasonality in ocean microbial communities. *Science*, *335*(6069), 671–676. https://doi.org/10.1126/science.1198078

Grimm, E. C. (1987). Coniss: A fortran 77 program for stratigraphically constrained cluster analysis by the method of incremental sum of squares. *Computers & Geosciences*, *13*(1), 13–35. https://doi.org/https://doi.org/10.1016/0098-3004(87)90022-7

Hansell, D. A., Carlson, C. A., Repeta, D. J., & Schlitzer, R. (2009). Dissolved organic matter in the ocean a controversy stim ulates new insights. *Oceanography*, *22*(SPL.ISS. 4), 202–211. https://doi.org/10.5670/oceanog.2009.109

Herndl, G. J. (1992). Marine snow in the northern adriatic sea: Possible causes and consequences for a shallow ecosystem. *Marine Microbial Food Webs*, *6*(2), 149–172.

Huete-Stauffer, T. M., Arandia-Gorostidi, N., Díaz-Pérez, L., & Morán, X. A. G. (2015). Temperature dependences of growth rates and carrying capacities of marine bacteria depart from metabolic theoretical predictions. *FEMS Microbiology Ecology*, *91*(10). https://doi.org/10.1093/femsec/fiv111

Juggins, S. (2020). *Rioja: Analysis of quaternary science data*. https://cran.r-project.org/package=rioja

Kharbush, J. J., Close, H. G., Van Mooy, B. A. S., Arnosti, C., Smittenberg, R. H., Le Moigne, F. A. C., Mollenhauer, G., Scholz-Böttcher, B., Obreht, I., Koch, B. P., Becker, K. W., Iversen, M. H., & Mohr, W. (2020). Particulate organic carbon deconstructed: Molecular and chemical composition of particulate organic carbon in the ocean. *Frontiers in Marine Science*, *7*, 518. https://doi.org/10.3389/fmars.2020.00518

Kirchman, D., K'nees, E., & Hodson, R. (1985). Leucine incorporation and its potential as a measure of protein synthesis by bacteria in natural aquatic systems. *Applied and Environmental Microbiology*, *49*(3), 599–607. https://aem.asm.org/content/49/3/599

Kralj, M., Lipizer, M., Čermelj, B., Celio, M., Fabbro, C., Brunetti, F., Francé, J., Mozetič, P., & Giani, M. (2019). Hypoxia and dissolved oxygen trends in the northeastern adriatic sea (gulf of trieste). *Deep Sea Research Part II: Topical Studies in Oceanography*, *164*, 74–88. https://doi.org/https://doi.org/10.1016/j.dsr2.2019.06.002

Langfelder, P., Zhang, B., & Horvath, S. (2007). Defining clusters from a hierarchical cluster tree: The Dynamic Tree Cut package for R. *Bioinformatics*, *24*(5), 719–720. https://doi.org/10.1093/bioinformatics/btm563

Legendre, P., Dallot, S., & Legendre, L. (1985). Succession of species within a community: Chronological clustering, with applications to marine and freshwater

zooplankton. *The American Naturalist*, *125*(2), 257–288. http://www.jstor.org/stable/2461635

Liaw, A., & Wiener, M. (2002). Classification and regression by randomforest. *R news*, *2*(3), 18–22.

Lipizer, M., De Vittor, C., Falconi, C., Comici, C., Tamberlich, F., & Giani, M. (2012). Effects of intense physical and biological forcing factors on CNP pools in coastal waters (Gulf of Trieste, Northern Adriatic Sea). *Estuarine, Coastal and Shelf Science*, *115*, 40–50. https://doi.org/10.1016/j.ecss.2012.03.024

Lønborg, C., Cuevas, L. A., Reinthaler, T., Herndl, G. J., Gasol, J. M., Morán, X. A. G., Bates, N. R., & Álvarez-Salgado, X. A. (2016). Depth dependent relationships between temperature and ocean heterotrophic prokaryotic production. *Frontiers in Marine Science*, *3*, 90. https://doi.org/10.3389/fmars.2016.00090

López-Urrutia, Á., & Morán, X. A. G. (2007). Resource limitation of bacterial production distorts the temperature dependence of oceanic carbon cycling. *Ecology*, *88*(4), 817–822. https://doi.org/https://doi.org/10.1890/06-1641

Lorenzen, C., & Jeffrey, S. (1980). Determination of chlorophyll in seawater. *Unesco technical papers in marine sciences*, *35*(1), 1–20.

Magazzù, G., Bruni, V., Decembrini, F., & Panella, S. (1989). La produzione primaria del picoplancton fotosintetico nei mari italiani. *Oebalia*, *4*, 463–478.

Malačič, V., Celio, M., Čermelj, B., Bussani, A., & Comici, C. (2006). Interannual evolution of seasonal thermohaline properties in the Gulf of Trieste (northern Adriatic) 1991–2003. *Journal of Geophysical Research*, *111*(C8), C08009. https://doi.org/10.1029/2005JC003267

Malfatti F, & Azam F. (2009). Atomic force microscopy reveals microscale networks and possible symbioses among pelagic marine bacteria. *Aquatic Microbial Ecology*, *58*(1), 1–14. https://www.int-res.com/abstracts/ame/v58/n1/p1-14/

Manna, V., Fabbro, C., Cerino, F., Bazzaro, M., Del Negro, P., & Celussi, M. (2019). Effect of an extreme cold event on the metabolism of planktonic microbes in the northernmost basin of the mediterranean sea. *Estuarine, Coastal and Shelf Science*, *225*, 106252. https://doi.org/https://doi.org/10.1016/j.ecss.2019.106252

Mihanović, H., Vilibić, I., Carniel, S., Tudor, M., Russo, A., Bergamasco, A., Bubić, N., Ljubešić, Z., Viličić, D., Boldrin, A., Malačič, V., Celio, M., Comici, C., & Raicich, F. (2013). Exceptional dense water formation on the Adriatic shelf in the winter of 2012. *Ocean Science*, *9*(3), 561–572. https://doi.org/10.5194/os-9-561-2013

Morán, X. A. G., Gasol, J. M., Pernice, M. C., Mangot, J. F., Massana, R., Lara, E., Vaqué, D., & Duarte, C. M. (2017). Temperature regulation of marine heterotrophic prokaryotes increases latitudinally as a breach between bottom-up and top-down controls. *Global Change Biology*, *23*(9), 3956–3964. https://doi.org/10.1111/gcb.13730

Moritz, S., & Bartz-Beielstein, T. (2017). Imputets: Time series missing value imputation in r. *The R Journal*, *9*(1), 207–218. https://doi.org/10.32614/RJ-2017-009

Moutin, T., Thingstad, T. F., Van Wambeke, F., Marie, D., Slawyk, G., Raimbault, P., & Claustre, H. (2002). Does competition for nanomolar phosphate supply explain the predominance of the cyanobacterium Synechococcus? *Limnology and Oceanography*, *47*(5), 1562–1567. https://doi.org/10.4319/lo.2002.47.5.1562

Mozetič, P., Solidoro, C., Cossarini, G., Socal, G., Precali, R., Francé, J., Bianchi, F., De Vittor, C., Smodlaka, N., & Fonda Umani, S. (2010). Recent Trends Towards Oligotrophication of the Northern Adriatic: Evidence from Chlorophyll a Time Series. *Estuaries and Coasts*, *33*(2), 362–375. https://doi.org/10.1007/s12237-009-9191-7

Paoli, A., Karuza, A., de Vittor, C., del Negro, P., & Umani, S. F. (2006). Daily variations of highly active bacteria in the Northern Adriatic Sea. *Journal of Plankton Research*, *28*(3), 325–335. https://doi.org/10.1093/plankt/fbi116

Paoli, A., Celussi, M., Del Negro, P., Fonda Umani, S., & Talarico, L. (2008). Ecological advantages from light adaptation and heterotrophic-like behavior in Synechococcus harvested from the Gulf of Trieste (Northern Adriatic Sea). *FEMS Microbiology Ecology*, *64*(2), 219–229. https://doi.org/10.1111/j.1574-6941.2008.00459.x

Pella, E., & Colombo, B. (1973). Study of carbon, hydrogen and nitrogen determination by combustion-gas chromatography. *Mikrochimica Acta*, *61*(5), 697–719. https://doi.org/10.1007/BF01218130

Pisano, A., Marullo, S., Artale, V., Falcini, F., Yang, C., Leonelli, F. E., Santoleri, R., & Buongiorno Nardelli, B. (2020). New evidence of mediterranean climate change and variability from sea surface temperature observations. *Remote Sensing*, *12*(1), 132. https://doi.org/10.3390/rs12010132

Pomati, F., Shurin, J. B., Andersen, K. H., Tellenbach, C., & Barton, A. D. (2020). Interacting temperature, nutrients and zooplankton grazing control phytoplankton size-abundance relationships in eight swiss lakes. *Frontiers in Microbiology*, *10*, 3155. https://doi.org/10.3389/fmicb.2019.03155

Pomeroy, L. R., & Wiebe, W. J. (2001). Temperature and substrates as interactive limiting factors for marine heterotrophic bacteria. *Aquatic Microbial Ecology*, *23*(2), 187–204. https://doi.org/10.3354/ame023187

Porter, K. G., & Feig, Y. S. (1980). The use of DAPI for identifying and counting aquatic microflora1. *Limnology and Oceanography*, *25*(5), 943–948. https://doi.org/https://doi.org/10.4319/lo.1980.25.5.0943

R Core Team. (2019). *R: A Language and Environment for Statistical Computing*. R Foundation for Statistical Computing. https://www.R-project.org/

Raicich, F., & Colucci, R. R. (2019). A near-surface sea temperature time series from trieste, northern adriatic sea (1899–2015). *Earth System Science Data*, *11*(2), 761–768. https://doi.org/10.5194/essd-11-761-2019

Raicich, F., Malačič, V., Celio, M., Giaiotti, D., Cantoni, C., Colucci, R. R., Čermelj, B., & Pucillo, A. (2013). Extreme air-sea interactions in the gulf of trieste (north adriatic) during the strong bora event in winter 2012. *Journal of Geophysical Research: Oceans*, *118*(10), 5238–5250. https://doi.org/https://doi.org/10.1002/jgrc.20398

Ribera d'Alcalà, M., Conversano, F., Corato, F., Licandro, P., Mangoni, O., Marino, D., Mazzocchi, M. G., Modigh, M., Montresor, M., Nardella, M., Saggiomo, V., Sarno, D., & Zingone, A. (2004). Seasonal patterns in plankton communities in a pluriannual time series at a coastal Mediterranean site (Gulf of Naples): An attempt to discern recurrences and trends. *Scientia Marina*, *68*(S1), 65–83. https://doi.org/10.3989/scimar.2004.68s165

Ribera d'Alcalà, M. (2019). Similarities, differences and mechanisms of climate impact on terrestrial vs. marine ecosystems. *Nature Conservation*, *34*, 505–523. https://doi.org/10.3897/natureconservation.34.30923

Riedel, T., & Dittmar, T. (2014). A Method Detection Limit for the Analysis of Natural Organic Matter via Fourier Transform Ion Cyclotron Resonance Mass Spectrometry. *Analytical Chemistry*, *86*(16), 8376–8382. https://doi.org/10.1021/ac501946m

Romagnan, J.-B., Legendre, L., Guidi, L., Jamet, J.-L., Jamet, D., Mousseau, L., Pedrotti, M.-L., Picheral, M., Gorsky, G., Sardet, C., & Stemmann, L. (2015). Comprehensive model of annual plankton succession based on the whole-plankton time series approach. *PLOS ONE*, *10*(3), 1–18. https://doi.org/10.1371/journal.pone.0119219

Sharp, J. H. (1974). Improved analysis for "particulate" organic carbon and nitrogen from seawater1. *Limnology and Oceanography*, *19*(6), 984–989. https://doi.org/10.4319/lo.1974.19.6.0984

Simon, M., & Azam, F. (1989). Protein content and protein synthesis rates of planktonic marine bacteria. *Marine Ecology Progress Series*, *51*, 201–213. https://doi.org/10.3354/meps051201

Smith, D. C. (1992). A simple, economical method for measuring bacterial protein synthesis rates in seawater using 3H-leucine. *Marine Microbial Food Webs*, *6*(2), 107–114.

Smith, M., Zeigler Allen, L., Allen, A., Herfort, L., & Simon, H. (2013). Contrasting genomic properties of free-living and particle-attached microbial assemblages within a coastal ecosystem. *Frontiers in Microbiology*, *4*, 120. https://doi.org/10.3389/fmicb.2013.00120

Šolić, M., Krstulović, N., Šantić, D., Šestanović, S., Kušpilić, G., Bojanić, N., Ordulj, M., Jozić, S., & Vrdoljak, A. (2017). Impact of the 3 °C temperature rise on bacterial growth and carbon transfer towards higher trophic levels: Empirical models for the Adriatic Sea. *Journal of Marine Systems*, *173*, 81–89. https://doi.org/10.1016/j.jmarsys.2017.01.001

Šolić, M., Šantić, D., Šestanović, S., Bojanić, N., Jozić, S., Ordulj, M., Vrdoljak Tomaš, A., & Kušpilić, G. (2020). Changes in the trophic pathways within the microbial food web in the global warming scenario: An experimental study in the adriatic sea. *Microorganisms*, *8*(4), 510. https://doi.org/10.3390/microorganisms8040510

Šolić, M., Šantić, D., Šestanović, S., Bojanić, N., Jozić, S., Vrdoljak, A., Ordulj, M., & Kušpilić, G. (2019). Temperature and phosphorus interacts in controlling the picoplankton carbon flux in the adriatic sea: An experimental versus field study. *Environmental Microbiology*, *21*(7), 2469–2484. https://doi.org/https://doi.org/10.1111/1462-2920.14634

Stravisi, F. (1977). Bora driven circulation in northern Adriatic. *Bollettino di Geofisica Teorica e Applicata*, *19*, 95–102.

Sugimura, Y., & Suzuki, Y. (1988). A high-temperature catalytic oxidation method for the determination of non-volatile dissolved organic carbon in seawater by direct injection of a liquid sample. *Marine Chemistry*, *24*(2), 105–131. https://doi.org/https://doi.org/10.1016/0304-4203(88)90043-6

Thomas, M. K., Fontana, S., Reyes, M., Kehoe, M., & Pomati, F. (2018). The predictability of a lake phytoplankton community, over time-scales of hours to years. *Ecology Letters*, *21*(5), 619–628. https://doi.org/https://doi.org/10.1111/ele.12927

Tinta, T., Vojvoda, J., Mozetič, P., Talaber, I., Vodopivec, M., Malfatti, F., & Turk, V. (2015). Bacterial community shift is induced by dynamic environmental parameters in a changing coastal ecosystem (northern adriatic, northeastern mediterranean sea) – a 2-year time-series study. *Environmental Microbiology*, *17*(10), 3581–3596. https://doi.org/https://doi.org/10.1111/1462-2920.12519

Vadrucci, M., Catalano, G., & Basset, A. (2005). Spatial and seasonal variability of fractionated phytoplankton biomass and primary production in the frontal region of the northern adriatic sea. *Mediterranean Marine Science*, *6*(1), 5–16. https://doi.org/10.12681/mms.189

Verdugo, P., Alldredge, A. L., Azam, F., Kirchman, D. L., Passow, U., & Santschi, P. H. (2004). The oceanic gel phase: A bridge in the DOM-POM continuum. *Marine Chemistry*, *92*(1-4), 67–85. https://doi.org/10.1016/j.marchem.2004.06.017

Wagner, S., Schubotz, F., Kaiser, K., Hallmann, C., Waska, H., Rossel, P. E., Hansman, R., Elvert, M., Middelburg, J. J., Engel, A., Blattmann, T. M., Catalá, T. S., Lennartz, S. T., Gomez-Saez, G. V., Pantoja-Gutiérrez, S., Bao, R., & Galy, V. (2020). Soothsaying dom: A current perspective on the future of oceanic dissolved organic carbon. *Frontiers in Marine Science*, *7*, 341. https://doi.org/10.3389/fmars.2020.00341

Weiss, M. S., Abele, U., Weckesser, J., Welte, W., Schiltz, E., & Schulz, G. E. (1991). Molecular architecture and electrostatic properties of a bacterial porin. *Science*, *254*(5038), 1627–1630. https://doi.org/10.1126/science.1721242

Wickham, H. (2016). *Ggplot2: Elegant Graphics for Data Analysis*. Springer-Verlag New York. https://ggplot2.tidyverse.org

Zaccone, R., & Caruso, G. (2019). Microbial enzymes in the Mediterranean Sea: Relationship with climate changes. *AIMS microbiology*, *5*(3), 251–271. https://doi.org/10.3934/microbiol.2019.3.251

3

Effect of an Extreme Cold Event on the Metabolism Of Planktonic Microbes in the Northernmost Basin of the Mediterranean Sea

This Chapter is adapted from: Manna, V., Fabbro, C., Cerino, F., Bazzaro, M., Del Negro, P., Celussi, M., 2019. Effect of an extreme cold event on the metabolism of planktonic microbes in the northernmost basin of the Mediterranean Sea. Estuarine, Coastal and Shelf Science, 225, 106252. https://doi.org/10.1016/j.ecss.2019.106252

3.1. Introduction

Heterotrophic bacteria and archaea are responsible for processing up to 50% of the organic carbon fixed in the ocean by planktonic photoautotrophs, playing thus a pivotal role in the global biogeochemical carbon cycle (Azam and Malfatti, 2007). In the marine environment, most of the organic matter is in a polymeric form and cannot be directly utilized since only small molecules (< 600 Da), such as amino acids and mono-saccharides, can cross the prokaryotic cell membrane due to the activity of permeases (Weiss et al., 1991). To exploit this huge reservoir, prokaryotes produce extracellular enzymes to hydrolyse high molecular weight organic matter into assimilable monomers (Chróst, 1992). Extracellular enzymes exist in two forms: cell-bound, localized on the outer cell wall of microbes, and cell-free, freely dissolved in the water or associated with particles of non-parental origin (Baltar, 2018; Martinez and Azam, 1993). Different sources of cell-free extracellular enzymes have been proposed so far, including the active release in response to an appropriate substrate, starvation, changes in cell permeability, viral lysis and grazing activity (see Baltar, 2018; Steen and Arnosti, 2011 and references therein). Regardless of their sources or forms, the ultimate goal of extracellular enzymes is to retrieve low molecular weight compounds that can be incorporated into cells and fuel prokaryotic growth.

Since the hydrolysis and the uptake of organic matter are affected by a wide range of different environmental factors (e.g., pH, UV radiation, organic matter quality and quantity, temperature, salinity, community composition), it is extremely complex to assess the effect of each variable on prokaryotic metabolism, especially in natural conditions. Among these variables, the temperature-substrate availability interaction has been recognized as a major factor controlling microbial metabolism (Ducklow and Carlson, 1992). Temperature affects the rates of all biochemical processes and could be regarded as an ever-present, interactive factor, ultimately modulating resources requirements (Morán et al., 2017; Pomeroy and Wiebe, 2001). Wiebe et al., 1992; Wiebe et al., 1993 exposed bacterial isolates from subtropical to polar environments to a wide range of temperature (0 – 30 °C) and substrate concentration (0.15 - 1500 mg L^{-1}). Comparing the growth rates, the authors found a consistent limiting effect of substrate concentration on isolates generation time when the temperature approached the lower limit for their growth. The deviation from the Arrhenius' linear response (Arrhenius, 1889) of prokaryotic growth to temperature was more evident in isolates from temperate water bodies, while psychrophilic bacteria, due to the shift of their optimal growth temperature range towards lower values, were able to overcome this effect when a higher substrate concentration was supplied. These results suggest that the control exerted on microbial metabolism by the interaction of temperature with substrate availability is enhanced in temperate water bodies during winter when water temperature is near the lower end of the optimal growth range (Pomeroy and Wiebe, 2001).

The Gulf of Trieste is a landlocked basin located in the northernmost part of the Adriatic Sea. Due to its limited depth (<26 m, Cozzi et al., 2012), the wind forcing plays a key role in shaping the variability of the water column profile, especially during winter, when severe heat loss and evaporation occur during outbreaks of local northeasterly wind, the Bora. These processes densify the resident water mass producing

the so-called Northern Adriatic Dense Water (NAdDW, Artegiani et al., 1989), including the northern Adriatic Sea among the three generation sites of dense shelf water in the Mediterranean Sea (Robinson et al., 2001). Occasionally, Bora outbreaks in the area can be very intense (up to 160 km h^{-1}) and last up to two weeks, enhancing dense water generation processes by inducing exceptional surface temperature drops (< 4°C, Mihanović et al., 2013). To date, the majority of the investigations on wintertime Bora outbreaks has focused on their contribution to dense water generation processes (Lee et al., 2005; Mihanović et al., 2013; Vilibić and Supić, 2005). The consequences on the biological compartment have been addressed only in the context of downward dense water flow (Luna et al., 2016), neglecting an assessment of the effect of these extreme events on the local planktonic microbial community. Likewise, on a broader picture, the science of extreme events has developed tools and methods to rapidly, objectively and quantitatively assess the changing nature of extreme weather risks at the local level (Otto et al., 2018), yet the effects of such phenomena on the ecosystems are rarely evaluated.

From 18th to 26th February 2018, the northern Adriatic Sea experienced an intense outbreak of Bora (wind speed peaking at 120 Km h^{-1}) which induced an exceptional drop in surface temperature (down to 5.7°C) in the coastal zone of the Gulf of Trieste. This study was designed to fill the knowledge gap on the effect of these events on the coastal microbial community, specifically investigating their potential negative effects on microbial standing stocks and on microbe-mediated organic matter processing (through the evaluation of the activities of the exoenzymes β-glucosidase, β-galactosidase, chitinase, lipase, alkaline-phosphatase and leucine aminopeptidase and organic matter uptake velocities). Additionally, we set up temperature manipulation experiments, aiming to evaluate whether the sudden temperature drop induced by the cold outbreak represented a lower thermal limit for microbial metabolic rates.

3.2. Materials and methods

3.2.1. Study area, sampling strategy and experimental design

The Gulf of Trieste is the northernmost part of the Adriatic Sea, with a surface area of ~600 Km^2) and an average depth of 17m (Celio et al., 2002). The main freshwater input in this shallow embayment comes from the Isonzo (Soča) river in the north-western part of the basin, while the freshwater runoff in the eastern part is of torrential nature (Comici and Bussani, 2007). Representing the main source of organic and inorganic nutrients, the river runoff shows a wide interannual variability (Comici and Bussani, 2007) and affects surface salinity, whose values range from 32 to 38 (Malačič et al., 2006). Surface temperature shows a clear seasonal pattern, from winter minima as low as 8°C in February and summer maxima >26°C (Malačič et al., 2006). Riverine outflows and significant heat fluxes induce a wide variability of the water column profile, further enhanced by the intense wind regime of the area (Stravisi, 1977), characterised by the alternance of cold and dry north-easterly winds (i.e., Bora) with milder south-easterly winds (i.e., Scirocco). All these features greatly affect the spatial and temporal dynamics of planktonic microbes, showing patterns very similar to typical temperate coastal environments (Milller, 2004), with exceptions determined by anomalous physical-chemical conditions (Celussi and Del Negro, 2012; Cibic et al.,

2018; Lipizer et al., 2012). The system is generally identified as meso- or oligotrophic (chlorophyll *a* concentration ranging from 0.1 to 3.8 µg L^{-1}; Celussi and Del Negro, 2012), with freshwater-triggered diatoms blooms in late winter, a nutrient-depleted summer when prokaryotic biomass prevails over the other plankton, and a second short-lasting fall bloom (Fonda Umani et al., 2012 and references therein). From 5 to 45% of prokaryotes in surface waters have been lately identified as Archaea, with Bacteria being the most abundant group (Vojvoda et al., 2014). While diatoms and nanoflagellates are the dominant components of phytoplankton through most of the year, cyanobacteria (*Synechococcus*) are the prevailing phototrophs in late summer (Fonda Umani et al., 2012).

From 26th February to 16th March 2018 a quasi-daily sampling was carried out, for a total of 13 data points (from 26th to 28th February, from 1st to 3rd, 5th, 8th and from 12th to 16th March), at a coastal station (45°42'25.1" N, 13°42'46.0" E) in the Gulf of Trieste. Samples for chemical and biological analysis were collected using a 5L Niskin bottle at ~1 m depth, transported to the laboratory into cooler boxes (approximately 15 minutes) and processed within 1 h after collection. Water temperature was measured *in situ* using a Hg thermometer. In order to evaluate the effect of a short-term temperature decrease on microbial metabolism, temperature manipulation experiments were carried out at every sampling day from 28th February to 16th March. Once in the laboratory, subsamples for exoenzymatic activity and heterotrophic carbon production were incubated at three different conditions: *in situ* temperature, *in situ* temperature lowered by 1°C (i.e., *in situ*-1°C) and *in situ* temperature lowered by 2°C (i.e., *in situ*-2°C). Samples were incubated in the dark for three hours in a cooled incubator (ST 1+, POL-EKO APARATURA).

3.2.2. Chemical analyses

Samples for salinity measurements were collected in 250 mL glass bottles and stored at 4°C until analysis. Salinity was analysed with a Guildline Autosal 8400B salinometer at the calibration facility of the OGS in Trieste (OGS-CTO) following international standard procedures. Particulate Organic Carbon (POC) and Particulate Nitrogen (PN) were measured using an elemental analyser CHNO-S Costech mod. ECS 4010 applying the methods performed by Pella and Colombo, 1973 and Sharp, 1974, as detailed by Celussi et al., 2017 (seawater volume range=0.72 – 4.0L). Samples for dissolved inorganic nitrogen (DIN=nitrites – $N\text{-}NO_2$ + nitrates –$N\text{-}NO_3$ + ammonium – $N\text{-}NH_4$), phosphate – $P\text{-}PO_4$, and silicates – Si -$Si(OH)_4$ were filtered onto precombusted (450°C for 4h) Whatman GF/F filters in acid-washed polyethylene vials and kept frozen (-20°C) until laboratory analysis. Inorganic nutrient concentrations were determined colourimetrically with a QuAAtro Seal Analytical autoanalyzer according to Hansen and Koroleff, 1999. Chlorophyll a (Chl *a*) concentration was determined spectrofluorimetrically according to Lorenzen and Jeffrey, 1980. Samples were filtered (volume range=2.0 – 3.5L) onto glass fibre filters (Whatman GF/F) and stored at -20°C. Extraction of Chl *a* was carried from the homogenate filter at 4 °C overnight in the dark, with 90% acetone. Chl *a* fluorescence was measured with a Jasco FP-6500 spectrofluorometer at 450 nm excitation and 665 nm emission wavelengths. Calibration was made with pure Chl *a* from spinach (Sigma Aldrich).

3.2.3. Flow cytometry

The abundance of *Synechococcus* (SYN), of heterotrophic prokaryotes (HP), of heterotrophic nanoflagellates (HNF) and of virus-like particles (VLP) was estimated by flow cytometry. A FACSCanto II (Becton Dickinson) instrument was used, equipped with an air-cooled laser at 488 nm and standard filter setup. Samples (1.7 mL) were fixed with 0.5% (final concentration, f.c.) glutaraldehyde solution (Grade I for EM analyses, Sigma Aldrich). Fixed samples were kept at 4 °C for approximately 15 minutes and then stored at -80°C until analysis (Brussaard, 2004). Prior to enumeration, samples were thawed at room temperature and diluted 1:10 (HP) and 1:50 (VLP) with 0.2 µm-filtered Tris-EDTA buffer 1× (Sigma Aldrich). Then samples were stained with SYBR Green I nucleic acid dye (Life Technologies), according to Marie et al., 1999, Christaki et al., 2011 and Brussaard, 2004 for HP, HNF and VLP, respectively. HP and HNF were stained (1× f.c.) and incubated for 10 minutes in the dark at room temperature. VLP were stained (0.5× f.c.) and incubated for 15 minutes in the dark at 80°C. Total virus abundance was obtained by correcting the total count for noise, with 0.2 µm-filtered Tris-EDTA buffer 1× (Sigma Aldrich) as blank. Data were acquired and processed with the FACSDiva software (Becton Dickinson). The flow rate was calibrated daily, by running distilled water and weighing it before and after the run (at least 5 replicates). The analysis carried out in duplicate on randomly selected samples (February 26th, March 5th and March 16th), showed a coefficient of variation between replicates ranging between 0.4 and 7.8%. Abundances were then calculated using the acquired cell counts and the respective flow rates. Subpopulations of relatively higher (HNA) or lower (LNA) nucleic acid content were distinguished (Gasol et al., 1999). Cell numbers of HP, SYN and HNF were converted to carbon biomass using a factor of 20 fg C $Cell^{-1}$ (Lee and Fuhrman, 1987), 200 fg C $Cell^{-1}$ (Caron et al., 1991) and 3.32 pg C $Cell^{-1}$ (Menden-Deuer and Lessard, 2000), respectively.

3.2.4. Phytoplankton

Samples for phytoplankton abundance and community composition were fixed with prefiltered and neutralized formaldehyde (1.6% f.c., Throndsen, 1978) and examined by an inverted microscope (LEICA DMi8) equipped with phase contrast. Depending on phytoplankton densities, a variable volume of seawater (25 - 50mL) was allowed to settle for 2 – 5d and examined following the Utermöhl method (Utermöhl, 1958. Cell counts were performed along transects (1 - 2) at a magnification of 400x. Half of the Utermöhl chamber was further examined at a magnification of 200x, to obtain a more correct evaluation of less abundant microphytoplankton taxa. To achieve a statistically acceptable estimation, ~200 cells of the most abundant species or at least 600 cells per sample were counted (Karlson et al., 2010). Identified taxa were reported per major groups such as diatoms, dinoflagellates, coccolithophores, cryptophytes and flagellates, the latter including all species/taxa detectable in light microscopy (i.e., >2µm). For the autotrophic biomass calculation, cell dimensions were used to calculate the biovolume choosing for each taxon the best fitting geometric shape (Hillebrand et al., 1999; Olenina et al., 2006). The carbon content was calculated from mean cell biovolumes using the formula introduced by Menden-Deuer and Lessard, 2000.

3.2.5. Extracellular enzymatic activity

Extracellular enzymatic activities (EEAs) were tested using fluorogenic substrate analogues (Hoppe, 1993) derived from 7-amino-4-methylcoumarin (AMC) and 4-methylumbelliferone (MUF). Leucine aminopeptidase activity (AMA) was assayed as the hydrolysis rate of leucine-AMC. Alkaline phosphatase (AP), β-galactosidase (BGAL), β-glucosidase (BGLU), chitinase (CHIT) and lipase (LIP) activities were assayed using MUF-phosphate, MUF-β-D-galactoside, MUF-N-acetyl-β-D-glucosaminide, MUF-β-D-glucoside, and MUF-oleate (Sigma Aldrich), respectively. Hydrolysis was measured by incubating 2mL subsamples with 200μM leucine-AMC, MUF-β-D-galactoside, MUF-β-D-glucoside, MUF-N-acetyl-β-D-glucosaminide, 50μM MUF-phosphate, 100μM MUF-oleate (saturating final concentrations, Celussi and Del Negro, 2012) for 3h in the dark at *in situ* or lowered temperature, according to the experimental design (see Section 3.2.1). Fluorescence increase due to AMC and MUF hydrolysed from the model substrates was measured using a Shimadzu RF-1501 spectrofluorometer (AMC=380nm excitation and 440nm emission; MUF=365nm excitation and 455nm emission). Triplicate calibration curves were performed daily, using 0.2μm-filtered seawater and 5μM standard solutions of AMC and MUF (Sigma Aldrich).

3.2.6. Heterotrophic carbon production

Heterotrophic carbon production (HCP) was measured with the method of ^{3}H-leucine (Leu) incorporation (Kirchman et al., 1985). Triplicate 1.7mL subsamples and one killed control (5% trichloroacetic acid - TCA - f.c.) were amended with 20nM radiotracer (52.9 Ci mmol^{-1}; Perkin Elmer) and incubated for 3h in the dark at *in situ* or lowered temperature, according to the experimental design (see Section 3.2.1). The extraction of ^{3}H-labelled proteins was carried out following the microcentrifugation method (Smith, 1992). After the addition of 1mL of scintillation cocktail (Ultima Gold™ MV; Packard), activity was determined by a TRI-CARB 2900 TR Liquid Scintillation Analyzer. Carbon biomass production was then estimated using the conversion factor of 3.1 kg C mol^{-1} Leu incorporated, assuming a two-fold isotope dilution (SSimon and Azam, 1989).

3.2.7. Statistical analyses

To highlight the patterns of microbial organic matter processing, a cluster analysis was performed using EEAs and HCP as variables. These were used to create a Bray-Curtis based dissimilarity matrix through the vegan R package (Oksanen et al., 2019). Samples were clustered applying Ward's minimum variance method (Murtagh and Legendre, 2014) and aggregated, according to their optimal cutting level, to form two clusters. Clustering method choice and the optimal number of clusters were identified using the R package clValid (Brock et al., 2008). Results of the cluster analysis were further used to generate a clustered heat map of the same variables, through the R package pheatmap (Kolde, 2019). For the samples gathered in each cluster, Friedman's ANOVA was used to test for differences between controls and experimental temperature manipulations, using Wilcoxon's matched pair test for post-hoc comparisons. A p-value of ≤0.05 was considered significant. To underline interactions among metabolic rates and between these and selected biogeochemical parameters, the

Spearman's correlation coefficient was computed after checking the non-normality of the dataset.

Chemical and biological data were compared to February, March and annual climatologies (median and interquartile range), computed on surface data (~-0.5m) recorded from 2000 to 2017 (when available) at the nearby Long-Term Ecological Research (LTER) station C1 (45°42'2" N, 13°42'36" E, Gulf of Trieste). An Arrhenius' plot (Arrhenius, 1889) was used to compare HCP values registered during the sampling period with climatological data.

The daily averaged air temperature, wind speed and Isonzo river flow rates for February and March were provided by ARPA – FVG.

Cluster analysis was performed with R version 3.5.0 (R Core Team, 2019). Friedman's ANOVA, Wilcoxon's matched pair test and Spearman's correlation were performed using the software STATISTICA (StatSoft, Inc., 2014, www.statsoft.com, ver. 12).

3.3. Results

3.3.1. Atmospheric and hydrological settings

Average Average wind speed (Fig. 3.1a) decreased steeply from 26th February to 2nd March (from 69 to 7Km h^{-1}), remaining then constant (~8Km h^{-1}) until the end of sampling, except for a small peak (20 Km h^{-1}) on 5th March. Air temperature (Fig. 3.1b) increased throughout the sampling period, from -4.7°C on 26th February to 10.3°C on 16th March, peaking on 12th March, when the maximum value was registered (12.8°C). During the sampling period, the Isonzo river flow rate (Fig. 3.1c) spanned over 3 order of magnitude, ranging between 0.73 and 781.65 m^3 s^{-1}. Lower and constant values characterised the period between 26th February and 9th March (3.25 ± 2.64 m^3 s^{-1}), while a steep increase was evident until 12th March, when the maximum freshwater discharge was registered. Afterwards, river discharge sharply declined until 15th March, increasing again on the last sampling day. Surface water temperature (Fig. 3.1d) dropped from 6.8 to 5.7°C between 26th February and 1st March, increasing then steadily until the end of the sampling period (10.3°C on 16th March). Surface salinity (Fig. 3.1d) ranged from 35.4 to 38.3, with higher and constant values until 8th March (38.2 ± 0.06; mean ± SD), decreasing then between 12th and 16th March, when the lowest salinity was measured.

3.3.2. Chemical analyses

Results of chemical analyses are summarized in Table 3.1. POC and PN followed the same general trend: after an initial drop between 26th and 28th February, a mild decreasing trend continued until 8th March, followed by a steady increase from 12th to 16th March. Minima of POC and PN (3.18 and 0.33 µM, respectively) were both measured on 5th March, while maxima were both found at the end of the sampling period, i.e. on 15th and 16th March (POC=11.34 µM; PN=2.08 µM). Dissolved inorganic nutrients time courses showed a clear temporal pattern, with lower or decreasing values between 26th February and 5th-8th March while higher and oscillating

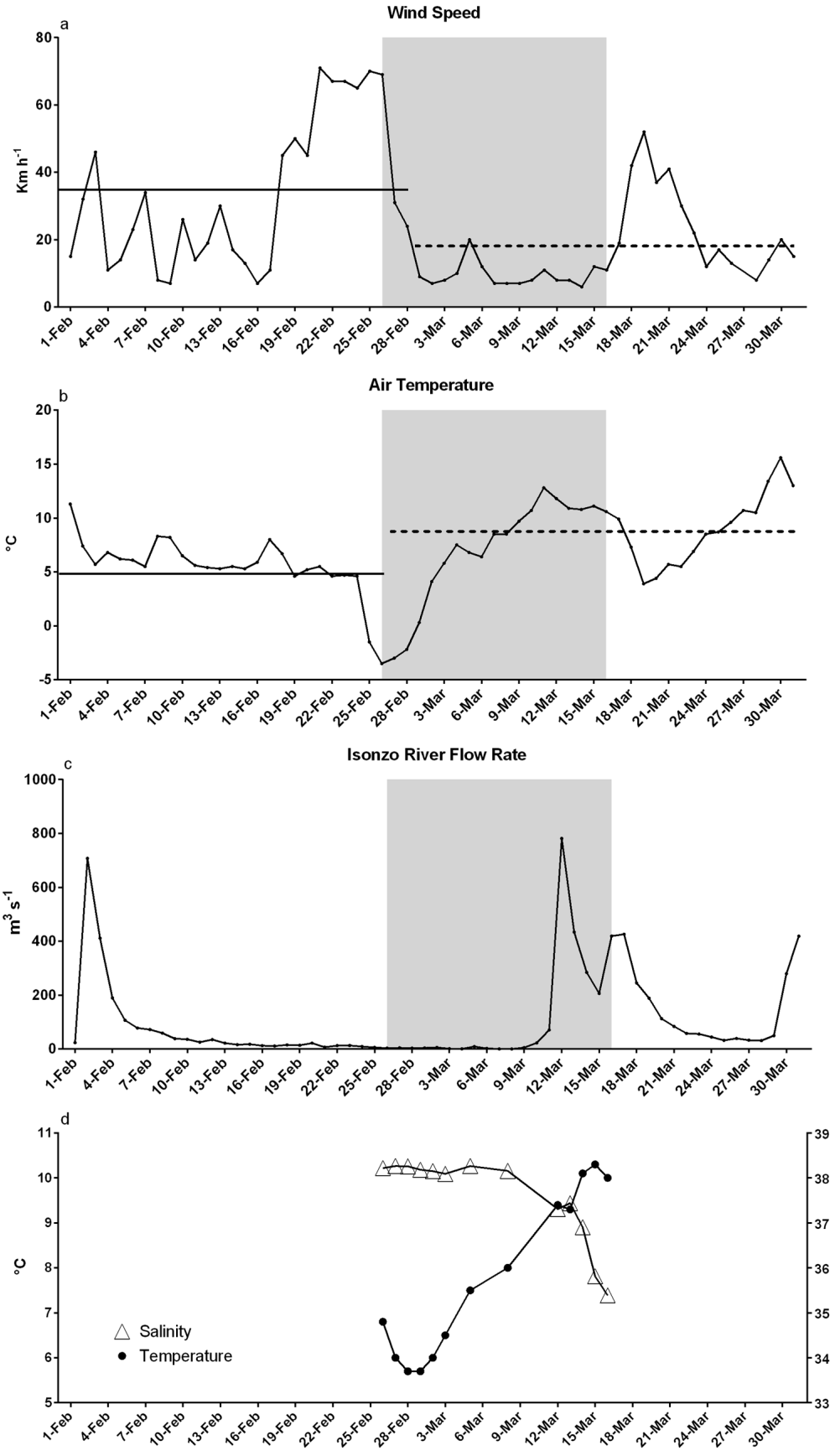

Figure 3.1: (Caption on the next page)

Figure 3.1: Time courses of a) wind speed, b) air temperature, c) Isonzo river discharge and d) water temperature and salinity. a), b) and c) represent daily averaged values for February and March 2018; d) depicts values measured during sampling. Horizontal lines on a) and b) indicate February (solid) and March (dashed) monthly average. Shaded areas in a), b) and c) indicate the sampling time frame.

concentrations were measured from 8th-12th to 16th March. Chlorophyll a concentration pattern followed those of the inorganic nutrients, i.e. mildly decreasing until 5th March (0.12 µg L^{-1}), then increasing until 14th March (0.55 µg L^{-1}) and finally declining until the end of the sampling period.

Table 3.1: Results of chemical analyses. POC=particulate organic C, PN=particulate N, DIN=dissolved inorganic N, PO_4=phosphate, $Si(OH)_4$=silicate, Chl *a*=chlorophyll *a*. Units are indicated in parentheses.

	26 Feb	27 Feb	28 Feb	1 Mar	2 Mar	3 Mar	5 Mar	8 Mar	12 Mar	13 Mar	14 Mar	15 Mar	16 Mar
POC (µM)	6.32	4.39	4.16	4.27	4.06	4.04	3.18	4.29	8.31	6.30	7.03	11.11	11.34
PN (µM)	1.04	0.54	0.46	0.43	0.46	0.50	0.33	0.38	1.24	1.20	1.12	2.08	2.06
DIN (µM)	1.27	1.49	1.51	1.69	1.70	1.67	1.47	1.91	3.64	3.09	3.66	5.61	4.50
PO_4 (µM)	0.02	0.02	0.03	0.03	0.03	0.02	0.02	0.03	0.05	0.05	0.04	0.03	0.01
$Si(OH)_4$ (µM)	3.18	3.31	3.45	4.04	3.37	3.58	3.26	3.20	4.34	3.59	5.10	6.00	5.17
Chl *a* (µg L^{-1})	0.30	0.23	0.20	0.16	0.24	0.18	0.12	0.14	0.36	0.33	0.55	0.44	0.49

3.3.3. Microbial community

SYN cell number (Fig. B.4) showed an overall negative trend during the sampling period (3.11 and 2.13 × 10^7 cell L^{-1} on 26th February and 16th March, respectively), characterised by a steep decline in the first days which, after a small peak on 3rd March, continued until 12th March, when the lowest abundance was measured (1.00 × 10^7 cell L^{-1}). Afterwards, a mildly increasing, but oscillating, trend continued until the end of sampling.

Heterotrophic prokaryotes abundance (Fig. 3.2a) ranged between 3.26 and 6.15 × 10^8 cell L^{-1}, with the highest values at the beginning of the sampling period, i.e. between 26th and 28th February. HP cell number dropped on 1st March, mildly decreasing until 5th March, when the minimum was measured. Between 12th and 16th March, HP abundance rose sharply and reached values comparable to those measured at the beginning of the sampling period. The initial (26th February - 8th March) prokaryotic assemblage was composed by a roughly equal proportion of high- and low- nucleic acid (HNA and LNA, respectively) cells, with an average HNA percent contribution to total HP abundance of 50.5 ± 3.9% (Fig. 3.2a). The subsequent increase in total prokaryotic abundance was instead dominated by HNA cells, which accounted for 68 ± 3.3% of total HP cell count between 12th and 16th March.

HNF abundance (Fig. B.5) showed an overall positive trend, increasing from 0.44 × 10^6 cell L^{-1} on 26th February to 2.44 x 10^6 cell L^{-1} on 16th March, characterised by lower and constant values in the first sampling days (26th February – 5th March, 0.39 ± 0.08 × 10^6 cell L^{-1}). Afterwards, HNF abundance steeply increased until 16th March,

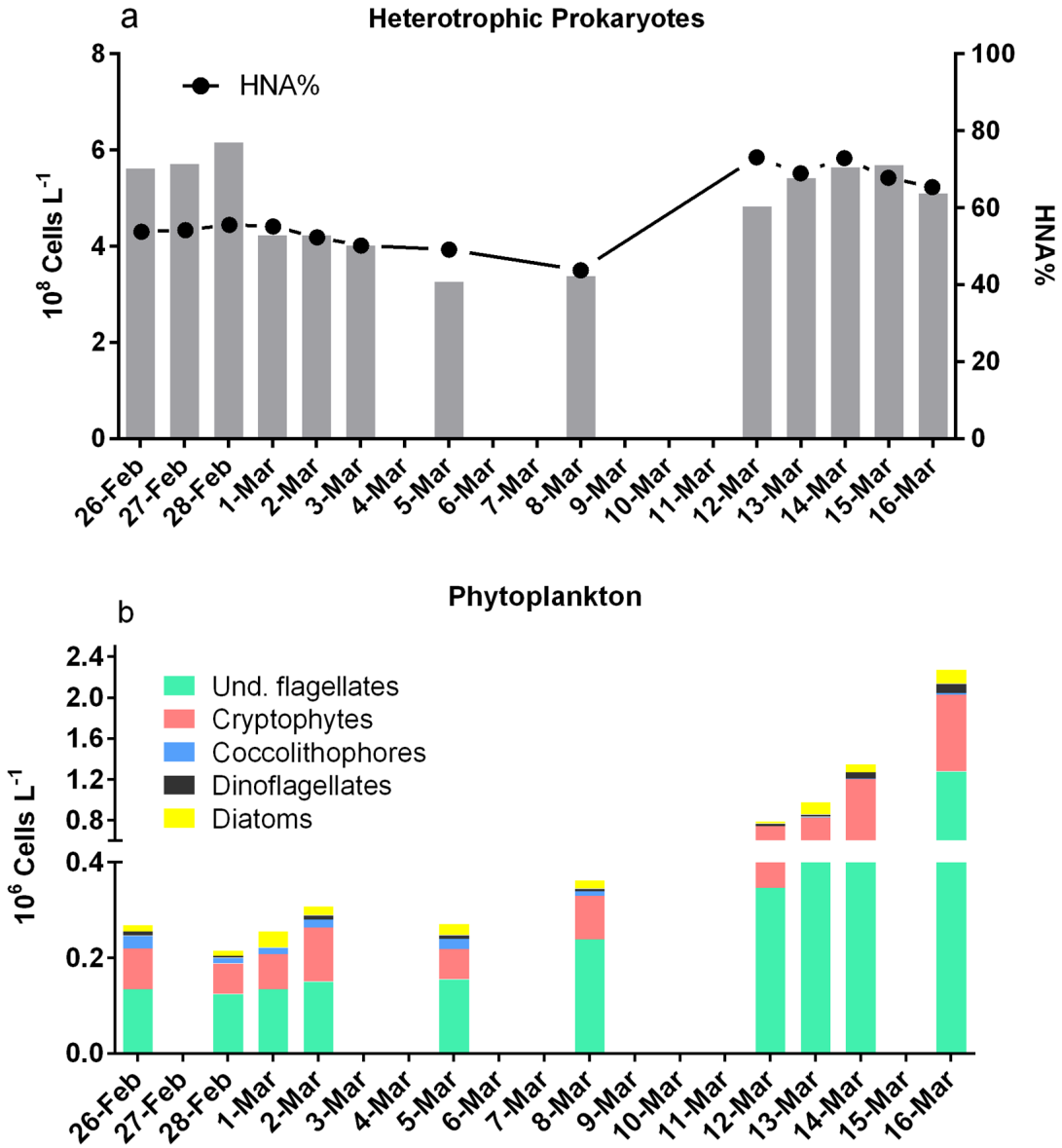

Figure 3.2: Time series of a) heterotrophic prokaryotes and relative contribution of HNA cells and b) phytoplankton abundance during the sampling period. Note that the Y-axis in b) is not linear.

when the maximum cell number was measured.

VLP abundance (Fig. B.6) ranged between 5.02 and 12.25 × 10 VLP L^{-1}, decreasing rapidly between 26th February and 28th February, when the minimum abundance was measured. Then, a steep increase took place, reaching the highest abundance on 15th March, slightly decreasing on the last sampling day.

Total phytoplankton abundance (Fig. 3.2b) ranged between 0.26 × 10^6 and 2.27 × 10^6 cell L^{-1}, with the highest and lowest values at the beginning and at the end of the sampling period, respectively. Throughout the sampling period, phytoplankton community was dominated by undetermined flagellates and cryptophytes (52.9 ± 6.5% and 33.5 ± 8.2%, respectively) while diatoms (2.5 – 13.1%), dinoflagellates (0.4 – 4.5%) and coccolithophorids (0.3 – 9.9%) contributed to a lesser extent.

3.3.4. Microbial metabolic activity

Time courses of enzymatic activities (EEAs) are reported in Fig. 3.3a and b. Overall, the EEAs tested showed low or decreasing hydrolysis rates between 26th February and 8th March. Afterwards, higher exoenzymatic activities were observed. β-glucosidase (BGLU, Fig. 3.3a) hydrolysis rates ranged between 0.69 ± 0.03 and 2.69 ± 0.12 nM h^{-1}, with minimum and maximum values on 27th February and 16th March, respectively. This activity was rather variable during the first part of the sampling period, peaking to near maximum (2.37 ± 0.10 nM h^{-1}) on 2nd March and then dropping again (0.80 ± 0.09 nM h^{-1}) on 5th March. β-galactosidase (BGAL, Fig. 3.3a) presented both the lowest and the highest hydrolysis rates (0.22 ± 0.01 and 4.02 ± 0.14 nM h^{-1}, respectively) among the tested glycolytic enzymes. BGAL activity mildly declined until 8th March, steadily increased until 15th March and finally dropped on the last sampling day. Chitinase (CHIT, Fig. 3.3a) activity was characterised by a slight decline from 26th February to 8th March (1.39 ± 0.02 and 1.06 ± 0.02 nM h^{-1}, respectively), followed by a ~3-fold increase on 12th March (3.07 ± 0.08 nM h^{-1}). Leucine aminopeptidase (AMA, Fig. 3.3b) rates were rather constant from 26th February to 8th March (5.94 ± 0.20 nM h^{-1}, on average). Then, AMA activity increased steeply until 15th March (39.67 ± 1.91 nM h^{-1}) and dropped on 16th March (28.37 ± 0.44 nM h^{-1}). With overall lower hydrolysis rates (0.58 ± 0.00 and 31.19 ± 1.37nM h^{-1}), lipase (LIP, Fig. 3.3b) followed the same pattern of AMA.

Minimum and maximum activities were respectively registered on 5th and 15th March, with a decrease of ~50% on the last sampling day. Alkaline phosphatase activity (AP, Fig. 3.3b) showed an overall increasing pattern (3.70 ± 0.35 - 14.94 ± 0.22 nM h^{-1}), with the lowest hydrolysis rates between 27th February and 1st March. Heterotrophic carbon production (Fig. 3.3c) followed the general trend described for the EEAs. Low and constant values (0.02 ± 0.00 µC L^{-1} h^{-1}) were observed from 26th February to 8th March and were, on average, 10-fold higher (0.20 ± 0.06 µgC L^{-1} h^{-1}) from 12th to 16th March, although quite variable.

3.3.5. Statistical analyses

The cluster analysis applied to EEAs and HCP gathered the samples in two main groups (Fig. 3.4). The first, formed by the samples collected from 26th February to 8th March, was characterised by low hydrolysis and HCP rates. By contrast, the

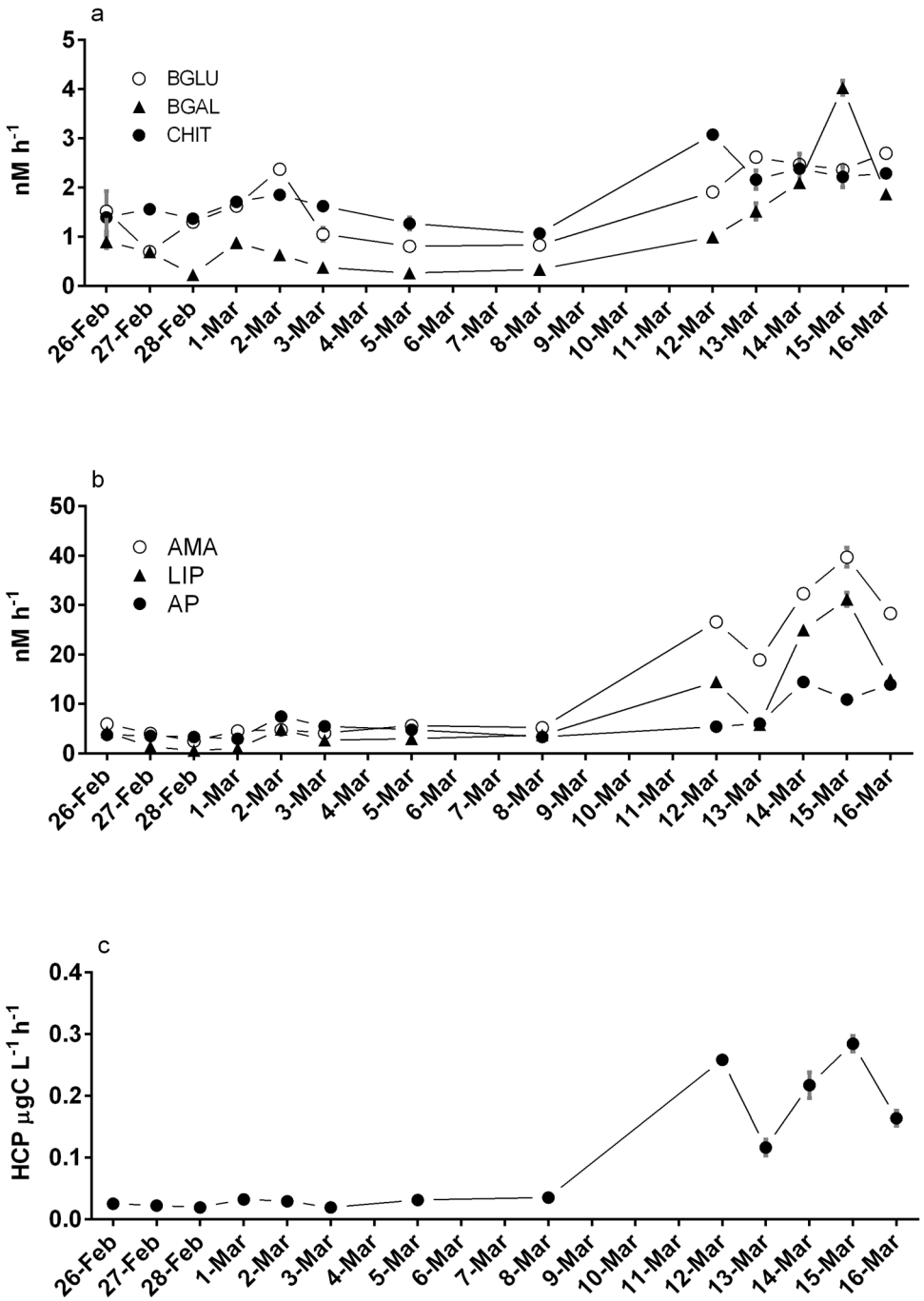

Figure 3.3: Time series of a) and b) exoenzymatic activities and c) heterotrophic carbon production Error bars represent the standard deviation of three analytical replicates. BGLU=β-glucosidase, BGAL=β-galactosidase, AP=alkaline phosphatase, LIP=lipase, CHIT=chitinase, AMA=leucine aminopeptidase, HCP=heterotrophic carbon production.

second group gathered the samples with faster microbial-mediated processes, i.e. those from 12th to 16th March (Fig. 3.4).

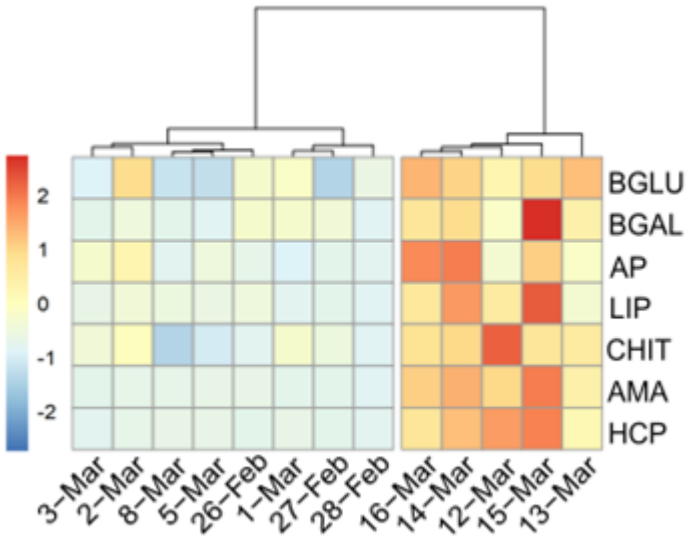

Figure 3.4: Clustered heatmap of exoenzymatic activities and heterotrophic carbon production. The dendrogram was built from a Bray-Curtis distance matrix, using Ward's minimum variance as aggregation method. The heat map depicts relative hydrolysis (EEAs) and leucine uptake (HCP) rates. For each variable, values were standardized, and the colour scale was balanced so that the blue colour will represent lower values and the red colour higher values. BGLU=β-glucosidase, BGAL=β-galactosidase, AP=alkaline phosphatase, LIP=lipase, CHIT=chitinase, AMA=leucine aminopeptidase, HCP=heterotrophic carbon production.

The rates measured during the temperature manipulation experiments were compared with those measured at *in situ* conditions (Fig 3.5). Overall, almost no significant effect of the temperature lowering was observed among samples gathered in the cold-affected cluster. Only BGLU hydrolysis rates were significantly different between *in situ* (control) and lowered temperature treatments (Friedman ANOVA, $N=6$, $p<0.05$), with lower velocities at *in situ*-2°C than in the control (Wilcoxon Matched Pairs Test, $Z=2.20$, $p<0.05$). The higher EEAs rates that characterised the samples of the second cluster (12th – 16th March, Fig. 3.5) decreased along with temperature. Friedman ANOVA highlighted significant differences between control and treatments for BGLU ($N=5$, $df=2$, $p<0.01$), CHIT ($N=5$, $df=2$, $p<0.05$), AMA ($N=5$, $df=2$, $p<0.01$) and HCP ($N=5$, $df=2$, $p<0.05$). BGLU and AMA activities were significantly different between all treatments (Wilcoxon Matched Pairs Test, $Z=2.02$, $p<0.05$). CHIT activity measured at *in situ*-2°C was significantly lower than the ones measured at *in situ* and *in situ*-1°C (Wilcoxon Matched Pairs Test, $Z=2.02$, $p<0.05$). Leucine incorporation rates at *in situ*-2°C were significantly lower than those at *in situ* temperature (Wilcoxon Matched Pairs Test, $Z=2.02$, $p<0.05$).

The computed February, March and annual climatology is presented in Table 2, alongside with values measured in the cold-affected and recovery periods (i.e., 26th February – 8th March and 12th – 16th March, respectively).

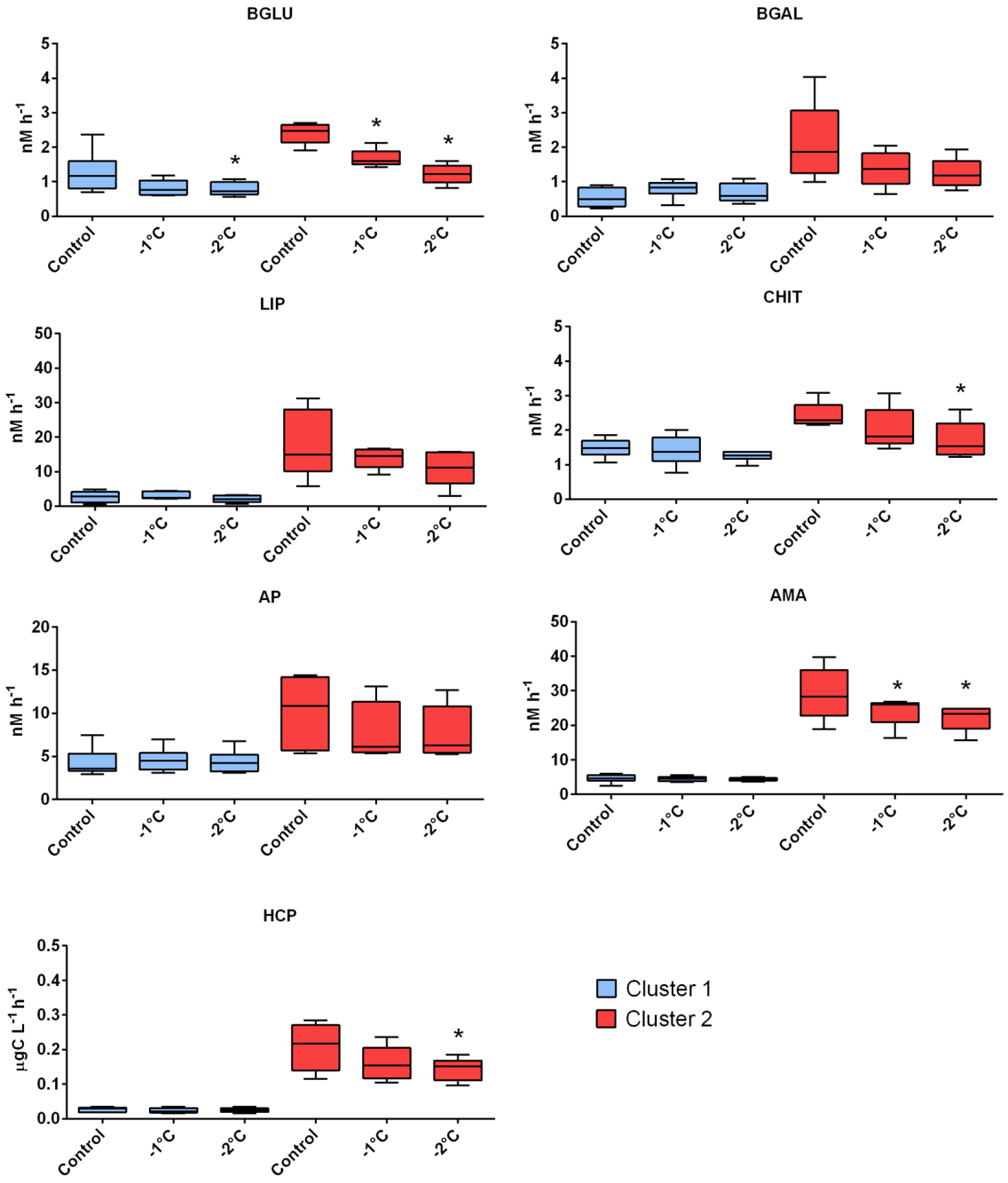

Figure 3.5: Box and whiskers plots of hydrolysis rates (EEAs, nM h-1) and heterotrophic carbon production µgC L^{-1} h^{-1}) during the experimental temperature manipulations. Samples included in cluster 1 (n=6) are coloured in blue, samples in cluster 2 (n=5) in red. Control=incubation at *in situ* temperature; -1°C=incubation at *in situ* temperature lowered by 1°C; -2°C=incubation at *in situ* temperature lowered by 2°C. Significant differences between treatments and control are indicated with an asterisks (*=p<0.05). BGLU=β-glucosidase, BGAL=β-galactosidase, AP=alkaline phosphatase, LIP=lipase, CHIT=chitinase, AMA=leucine aminopeptidase, HCP=heterotrophic carbon production.

Table 3.2: Median and interquartile ranges (in parentheses) of sampled parameters in cold-affected and recovery period, compared with February, March and annual climatologies computed on surface values (~-0.5m) measured at st. C1 from 2000 to 2017. PO_4=phosphate; DIN=dissolved inorganic nitrogen; POC=particulate organic carbon; Chl *a*=chlorophyll a; DOC=dissolved organic carbon; SYN=*Synechococcus* abundance; HP=heterotrophic prokaryotes abundance; HNF=heterotrophic nanoflagellates abundance; VLP=virus-like particles abundance. Units are given in parentheses.

	Cold-affected Period	Recovery Period	February Climatology	March Climatology	Annual Climatology
Temperature (°C)	6.25 (5.92 - 6.97)	10.00 (9.40 - 10.10)	8.39 (7.12 - 9.34)	9.42 (8.69 - 10.12)	15.65 (10.78 - 20.83)
Salinity	38.20 (38.15 - 38.25	36.90 (35.81 - 37.30)	37.51 (37.21 - 37.97)	37.57 (36.86 - 37.84)	37.33 (36.79 - 37.70)
PO_4 (µM)	0.02 (0.02 - 0.02)	0.03 (0.02 - 0.04)	0.04 (0.02 - 0.06)	0.03 (0.02 - 0.07)	0.04 (0.02 - 0.07)
DIN (µM)	1.58 (1.48 - 1.69)	3.65 (3.63 - 4.49)	2.33 (1.89 - 4.96)	3.06 (1.26 - 4.53)	2.09 (1.19 - 3.45)
POC (µM)	3.87 (3.73 - 4.00)	8.30 (7.02 - 10.70)	18.2 (13.04 - 20.93)	19.98 (19.06 - 21.29)	16.99 (12.19 - 22.06)
Chl *a* (µg L^{-1})	0.18 (0.15 - 0.22)	0.44 (0.36 - 0.48)	0.86 (0.55 - 1.13)	0.58 (0.41 - 0.88)	0.76 (0.48 - 1.11)
DOC (µM)	NA	NA	81 (75.76 - 83.73)	84.09 (77.42 - 84.50)	96.91 (84.29 - 112.24)
SYN* (10^7 Cell L^{-1})	1.64 (1.34 - 1.95)	1.52 1.43 - 2.04)	0.64 (0.45 - 0.84)	1.2 (0.78 - 1.79)	2.84 (1.45 - 5.89)
HP* (10^8 Cell L^{-1})	4.23 (3.85 - 5.64)	5.41 (5.09 - 5.64)	4.75 (3.82 - 5.67)	4.13 (4.01 - 4.24)	10.39 (6.84 - 13.72)
HNF* (10^6 Cell L^{-1}	0.45 (0.34 - 0.48)	1.60 (1.19 - 2.04)	1.16 (1.16 - 1.16)	1.51 (1.38 - 1.65)	1.77 (1.36 - 2.37)
VLP* (10^9 VLP L^{-1})	6.48 (5.99 - 6.96)	10.42 (10.33 - 10.83)	14.32 (14.32 - 14.32)	17.31 (16.12 - 18.43)	24.32 (19.23 - 30.13)

NA=not available; *=climatology computed only for 2016 and 2017.

3.4. Discussion

In In the Gulf of Trieste, the annual variability of temperature and salinity is mainly controlled by wind stress and freshwater inputs (Lipizer et al., 2012) therefore extreme meteorological events greatly affect the hydrological properties of this landlocked basin. Following the Bora event between 26th February and 8th March, both surface water temperature and salinity (Fig. 3.1d) deviated from the basin climatology (2000-2017, Table 3.2), falling closer to values previously measured in the area as the effect of intense, long-lasting cold air outbreaks (e.g., February 2012, Mihanović et al., 2013). The unusually higher values of surface salinity were due to a limited freshwater runoff at the sampling station (Fig. 3.1c) and wind-enhanced evaporation. Given the importance of riverine inputs in supplying the Gulf of Trieste with inorganic nutrients and organic matter (Cozzi and Giani, 2011), the limited freshwater inputs would explain the remarkably low dissolved inorganic nitrogen concentration (Table 3.2) between 26th February and 8th March, as up to 60% of inorganic N in the area is supplied by riverine inputs (Cozzi et al., 2014). A highly significant negative correlation was found between nutrients and salinity (Spearman's rank correlation: salinity vs. DIN, ρ_s=-0.92, p<0.001; salinity vs. POC, ρ_s=-0.80, p<0.001) suggesting that the increased nutrients (inorganic and organic) availability between 12th and 16th March (Table 3.1) was due to the re-established freshwater supply in the area (Fig. 3.1c).

As pointed out by several phytoplankton and Chl *a* time series data (Bernardi Aubry et al., 2012; Cabrini et al., 2012; Mozetič et al., 2010), because of a reduced freshwater discharge, the northern Adriatic Sea and the Gulf of Trieste are experiencing a progressive oligotrophication, inducing a shift towards a small cells-dominated phytoplankton community. Albeit on a much smaller spatial and temporal scale, this general framework applies also in the present study. Indeed, the reduced freshwater inputs in the sampling area following the cold-outbreak (Fig. 3.1c) may have concurred to induce a transient oligotrophy between 26th February and 8th March, affecting the phytoplankton abundance and composition at the sampling station. Remarkably, this condition prevented (or postponed) the onset of the late-winter diatom bloom, usually occurring in the area in late February – early March, a phenomenon often observed in the Gulf of Trieste when the river runoff is reduced (Cabrini et al., 2012). The autotrophic community was instead dominated by small cells (i.e., undetermined flagellates and cryptophytes, Fig. 3.2b), with a consistent contribution of SYN in the first part of the sampling period (Fig. B.4 and Table 3.2). Indeed, due to their high surface to volume ratio, smaller cells are able to outcompete bigger cells in nutrient-limiting conditions, because of their higher efficiency in nutrients utilization (Moutin et al., 2002). The overall dominance of small phytoplankton taxa observed in the present study (Fig. 3.2b) determined an exceptionally low phytoplanktonic biomass (Chl *a* lower than median climatological values, 2000 - 2017, Table 3.2), suggesting a limited system (primary) productivity (Finkel et al., 2010).

Since heterotrophic prokaryotes consume up to 50% of the carbon fixed by phytoplankton in the marine environment (Fuhrman and Azam, 1982), a reduced primary productivity would greatly affect prokaryotic dynamics. Indeed, except for the period between 26th and 28th February, the trend of prokaryotic abundance (Fig. 3.2a) mirrored the variability pattern of Chl *a* (Table 3.1), implying a tight dependence of prokary-

otic growth on phytoplankton-derived organic matter. Over the sampling period, fluctuations of HP abundance (Fig. 3.2a) over time were mostly due to the variability of the HNA fraction. The two main NA fractions (i.e., HNA and LNA) could be dissimilar due to distinct cell or genome size, physiological state (Bouvier et al., 2007) or even to taxonomic community composition (Vila-Costa et al., 2012), thus implying a different response of the two fractions to environmental changes. Since the cytometric signature of a prokaryotic assemblage retains all these information, phylogenetic or metabolic changes can be inferred through cytometric fingerprinting (Props et al., 2016; Quiroga et al., 2017; Wanderley et al., 2019).

Over the sampling period, cytograms clustered according to their relative contribution of the HNA fraction to the bulk of HP, identifying three distinct groups (Fig. B.3). The first cluster (1st – 5th March) grouped samples characterised by the lowest values of Chl *a*, DIN, POC and HP, with a higher contribution of LNA cells (Fig. 3.2a), highlighting the development of a peculiar prokaryotic assemblage following the Bora outbreak, which persisted several days after the event ceased. Initial (26th – 28th February) and final (12th, 14th – 16th March) assemblages, were gathered together (Fig. B.3) displaying similar optical features, despite a rather different metabolic pattern (Fig. 3.4). The different cytometric properties of the prokaryotic assemblage analysed in the present study may thus be mainly due to shifts in the physiological/metabolic state of the cells, rather to changes in the microbial community phylogenetic structure. These results agree with the findings of several *in situ*, modelling and experimental studies (Bouvier et al., 2007; Gasol et al., 1999; Morán et al., 2007; Zubkov et al., 2004), suggesting a relationship between the trophic status of the system and the contribution of NA fractions to the bulk of heterotrophic prokaryotes. High nucleic acid cells can be viewed as “opportuni-trophs”, i.e. they are able to capitalize their genomic flexibility by exploiting the heterogeneous organic matter produced by actively growing phytoplankton. Conversely, LNA cells, also because of their smaller genomes, are able to thrive under oligotrophic conditions focusing on a narrower range of substrates (Polz et al., 2006).

Consistently with this view, the HNA abundance positively correlated with Chl *a* (Spearman’s rank correlation: ρ_s=0.84, p<0.001), suggesting that the variability pattern of the HNA fraction was significantly controlled by phytoplankton-derived organic matter availability. This is in agreement with the results of Morán et al., 2010, who reported a higher degree of bottom-up control on the HNA fraction in cooler waters. Since predation by HNF and viral lysis are considered the main top-down controlling factors on HP abundance (Hunter and Price, 1992), the lack of any significant relationship between HP and HNF or VLP abundance (Spearman’s rank correlation: HP vs HNF, ρ_s=0.26, p>0.05; HP vs VLP, ρ_s=0.45, p>0.05) would indicate a limited top-down control on the HP community, at least during the cold-affected period, when the HNF abundance was at its minimum (Fig. B.5).

The functional cluster analysis (Fig. 3.4) highlighted a sharp temporal pattern during the sampling period. The modification of the biogeochemical features of the sampling area following the wind outbreak (i.e., 26th February to 8th March, Table 3.2) exerted an inhibitory effect on the microbial metabolic rates. A subsequent functional recovery (i.e., increased exoenzymatic activities, carbon production and planktonic

respiration rates, Fig. 3.3 and Fig. B.2) was evident from 12th to 16th March, when biogeochemical variables showed ranges comparable to the long-term climatology of the sampling area (Table 3.2). Higher metabolic rates were coupled with higher temperature, with AMA, LIP and HCP showing the tightest correlations (Spearman's rank correlation: Temperature vs. AMA, ρ_s=0.93, p<0.001; Temperature vs. LIP, ρ_s=0.91, p<0.001; Temperature vs. HCP, ρ_s=0.85, p<0.001). Leucine aminopeptidase activity is implicated in the recovery of amino acids and labile polypeptides (Sala et al., 2001), while lipase is involved in the hydrolysis of a wide range of phosphorous- and carbon-containing organic compounds (Gupta et al., 2004). AMA and LIP reached the fastest hydrolysis rates (39.67 and 31.19 nM h^{-1}, respectively, Fig. 3.3b), highlighting the importance of these generalists, broad-spectrum enzymes in supplying readily utilizable substrates to microbial metabolism (Baltar et al., 2017). While enhancing the total exoenzymatic activity, higher temperature induced a decrease in the proportion of cell-free relative to total EEA (Appendix B.1.1, Fig. B.1; Spearman's rank correlation: Temperature vs % cell-free BGAL, ρ_s=-0.80, p<0.01; Temperature vs % cell-free AP, ρ_s=-0.67, p<0.05; Temperature vs % cell-free AMA, ρ_s=-0.74, p<0.05). Despite the narrow temperature range considered in the present study, these results agree with the findings of several investigations (Baltar, 2018 and references therein), highlighting that temperature is one of the main controlling factors affecting the activity and the contribution of cell-free relative to total EEA.

Four of the assayed exoenzymatic activities showed a strong inverse correlation with salinity (Spearman's rank correlation: salinity vs. BGLU, ρ_s=-0.80, p<0.001; salinity vs. BGAL, ρ_s=-0.78, p<0.01; salinity vs. AP, ρ_s=-0.78, p<0.01; salinity vs. CHIT, ρ_s=-0.82, p<0.001; salinity vs. LIP, ρ_s=-0.82, p<0.001), suggesting that a significant fraction of the organic matter fuelling the microbial metabolism was related to freshwater inputs. Indeed, organic matter loads in the Gulf of Trieste are mainly driven by river runoff (Lipizer et al., 2012) either by direct advection of land-born organic matter or by delivering inorganic nutrients, which in turn stimulate autochthonous organic matter production. In the present study, no measure of dissolved organic carbon (DOC) concentration was carried out. Literature values in the study area (De Vittor et al., 2008) report an annual DOC concentration range between 72.51 and 138.50 µM (Table 3.2), with winter minima and late summer maxima. Values of DOC concentration measured during previous cold events (i.e., February 2012 and January 2017) were within the ranges of the climatological variability in the area (76.33 and 73.34 µM for February 2012 and January 2017, respectively, Table 3.2, C. De Vittor, unpublished data), suggesting that the magnitude of the DOC pool is not substantially altered during intense cold-outbreaks in the Gulf of Trieste. Therefore, in terms of substrate availability, the variability in the measured metabolic rates is more likely related to POC dynamics rather than to those of the dissolved organic matter pool.

In the present study, glycolytic activities (BGLU and BGAL, Fig. 3.3a) had the lowest hydrolysis rates among the tested EEAs. These results agree with previous surveys conducted in the Northern Adriatic Sea (Celussi et al., 2011; Celussi and Del Negro, 2012; Celussi et al., 2015) generally reporting slower BGLU and BGAL hydrolysis rates in comparison to other EEAs. Since Chl *a* concentration measured over the sampling period was exceptionally low (Table 3.2), the slow glycolytic rates can

be viewed as a consequence of the lack of suitable substrate, as polysaccharide hydrolysis is reported to be substrate-inducible (Sinsabaugh and Follstad Shah, 2012). However, Celussi et al., 2015 reported pronounced affinities of BGLU and BGAL for their substrates, suggesting that the low activity can, in turn, be compensated by the higher hydrolytic performance of the enzymes. Furthermore, BGLU was the only EEA which did not show a significant relationship with temperature, a condition already reported for the study area (Celussi and Del Negro, 2012), although over a much broader temperature range. Considering that polysaccharides are estimated to support 20% of prokaryotic production in marine ecosystems (Kirchman, 2003; Piontek et al., 2011), it is possible that heterotrophic prokaryotes adopt a metabolic strategy aimed at producing highly-performing, thermostable (over a well-defined temperature range) glycolytic enzymes in order to cope with the broad biogeochemical variability of coastal systems. The results of temperature manipulation experiments (Fig. 3.5) would confirm this hypothesis, as BGLU was the only extracellular enzyme that showed temperature-dependent hydrolysis rates in the cold-affected period. All the other tested hydrolysis rates were not affected by the experimental temperature lowering (Fig. 3.5), suggesting that the exceptionally low water temperature, coupled with the limited substrate availability during the cold-affected period, represented a lower thermal limit for the microbial processing of organic matter. The results of temperature manipulation experiments in samples belonging to the recovery cluster (12th – 16th March) are more ambiguous, as only BGLU, CHIT and AMA showed decreased hydrolysis rates with temperature (Fig. 3.5). This result might be explained by a different degree of temperature-substrate control on each EEA. Enzymes showing a temperature-dependence in the second cluster (i.e., with potentially non-limiting substrate concentrations and warmer water) could be more controlled by the kinetic effect of temperature, while hydrolytic activities not suppressed by the lowered temperature, are more prone to be affected by a substrate-induced feedback mechanism.

HCP rates measured during the cold-affected period were not significantly affected by the experimental temperature lowering (Fig. 3.5), suggesting that the temperature drop that followed the Bora event pushed carbon production rates at their lower thermal limit. Since between 26th February and 8th March both HNF and VLP abundances were lower than climatological values (Table 3.2), it is likely that microbial growth during the cold-affected period was mainly bottom-up controlled. The lack of the Arrhenius' linear response of HCP to temperature (Fig. 3.6) of samples gathered in the first cluster, corroborate the hypothesis that microbial growth during the cold-affected period was mainly controlled by bottom-up factors, such as temperature and substrate availability (Pomeroy and Wiebe, 2001). A similar response of HCP to temperature in the middle and central Adriatic Sea was reported by Šolić et al., 2017, who found a major effect of P-limitation in controlling prokaryotic growth rates at a lower temperature (i.e., <16°C). In the present study, the AP to AMA ratio, often used as a proxy of P-limitation of microbial communities (Sala et al., 2001; Williams and Jochem, 2006), was always low (<2) indicating that the prokaryotic community was not limited by the inorganic phosphorous availability, in agreement with previous findings reported for the study area (Celussi and Del Negro, 2012). Thus, as suggested by the low Chl *a* concentration between 26th February and 8th March (Table 3.1), the non-linearity of the HCP - temperature relation during the cold affected period was likely to be due

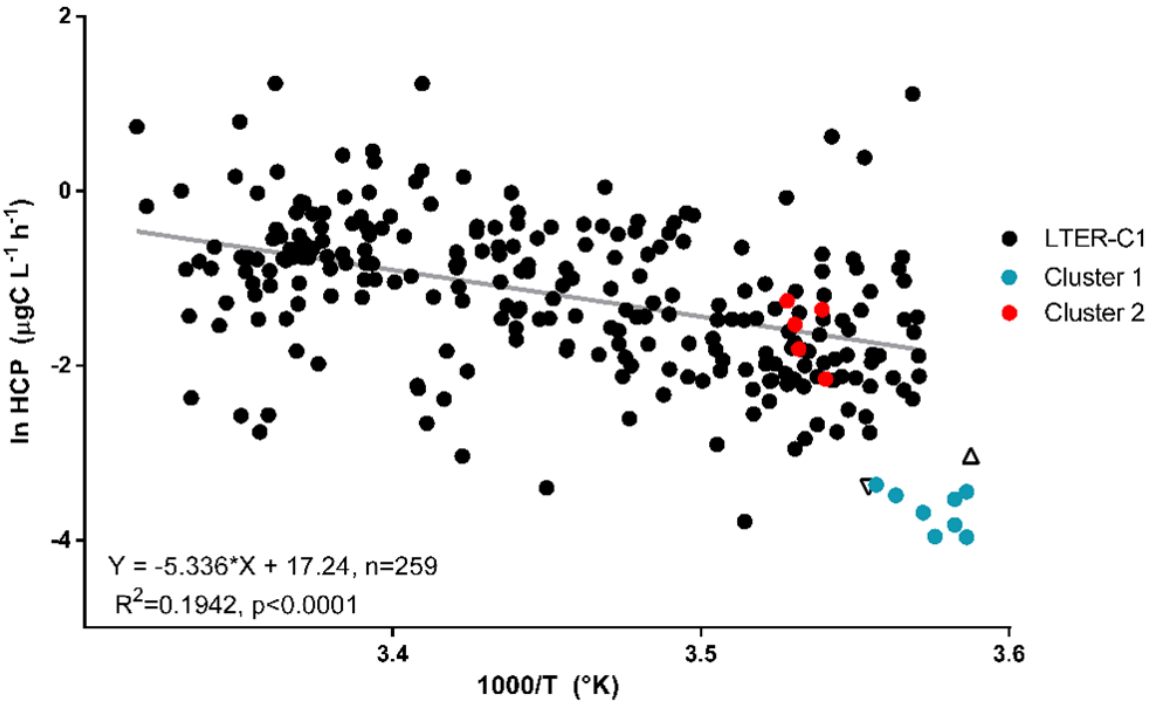

Figure 3.6: Arrhenius plot of the natural logarithm of the heterotrophic carbon production (ln HCP) against the inverse absolute temperature (1000/T) of values measured during sampling (marked in blue and red for samples in cluster 1 and 2, respectively) and at LTER-C1 from 2000 to 2017 in the surface layer (in black). The grey line represents the linear regression trendline. Upward and downward triangles mark HCP rates measured in February 2012 and January 2017, respectively.

to the reduced availability of organic substrates, which, coupled with the anomalous temperature drop, exceptionally constrained prokaryotic growth following the intense Bora outbreak. The low rates of planktonic respiration during the cold affected period (Appendix B.1.2, Fig. B.2) would support this hypothesis, further implying that the basal prokaryotic metabolism was extremely limited, even several days after the event ceased (1st – 5th March). Noteworthy, HCP rates measured in February 2012 and January 2017 at the LTER – C1 sampling station fell in the same range of rates measured in the present study (Fig. 3.6), suggesting a systematic limitation of the prokaryotic carbon production following intense cold outbreaks in the northernmost basin of the Mediterranean Sea.

Comparing our data with the trophodynamics scheme developed by Fonda Umani et al., 2012, conceptualizing the pelagic winter carbon fluxes in the Gulf of Trieste, we found a 98% reduction of the phytoplankton carbon stock following the Bora outbreak. This result highlighted an exceptionally reduced carbon transfer to higher trophic levels via the classical grazing food web (i.e., microphytoplankton->zooplankton->fishes). Conversely, we found a 61% increase of SYN carbon reservoir, confirming the shift towards a smaller photoautotrophic community during the cold-affected period. In addition, this comparison underlined a 21% decrease in HP biomass, which was coupled with a similar reduction of HNF carbon stock (22%), indicating that also the carbon flux mediated by the microbial food web was compromised following the intense

Bora event. Indeed, we found an average HCP of 0.64 ± 0.14 µg C L^{-1} d^{-1} during the cold-affected period, which, compared to the winter value reported by Fonda Umani et al. (2012) (7.00 µg C L^{-1} d^{-1}) pinpoints an extremely reduced microbe-mediated carbon channelling to higher trophic levels. Although these computations are referred to the study area, similar scenarios can be envisioned in other coastal systems characterised by strong Bora outbreaks, such as the Croatian coast of the Adriatic Sea (Vilibić and Supić, 2005) or the northern Black Sea coast (Onea and Rusu, 2014), as well as in temperate areas affected by other katabatic winds, such as, for example, the Mistral in the Gulf of Lion (Wrathall, n.d.) or the Oroshi in the central-east Japan (Kurose et al., 2002).

3.5. Conclusions

The intense and long-lasting Bora outbreak registered in the Gulf of Trieste in late February 2018 remarkably modified the biogeochemistry of its coastal system, inducing a transient oligotrophy which determined an exceptionally low organic matter availability throughout the cold-affected period. The sudden drop in temperature induced by the cold outbreak constrained the microbial processing of organic matter, inducing a "cold-footprint" (i.e., the time window comprised between 2nd and 8th March characterised by lower metabolic rates despite being not directly affected by the temperature drop), which further inhibited the functional metabolic recovery once the event ceased. Furthermore, our results demonstrate that following intense and long-lasting Bora outbreaks, the prokaryotic growth is exceptionally constrained by the interactive effect of temperature and substrate availability. By limiting the microbial processing of organic matter, extreme meteorological events of this kind have the potential to affect the structure of local trophic webs, altering the functioning of the entire planktonic compartment for several days during and after the onset of the phenomenon.

Acknowledgements

We would like to thank B. Cataletto for his help in sampling activities, F. Malfatti for her suggestions during the experimental activities, F. Relitti for POC and PN, L. Urbini for inorganic nutrients analysis , the calibration facility of the OGS in Trieste (OGS-CTO) for salinity analysis and M. Giani for providing Isonzo river discharge data. We thank A. Franzo for her suggestions during the early stages of the manuscript preparation. This study was partly supported by fundings from the Friuli Venezia Giulia autonomous region and from the flagship project RITMARE – La Ricerca ITaliana per il MARE (coordinated by the National Research Council and funded by the Italian Ministry of Education, University and Research).

References

Arrhenius, S. (1889). Über die Reaktionsgeschwindigkeit bei der Inversion von Rohrzucker durch Säuren. *Zeitschrift für Physikalische Chemie*, *4U*(1). https://doi.org/10.1515/zpch-1889-0416

Artegiani, A., Azzolini, R., & Salusti, E. (1989). On dense water in the Adriatic Sea. *Oceanologica Acta*, *12*, 151–160.

Azam, F., & Malfatti, F. (2007). Microbial structuring of marine ecosystems. *Nature Reviews Microbiology*, *5*(10), 782–791. https://doi.org/10.1038/nrmicro1747

Baltar, F. (2018). Watch out for the "living dead : Cell-free enzymes and their fate. *Frontiers in Microbiology*, *8*(JAN), 2438. https://doi.org/10.3389/fmicb.2017.02438

Baltar, F., Morán, X. A. G., & Lønborg, C. (2017). Warming and organic matter sources impact the proportion of dissolved to total activities in marine extracellular enzymatic rates. *Biogeochemistry*, *133*(3), 307–316. https://doi.org/10.1007/s10533-017-0334-9

Bernardi Aubry, F., Cossarini, G., Acri, F., Bastianini, M., Bianchi, F., Camatti, E., De Lazzari, A., Pugnetti, A., Solidoro, C., & Socal, G. (2012). Plankton communities in the northern Adriatic Sea: Patterns and changes over the last 30 years. *Estuarine, Coastal and Shelf Science*, *115*, 125–137. https://doi.org/10.1016/j.ecss.2012.03.011

Bouvier, T., del Giorgio, P. A., & Gasol, J. M. (2007). A comparative study of the cytometric characteristics of High and Low nucleic-acid bacterioplankton cells from different aquatic ecosystems. *Environmental Microbiology*, *9*(8), 2050–2066. https://doi.org/10.1111/j.1462-2920.2007.01321.x

Brock, G., Pihur, V., Datta, S., & Datta, S. (2008). clValid: An R Package for Cluster Validation. *Journal of Statistical Software; Vol 1, Issue 4 (2008)*. https://www.jstatsoft.org/v025/i04

Brussaard, C. P. (2004). Viral control of phytoplankton populations - A review. *Journal of Eukaryotic Microbiology*, *51*(2), 125–138. https://doi.org/10.1111/j.1550-7408.2004.tb00537.x

Cabrini, M., Fornasaro, D., Cossarini, G., Lipizer, M., & Virgilio, D. (2012). Phytoplankton temporal changes in a coastal northern Adriatic site during the last 25 years. *Estuarine, Coastal and Shelf Science*, *115*, 113–124. https://doi.org/10.1016/j.ecss.2012.07.007

Caron, D., Lim, E., Miceli, G., Waterbury, J., & Valois, F. (1991). Grazing and utilization of chroococcoid cyanobacteria and heterotrophic bacteria by protozoa in laboratory cultures and a coastal plankton community. *Marine Ecology Progress Series*, *76*, 205–217. https://doi.org/10.3354/meps076205

Celio, M., Comici, C., & Bussani, A. (2002). Thermohaline Anomalies in the Spring and Early Summer of 2000 in the Gulf of Trieste. *Marine Ecology*, *23*(s1), 101–110. https://doi.org/10.1111/j.1439-0485.2002.tb00011.x

Celussi, M., Bussani, A., Cataletto, B., & Del Negro, P. (2011). Assemblages' structure and activity of bacterioplankton in northern Adriatic Sea surface waters: A 3-year case study: Northern Adriatic Sea bacterioplankton assemblages. *FEMS*

Microbiology Ecology, *75*(1), 77–88. https://doi.org/10.1111/j.1574-6941.2010.00997.x

Celussi, M., & Del Negro, P. (2012). Microbial degradation at a shallow coastal site: Long-term spectra and rates of exoenzymatic activities in the NE Adriatic Sea. *Estuarine, Coastal and Shelf Science*, *115*, 75–86. https://doi.org/10.1016/j.ecss.2012.02.002

Celussi, M., Fabbro, C., Bastianini, M., Urbani, R., & Del Negro, P. (2015). Polysaccharide degradation and utilisation during a spring phytoplankton bloom in the north-western Adriatic Sea. *Hydrobiologia*, *757*(1), 209–222. https://doi.org/10.1007/s10750-015-2253-x

Celussi, M., Malfatti, F., Ziveri, P., Giani, M., & Del Negro, P. (2017). Uptake-release dynamics of the inorganic and organic carbon pool mediated by planktonic prokaryotes in the deep Mediterranean Sea. *Environmental Microbiology*, *19*(3), 1163–1175. https://doi.org/https://doi.org/10.1111/1462-2920.13641

Christaki, U., Courties, C., Massana, R., Catala, P., Lebaron, P., Gasol, J. M., & Zubkov, M. V. (2011). Optimized routine flow cytometric enumeration of heterotrophic flagellates using SYBR Green I: FC analysis of HF. *Limnology and Oceanography: Methods*, *9*(8), 329–339. https://doi.org/10.4319/lom.2011.9.329

Chróst, R. J. (1992). Significance of bacterial ectoenzymes in aquatic environments. *Hydrobiologia*, *243-244*(1), 61–70. https://doi.org/10.1007/BF00007020

Cibic, T., Cerino, F., Karuza, A., Fornasaro, D., Comici, C., & Cabrini, M. (2018). Structural and functional response of phytoplankton to reduced river inputs and anomalous physical-chemical conditions in the Gulf of Trieste (northern Adriatic Sea). *Science of The Total Environment*, *636*, 838–853. https://doi.org/10.1016/j.scitotenv.2018.04.205

Comici, C., & Bussani, A. (2007). Analysis of the River Isonzo discharge (1998-2005). *Bollettino di Geofisica Teorica ed Applicata*, *48*, 435–454.

Cozzi, S., Falconi, C., Comici, C., Čermelj, B., Kovac, N., Turk, V., & Giani, M. (2012). Recent evolution of river discharges in the Gulf of Trieste and their potential response to climate changes and anthropogenic pressure. *Estuarine, Coastal and Shelf Science*, *115*, 14–24. https://doi.org/10.1016/j.ecss.2012.03.005

Cozzi, S., & Giani, M. (2011). River water and nutrient discharges in the Northern Adriatic Sea: Current importance and long term changes. *Continental Shelf Research*, *31*(18), 1881–1893. https://doi.org/10.1016/j.csr.2011.08.010

Cozzi, S., Mistaro, A., Sparnocchia, S., Colugnati, L., Bajt, O., & Toniatti, L. (2014). Anthropogenic loads and biogeochemical role of urea in the Gulf of Trieste. *Science of The Total Environment*, *493*, 271–281. https://doi.org/10.1016/j.scitotenv.2014.05.148

De Vittor, C., Paoli, A., & Fonda Umani, S. (2008). Dissolved organic carbon variability in a shallow coastal marine system (Gulf of Trieste, northern Adriatic Sea). *Estuarine, Coastal and Shelf Science*, *78*(2), 280–290. https://doi.org/10.1016/j.ecss.2007.12.007

Ducklow, H. W., & Carlson, C. A. (1992). Oceanic Bacterial Production. In K. C. Marshall (Ed.), *Advances in Microbial Ecology* (pp. 113–181). Springer US. https://doi.org/10.1007/978-1-4684-7609-5_3

Finkel, Z. V., Beardall, J., Flynn, K. J., Quigg, A., Rees, T. A. V., & Raven, J. A. (2010). Phytoplankton in a changing world: Cell size and elemental stoichiometry. *Journal of Plankton Research*, *32*(1), 119–137. https://doi.org/10.1093/plankt/fbp098

Fonda Umani, S., Malfatti, F., & Del Negro, P. (2012). Carbon fluxes in the pelagic ecosystem of the Gulf of Trieste (Northern Adriatic Sea). *Estuarine, Coastal and Shelf Science*, *115*, 170–185. https://doi.org/10.1016/j.ecss.2012.04.006

Fuhrman, J. A., & Azam, F. (1982). Thymidine incorporation as a measure of heterotrophic bacterioplankton production in marine surface waters: Evaluation and field results. *Marine Biology*, *66*(2), 109–120. https://doi.org/10.1007/BF00397184

Gasol, J. M., Zweifel, U. L., Peters, F., Fuhrman, J. A., & Hagström, A. (1999). Significance of size and nucleic acid content heterogeneity as measured by flow cytometry in natural planktonic bacteria. *Applied and environmental microbiology*, *65*(10), 4475–4483. https://doi.org/10.1128/AEM.65.10.4475-4483.1999

Gupta, R., Gupta, N., & Rathi, P. (2004). Bacterial lipases: An overview of production, purification and biochemical properties. *Applied Microbiology and Biotechnology*, *64*(6), 763–781. https://doi.org/10.1007/s00253-004-1568-8

Hansen, H. P., & Koroleff, F. (1999). Determination of nutrients. In K. Grasshoff, K. Kremling, & M. Ehrhardt (Eds.), *Methods of Seawater Analysis* (pp. 159–228). Wiley-VCH Verlag GmbH. https://doi.org/10.1002/9783527613984.ch10

Hillebrand, H., Dürselen, C.-D., Kirschtel, D., Pollingher, U., & Zohary, T. (1999). BIOVOLUME CALCULATION FOR PELAGIC AND BENTHIC MICROALGAE. *Journal of Phycology*, *35*(2), 403–424. https://doi.org/10.1046/j.1529-8817.1999.3520403.x

Hoppe, H.-G. (1993). Use of Fluorogenic Model Substrates for Extracellular Enzyme Activity (EEA) Measurement of Bacteria. In P. F. Kemp, B. F. Sherr, E. B. Sherr, & J. J. Cole (Eds.), *Handbook of Methods in Aquatic Microbial Ecology* (1st ed., pp. 423–431). Routledge. https://doi.org/10.1201/9780203752746-49

Hunter, M. D., & Price, P. W. (1992). Playing Chutes and Ladders: Heterogeneity and the Relative Roles of Bottom-Up and Top-Down Forces in Natural Communities. *Ecology*, *73*(3), 724–732. https://doi.org/10.2307/1940152

Karlson, B., Cusack, C., & Bresnan, E. (2010). Microscopic and molecular methods for quantitative phytoplankton analysis.

Kirchman, D., K'nees, E., & Hodson, R. (1985). Leucine incorporation and its potential as a measure of protein synthesis by bacteria in natural aquatic systems. *Applied and Environmental Microbiology*, *49*(3), 599–607. https://aem.asm.org/content/49/3/599

Kirchman, D. (2003). The Contribution of Monomers and other Low-Molecular Weight Compounds to the Flux of Dissolved Organic Material in Aquatic Ecosystems. *Aquatic Ecosystems* (pp. 217–241). Elsevier. https://doi.org/10.1016/B978-012256371-3/50010-X

Kolde, R. (2019). *Pheatmap: Pretty Heatmaps*. https://CRAN.R-project.org/package=pheatmap

Kurose, Y., Ohba, K., Maruyama, A., & Maki, T. (2002). Characteristics of Local Wind "aso Oroshi". *Journal of Agricultural Meteorology*, *58*(2), 93–101. https://doi.org/10.2480/agrmet.58.93

Lee, C. M., Askari, F., Book, J., Carniel, S., Cushman-Roisin, B., Dorman, C., Doyle, J., Flament, P., Harris, C. K., Jones, B. H., Kuzmic, M., Martin, P., Ogston, A., Orlic, M., Perkins, H., Poulain, P.-M., Pullen, J., Russo, A., Sherwood, C., … Thaler, D. (2005). Northern Adriatic response to a wintertime bora wind event. *Eos, Transactions American Geophysical Union*, *86*(16), 157. https://doi.org/10.1029/2005EO160001

Lee, S., & Fuhrman, J. A. (1987). Relationships between Biovolume and Biomass of Naturally Derived Marine Bacterioplankton. *Applied and environmental microbiology*, *53*(6), 1298–1303. https://doi.org/10.1128/AEM.53.6.1298-1303.1987

Lipizer, M., De Vittor, C., Falconi, C., Comici, C., Tamberlich, F., & Giani, M. (2012). Effects of intense physical and biological forcing factors on CNP pools in coastal waters (Gulf of Trieste, Northern Adriatic Sea). *Estuarine, Coastal and Shelf Science*, *115*, 40–50. https://doi.org/10.1016/j.ecss.2012.03.024

Lorenzen, C., & Jeffrey, S. (1980). Determination of chlorophyll in seawater. *Unesco technical papers in marine sciences*, *35*(1), 1–20.

Luna, G. M., Chiggiato, J., Quero, G. M., Schroeder, K., Bongiorni, L., Kalenitchenko, D., & Galand, P. E. (2016). Dense water plumes modulate richness and productivity of deep sea microbes: Dense waters influence on bacterioplankton. *Environmental Microbiology*, *18*(12), 4537–4548. https://doi.org/10.1111/1462-2920.13510

Malačič, V., Celio, M., Čermelj, B., Bussani, A., & Comici, C. (2006). Interannual evolution of seasonal thermohaline properties in the Gulf of Trieste (northern Adriatic) 1991–2003. *Journal of Geophysical Research*, *111*(C8), C08009. https://doi.org/10.1029/2005JC003267

Marie, D., Brussaard, C. P. D., Thyrhaug, R., Bratbak, G., & Vaulot, D. (1999). Enumeration of Marine Viruses in Culture and Natural Samples by Flow Cytometry. *Applied and Environmental Microbiology*, *65*(1), 45–52. https://doi.org/10.1128/AEM.65.1.45-52.1999

Martinez, J., & Azam, F. (1993). Penplasmic aminopeptidase and alkaline phosphatase activities in a marine bacterium- implications for substrate processing in the sea. *Marine Ecology Progress Series*, *92*, 89–97. https://doi.org/10.3354/meps092089

Menden-Deuer, S., & Lessard, E. J. (2000). Carbon to volume relationships for dinoflagellates, diatoms, and other protist plankton. *Limnology and Oceanography*, *45*(3), 569–579. https://doi.org/10.4319/lo.2000.45.3.0569

Mihanović, H., Vilibić, I., Carniel, S., Tudor, M., Russo, A., Bergamasco, A., Bubić, N., Ljubešić, Z., Viličić, D., Boldrin, A., Malačič, V., Celio, M., Comici, C., & Raicich, F. (2013). Exceptional dense water formation on the Adriatic shelf in the winter of 2012. *Ocean Science*, *9*(3), 561–572. https://doi.org/10.5194/os-9-561-2013

Milller, C. B. (2004). The spring phytoplankton bloom. In C. B. Miller (Ed.), *Biological Oceanography* (pp. 1–19). Blackwell Publishing.

Morán, X., Bode, A., Suárez, L., & Nogueira, E. (2007). Assessing the relevance of nucleic acid content as an indicator of marine bacterial activity. *Aquatic Microbial Ecology*, *46*, 141–152. https://doi.org/10.3354/ame046141

Morán, X., Calvo-Díaz, A., & Ducklow, H. (2010). Total and phytoplankton mediated bottom-up control of bacterioplankton change with temperature in NE Atlantic

shelf waters. *Aquatic Microbial Ecology*, *58*, 229–239. https://doi.org/10.3354/ame01374

Morán, X. A. G., Gasol, J. M., Pernice, M. C., Mangot, J. F., Massana, R., Lara, E., Vaqué, D., & Duarte, C. M. (2017). Temperature regulation of marine heterotrophic prokaryotes increases latitudinally as a breach between bottom-up and top-down controls. *Global Change Biology*, *23*(9), 3956–3964. https://doi.org/10.1111/gcb.13730

Moutin, T., Thingstad, T. F., Van Wambeke, F., Marie, D., Slawyk, G., Raimbault, P., & Claustre, H. (2002). Does competition for nanomolar phosphate supply explain the predominance of the cyanobacterium Synechococcus? *Limnology and Oceanography*, *47*(5), 1562–1567. https://doi.org/10.4319/lo.2002.47.5.1562

Mozetič, P., Solidoro, C., Cossarini, G., Socal, G., Precali, R., Francé, J., Bianchi, F., De Vittor, C., Smodlaka, N., & Fonda Umani, S. (2010). Recent Trends Towards Oligotrophication of the Northern Adriatic: Evidence from Chlorophyll a Time Series. *Estuaries and Coasts*, *33*(2), 362–375. https://doi.org/10.1007/s12237-009-9191-7

Murtagh, F., & Legendre, P. (2014). Ward's Hierarchical Agglomerative Clustering Method: Which Algorithms Implement Ward's Criterion? *Journal of Classification*, *31*(3), 274–295. https://doi.org/10.1007/s00357-014-9161-z

Oksanen, J., Blanchet, F. G., Friendly, M., Kindt, R., Legendre, P., McGlinn, D., Minchin, P. R., O'Hara, R. B., Simpson, G. L., Solymos, P., Stevens, M. H. H., Szoecs, E., & Wagner, H. (2019). *Vegan: Community Ecology Package*. https://CRAN.R-project.org/package=vegan

Olenina, I., Hajdu, S., Edler, L., Andersson, A., Wasmund, N., Busch, J., Göbel, J., Gromisz, S., Huseby, S., Huttunen, M., Jaanus, A., Kokkonen, P., Ledaine, I., & Niemkiewicz, E. (2006). Biovolumes and size-classes of phytoplankton in the baltic sea. *HELCOM Baltic Sea Environment Proceedings*, 144.

Onea, F., & Rusu, E. (2014). Wind energy assessments along the Black Sea basin: Wind energy assessments in the Black Sea. *Meteorological Applications*, *21*(2), 316–329. https://doi.org/10.1002/met.1337

Otto, F. E. L., Philip, S., Kew, S., Li, S., King, A., & Cullen, H. (2018). Attributing high-impact extreme events across timescales—a case study of four different types of events. *Climatic Change*, *149*(3-4), 399–412. https://doi.org/10.1007/s10584-018-2258-3

Pella, E., & Colombo, B. (1973). Study of carbon, hydrogen and nitrogen determination by combustion-gas chromatography. *Mikrochimica Acta*, *61*(5), 697–719. https://doi.org/10.1007/BF01218130

Piontek, J., Händel, N., De Bodt, C., Harlay, J., Chou, L., & Engel, A. (2011). The utilization of polysaccharides by heterotrophic bacterioplankton in the Bay of Biscay (North Atlantic Ocean). *Journal of Plankton Research*, *33*(11), 1719–1735. https://doi.org/10.1093/plankt/fbr069

Polz, M. F., Hunt, D. E., Preheim, S. P., & Weinreich, D. M. (2006). Patterns and mechanisms of genetic and phenotypic differentiation in marine microbes. *Philosophical transactions of the Royal Society of London. Series B, Biological sciences*, *361*(1475), 2009–2021. https://doi.org/10.1098/rstb.2006.1928

Pomeroy, L. R., & Wiebe, W. J. (2001). Temperature and substrates as interactive limiting factors for marine heterotrophic bacteria. *Aquatic Microbial Ecology*, *23*(2), 187–204. https://doi.org/10.3354/ame023187

Props, R., Monsieurs, P., Mysara, M., Clement, L., & Boon, N. (2016). Measuring the biodiversity of microbial communities by flow cytometry (D. Hodgson, Ed.). *Methods in Ecology and Evolution*, *7*(11), 1376–1385. https://doi.org/10.1111/2041-210X.12607

Quiroga, M. V., Mataloni, G., Wanderley, B. M. S., Amado, A. M., & Unrein, F. (2017). Bacterioplankton morphotypes structure and cytometric fingerprint rely on environmental conditions in a sub-Antarctic peatland. *Hydrobiologia*, *787*(1), 255–268. https://doi.org/10.1007/s10750-016-2969-2

R Core Team. (2019). *R: A Language and Environment for Statistical Computing*. R Foundation for Statistical Computing. https://www.R-project.org/

Robinson, A., Leslie, W., Theocharis, A., & Lascaratos, A. (2001). Mediterranean Sea Circulation. *Encyclopedia of Ocean Sciences* (pp. 1689–1705). Elsevier. https://doi.org/10.1006/rwos.2001.0376

Sala, M., Karner, M., Arin, L., & Marrasé, C. (2001). Measurement of ectoenzyme activities as an indication of inorganic nutrient imbalance in microbial communities. *Aquatic Microbial Ecology*, *23*, 301–311. https://doi.org/10.3354/ame023301

Sharp, J. H. (1974). Improved analysis for "particulate" organic carbon and nitrogen from seawater1. *Limnology and Oceanography*, *19*(6), 984–989. https://doi.org/10.4319/lo.1974.19.6.0984

Simon, M., & Azam, F. (1989). Protein content and protein synthesis rates of planktonic marine bacteria. *Marine Ecology Progress Series*, *51*, 201–213. https://doi.org/10.3354/meps051201

Sinsabaugh, R. L., & Follstad Shah, J. J. (2012). Ecoenzymatic Stoichiometry and Ecological Theory. *Annual Review of Ecology, Evolution, and Systematics*, *43*(1), 313–343. https://doi.org/10.1146/annurev-ecolsys-071112-124414

Smith, D. C. (1992). A simple, economical method for measuring bacterial protein synthesis rates in seawater using 3H-leucine. *Marine Microbial Food Webs*, *6*(2), 107–114.

Šolić, M., Krstulović, N., Šantić, D., Šestanović, S., Kušpilić, G., Bojanić, N., Ordulj, M., Jozić, S., & Vrdoljak, A. (2017). Impact of the 3 °C temperature rise on bacterial growth and carbon transfer towards higher trophic levels: Empirical models for the Adriatic Sea. *Journal of Marine Systems*, *173*, 81–89. https://doi.org/10.1016/j.jmarsys.2017.01.001

Steen, A. D., & Arnosti, C. (2011). Long lifetimes of β-glucosidase, leucine aminopeptidase, and phosphatase in Arctic seawater. *Marine Chemistry*, *123*(1-4), 127–132. https://doi.org/10.1016/j.marchem.2010.10.006

Stravisi, F. (1977). Bora driven circulation in northern Adriatic. *Bollettino di Geofisica Teorica e Applicata*, *19*, 95–102.

Throndsen, J. (1978). Preservation and storage. *Phytoplankton manual* (pp. 69–74). Unesco.

Utermöhl, H. (1958). Zur vervollkommnung der quantitativen phytoplankton-methodik: Mit 1 Tabelle und 15 abbildungen im Text und auf 1 Tafel. *Internationale Vereinigung für theoretische und angewandte Limnologie: Mitteilungen*, *9*(1), 1–38.

Vila-Costa, M., Gasol, J. M., Sharma, S., & Moran, M. A. (2012). Community analysis of high- and low-nucleic acid-containing bacteria in NW Mediterranean coastal waters using 16S rDNA pyrosequencing: Bacterial composition of different cytometric populations in Mediterranean waters. *Environmental Microbiology*, *14*(6), 1390–1402. https://doi.org/10.1111/j.1462-2920.2012.02720.x

Vilibić, I., & Supić, N. (2005). Dense water generation on a shelf: The case of the Adriatic Sea. *Ocean Dynamics*, *55*(5-6), 403–415. https://doi.org/10.1007/s10236-005-0030-5

Vojvoda, J., Lamy, D., Sintes, E., Garcia, J., Turk, V., & Herndl, G. (2014). Seasonal variation in marine-snow-associated and ambient-water prokaryotic communities in the northern Adriatic Sea. *Aquatic Microbial Ecology*, *73*(3), 211–224. https://doi.org/10.3354/ame01718

Wanderley, B. M. S., A. Araújo, D. S., Quiroga, M. V., Amado, A. M., Neto, A. D. D., Sarmento, H., Metz, S. D., & Unrein, F. (2019). flowDiv: A new pipeline for analyzing flow cytometric diversity. *BMC Bioinformatics*, *20*(1), 274. https://doi.org/10.1186/s12859-019-2787-4

Weiss, M. S., Abele, U., Weckesser, J., Welte, W., Schiltz, E., & Schulz, G. E. (1991). Molecular architecture and electrostatic properties of a bacterial porin. *Science*, *254*(5038), 1627–1630. https://doi.org/10.1126/science.1721242

Wiebe, W. J., Sheldon, W. M., & Pomeroy, L. R. (1992). Bacterial Growth in the Cold: Evidence for an Enhanced Substrate Requirement. *Applied and Environmental Microbiology*, *58*(1), 359–364. https://aem.asm.org/content/58/1/359

Wiebe, W. J., Sheldon, W. M., & Pomeroy, L. R. (1993). Evidence for an enhanced substrate requirement by marine mesophilic bacterial isolates at minimal growth temperatures. *Microbial Ecology*, *25*(2), 151–159. https://doi.org/10.1007/BF00177192

Williams, C. J., & Jochem, F. J. (2006). Ectoenzyme kinetics in Florida Bay: Implications for bacterial carbon source and nutrient status. *Hydrobiologia*, *569*(1), 113–127. https://doi.org/10.1007/s10750-006-0126-z

Wrathall, J. E. (n.d.). The mistral and forest fires in provence côte d'azur, southern france. *Weather*.

Zubkov, M., Allen, J., & Fuchs, B. (2004). Coexistence of dominant groups in marine bacterioplankton community—a combination of experimental and modelling approaches. *Journal of the Marine Biological Association of the United Kingdom*, *84*(3), 519–529. https://doi.org/10.1017/S002531540400952Xh

4

Prokaryotic Response to Phytodetritus-Derived Organic Material in Epi- and Mesopelagic Antarctic Waters

This Chapter is adapted from: Manna V., Malfatti F., Banchi E., Cerino F., De Pascale .F, Franzo A., Schiavon R., Vezzi A., Del Negro, P. and Celussi, M., 2020. Prokaryotic Response to Phytodetritus-Derived Organic Material in Epi- and Mesopelagic Antarctic Waters. Frontiers in Microbiology, 11:1242. https://doi.org/10.3389/fmicb.2020.01242

4.1. Introduction

Whether organic particles derive from phytoplankton, zooplankton or dissolved organic matter (DOM) aggregation, they represent a hotspot of microbial activity in aquatic ecosystems (Grossart and Simon, 1993; Kiørboe, 2001). To process and consume the particulate organic matter (POM), particle-associated microbes need a complex suite of enzymes that hydrolyze high molecular weight (HMW) substrates, but not all microorganisms possess the enzymatic capabilities to hydrolyze all organic matter moieties (Arnosti, 2011; Kiørboe et al., 2002). On one hand, this means that the POM quality selects for a subset of microbes, capable to degrade that specific pool of organic matter (Kiørboe et al., 2004). On the other hand, selective degradation of particles' constituents leads to shifts in quality and quantity of carbon, driving changes in the particle-associated community over time (Datta et al., 2016). Therefore, changes in POM composition will affect the dynamics of the associated communities (Eiler and Bertilsson, 2004; Grossart, 1999; Grossart et al., 2005; LeCleir et al., 2014).

The export of POM represents the underlying principle of the biological carbon pump which annually removes about one third of anthropogenic atmospheric CO_2 via the export of organic carbon produced by phytoplankton in the euphotic ocean toward the deep ocean (Boyd et al., 2019; Sabine et al., 2004). The POM settling rate is a central factor in determining the efficiency of carbon sequestration: the deeper the particles sink, the longer the carbon of which they are made will be removed from the atmospheric and upper-oceanic reservoirs (Kwon et al., 2009; Passow and Carlson, 2012). However, only a small fraction, between 5 and 25% of the POM produced in the upper ocean, reaches the mesopelagic realm (Buesseler and Boyd, 2009; Rocha and Passow, 2007). Organic particles are indeed subjected to remineralization as they sink to the ocean interior, leading to the release of CO_2 and DOM and causing a reduction in the biological carbon pump efficiency (Rocha and Passow, 2007). Remineralization processes are mainly carried out by particle-associated prokaryotes, which can respire more than 70% of the sinking POM (Giering et al., 2014).

The Southern Ocean (SO) makes up approximately 10% of the world's ocean (Rogers et al., 2020), yet it is responsible for the ventilation of the global ocean as well as for a conspicuous drawdown (ca. 10%) of the anthropogenic CO_2 emissions (THauck et al., 2015; Turner et al., 2009). The SO is a high nutrient-low chlorophyll system because of the limitation of the primary producer growth by micronutrients such as iron (Boyd et al., 2012; Strzepek et al., 2011). Nevertheless, its coastal, shallower zones represent hotspots of primary production (Smetacek and Nicol, 2005). Among them, the Ross Sea is widely recognized as one of the most productive sectors of the SO, supporting 1/3 of its total annual productivity and accounting for more than 25% of its total CO_2 uptake (Arrigo et al., 2008; Smith et al., 2014). About half of the carbon fixed into biomass by primary producers in the Ross Sea surface layer is exported as POM in the mesopelagic system, a flux that may represent up to 40% of the global POM export (Catalano et al., 2010; Ducklow et al., 2001). Cumulative evidence demonstrates that a significant fraction of this POM is represented by healthy or at least intact phytoplankton cells (DiTullio et al., 2000; Rembauville et al., 2015; Zoccarato et al., 2016). Furthermore, Agusti et al., 2015 demonstrated that the presence at depth of phytoplankton is widespread at a global scale, unravelling a previously overlooked source

of organic matter in the dark ocean.

While marine snow associated community dynamics are well characterized by both experimental and environmental studies (e.g., Bižić-Ionescu et al., 2018; Bižić-Ionescu et al., 2015; Datta et al., 2016; Duret et al., 2019; Fontanez et al., 2015; Pelve et al., 2017), limited information exist on the degradation mechanisms of phytodetrital particles and on their associated prokaryotic communities (Becquevort and Smith, 2001; Bidle et al., 2002). To fill this gap, during austral summer 2017, we performed 8 microcosm incubation experiments by providing freshly produced algal detritus, generated from on-site collected microplankton net tows, to free-living prokaryotic communities (<1 µm) from the surface and from the mesopelagic zone (548 to 1051 m) of a coast-offshore transect in the Ross Sea. We measured the functional (i.e., extracellular enzymatic activities, heterotrophic carbon production and dark dissolved inorganic carbon uptake) as well as the taxonomic community response (16S rRNA Illumina amplicon sequencing) under the hypothesis that different detrital pools yield distinct metabolic and community shifts.

4.2. Materials and methods

4.2.1. Sampling

The sampling stations (Table 4.1 and Fig. C.1) were placed along a transect heading N-E from Terra Nova Bay based on previous studies (e.g., Celussi et al., 2009; Zoccarato et al., 2016). The sampling was performed during the XXXII Italian Antarctic Expedition in 2017. Water samples were collected by means of 12-L Niskin bottles mounted on a Rosette carousel equipped with a SBE 9/11 Plus CTD profiler. Samples were collected at surface (ca. 2 m) and at the bottom layer (ranging from 548 to 1051 m) at each of the four stations. Right after the CTD casts, 7 plankton tows were performed at each station by means of a 20-µm mesh-sized net in order to achieve collect a final plankton sample volume equal to 1.5 L. The depth of the net deployment was chosen according to the CTD chlorophyll a fluorescence profiles and ranged between 60 and 120 m (Fig. C.2).

Table 4.1: Details of the sampling stations (coordinates, bottom depth and sampling depth) in the Ross Sea.

Station	Date	Longitude (°E)	Latitude (°N)	Bottom depth	Sampling depth
B	17 Jan 2017	175.089	-74	578 m	~2;565 m
C1	01 Feb 2017	170.9092	-74.1877	563 m	~2;548 m
C2	23 Jan 2017	166.8105	-74.75716	905 m	~2;899 m
D	08 Jan 2017	164.5333	-75.12672	1057 m	~2;1051 m

4.2.2. Experimental design and setup

Microcosm (Hcl-washed 2-L Nalgene PC bottles) experiments were set-up on board the R/V Italica. Seawater was filtered through 1 µm PC filters (Whatman) in order to keep free-living prokaryotes only. The pore-size was chosen considering the cell-size frequency distribution study by La Ferla et al., 2015 in the same geographical area. For each experiment, 1 µm-filtered seawater from surface and bottom layers of the four stations was amended with phytodetritus in order to achieve final concentrations of 1 µg and 10 µg of Chlorophyll *a* equivalent per liter (hereinafter 1 µg L^{-1} and 10 µg L^{-1}, respectively). Unamended 1 µm-filtered seawater was used as control. A conceptual scheme of the experimental setup is depicted in Fig. C.3. All treatments and controls were run in experimental duplicates and were incubated in the dark, at *in situ* temperature for four days. Sampling within the microcosms were performed at day (d) 0, right after the amendments, and after 1, 2 and 4 days. The phytodetritus was generated by plankton net samples through 7 cycles of freezing (-80°C)/thawing (80°C) (Bidle and Azam, 2001). Unwashed aliquots of the detritus were then added to the 2-L microcosms containing 1µm-filtered seawater at 1 and 10 µg L^{-1} of Chlorophyll *a* equivalent (See Section 4.2.3). These pigment concentrations were selected in order to mimic mild and dense bloom conditions (e.g. Schine et al., 2016) in the Ross Sea. At every time point, samples were collected for the determination of free-living heterotrophic prokaryote abundance, viral abundance, heterotrophic carbon production rates and the activity of the exoenzymes β-glucosidase, lipase, and leucine aminopeptidase. Additional aliquots were collected at d0, and after 1 and 4 days for the estimation of the abundance of particle-attached prokaryotes. Dark Dissolved Inorganic Carbon (DDIC) fixation rates were measured only at d0 since the incubation time for the analysis was 96 h (see Section 4.2.6). At the end of the experiments, the remaining seawater volume in the PC bottles was >1.75 L. At d0 and at the end of the experiments, DNA was collected as described in Section 4.2.7.

4.2.3. Chemical analyses

Clorophyll *a* concentration in the net samples was determined by the fluorometric method by Lorenzen and Jeffrey, 1980. Briefly, triplicate 3 mL aliquots were filtered onto glass fiber filters (Whatman GF/F) and the extraction was performed with 90% v/v acetone at 4°C in the dark for 4 h (Holm-Hansen et al., 1965). Holm-Hansen et al., 2000 proposed to use at least 2 h extraction incubation prior fluorometric reading for Antarctic seawater samples. This quick procedure was chosen in order to expedite the experimental setup since we needed to titrate the phytodetritus prior amendment. Fluorometric reads were performed before and after acidification with two drops of HCl 1N by means of a Shimadzu RF-1501 spectrofluorometer at 450 nm excitation and 665 nm emission wavelength. Calibration curves were made with pure Chlorophyll *a* standard from spinach (Sigma-Aldrich). The analysis of particulate and dissolved organic C concentration within the generated phytodetritus was carried out by standard protocols, as detailed in Section C.1.

4.2.4. Phytodetritus composition

The analysis of microplankton net tows was carried out by an inverted microscope (LEICA DMi8) equipped with phase contrast after fixation with neutralized formaldehyde (1.6% final concentration, f.c., Throndsen, 1978). To obtain the relative abundance of microplankton taxa, the samples were allowed to settle in a Utermöhl chamber and examined following the Utermöhl method (Utermöhl, 1958). Cell counts were performed along transects or fields at a magnification of 400× counting a minimum of 200 cells.

4.2.5. Heterotrophic prokaryotes and viruses

The abundance of free-living heterotrophic prokaryotes (FL-HP) and of virus-like particles (VLP) was estimated by flow cytometry. A FACSCanto II (Becton Dickinson) instrument was used, equipped with an air-cooled laser at 488 nm and standard filter setup. Samples (1.7 mL) were fixed with 0.5% (f.c.) glutaraldehyde solution (Grade I for EM analyses, Sigma Aldrich). Fixed samples were kept at 4°C for approximately 15 minutes and then stored at -80°C until analysis (Brussaard, 2004). Prior to enumeration, samples were thawed at room temperature and diluted 1:10 (FL-HP) and 1:50 (VLP) with 0.2 µm-filtered Tris-EDTA buffer 1× (Sigma Aldrich). Then samples were stained with SYBR Green I nucleic acid dye (Life Technologies), according to Marie et al., 1999 and Brussaard, 2004 for FL-HP and VLP, respectively. FL-HP were stained (1×, f.c.) and incubated for 10 minutes in the dark at room temperature. Virus-like particles were stained (0.5×, f.c.) and incubated for 15 minutes in the dark at 80°C. Total virus abundance was obtained by correcting the total count for noise, with 0.2 µm-filtered Tris-EDTA buffer 1× (Sigma Aldrich) as blank. Data were acquired and processed with the FACSDiva software (Becton Dickinson). The flow rate was calibrated daily, by running distilled water and weighing it before and after the run (at least 5 replicates). Abundances were then calculated using the acquired cell counts and the respective flow rates.

From the same glutaraldehyde-fixed samples, particle-attached (PA) prokaryotes were counted at the home laboratory by epifluorescence microscopy after staining the cells with 4,6-diamidino-2-phenylindole (DAPI, Sigma Aldrich) following the protocol of Porter and Feig, 1980 with slight modifications, as reported in Celussi, Malfatti, Annalisa, et al., 2017. Briefly, 1.5 mL aliquots were filtered in duplicates onto 0.2 µm black polycarbonate membranes (Whatman) that were subsequently placed on a drop (50 µL) of DAPI (30 µg mL^{-1} in an autoclaved 3.7% NaCl solution) for 15 min in the dark. The back of the filters were gently dried onto a kimwipe tissue, mounted between layers of immersion oil (Type A, Cargille) and stored at -20°C. Particle-attached prokaryotes (PA) were counted at 1000× magnification (Olympus BX 60 FS) under a UV filter set (BP 330-385 nm, BA 420 nm). A minimum of 300 cells was counted for each membrane in at least 20 randomly selected fields.

4.2.6. Microbial metabolic activities

Extracellular enzymatic activities (EEAs) were tested using fluorogenic substrate analogues derived from 7-amino-4-methylcoumarin (AMC) and 4-methylumbelliferone (MUF) (Hoppe, 1993). Leucine-aminopeptidase activity (AMA) was assayed as the

hydrolysis rate of leucine-AMC. Lipase (LIP) and β-glucosidase (BGLU) activities were assayed using MUF-oleate and MUF-β-D-glucoside (Sigma Aldrich), respectively. Hydrolysis was measured by incubating 2.5 mL subsamples with 200 µM leucine-AMC, MUF-β-D-glucoside, 100 µM MUF-oleate (saturating final concentrations, Celussi et al., 2009) for 3–7 h in the dark at *in situ* temperature. Fluorescence increase due to AMC and MUF hydrolyzed from the model substrates was measured using a Shimadzu RF-1501 spectrofluorometer (AMC= 380 nm excitation and 440 nm emission; MUF= 365 nm excitation and 455 nm emission). Triplicate calibration curves were performed daily, using 0.2 µm-filtered seawater and 5 µM standard solutions of AMC and MUF (Sigma Aldrich). EEAs were measured also on diluted (1:1000) aliquots of detritus, and hydrolysis rates were not measurable or negligible (< 0.01 nM h^{-1}).

Heterotrophic carbon production (HCP) was measured with the method of $_3$H-leucine (Leu) incorporation (Kirchman et al., 1985). Triplicate 1.7 mL subsamples and one killed control (5% trichloroacetic acid - TCA - f.c.) were amended with 20 nM radiotracer (50.2 Ci $mmol^{-1}$; Perkin Elmer) and incubated for 3–7 h in the dark at *in situ* temperature. The extraction of $_3$H-labelled proteins was carried out following the microcentrifugation method (Smith et al., 1992). After the addition of 1 mL of scintillation cocktail (Ultima Gold™ MV; Packard), the activity was determined by a TRI-CARB 2900 TR Liquid Scintillation Analyzer.

Rates of Dark Dissolved Inorganic Carbon fixation (DDIC) were determined by the incorporation of $NaH^{14}CO_3$ (Herndl et al., 2005; Yakimov et al., 2011), as described previously (Celussi, Malfatti, Ziveri, et al., 2017). Samples were collected from the microcosms at d0 in 2 replicates (40 mL each) plus one killed control (treated with 2% formalin, f.c.). Each tube was spiked with 100 µL of a $NaH^{14}CO_3$ solution (42.1 mCi $mmol^{-1}$; DHI) to yield a final activity of 0.25 µCi mL^{-1}. Samples were incubated in the dark for 96 h at *in situ* temperature and then fixed with 2% dolomite-buffered formalin. The whole volume in each tube was filtered through 0.2 µm-pore-size polycarbonate membranes (Whatman). Filters were washed twice with 10 mL of an autoclaved NaCl (3.8% w/v) solution, acidified with HCl fumes in scintillation vials for 12–16 h and frozen at -20°C. Once in the laboratory, the scintillation vials were filled with 5 mL scintillation cocktail (Filter-CountTM, Perkin Elmer) and the activity was determined by a TRICARB 2900 TR Liquid Scintillation Analyzer. The filtration and the acidification steps were performed within 24 h from fixation with formalin. DDIC was determined according to the following equation (Nielsen, 1952):

$$DDIC = \frac{DIC \times DPM_{(sample-control)} \times 1.05 \times 12}{DPM_{added} \times T}$$

where DIC is the concentration of dissolved inorganic carbon in samples (2.16 and 2.24 mmol L^{-1}, for surface and bottom experiments respectively, G. Ingrosso, unpublished data from previous surveys in the Ross Sea), 1.05 is the correction factor for slower assimilation of $_{14}$C than $_{12}$C, 12 is the molecular weight of C, $DPM_{sample-control}$ are the DPM measured in every replicate corrected for the ones in the control, DPM_{added} is the activity (certified by the provider) of the $NaH^{14}CO_3$ solution spiked in each tube and T is the incubation time.

4.2.7. DNA extraction, amplicon library preparation and sequencing

At the beginning of the experiments the native free-living prokaryotic community (1 µm-filtered) was collected on 0.2 µm polyether-sulfone membrane filters (SUPOR 200, Pall) and stored at -80°C for DNA analyses. The filtered volumes were 2 to 4 L for surface experiments and 8 L for deep water experiments. The same protocol was used at the end of the experiments (d4), by filtering the remaining volume in each bottle, approximately 1.75 L. DNA was extracted using the DNeasy PowerWater kit (Qiagen) following the manufacturer's instructions. The quantity of DNA extracts was measured by Qubit Fluorometer (ThermoFisher Scientific). Extracted DNA was stored at -20°C until further analysis.

To generate prokaryotic barcodes, the primer pair 515F-Y (5'-GTGYCAGCMGCCGC GGTAA-3') and 926R (5'-CGYCAATTYMTTTRAGTTT-3'), encompassing the V4 and V5 hypervariable loops of 16S rRNA genes (Parada et al., 2016) were used. PCR mixtures (25 µL final volume) were as follows: 5 ng of template DNA, 0.5 U of Phusion High-Fidelity DNA polymerase (ThermoFisher Scientific), 1× Phusion HF buffer, 200 µM of each dNTP, and 0.5 µM of each primer. PCR amplifications (98°C for 4 min; 25 cycles of 98°C for 20 s, 57°C for 30s, 72°C for 30s; 72°C for 5 min) were carried out in duplicate in order to smooth possible intra-sample variance. PCR products were visualized on 1.5% agarose gels, then amplicon duplicates were pooled and purified using 0.8× volumes of AMPure XP beads (Beckman Coulter). All the purified products were finally quantified with a Qubit Fluorometer (ThermoFisher Scientific).

PCR indexing and normalization were based on the "16S Metagenomic Sequencing Library Preparation" protocol provided by Illumina, with the following major modifications: 1) PCR mixtures were in 25 µL final volume, using 2.5 µL of template DNA, 0.5 U of Phusion High-Fidelity DNA polymerase (ThermoFisher Scientific), 1× Phusion HF buffer, 200 µM of each dNTP, and 5 µL of each index primer. 2) PCR amplicons were normalized using a SequalPrep Normalization Plate (ThermoFisher Scientific). Finally, amplicon libraries were equally pooled and sequenced using the Illumina MiSeq system (2 × 300 base pairs). The 16S amplicon sequences generated for this study can be found in the Sequence Reads Archive (SRA) at NCBI under the accession number PRJNA609227. All the activities described in this subsection have been carried out at University of Padova laboratories.

4.2.8. Bioinformatic pipeline

Sequenced reads from 16S amplicon libraries were analyzed with QIIME2 version 2019.7 (Bolyen et al., 2019). Denoising and amplicon sequence variants (ASVs) were identified using DADA2 (Callahan et al., 2016) QIIME2 plugin, trimming for low quality bases (q2-cutadapt DADA2 plugin; forward reads at 290 bp length and reverse reads at 220 or 240 bp according to quality; indicated lenghts refer to reads with primers included). Resulting ASVs were aligned with mafft aligner (Katoh et al., 2002) via q2-alignment plugin. The resulting multi-alignment was used to reconstruct phylogeny with fasttree2 (Price et al., 2010) via q2-phylogeny. Rarefaction curves were constructed using q2-diversity. Taxonomy was assigned to ASVs using the q2-feature classifier plugin (Bokulich et al., 2018) that embeds a naïve Bayesian taxonomy classifier against SILVA database v 132 clustered at 99% identity (Quast et al., 2013).

4.2.9. Statistical analyses

Differences in the final (d4) community structure among sampling sites, sampling depths and treatments were tested with analysis of similarity (ANOSIM) and visualized with non-metric multidimensional scaling plots (NMDS). To estimate the amount of variance associated with individual factors (station, depth and treatment), permutational multivariate analysis of variance (PERMANOVA, function *adonis* in package *vegan*, Oksanen et al., 2019) with pairwise analysis was used. All permutations tests were considered significant at $p<0.05$ with 9999 permutations. For the analyses related to beta diversity hypothesis testing, Bray-Curtis dissimilarity matrices were constructed using normalized read abundances (function *vegdist* in package *vegan*, Oksanen et al., 2019). Visualization of the microbial diversity data was done using normalized genera abundance, with the package *ggplot2* (Wickham, 2016).

The quality of 16S rRNA sequencing replicates was checked computing Spearman's rank correlation coefficients between raw ASVs counts of experimental duplicates.

The compositional change in the prokaryotic community was investigated by calculating the average (across experimental duplicates) relative abundance (RA) change of each genus (deepest taxonomic resolution). ASVs that were not present at 1% RA as a minimum, in at least one sample, were pooled as 'Others'. Changes in control samples were compared against the starting community (d0), whereas the effect of detrital particles amendments was compared against the controls. This comparison allowed to highlight both positive and negative responses of each genus to (i) the enclosure itself and (ii) to the enrichments with phytodetritus.

To test if the composition of detrital particles (i.e., taxa composition within plankton samples) drove differential response in the number of attached prokaryotes, we fitted Generalized Linear Models (GLMs) using attached prokaryotes abundance as response variable and phytodetrital composition as independent variables. Models were fitted separately for each time point (i.e., d0, d1 and d4) using the function *glm.nb* embedded in the *MASS* package (Venables and Ripley, 2013). The Shapiro-Wilk test was used to check if residuals met the assumption of normal distribution.

The Mann-Whitney test was also used to detect statistically significant differences between control and amended microcosms at day 4 and to test for significant differences in variables among two or more factors. The Spearman's rank correlation coefficient was calculated among selected variables. All the above tests were considered significant at $p<0.05$ after correction for false discovery rate (fdr, Benjamini and Hochberg, 1995). All the statistical analyses were conducted in the R environment (v. 3.6.1, R Core Team, 2019).

4.3. Results

4.3.1. Methodological considerations

The results of chemical analyses on the four detrital pools are summarized in Table C.1. To estimate the magnitude of organic C enrichments following the phytodetritus addition, we calculated the enrichment factors (EF) of DOC and POC in the

amended bottles according to Hardy et al., 1997 with the formula:

$$EF = \frac{[XOC]_{(added+environmental)}}{[XOC]_{environmental}}$$

where $[XOC]_{(added+environmental)}$ is the concentration of either DOC or POC in the amended bottles and $[XOC]_{environmental}$ is the POC or DOC environmental concentration (i.e., before the amendments). Since the seawater was filtered onto 1 µm pore size prior to the detritus enrichments, we assumed that prokaryotic cells represented the only source of POC in the pre-amended microcosms. Thus, POC concentration was calculated converting prokaryotic abundance into carbon using the conversion factor of 13 fgC Cell^{-1} derived from Carlson et al., 1999 for prokaryotic cells in the Ross Sea. Environmental DOC concentrations in surface and bottom samples were provided by F. Relitti (unpublished data).

Enrichment factors (Table C.2) for DOC ranged between 1.0 and 1.1 and from 1.2 and 2.3 for the 1 and 10 µg L^{-1} treatments, respectively. Amendments with detritus resulted in consistently higher POC enrichment factors, ranging between 6.5 and 67.7 in 1 µg L^{-1} and between 56 and 906.3 in 10 µg L^{-1}. These calculations highlight that POC enrichment factors following phytodetritus amendments were up to 2 orders of magnitude greater than DOC ones.

We are aware that some uncertainties in the metabolic rates and community composition might arise from the ambient pressure characterizing our incubations. Metabolic rates of bathypelagic prokaryotes have been shown to be overestimated at ambient pressure (Tamburini et al., 2013) while, from a community perspective, some evidence suggest that the effect might be group specific (La Cono et al., 2015). However, there still is a lack of general consensus about the effect of decompression on the metabolism of deep-sea microorganisms (Tamburini et al., 2013 and references therein). Our inferences consider both metabolic and community changes in relative terms, i.e., enhanced or suppressed by the detrital addition and/or composition. Hence, even if the absolute measured rates may be biased, our findings are likely not impaired by the depressurized incubation.

4.3.2. Phytodetritus composition

The plankton net samples used to generate the phytodetritus showed marked compositional differences among stations (Fig. 4.1). Plankton assemblages of stations B and D were dominated by *Phaeocystis antarctica*, accounting for 77 and 52% of the total pool, respectively. Diatom taxa were underrepresented in station B (4%), and accounted for 25% of microplankton cells at station D. The microplankton net sample of station C2 was instead dominated by diatom taxa, which accounted for 90% of the sampled community. Members of the *Pseudo-nitzschia* genus were the most abundant (52%), followed by the genus *Chaetoceros* (20%). A similar pattern was observed for C1 net samples, in which diatom taxa made up 50% of total pool. Representatives of the *Pseudo-nitzschia* genus were the most abundant (25%), followed by *Chaetoceros* spp. (10%). Choanoflagellates (23%) and *Phaeocystis antarctica* (18%) considerably contributed to the microplanktonic community retrieved at station C1.

4.3.3. Viruses, free-living and particle-attached prokaryotes

Experiments B and C1 showed a low variability of VLPs abundance, which was remarkably constant over time and among treatments, with similar values in surface and bottom microcosms (Fig. C.4). Bottles amended with detritus generated from the stations C2 and D showed a more variable temporal pattern, although rather similar among treatments (Fig. C.4). In C2 surface bottles, both treatments resulted in a decreasing trend over time, even though abundance values were very similar to those in control bottles. Lower VLPs abundances were measured in bottom microcosms, which showed a rather similar decreasing trend over time, regardless of the treatment. An increase of VLPs over time was measured only in bottles amended with D detritus. A steep increase, deviating from the general pattern was evident on d4 in 10 µg L^{-1}, , resulting in the highest values measured in both surface and bottom enclosures (8.19 ± 3.48 and 5.24 ± 3.19 × 10^9 VLPs L^{-1}, respectively, Fig. C.4).

Abundance of FL-HP (Fig. C.4) showed a general increasing trend over time, more evident in 10 µg L^{-1} microcosms. Station B enclosures were a remarkable exception to this pattern, with FL-HP abundance extremely constant across time, treatment and depth (on average, 0.10 ± 0.01 × 10^9 cells L^{-1}, Fig. C.4). In C1 and C2 bottles, the effect of the detritus addition became evident only on d4, whereas between d0 and d2, FL-HP abundances were very similar to those in control samples. The addition of detritus at 10 µg L^{-1} resulted in a steep increase of FL-HP abundance in surface C1 samples (approximately 5 times higher than control, Fig. C.4), whereas in bottom samples FL-HP abundance was not clearly affected by the particles enrichment. Station C2 enclosures showed an inverse pattern, with a stronger response of bottom samples to particles addition (~6 times higher than control on d4). The highest cell numbers were measured in D samples in both surface (5.49 ± 0.35 × 10^9 Cells L^{-1}) and bottom samples (1.92 ± 0.83 × 10^9 Cells L^{-1}). Addition of 1 µg Chl *a* L^{-1} equivalent in surface samples had mild effect on FL-HP abundance, whereas the strongest amendment yielded a steep increase of FL-HP cells in both surface and bottom samples (Fig. C.4).

The abundance of PA ranged between 0.49 ± 0.09 and 71.71 ± 7.67 × 10^6 Cells L^{-1} (Fig. 4.2). The lowest number of attached cells was measured on d0 in B surface bottles amended with 1 µg Chl *a* L^{-1}, while the highest number of PA cells was found on d4 in C2 bottom samples with 10 µg L^{-1}. Over time, PA abundance was constant or decreasing between d0 and d1, followed by an increase on d4 (Fig. 4.2). B experiments showed the lowest abundance of particle-attached prokaryotes, in both surface and bottom microcosms, whereas station C2 presented the highest PA abundance. PA abundance on d0 was higher in surface enclosures, except for B bottles, where the initial PA cells number was higher in bottom samples (Fig. 4.2). On d4, bottom microcosms presented a higher PA abundance than surface ones, except for C2 samples (Fig. 4.2)

4.3.4. Microbial metabolic activities

Minima of the three EEAs were all measured in bottom C1 bottles (BGLU: 0.01 ± 0.00 nM h^{-1}; AMA: 0.79 ± 0.08 nM h^{-1}; LIP: 0.86 ± 0.07 nM h^{-1}; Fig. 4.3). Maxima of BGLU and AMA were measured in surface bottles amended with station D phytodetritus (7.19 ± 0.00 and 1622.24 ± 113.55 nM h^{-1}, respectively, Fig. 4.3), while the

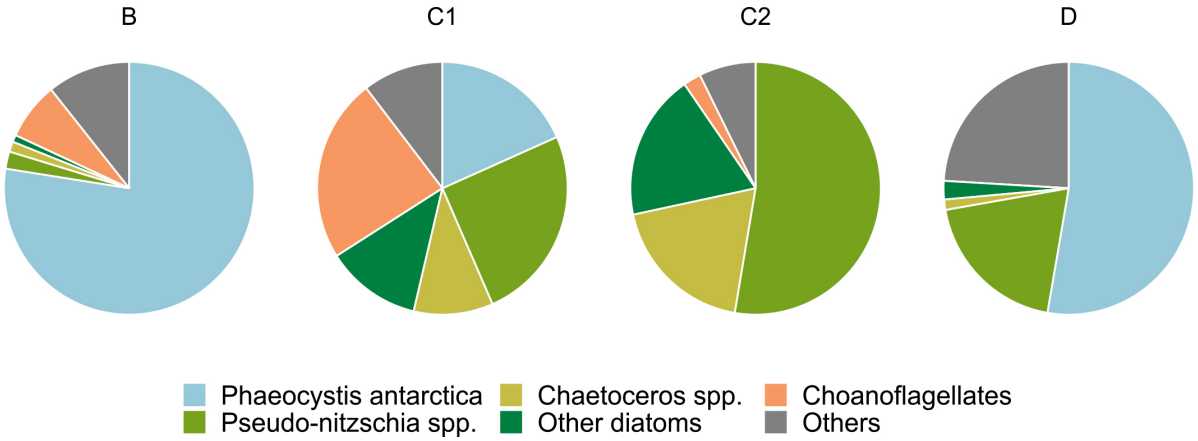

Figure 4.1: Compositional pie charts of plankton net samples used to generate phytodetritus.

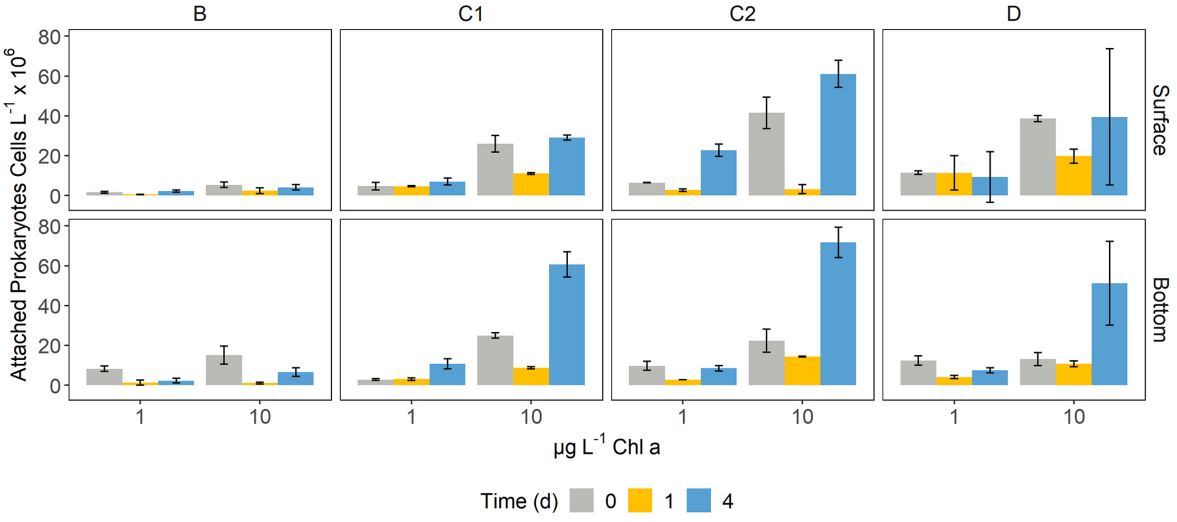

Figure 4.2: Bar plots showing the abundance of attached prokaryotes on d0, d1 and d4 in each of the microcosms. Error bars represent the standard deviation of two experimental replicates.

fastest lipid degradation was found in bottom microcosms supplemented with C1 detrital particles (78.61 ± 32.65 nM h^{-1}, Fig. 4.3).

Protease activity showed a general increasing trend in all the experiments, with steeper slopes between days 2 and 4 (Fig. 4.3). Slower rates were observed in B bottles, while maxima were measured in bottles amended with particles from station D (Fig. 4.3). Treatments at 10 µg L^{-1} yielded the strongest increase in peptidase activity in bottom bottles enriched with detritus from stations C1, C2 and D compared to controls on d4 (approximately 35, 30 and 10 times, respectively, Fig. 4.3). The amendment of B bottom microcosms with 1 µg L^{-1} sustained a ~3 times higher AMA activity compared to control and 10 µg L^{-1} treatment (Fig. 4.3).

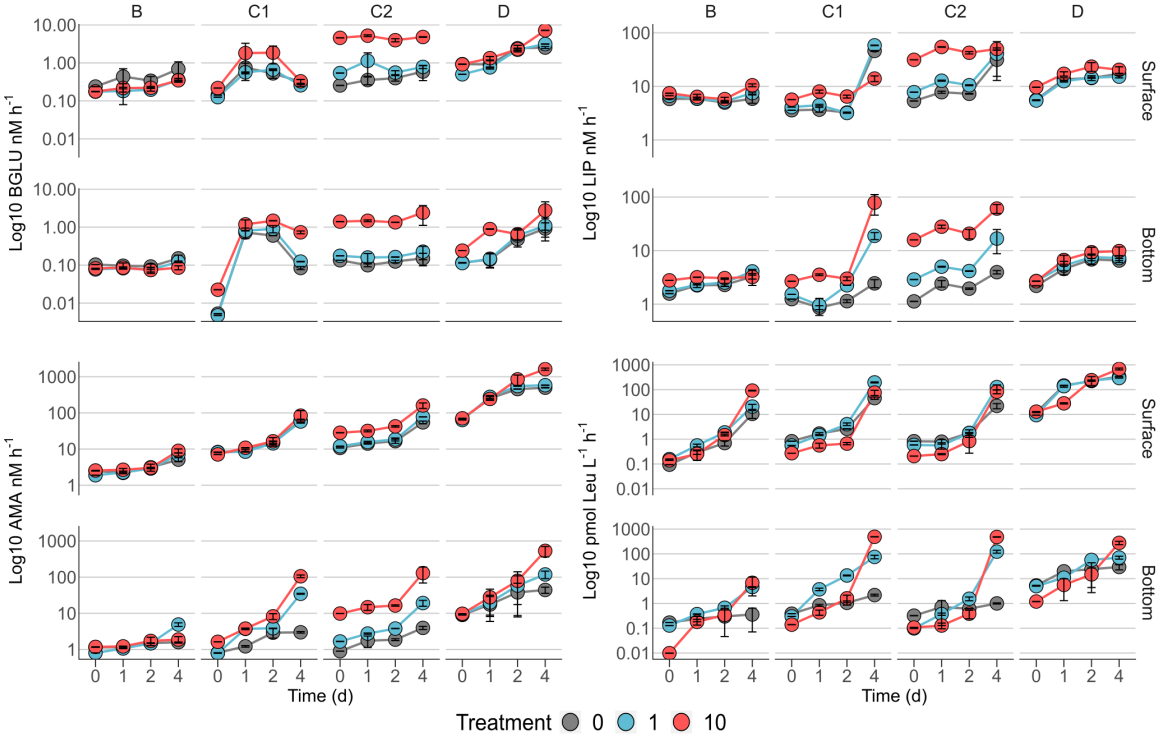

Figure 4.3: Time courses of β-glucosidase (BGLU), lipase (LIP), leucine-aminopeptidase activities (AMA) and heterotrophic carbon production (HCP). 0: controls; 1: 1 µg L^{-1} Chl *a*; 10: 10 µg LL^{-1} Chl *a*. To ease comparison, metabolic rates are plotted on Log Y-axes, which are differentially scaled. Error bars represent the standard deviation of two experimental replicates; where not visible, they are embedded in the symbol.

Lipid degradation was slower in experiments B and D in both surface and bottom bottles. Experiments C1 and C2 showed the highest values of lipase activity in bottom microcosms, where the maximum value was measured (experiment C1, Fig. 4.3). A mild effect of the detritus enrichments was visible in surface B and D bottles, while bottom experiments were not clearly affected by particle amendments (Fig. 4.3). The enrichment with 10 µg L^{-1} in surface C1 bottles resulted in a ~4 times lower rates compared to control and 1 µg L^{-1} at day 4 (Fig. 4.3). In bottom C1 bottles, the highest Chl *a* amendment yielded an increase in LIP activity of approximately 40 and 15 times compared to control and 1 µg L^{-1}, respectively (Fig. 4.3). A similar trend was observed

for C2 experiments, although with a milder increase (Fig. 4.3). Surface C2 bottles were characterized by higher LIP rates in the 10 µg L^{-1} throughout the experiment, compared to control and 1 µg L^{-1} (Fig. 4.3).

Carbohydrate hydrolysis showed a peculiar response in each of the experiments (i.e., B, C1, C2 and D), highly conserved in both surface and bottom bottles. The lowest BGLU activity was measured in station B microcosms. In station C1 experiments, enrichments at 10 µg L^{-1} induced slightly higher BGLU rates compared to control and 1 µg L^{-1}. The general pattern, showing a steep increase in the first 24 h and then a drop to initial values on d4, was common to all the experimental conditions (Fig. 4.3). Amendments with C2 detritus (Fig. 4.3) yielded the strongest response in the 10 µg L^{-1} treatment, with rates ~8 and 17 times higher than 1 µg L^{-1} treatment and control, respectively. An increasing trend over time was measured in both surface and bottom D bottles. While the addition of detrital particles at 1 µg L^{-1} did not produce a clear effect on glycolytic rates (Fig. 4.3), enrichments at 10 µg L^{-1} resulted in a steeper increase of BGLU activity on day 4, which was approximately 3 times higher than control and 1 µg L^{-1} in both surface and bottom bottles (Fig. 4.3).

Heterotrophic carbon production (Fig. 4.3) showed an overall strong response to detritus enrichment, especially on d4. Rates of prokaryotic production spanned over 4 orders of magnitude, ranging between 0.01 ± 0 and 682.83 ± 57.66 pmol Leu L^{-1} h^{-1}. Range extrema were measured at the highest Chl *a* concentration (10 µg L^{-1}) in bottom B bottles and surface D bottles, respectively (Fig. 4.3). As observed for the EEAs, overall slower prokaryotic production rates were observed in B experiments, with higher values in surface bottles. Amendments with detritus yielded the strongest response at 10 µg L^{-1}, with HCP rates approximately 9 and 16 times higher than control in surface and bottom bottles, respectively (Fig. 4.3). Enrichment at 1 µg L^{-1} in experiment C1 resulted in a steep increase of prokaryotic production on d4, with rates ~4 and 3 times higher than control and 10 µg L^{-1}, respectively (Fig. 4.3). In bottom C1 bottles, HCP rates strongly increased in response to 10 µg L^{-1} amendments, peaking at 489.00 ± 6.29 pmol Leu L^{-1} h^{-1}, the maximum value measured in bottom samples (Fig. 4.3). Experiment C2 showed a similar response in both surface and bottom bottles (Fig. 4.3). Experiment D microcosms showed a steady increasing trend of Leucine incorporation rates over time. The detritus enrichment induced the strongest response at the highest concentration (10 µg L^{-1}), resulting in HCP rates approximately 3 and 4 times higher than control in surface and bottom bottles, respectively (Fig. 4.3).

DDIC is an often neglected channeling of environmental C into prokaryotes and can be associated both to heterotrophic and autotrophic metabolism (see Section 4.4.2) The enrichments with detritus at the lowest concentration stimulated dark DIC uptake in C1 and C2 enclosures, with a stronger effect on the latter (~2 times higher than control, Table 4.2), while negatively affecting D and B enclosures (Table 4.2). The enrichments at 10 µg L^{-1} strongly enhanced DDIC rates in station D, C1 and C2 (approximately 10, 5 and 6 times higher than control, respectively), while had a slight negative effect on B microcosms (Table 4.2). Bottom DDIC uptake rates were unaffected by the particle amendments at 1 µg L^{-1}, while the strongest enrichments yielded a remarkable enhancement of dark DIC uptake in B and C2 bottles (~2 and 6 times relative to controls, respectively).

Table 4.2: Dark dissolved inorganic carbon (DDIC, ngC L^{-1} d^{-1}) uptake rates in control and amended microcosms measured on d0 (See Section 4.2.6). Results are presented as mean ± SD of two experimental replicates.

Depth	Treatment	B	C1	C2	D
Surface	Control	2.60±0.19	0.40±0.00	14.39±4.95	13.26±2.90
	1 µg L^{-1} Chl *a*	1.91±0.77	1.40±1.42	31.88±8.43	3.69±1.64
	10 µg L^{-1} Chl *a*	1.64±0.19	2.00±0.57	94.23±47.84	166.41±1.74
Bottom	Control	2.41±1.80	3.94±2.05	6.71±3.42	8.49±0.00
	1 µg L^{-1} Chl *a*	1.42±0.40	3.74±0.59	10.20±4.55	10.19±3.20
	10 µg L^{-1} Chl *a*	4.67±0.20	3.11±0.88	41.73±20.30	2.97±1.40

4.3.5. Prokaryotic diversity and community composition

Following the bioinformatic pipeline, the 16S rRNA dataset comprised 1950252 reads from the 56 analyzed samples, with, on average, 34825.92 reads per sample, totaling 420 prokaryotic ASVs. The lowest number of reads was found in the initial (d0) C2 surface sample (n= 12110), while sample replicate 2 of bottom D sample amended with 10 µg L^{-1} scored the highest value (n= 81610). The whole prokaryotic diversity was captured by the chosen sequencing effort, as shown by the rarefaction curves (Fig. C.5). ASVs richness (i.e., number of unique ASVs retrieved) ranged between 43 and 219. Both values were measured in C2 bottom enclosures, in replicate 2 of the 10 µg L^{-1} amendment on d4 and d0, respectively. A general decreasing trend in richness (Fig. C.6) was observed with increasing Chl *a* concentration (i.e., 0, 1 and 10 µg L^{-1}), particularly evident in bottom samples, whose initial communities were characterized by a significantly higher richness compared to surface ones (Mann–Whitney, $p < 0.05$). Segregation by depth did not reveal significant differences in richness between stations (Mann–Whitney, $p > 0.05$). The sequencing duplicates were highly consistent, being significantly correlated at $p<0.001$, with Spearman's rho values ranging between 0.60 and 0.90 (Fig. C.7).

In terms of initial community composition, the relative abundance of major taxa (RA >1%, Fig. 4.4 and Fig. C.8) significantly varied with depth (ANOSIM R= 0.83, $p < 0.05$). Surface samples of station B and D were respectively dominated by ASVs mapping to the SAR11 clade (61.85%) and to the *Polaribacter* genus (75.99%). The latter represented the most abundant taxon in stations C1 and C2 too (22.68 and 24.87%, respectively), sided by SAR11 ASVs at station C1 (13.50%) and by members of the Gammaproteobacterial family *Nitrincolaceae* at station C2 (13.45%). Initial bottom communities (Fig. 4.4 and Fig. C.8) were dominated by members of the phyla Proteobacteria (30.15 ± 6.32%) and Bacteroidetes (24.54 ± 9.5%). The former characterized the communities of stations B and D (39.47 and 28.77%, respectively), whereas stations C1 and C2 were dominated by the latter (34.97 and 29.66%, respectively). Classes Alpha- and Gamma-proteobacteria accounted for most of the Proteobacterial sequences (11.53 ± 1.84 and 14.74 ± 3.78%, respectively) in these stations, while most of the *Bacteroidetes* abundance was made up by *Flavobacteriales* (22.82

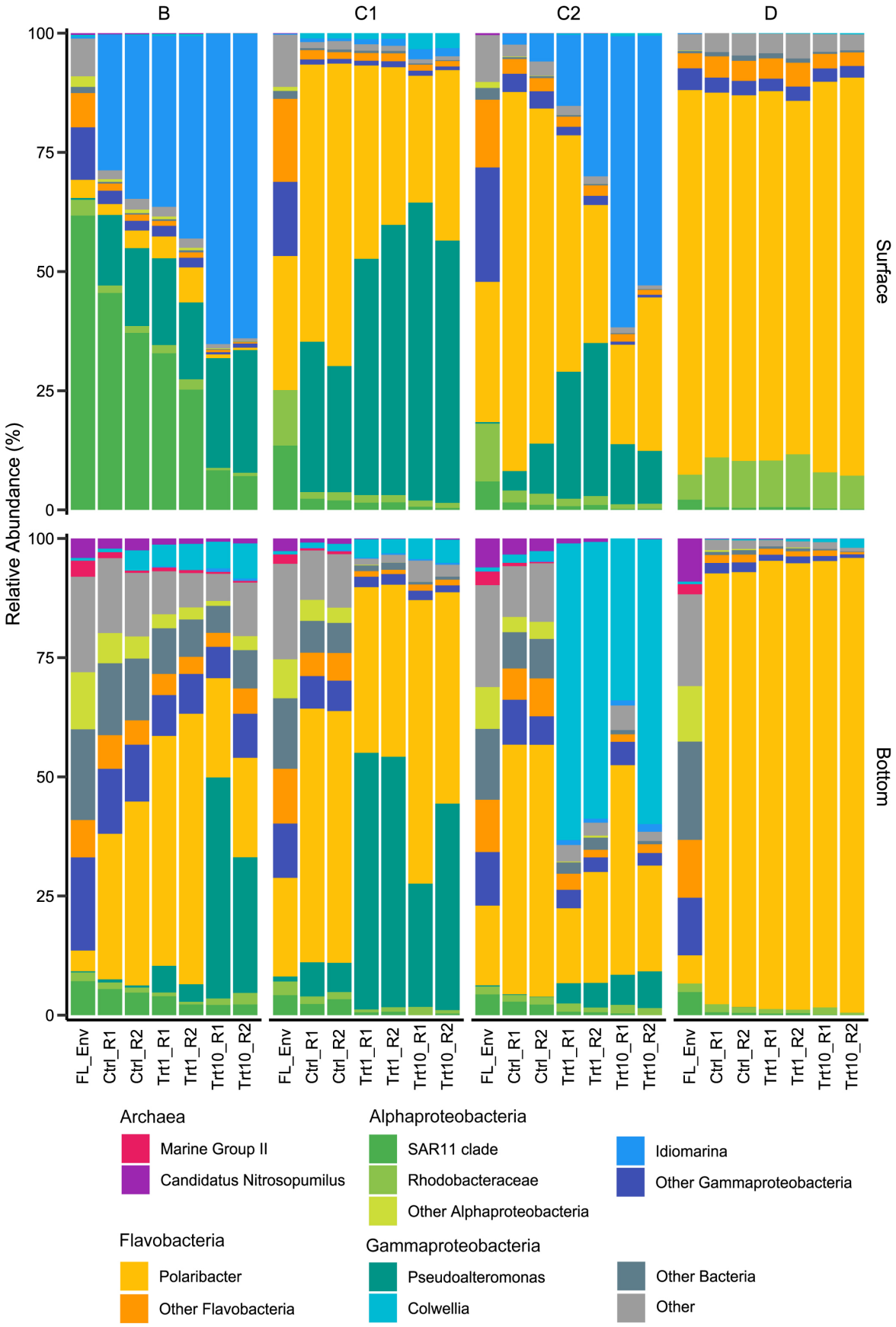

Figure 4.4: (Caption on the next page.)

Figure 4.4: Relative abundance plots of major taxa (>1% in at least one sample). FL_Env: initial free-living (1 µm-filtered) community, Ctrl: control samples; Trt1: amendments at 1 µg L^{-1} Chl *a*; Trt10: amendments at 10 µg L^{-1} Chl *a*; R1 and R2 identify the two experimental replicates. A detailed version of the figure with all subgroups showed is available in Appendix C.3.1.

± 9.16%).Among the Alpha-proteobacteria, members of the SAR11 clade represented approximately half of the retrieved sequences (5.03 ± 1.55%), with the highest relative abundance observed in station B samples (7.30%). Gamma-proteobacteria were mostly represented by sequences assigned to the family *Thiomicrospirales*, especially abundant at station B (10.69%, Fig. C.8), and *Oceanospirillales* (on average, 4.69 ± 4.02 and 4.27 ± 0.73%, respectively, Fig. C.8). Archaeal ASVs, belonging to Marine Group II and Nitrosopumilaceae, represented, on average, 8.08 ± 2.71% of the bottom initial community (Fig. 4.4 and Fig. C.8).

NMDS plot of the final prokaryotic communities showed that samples separated well according to sampling station and depth (Fig. 4.5). The highest amount of variance was explained by the sampling site (40%, Table 4.3), highlighting both the effect of the "seed" community and of the addition of different kinds of detrital particles on the observed differences.

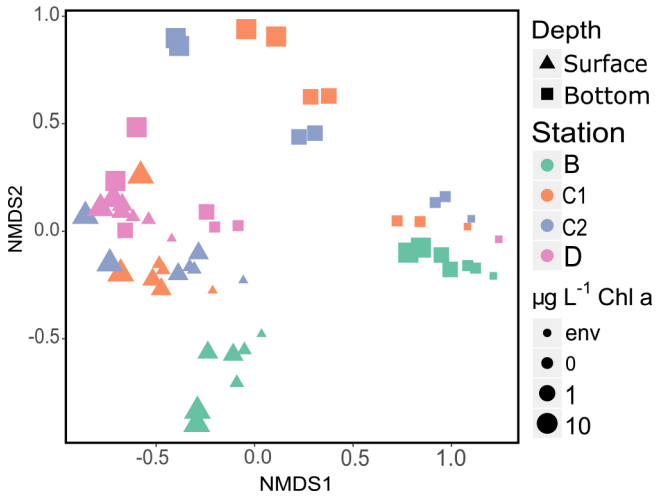

Figure 4.5: NMDS plot (stress= 0.11) showing Bray-Curtis dissimilarity in community composition. Samples are color, shape and size coded according to sampling site, sampling depth and treatment, respectively (see legend). Env: initial community d0, 1 µm-filtered); s: surface; b: bottom. Both replicates for each sample are plotted.

The enclosure of the initial prokaryotic communities led to an overall increase in the relative abundance of members of the *Flavobacteriaceae* family, mostly due to ASVs mapping to the *Polaribacter* genus (Fig. 4.6 and Fig. C.9). Station B represented an exception to this pattern, with changes in relative abundance mostly due to the genera *Idiomarina* (*Alteromonadales*) in surface samples and *Polaribacter* (*Flavobacteriales*) in bottom ones (Fig. 4.6). Community changes in samples amended with detrital particles were mainly driven by the increase of the relative abundance of members of the order Alteromonadales to the detriment of *Flavobacteriales* representatives (Fig. 4.6). Distinct *Alteromonadales* genera characterized the observed changes across

Table 4.3: Results of permutational multivariant analysis of variance (PERMANOVA) of final prokaryotic communities based on Bray-Curtis dissimilarities of read relative abundance. The factor 'Sampling Site' represents both the effect of the "seed" community and of the amendment with the site-specific detrital pool.

Factor	d.f.	SS	Pseudo F	R^2
Sampling Site	3	4.4	14.65	0.40*
Sampling Depth	1	1.87	18.72	0.17*
Treatment	2	0.63	3.15	0.05
Residuals	48	4.11		0.37
Total	55	11.03		1

d.f.: degrees of freedom; SS: sum of squares.
*denotes significance at p< 0.001, calculated after 9999 permutations

sampling sites and depths. The genus *Idiomarina* increased in surface B and C2 enriched samples, particularly in the 10 µg L^{-1} Chl *a* treatment, while the genus *Colwellia* was largely responsible for the changes observed in amended C2 bottom samples (Fig. 4.6). The genus Fig. 4.6 was positively affected by the detritus addition in both surface and bottom samples of station C1 and in bottom B bottles (Fig. 4.6). Surface D enclosures showed very few changes in relative abundance in response to both the enclosure and to the amendment with phytodetritus (Fig. 4.6). The enclosure of bottom D samples strongly selected for *Polaribacter* ASVs, with relative abundance increasing ~40 times compared to environmental samples (Fig. 4.6). At station D the amendments with detrital particles induced only minor community changes in both surface and bottom samples.

4.4. Discussion

4.4.1. Detritus-induced changes in prokaryotic abundance and community structure

Our analyses identified sampling site and depth as the main driving factors explaining the observed differences in final (d4) communities (see Section 4.3.4 and Fig. 4.5). The addition of 'small' amount of detritus (1 µg L^{-1} Chl *a* equivalent) was enough to select for the growth of specific prokaryotic taxa within the *in situ* free-living communities In fact, we did not find a significant effect of phytodetritus concentration (i.e., 1 vs 10 µg L^{-1}, Table 4.3) on the final prokaryotic communities, suggesting that the major drivers of the observed changes were the features of the phytodetrital particles rather than their concentration. These results suggest that the interaction of the initial free-living assemblage with the particulate detrital pool resulted in site-specific changes, differentially affecting surface and bottom assemblages.

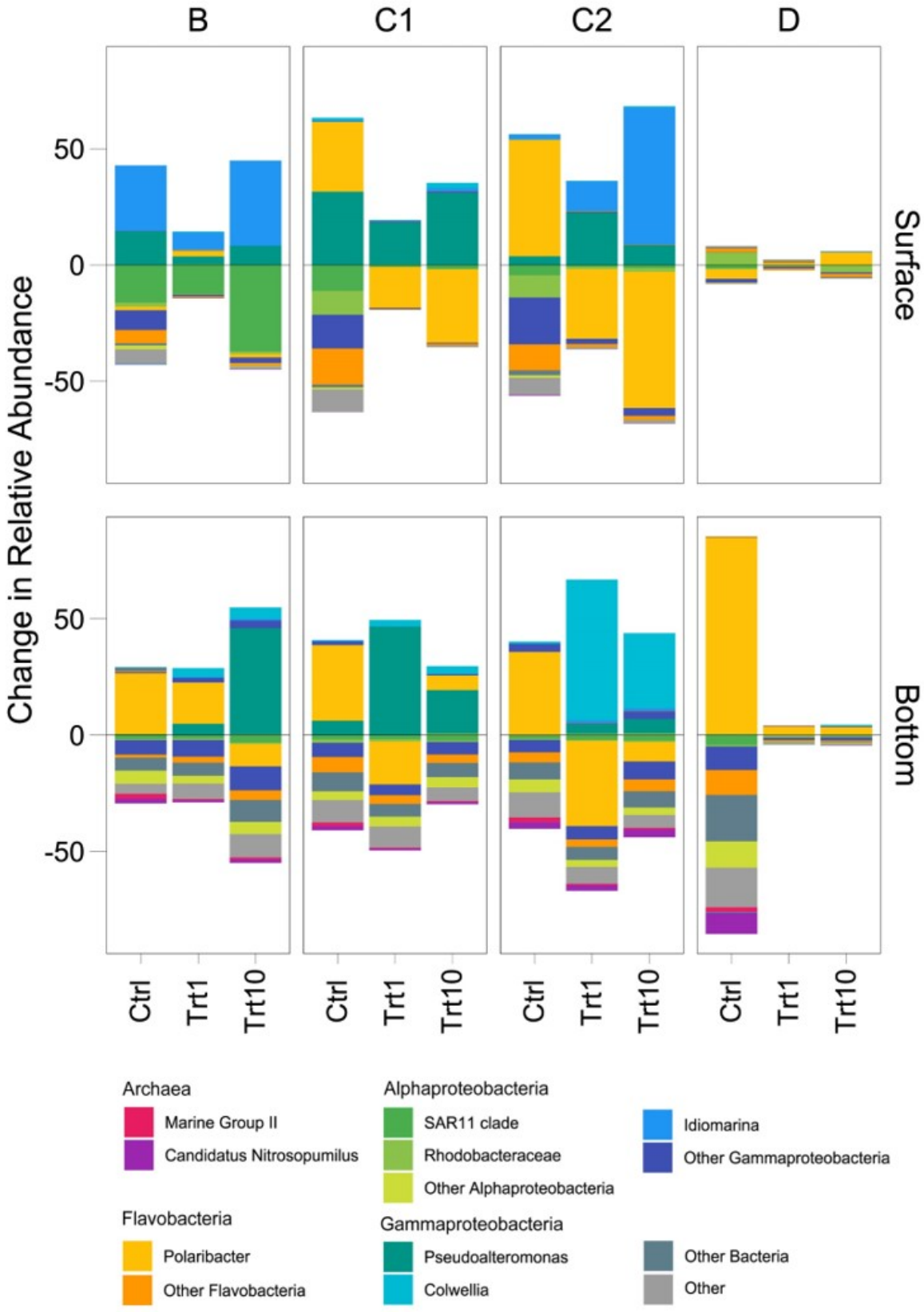

Figure 4.6: (Caption on the next page.)

Figure 4.6: Treatment-related shifts in prokaryotic community. Shifts in controls are compared to the initial (d0, 1 µm-filtered) community, whereas taxa shifts in treatments (i.e., 1 and 10 µg L^{-1}) are compared against the controls (both on d4). Ctrl: control samples; Trt1: amendments at 1 µg L^{-1} Chl *a*; Trt10: amendments at 10 µg L^{-1} Chl *a*. A detailed version of the figure with all subgroups showed is available in Appendix C.3.1.

Enrichments with Phaeocystis-derived detrital particles yielded significantly higher FL-HP abundance in surface samples amended with 10 µg L^{-1} and in bottom bottles amended with 1 µg L^{-1} (stations B and D, Fig. 4.7). This pattern suggests that, in surface samples, mild detritus enrichments induced a community-level response (i.e., shifts in community structure with constant cell abundance, Reintjes et al., 2019) to the POM features, while stronger enrichments select for specific fast-responsive taxa (i.e., *Alteromonadales* in B and *Flavobacteriales* in D, Fig. 4.6). It is noteworthy that bottom samples showed an exact inverse pattern (Fig. 4.7), highlighting that small pulses of organic matter are rapidly exploited by conditionally rare copiotrophs, while more consistent loads of POM re-shuffle the whole community. At stations C1 and C2, enrichments with diatom-derived detritus yielded significantly higher FL-HP abundance than control samples. The increase in FL-HP in those samples was coupled with the marked increase in the relative abundance of *Pseudoalteromonas* and *Idiomarina* genera, respectively (Fig. 4.6), suggesting that the changes in community composition were the result of the emergence of these genera rather than a community-level response to the detritus addition.

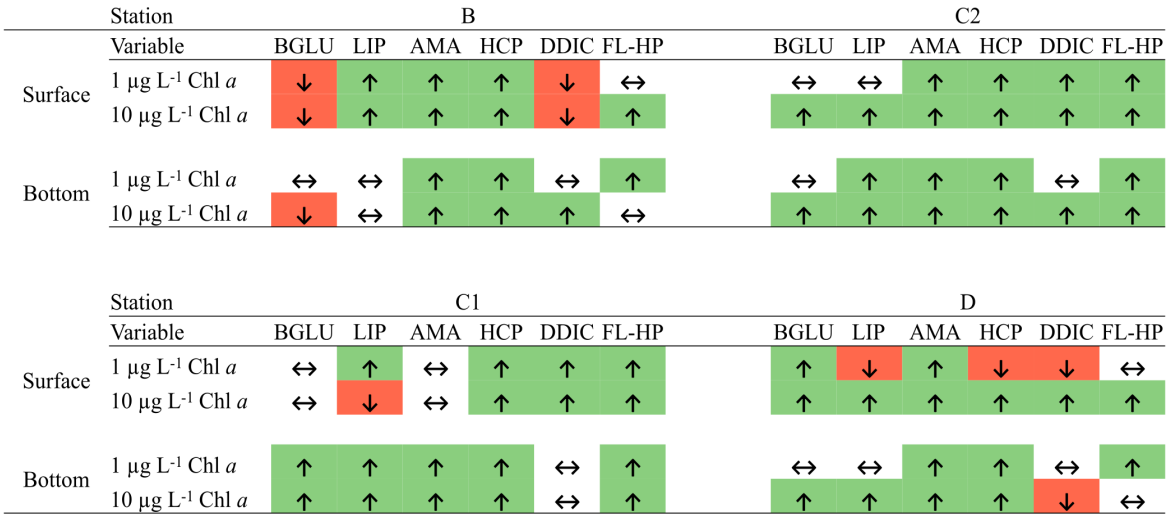

Figure 4.7: Significant differences between control and amended microcosm at day 4 (Mann-Whitney test, p<0.05). ↑: enhanced by phytodetritus; ↓: inhibited by phytodetritus; ↔: no significant variation detected. BGLU: β-glucosidase activity; LIP: lipase activity; AMA: leucine-aminopeptidase activity; HCP: heterotrophic carbon production; DDIC: dark dissolved inorganic C uptake rates; FL-HP: free-living heterotrophic prokaryotes abundance.

Starting communities (Fig. 4.4 and Fig. C.8) comprised typical free-living lineages as SAR11, SAR86 and AEGEAN-169 (Dupont et al., 2012; Giovannoni et al., 2014) sided by clades often observed associated with phytoplankton blooms or reported as feed-

ers on algal-derived compounds (e.g., NS3 and NS5 marine groups and *Rhodobacteraceae*; Amin et al., 2015; Halsey et al., 2012; Teeling et al., 2016). The latter were more represented in bottom initial communities, suggesting that, albeit free-living, those communities harbored the potential to find, colonize and degrade phytodetrital particles. Starting bottom assemblages were compositionally similar, as expected, since they were collected within the same deep-water mass (High Salinity Shelf Water). Indeed, in the same area, in previous studies we had observed a segregation of deep prokaryotic (Celussi et al., 2010) and protist (Zoccarato et al., 2016) communities according to the water mass they were sampled in. On the other hand, due to the strong physical and biological spatial gradients of the upper water column (Rivaro et al., 2019), surface initial communities widely varied across sampling site (Fig. 4.5). Flavobacteria and SAR11 clades drove the observed differences, accounting for the 75.99 and 61.55% of the sequences retrieved in D and B, respectively (Fig. 4.4).

Flavobacteria are well-known degraders of complex organic molecules, such as proteins and polysaccharides, being less effective in the uptake of smaller and simpler organic substrates (Fourquez et al., 2016; Wietz et al., 2015). These experimentally-observed traits are supported by comparative genomic studies showing a conspicuous repertoire of genes involved in high molecular weight (HMW) compounds transport and degradation, sided by a lower number of genes devoted to handle simpler organic substrates (Fernández-Gómez et al., 2013; Gómez-Pereira et al., 2012; González et al., 2008; Williams et al., 2013). It is, therefore, not surprising that *Flavobacteria*, mainly represented by the *Polaribacter* genus, constituted a significant fraction of the microcosms community (except for B surface enclosures, Fig. 4.4 and Fig. C.8). At the time of sampling, a diatom bloom was in place in the station D surface layer (Section C.2.1), thus explaining the dominance of Flavobacterial ASVs in this sample. Indeed, most of those ASVs mapped to the genus *Polaribacter*, a taxon reported as associated with diatom-derived organic matter in both environmental surveys (Teeling et al., 2012; Teeling et al., 2016) and experimental enclosures (Landa et al., 2018; Wietz et al., 2015). Noteworthy, amendments with detrital particles at both concentrations in station D samples showed very little community changes (Fig. 4.6 and Fig. C.9). While this was expected in surface samples, as the initial community (i.e., 1 µm-filtered) was already dominated by *Polaribacter* ASVs (Fig. 4.4), the fact that bottom samples showed the same dynamics, in the face of a highly diverse initial community (Fig. 4.6 and Fig. C.9), was rather puzzling. Although we cannot rule out the influence of the bottle effect, one possible explanation relies on the phytodetrital composition which, besides the high number of diatoms, was mainly composed by *Phaeocystis antarctica* (>50%, Fig. 4.1). Colonial forms of *P. antarctica* allocate ~50% of carbon production to the extracellular mucus that makes up the scaffold of the colonial matrix (DiTullio et al., 2000), making the Phaeocystis-derived detritus a source of HMW polysaccharides. Previous enrichment experiments with Phaeocystis-derived material have shown how the degradation of this organic pool is mostly carried out by *Flavobacteria* (Brussaard et al., 2005), further explaining their dominance in D samples. Flavobacterial ASVs, mostly represented by the *Polaribacter* genus, contributed to a consistent part of the final prokaryotic community in all bottom unamended microcosms (Fig. 4.4 and Fig. C.8). Recent *in vivo* and *in vitro* studies (Reintjes et al., 2019; Reintjes et al., 2017) have demonstrated that *Flavobacteria* representatives are able to assim-

ilate large polysaccharides in their periplasmic space, where subsequent hydrolysis and uptake processes take place. This mechanism, defined as "selfish" uptake, is highly competitive as it implies a reduced diffusive loss of hydrolysis products. The dominance of Flavobacterial representatives in control samples is therefore explained by their capability to efficiently utilize HMW DOM, outcompeting other members of the community. Previous experiments with organic matter enrichments showed similar results (Landa et al., 2018; Luria et al., 2017; Wietz et al., 2015), confirming the ability of this group to efficiently utilize HMW organic matter.

SAR11 is a diverse group, widespread in oligotrophic water across the global ocean (Giovannoni, 2017). Genomic analysis on both environmental and cultivated members of this clade have pointed out peculiar adaptations to thrive in nutrient-poor environments (Sowell et al., 2009; Thompson et al., 2013). This lineage is not able to degrade HMW organic matter, supplying this lack with a high abundance of LMW organic matter transporters (i.e., amino-acids and sugars, Tripp, 2013). Although the relative abundance of SAR11 clade members decreased with the addition of detrital particles, it represented a consistent fraction in all samples (>1%, Fig. 4.4), showing a higher occurrence in samples where Flavobacterial ASVs were poorly represented (e.g., station B experiments, Fig. 4.4). Within their conceptual model, Arnosti et al., 2018 put out a third player, the "scavenging" bacteria, not able to degrade HMW organic matter on their own but rather "scavenging" hydrolysis products produced by external degraders. The SAR11 clade remarkably fits this role, and its "scavenging" behavior has been confirmed in their *in vivo* experiments. Our results confirm these findings, linking the presence of SAR11 to the prevalence of external hydrolysis of organic matter (as suggested by the high RA of *Alteromonadales*, Fig. 4.4) and further suggest that, under the appropriate conditions, "scavenging" behavior may be more effective than "selfish" hydrolysis.

ASVs belonging to the Gammaproteobacterial family *Alteromonadales* were initially rare, yet they became prevalent in all the enriched bottles of station B, C1 and C2 (Fig. 4.6). A similar pattern has been previously observed in HMW organic matter amendment experiments (Balmonte et al., 2019; Luria et al., 2017) and all these findings point out a major role of these conditionally rare, copiotroph taxa in exploiting organic matter pulses. The increase in *Alteromonadales* ASVs was always at the detriment of Flavobacterial representatives (Fig. 4.6), in agreement with what has been observed in DOM enrichment experiments in the Southern Ocean (Landa et al., 2018; Luria et al., 2017). *Alteromonadales* can rapidly take advantages of transient sources of organic matter through their flexible metabolism, which allow them to utilize a wide array of phytoplankton-derived organic molecules (Liu et al., 2017; Sperling et al., 2017). These characteristics make this family the archetype of the r-strategist (Pedler et al., 2014), explaining its dominance in the amended samples. It is interesting to note that within the *Alteromonadales* order, three different genera dominated in different groups of experiments: *Pseudoalteromonas* and *Idiomarina* co-occurred in B and C1 samples and in C2 surface samples, whereas the genus *Colwellia* was dominant in C2 bottom enclosures (Fig. 4.4 and Fig. 4.6). These three genera have been shown to be able to degrade dimethylsulfoniopropionate (DMSP), a sulfur-containing molecule produced by phytoplankton (Zeng, 2019). As DMSP is mainly produced by

diatoms and *Phaeocystis* spp., the ability to degrade this compound may have been a prominent factor driving the observed *Alteromonadales* prevalence in amended samples. Among the three genera, *Pseudoalteromonas* is the only one able to grow using DMSP as a sole source of carbon (Zeng, 2019), a characteristic that may explain its exclusive dominance in samples amended with C1 detritus, the particles pool of which was almost exclusively composed by diatoms (Fig. 4.1). In agreement with our results, specific taxa within this bacterial family have been observed to success during different stages of phytoplankton blooms, indicating (i) that these taxa possess the hydrolytic machinery necessary to rapidly process HMW organic matter and (ii) that different organic matter source drives specific community changes (Buchan et al., 2014; Teeling et al., 2012; Teeling et al., 2016).

A conspicuous amount of Archaeal ASVs was retrieved in bottom samples at all stations (~10%, Fig. 4.4). Albeit by the end of the experiment most of the Archaeal community was wiped out by bacterial ASVs, their presence throughout the incubation was noteworthy (~1% on d4, Fig. 4.4). Most of the Archaeal ASVs retrieved in our samples belonged to members of Marine Group II (MG II, *Euryarchaeota*), a group identified as a consistent member of prokaryotic community in both temperate and polar oceans (Quero et al., 2020; Zhang et al., 2015). Metagenomic-inferred physiology suggest that members of MG II possess abundant genes deputed to the handling and utilization of HMW organic matter (Deschamps et al., 2014). Consistent with these findings, Orsi et al., 2015 found an enrichment of MGII sequences in the particle-attached fraction, indicating physical association with particles and therefore, the presence of detrital particles in our experiments may have provided MG II with exploitable substrates, granting their persistence throughout the incubation period.

The particle type, taken as a proxy of the organic matter quality, has been suggested to play a key role in the processes governing the activity and composition of the particle attached bacterial community (Grossart et al., 2005; Teeling et al., 2012). Indeed, we found significant differences in the number of PA prokaryotes according to the detrital pool supplied, with diatom-based detritus yielding the highest number of associated bacteria on d4 (Fig. 4.2). Albeit compositionally different, the final communities were rather similar in terms of potential interaction with particles, harboring two of the major players in particles colonization and degradation (i.e., *Flavobacteriales* and *Alteromonadales*). The results of the GLMs showed that *Pseudo-nitzschia* genus abundance was the only significant factor driving the number of attached bacteria on d0 ($p < 0.05$), whereas on d4 the response of PA bacteria was significantly related to all the other microplankton taxa ($p < 0.001$ for *Pseudo-nitzschia* and *Phaeocystis* spp., $p < 0.05$ for *Chaetoceros* spp., Table C.3). Given these results, we hypothesize that the observed increase of attached prokaryotes over time may be due to the intrinsic properties of the detrital pool supplied. Diatom-derived detritus indeed, may have represented a more suitable colonization substrate than Phaeocystis-dominated one, providing more particulate material per unit Chl *a* (Table C.1). The utterly complex shape of diatom-derived aggregates may enhance prokaryotic colonization by making available a wide variety of microniches as well as by enhancing coagulation with other particles (Zetsche et al., 2020). These properties likely explain the higher number of attached cells that we found on diatom-containing detrital pools. Furthermore,

we found significant positive correlation between viruses and diatom abundance in net samples (Spearman's rho: *Pseudo-nitzschia* spp.= 0.31; *Chaetoceros* spp.= 0.19; other diatoms= 0.19, p (fdr)< 0.01, n= 128), suggesting that especially diatom-derived phytodetritus represented hot-spots of viral activity during the incubations. This intense activity could thus have caused lysis-derived DOM to diffuse from the aggregates, increasing particles detectability by chemotactic prokaryotes and thus the PA abundance (Kiørboe and Jackson, 2001; Riemann and Grossart, 2008). In addition, this DOM may have represented an additional source of organic matter for FL-HP, contributing to their significant increase in amended samples relative to control ones (Fig. 4.7). It must be noted, however, that the abundance of virus-like-particles was remarkably constant in our microcosms, except for bottles amended with detritus D (Fig. C.4). This suggests a dynamic balance between production and loss processes, possibly represented by detritus-enhanced prokaryotic activity (and thus viral production) vs. detritus-enhanced viral adsorption by particles (Fuhrman, 1999).

Despite the similar detrital composition, Stations D and B showed a remarkable difference in colonization yield (Fig. 4.2). Shifts in microbial community composition as the particle ages or sink are correlated with changes in community functioning (Fontanez et al., 2015), leading in turn to modifications of the nutritional properties of the particles (Martinez et al., 1996; Smith et al., 1992). Moreover, the process of particle colonization is highly dynamic (Kiørboe et al., 2004), thus if the particle-OM labile pool is exhausted or selective degradation reduces its palatability for the resident prokaryotes, the most cost-effective strategy consists in finding another particle to exploit, thus increasing the probability to find free-living cells. Furthermore, albeit both detrital pools were Phaeocystis-dominated, a consistent fraction of station D detritus was composed by diatoms (Fig. 4.1), which contain more particles (active surfaces) per Chl *a* unit than *Phaeocystis* (DiTullio and Smith Jr., 1996; Table C.1), thus providing prokaryotes with a physical scaffold for colonization.

4.4.2. Detritus-induced functional changes

In terms of functional response to phytodetritus addition (Fig. 4.7), diatom-derived organic matter mostly exerted a positive effect on metabolic rates, whereas when enriched with Phaeocystis-derived detritus, microbial communities showed shifts in organic matter degradation patterns.

Metabolic rates measured in microcosms amended with B detritus were consistently the lowest among the four groups of samples (Fig. 4.3). This may be explained by two hypotheses, regarding (i) the composition of the supplied detritus and (ii) the native prokaryotic community composition. The detritus supplied to B bottles was mainly composed by *Phaeocystis antarctica*, which allocates a significant fraction of its carbon content to carbohydrates (Mathot et al., 2000) that are stored in the forms of glucan or polysaccharides as the growth progress towards senescence (Alderkamp et al., 2007). Our measurement of carbohydrate degradation is limited to the activity of β-glucosidase and thus is it possible that, while this enzyme showed a reduced activity following the addition of detrital particles, a whole, untested, set of polysaccharide degrading enzymes may have been produced to cope with the complexity of the organic matter in this detrital pool. Recent experiments have demon-

strated how following the addition of HMW organic matter, many different glycolytic enzymes, are produced (Balmonte et al., 2019), corroborating our hypothesis. Culture and mesocosm-based experiments have shown that *Flavobacteria* was the major bacterial group involved in Phaeocystis-derived organic matter processing (Alderkamp et al., 2006; Brussaard et al., 2005) and thus their low proportion in B enclosures may explain the low exoenzymatic activities. Consistent with this hypothesis, we observed a shift from carbohydrate to lipid degradation in surface samples (Fig. 4.7). This observation was coupled with the increase in RA of *Idiomarina* in amended samples. It has been reported that the genome of *Idiomarina* representatives shows a higher proportion of lipid metabolism-related genes compared to substantial loss of sugar metabolism genes (Hou et al., 2004). The enhancement of BGLU rates in D experiments, despite the similar detrital composition, further corroborate our hypothesis, linking Phaeocystis-derived organic matter degradation with a Flavobacteria-dominated community (Figs. 4.4 and 4.7).

DDIC fixation rates were differentially affected by the distinct pools of phytodetrital particles supplied (Table 4.2 and Fig. 4.7). Diatom-derived detritus significantly enhanced DDIC uptake, congruently with the other measured metabolic rates, whereas samples amended with Phaeocystis-dominated phytodetritus showed a more puzzling pattern. The highest inorganic carbon fixation rates were found in surface microcosms C2 and D and were correlated to exoenzymatic activities (Spearman's Rho: BGLU=0.50, LIP=0.32, AMA=0.52; p (fdr)<0.05; n=32). Similar findings are reported in Baltar et al., 2016, where DDIC fixation rates and associated transcripts were enhanced following a sudden intensification of bacterial heterotrophic metabolism. Indeed, DDIC is not a prerogative pathway of autotrophs (photo- or chemo-) but heterotrophs can take up and effectively use CO_2 through metabolic pathways implicated in the synthesis of fatty acids, nucleotides, and amino acids, as well as in anaplerotic reactions (Alonso-Sáez et al., 2010), making the heterotrophic CO_2 assimilation a relevant process for the global carbon cycle (Erb, 2011). Therefore, we hypothesize that the observed steep increase in DDIC fixation rates in microcosms C2 and D was mainly due to an intensified anaplerotic activity, deputed to fuel the intense heterotrophic activity. Moreover, representatives of *Polaribacter*, *Colwellia* and *Pseudoalteromonas* genera have been shown to significantly contribute to DIC uptake (DeLorenzo et al., 2012). These taxa were preponderant members of the community in the enclosures with higher rates of dark DIC fixation, further corroborating our hypothesis of the prevalence of anaplerotic DDIC fixation. It is also worth mentioning that the putatively chemosynthetic taxa *Nitrosopumilus* (*Thaumarchaeota*), *Nitrospina* and LS-NOB (*Nitrospinaceae*) decreased in relative abundance along with time and detritus concentration, thus suggesting a tuning of DIC uptake from (at least partially) autotrophic to heterotrophic pathways in our 4-day incubations.

Remarkably, we found significant positive correlations between all the metabolic activities tested and attached prokaryotes (Spearman's rho: BGLU= 0.42; LIP= 0.41; AMA= 0.55; HCP=0.29; DDIC= 0.51; p (fdr)<0.01; n=96 for BGLU, LIP, AMA and HCP; n=32 for DDIC) suggesting that detrital particles represented a significant hotspot of prokaryotic activity during our incubations.

4.4.3. Conclusions

We hypothesized that in response to phytodetrital features and concentration, distinct microbial communities would show a different structural and functional response. The artificially generated phytodetritus well captured the peculiar duality of the phytoplankton in the Ross Sea, which is either dominated by *Haptophytes* (e.g., *Phaeocystis* spp.) or diatoms (Smith et al., 2014). Amendments with diatom-derived POM induced marked shifts in both surface and bottom communities, led by a consistent increase of *Alteromonadales*. Enrichments with Phaeocystis-derived material produced different effects on surface and bottom communities. Mild enrichments induced a community-level response while stronger enrichments induced the growth of specific, fast-responsive, taxa (i.e. *Alteromonadales* and *Flavobacteriales*). Bottom samples showed an exact inverse pattern highlighting that small pulses of POM are rapidly exploited while more consistent loads of OM re-shuffle the whole community. Our results show that several rare or undetected taxa in the initial community became dominant in the time course of the incubation (4 days). Furthermore, diverse organic matter sources induced site-specific changes in microbial communities, selecting for specific genera which differ in their capabilities to degrade organic matter. These experiments, in combination with the present knowledge of the metabolic strategies of those taxa, suggest that free-living communities represent functional seedbanks for the degradation of particulate organic matter of detrital origin. The emergence of bacterial groups that were also abundant in environmental and experimental phytoplankton-derived organic matter enrichments in the Southern Ocean (i.e., Landa et al., 2016; Landa et al., 2018) emphasize the relevance of our study in shedding light on the microbial community response of this ecosystem to organic matter pulses. Finally, our study provides novel insights on the mechanisms underlying the prokaryotic utilization of detrital particles in the mesopelagic realm, that harbor an overlooked, but significant, pool of organic matter in the dark ocean.

Acknowledgements

The help of the officers and of the crew of the R/V Italica is kindly acknowledged. The authors would like to thank the staff of the Dipartimento di Scienze e Tecnologie, University of Naples Parthenope, led by P. Falco, for CTD casts and for providing the related data, F. Relitti for DOC and POC data, A. Baričević and M. Smodlaka Tanković for flow cytometry measurements and S. Maggiore for epifluorescence microscope analysis. This study was supported by the project PRIAMO (PRokaryotes Interactions with Antarctic phytodetritus: a Micro- to macroscale voyage from the surface to the deep Ocean) in the framework of the Italian Program for Research in Antarctica (project no. PNRA16_00103), with funds from the Italian Ministry for Education, University and Research.

References

Agusti, S., González-Gordillo, J. I., Vaqué, D., Estrada, M., Cerezo, M. I., Salazar, G., Gasol, J. M., & Duarte, C. M. (2015). Ubiquitous healthy diatoms in the deep sea confirm deep carbon injection by the biological pump. *Nature Communications*, *6*(1), 7608. https://doi.org/10.1038/ncomms8608

Alderkamp, A.-C., Sintes, E., & Herndl, G. J. (2006). Abundance and activity of major groups of prokaryotic plankton in the coastal North Sea during spring and summer. *Aquatic Microbial Ecology*, *45*(3), 237–246. https://www.int-res.com/abstracts/ame/v45/n3/p237-246/

Alderkamp, A.-C., Buma, A. G. J., & van Rijssel, M. (2007). The carbohydrates of Phaeocystis and their degradation in the microbial food web. In M. A. van Leeuwe, J. Stefels, S. Belviso, C. Lancelot, P. G. Verity, & W. W. C. Gieskes (Eds.), *Phaeocystis, major link in the biogeochemical cycling of climate-relevant elements* (pp. 99–118). Springer Netherlands. https://doi.org/10.1007/978-1-4020-6214-8_9

Alonso-Sáez, L., Galand, P. E., Casamayor, E. O., Pedrós-Alió, C., & Bertilsson, S. (2010). High bicarbonate assimilation in the dark by Arctic bacteria. *The ISME Journal*, *4*(12), 1581–1590. https://doi.org/10.1038/ismej.2010.69

Amin, S. A., Hmelo, L. R., van Tol, H. M., Durham, B. P., Carlson, L. T., Heal, K. R., Morales, R. L., Berthiaume, C. T., Parker, M. S., Djunaedi, B., Ingalls, A. E., Parsek, M. R., Moran, M. A., & Armbrust, E. V. (2015). Interaction and signalling between a cosmopolitan phytoplankton and associated bacteria. *Nature*, *522*(7554), 98–101. https://doi.org/10.1038/nature14488

Arnosti, C., Reintjes, G., & Amann, R. (2018). A mechanistic microbial underpinning for the size-reactivity continuum of dissolved organic carbon degradation. *Marine Chemistry*, *206*, 93–99. https://doi.org/10.1016/j.marchem.2018.09.008

Arnosti, C. (2011). Microbial Extracellular Enzymes and the Marine Carbon Cycle. *Annual Review of Marine Science*, *3*(1), 401–425. https://doi.org/10.1146/annurev-marine-120709-142731

Arrigo, K. R., van Dijken, G. L., & Bushinsky, S. (2008). Primary production in the Southern Ocean, 1997–2006. *Journal of Geophysical Research: Oceans*, *113*(C8). https://doi.org/https://doi.org/10.1029/2007JC004551

Balmonte, J. P., Buckley, A., Hoarfrost, A., Ghobrial, S., Ziervogel, K., Teske, A., & Arnosti, C. (2019). Community structural differences shape microbial responses to high molecular weight organic matter. *Environmental Microbiology*, *21*(2), 557–571. https://doi.org/https://doi.org/10.1111/1462-2920.14485

Baltar, F., Lundin, D., Palovaara, J., Lekunberri, I., Reinthaler, T., Herndl, G. J., & Pinhassi, J. (2016). Prokaryotic Responses to Ammonium and Organic Carbon Reveal Alternative CO2 Fixation Pathways and Importance of Alkaline Phosphatase in the Mesopelagic North Atlantic. *Frontiers in Microbiology*, *7*, 1670. https://doi.org/10.3389/fmicb.2016.01670

Becquevort, S., & Smith, W. O. (2001). Aggregation, sedimentation and biodegradability of phytoplankton-derived material during spring in the Ross Sea, Antarctica. *Deep Sea Research Part II: Topical Studies in Oceanography*, *48*(19), 4155–4178. https://doi.org/https://doi.org/10.1016/S0967-0645(01)00084-4

Benjamini, Y., & Hochberg, Y. (1995). Controlling the False Discovery Rate: A Practical and Powerful Approach to Multiple Testing. *Journal of the Royal Statistical Society: Series B (Methodological)*, *57*(1), 289–300. https://doi.org/https://doi.org/10.1111/j.2517-6161.1995.tb02031.x

Bidle, K. D., & Azam, F. (2001). Bacterial control of silicon regeneration from diatom detritus: Significance of bacterial ectohydrolases and species identity. *Limnology and Oceanography*, *46*(7), 1606–1623. https://doi.org/https://doi.org/10.4319/lo.2001.46.7.1606

Bidle, K. D., Manganelli, M., & Azam, F. (2002). Regulation of Oceanic Silicon and Carbon Preservation by Temperature Control on Bacteria. *Science*, *298*(5600), 1980–1984. https://doi.org/10.1126/science.1076076

Bižić-Ionescu, M., Ionescu, D., & Grossart, H.-P. (2018). Organic Particles: Heterogeneous Hubs for Microbial Interactions in Aquatic Ecosystems. *Frontiers in Microbiology*, *9*, 2569. https://doi.org/10.3389/fmicb.2018.02569

Bižić-Ionescu, M., Zeder, M., Ionescu, D., Orlić, S., Fuchs, B. M., Grossart, H.-P., & Amann, R. (2015). Comparison of bacterial communities on limnic versus coastal marine particles reveals profound differences in colonization. *Environmental Microbiology*, *17*(10), 3500–3514. https://doi.org/https://doi.org/10.1111/1462-2920.12466

Bokulich, N. A., Kaehler, B. D., Rideout, J. R., Dillon, M., Bolyen, E., Knight, R., Huttley, G. A., & Gregory Caporaso, J. (2018). Optimizing taxonomic classification of marker-gene amplicon sequences with QIIME 2's q2-feature-classifier plugin. *Microbiome*, *6*(1), 90. https://doi.org/10.1186/s40168-018-0470-z

Bolyen, E., Rideout, J. R., Dillon, M. R., Bokulich, N. A., Abnet, C. C., Al-Ghalith, G. A., Alexander, H., Alm, E. J., Arumugam, M., Asnicar, F., Bai, Y., Bisanz, J. E., Bittinger, K., Brejnrod, A., Brislawn, C. J., Brown, C. T., Callahan, B. J., Caraballo-Rodríguez, A. M., Chase, J., … Caporaso, J. G. (2019). Reproducible, interactive, scalable and extensible microbiome data science using QIIME 2. *Nature Biotechnology*, *37*(8), 852–857. https://doi.org/10.1038/s41587-019-0209-9

Boyd, P. W., Arrigo, K. R., Strzepek, R., & van Dijken, G. L. (2012). Mapping phytoplankton iron utilization: Insights into Southern Ocean supply mechanisms. *Journal of Geophysical Research: Oceans*, *117*(C6). https://doi.org/https://doi.org/10.1029/2011JC007726

Boyd, P. W., Claustre, H., Levy, M., Siegel, D. A., & Weber, T. (2019). Multi-faceted particle pumps drive carbon sequestration in the ocean. *Nature*, *568*(7752), 327–335. https://doi.org/10.1038/s41586-019-1098-2

Brussaard, C. P. D., Mari, X., Bleijswijk, J. D. L. V., & Veldhuis, M. J. W. (2005). A mesocosm study of Phaeocystis globosa (Prymnesiophyceae) population dynamics: II. Significance for the microbial community. *Harmful Algae*, *4*(5), 875–893. https://doi.org/https://doi.org/10.1016/j.hal.2004.12.012

Brussaard, C. P. D. (2004). Optimization of Procedures for Counting Viruses by Flow Cytometry. *Applied and Environmental Microbiology*, *70*(3), 1506–1513. https://doi.org/10.1128/AEM.70.3.1506-1513.2004

Buchan, A., LeCleir, G. R., Gulvik, C. A., & González, J. M. (2014). Master recyclers: Features and functions of bacteria associated with phytoplankton blooms. *Nature Reviews Microbiology*, *12*(10), 686–698. https://doi.org/10.1038/nrmicro3326

Buesseler, K. O., & Boyd, P. W. (2009). Shedding light on processes that control particle export and flux attenuation in the twilight zone of the open ocean. *Limnology and Oceanography*, *54*(4), 1210–1232. https://doi.org/https://doi.org/10.4319/lo.2009.54.4.1210

Callahan, B. J., McMurdie, P. J., Rosen, M. J., Han, A. W., Johnson, A. J. A., & Holmes, S. P. (2016). DADA2: High-resolution sample inference from Illumina amplicon data. *Nature Methods*, *13*(7), 581–583. https://doi.org/10.1038/nmeth.3869

Carlson, C. A., Bates, N. R., Ducklow, H. W., & Hansell, D. A. (1999). Estimation of bacterial respiration and growth efficiency in the ross sea, antarctica. *Aquatic Microbial Ecology*, *19*(3), 229–244. https://www.int-res.com/abstracts/ame/v19/n3/p229-244/

Catalano, G., Budillon, G., La Ferla, R., Povero, P., Ravaioli, M., Saggiomo, V., Accornero, A., Azzaro, M., Carrada, G., Giglio, F., Langone, L., Mangoni, O., Misic, C., & Modigh, M. (2010). The Ross Sea. In L. Liu, K.-K. Atkinson, L. Quinones, & R. Talaue-McManus (Eds.), *Carbon and nutrient fluxes in continental margins: A global synthesis* (pp. 303–318). Springer.

Celussi, M., Bergamasco, A., Cataletto, B., Umani, S. F., & Del Negro, P. (2010). Water masses' bacterial community structure and microbial activities in the Ross Sea, Antarctica. *Antarctic Science*, *22*(4), 361–370. https://doi.org/10.1017/S0954102010000192

Celussi, M., Cataletto, B., Fonda Umani, S., & Del Negro, P. (2009). Depth profiles of bacterioplankton assemblages and their activities in the Ross Sea. *Deep Sea Research Part I: Oceanographic Research Papers*, *56*(12), 2193–2205. https://doi.org/10.1016/j.dsr.2009.09.001

Celussi, M., Malfatti, F., Annalisa, F., Gazeau, F., Giannakourou, A., Pitta, P., Tsiola, A., & Del Negro, P. (2017). Ocean acidification effect on prokaryotic metabolism tested in two diverse trophic regimes in the Mediterranean Sea. *Ocean acidification in the Mediterranean Sea: pelagic mesocosm experiments*, *186*, 125–138. https://doi.org/10.1016/j.ecss.2015.08.015

Celussi, M., Malfatti, F., Ziveri, P., Giani, M., & Del Negro, P. (2017). Uptake-release dynamics of the inorganic and organic carbon pool mediated by planktonic prokaryotes in the deep Mediterranean Sea. *Environmental Microbiology*, *19*(3), 1163–1175. https://doi.org/https://doi.org/10.1111/1462-2920.13641

Datta, M. S., Sliwerska, E., Gore, J., Polz, M. F., & Cordero, O. X. (2016). Microbial interactions lead to rapid micro-scale successions on model marine particles. *Nature Communications*, *7*(1), 11965. https://doi.org/10.1038/ncomms11965

DeLorenzo, S., Bräuer, S. L., Edgmont, C. A., Herfort, L., Tebo, B. M., & Zuber, P. (2012). Ubiquitous Dissolved Inorganic Carbon Assimilation by Marine Bacteria in the Pacific Northwest Coastal Ocean as Determined by Stable Isotope Probing. *PLOS ONE*, *7*(10), 1–15. https://doi.org/10.1371/journal.pone.0046695

Deschamps, P., Zivanovic, Y., Moreira, D., Rodriguez-Valera, F., & López-García, P. (2014). Pangenome Evidence for Extensive Interdomain Horizontal Transfer Affecting Lineage Core and Shell Genes in Uncultured Planktonic Thaumarchaeota and Euryarchaeota. *Genome Biology and Evolution*, *6*(7), 1549–1563. https://doi.org/10.1093/gbe/evu127

DiTullio, G. R., Grebmeier, J. M., Arrigo, K. R., Lizotte, M. P., Robinson, D. H., Leventer, A., Barry, J. P., VanWoert, M. L., & Dunbar, R. B. (2000). Rapid and early export of Phaeocystis antarctica blooms in the Ross Sea, Antarctica. *Nature*, *404*(6778), 595–598. https://doi.org/10.1038/35007061

DiTullio, G. R., & Smith Jr., W. O. (1996). Spatial patterns in phytoplankton biomass and pigment distributions in the Ross Sea. *Journal of Geophysical Research: Oceans*, *101*(C8), 18467–18477. https://doi.org/https://doi.org/10.1029/96JC00034

Ducklow, H. W., Steinberg, D. K., & Buesseler, K. O. (2001). Upper ocean carbon export and the biological pump. *Oceanography*, *14*(SPL.ISS. 4), 50–58. https://doi.org/10.5670/oceanog.2001.06

Dupont, C. L., Rusch, D. B., Yooseph, S., Lombardo, M.-J., Alexander Richter, R., Valas, R., Novotny, M., Yee-Greenbaum, J., Selengut, J. D., Haft, D. H., Halpern, A. L., Lasken, R. S., Nealson, K., Friedman, R., & Craig Venter, J. (2012). Genomic insights to SAR86, an abundant and uncultivated marine bacterial lineage. *The ISME Journal*, *6*(6), 1186–1199. https://doi.org/10.1038/ismej.2011.189

Duret, M. T., Lampitt, R. S., & Lam, P. (2019). Prokaryotic niche partitioning between suspended and sinking marine particles. *Environmental Microbiology Reports*, *11*(3), 386–400. https://doi.org/https://doi.org/10.1111/1758-2229.12692

Eiler, A., & Bertilsson, S. (2004). Composition of freshwater bacterial communities associated with cyanobacterial blooms in four Swedish lakes. *Environmental Microbiology*, *6*(12), 1228–1243. https://doi.org/https://doi.org/10.1111/j.1462-2920.2004.00657.x

Erb, T. J. (2011). Carboxylases in Natural and Synthetic Microbial Pathways. *Applied and Environmental Microbiology*, *77*(24), 8466–8477. https://doi.org/10.1128/AEM.05702-11

Fernández-Gómez, B., Richter, M., Schüler, M., Pinhassi, J., Acinas, S. G., González, J. M., & Pedrós-Alió, C. (2013). Ecology of marine Bacteroidetes: A comparative genomics approach. *The ISME Journal*, *7*(5), 1026–1037. https://doi.org/10.1038/ismej.2012.169

Fontanez, K. M., Eppley, J. M., Samo, T. J., Karl, D. M., & DeLong, E. F. (2015). Microbial community structure and function on sinking particles in the North Pacific Subtropical Gyre. *Frontiers in Microbiology*, *6*, 469. https://doi.org/10.3389/fmicb.2015.00469

Fourquez, M., Beier, S., Jongmans, E., Hunter, R., & Obernosterer, I. (2016). Uptake of Leucine, Chitin, and Iron by Prokaryotic Groups during Spring Phytoplankton Blooms Induced by Natural Iron Fertilization off Kerguelen Island (Southern Ocean). *Frontiers in Marine Science*, *3*, 256. https://doi.org/10.3389/fmars.2016.00256

Fuhrman, J. A. (1999). Marine viruses and their biogeochemical and ecological effects. *Nature*, *399*(6736), 541–548. https://doi.org/10.1038/21119

Giering, S. L. C., Sanders, R., Lampitt, R. S., Anderson, T. R., Tamburini, C., Boutrif, M., Zubkov, M. V., Marsay, C. M., Henson, S. A., Saw, K., Cook, K., & Mayor, D. J. (2014). Reconciliation of the carbon budget in the ocean's twilight zone. *Nature*, *507*(7493), 480–483. https://doi.org/10.1038/nature13123

Giovannoni, S. J. (2017). SAR11 Bacteria: The Most Abundant Plankton in the Oceans. *Annual Review of Marine Science*, *9*(1), 231–255. https://doi.org/10.1146/annurev-marine-010814-015934

Giovannoni, S. J., Cameron Thrash, J., & Temperton, B. (2014). Implications of streamlining theory for microbial ecology. *The ISME Journal*, *8*(8), 1553–1565. https://doi.org/10.1038/ismej.2014.60

Gómez-Pereira, P. R., Schüler, M., Fuchs, B. M., Bennke, C., Teeling, H., Waldmann, J., Richter, M., Barbe, V., Bataille, E., Glöckner, F. O., & Amann, R. (2012). Genomic content of uncultured Bacteroidetes from contrasting oceanic provinces in the North Atlantic Ocean. *Environmental Microbiology*, *14*(1), 52–66. https://doi.org/https://doi.org/10.1111/j.1462-2920.2011.02555.x

González, J. M., Fernández-Gómez, B., Fernàndez-Guerra, A., Gómez-Consarnau, L., Sánchez, O., Coll-Lladó, M., del Campo, J., Escudero, L., Rodríguez-Martínez, R., Alonso-Sáez, L., Latasa, M., Paulsen, I., Nedashkovskaya, O., Lekunberri, I., Pinhassi, J., & Pedrós-Alió, C. (2008). Genome analysis of the proteorhodopsin-containing marine bacterium Polaribacter sp. MED152 (Flavobacteria). *Proceedings of the National Academy of Sciences*, *105*(25), 8724–8729. https://doi.org/10.1073/pnas.0712027105

Grossart, H.-P. (1999). Interactions between marine bacteria and axenic diatoms (Cylindrotheca fusiformis, Nitzschia laevis, and Thalassiosira weissflogii) incubated under various conditions in the lab. *Aquatic Microbial Ecology*, *19*(1), 1–11. https://www.int-res.com/abstracts/ame/v19/n1/p1-11/

Grossart, H.-P., Levold, F., Allgaier, M., Simon, M., & Brinkhoff, T. (2005). Marine diatom species harbour distinct bacterial communities. *Environmental Microbiology*, *7*(6), 860–873. https://doi.org/https://doi.org/10.1111/j.1462-2920.2005.00759.x

Grossart, H.-P., & Simon, M. (1993). Limnetic macroscopic organic aggregates (lake snow): Occurrence, characteristics, and microbial dynamics in Lake Constance. *Limnology and Oceanography*, *38*(3), 532–546. https://doi.org/https://doi.org/10.4319/lo.1993.38.3.0532

Halsey, K. H., Carter, A. E., & Giovannoni, S. J. (2012). Synergistic metabolism of a broad range of C1 compounds in the marine methylotrophic bacterium HTCC2181. *Environmental Microbiology*, *14*(3), 630–640. https://doi.org/https://doi.org/10.1111/j.1462-2920.2011.02605.x

Hardy, J. T., Hunter, K. A., Calmet, D., Cleary, J. J., Duce, R. A., Forbes, T. L., Gladyshev, M. L., Harding, G., Shenker, J. M., Tratnyek, P., & al et, e. (1997). Report Group 2 – Biological effects of chemical and radiative change in the sea surface. In P. S. Liss & R. A. Duce (Eds.), *The Sea Surface and Global Change* (pp. 35–70). Cambridge University Press. https://doi.org/10.1017/CBO9780511525025.003

Hauck, J., Völker, C., Wolf-Gladrow, D. A., Laufkötter, C., Vogt, M., Aumont, O., Bopp, L., Buitenhuis, E. T., Doney, S. C., Dunne, J., Gruber, N., Hashioka, T., John, J., Quéré, C. L., Lima, I. D., Nakano, H., Séférian, R., & Totterdell, I. (2015). On the Southern Ocean CO2 uptake and the role of the biological carbon pump in the 21st century. *Global Biogeochemical Cycles*, *29*(9), 1451–1470. https://doi.org/https://doi.org/10.1002/2015GB005140

Herndl, G. J., Reinthaler, T., Teira, E., van Aken, H., Veth, C., Pernthaler, A., & Pernthaler, J. (2005). Contribution of Archaea to Total Prokaryotic Production in the Deep Atlantic Ocean. *Applied and Environmental Microbiology*, *71*(5), 2303–2309. https://doi.org/10.1128/AEM.71.5.2303-2309.2005

Holm-Hansen, O., Amos, A. F., & Hewes, C. D. (2000). Reliability of estimating chlorophyll a concentrations in Antarctic waters by measurement of in situ chlorophyll a fluorescence. *Marine Ecology Progress Series*, *196*, 103–110. http://www.jstor.org/stable/24855096

Holm-Hansen, O., Lorenzen, C. J., Holmes, R. W., & Strickland, J. D. H. (1965). Fluorometric Determination of Chlorophyll. *ICES Journal of Marine Science*, *30*(1), 3–15. https://doi.org/10.1093/icesjms/30.1.3

Hoppe, H.-G. (1993). Use of Fluorogenic Model Substrates for Extracellular Enzyme Activity (EEA) Measurement of Bacteria. In P. F. Kemp, B. F. Sherr, E. B. Sherr, & J. J. Cole (Eds.), *Handbook of Methods in Aquatic Microbial Ecology* (1st ed., pp. 423–431). Routledge. https://doi.org/10.1201/9780203752746-49

Hou, S., Saw, J. H., Lee, K. S., Freitas, T. A., Belisle, C., Kawarabayasi, Y., Donachie, S. P., Pikina, A., Galperin, M. Y., Koonin, E. V., Makarova, K. S., Omelchenko, M. V., Sorokin, A., Wolf, Y. I., Li, Q. X., Keum, Y. S., Campbell, S., Denery, J., Aizawa, S.-I., … Alam, M. (2004). Genome sequence of the deep-sea γ-proteobacterium Idiomarina loihiensis reveals amino acid fermentation as a source of carbon and energy. *Proceedings of the National Academy of Sciences*, *101*(52), 18036–18041. https://doi.org/10.1073/pnas.0407638102

Katoh, K., Misawa, K., Kuma, K.-i., & Miyata, T. (2002). MAFFT: A novel method for rapid multiple sequence alignment based on fast Fourier transform. *Nucleic Acids Research*, *30*(14), 3059–3066. https://doi.org/10.1093/nar/gkf436

Kiørboe, T. (2001). Formation and fate of marine snow: Small-scale processes with large- scale implications. *Scientia Marina*, *65*(S2), 57–71. https://doi.org/10.3989/scimar.2001.65s257

Kiørboe, T., Grossart, H. P., Ploug, H., Tang, K. W., & Auer, B. (2004). Particle-associated flagellates: Swimming patterns, colonization rates, and grazing on attached bacteria. *Aquatic Microbial Ecology*, *35*(2), 141–152. https://doi.org/10.3354/ame035141

Kiørboe, T., Grossart, H., Ploug, H., & Tang, K. (2002). Mechanisms and rates of bacterial colonization of sinking aggregates. *Applied and Environmental Microbiology*, *68*(8), 3996–4006. https://doi.org/10.1128/AEM.68.8.3996-4006.2002

Kiørboe, T., & Jackson, G. A. (2001). Marine snow, organic solute plumes, and optimal chemosensory behavior of bacteria. *Limnology and Oceanography*, *46*(6), 1309–1318. https://doi.org/https://doi.org/10.4319/lo.2001.46.6.1309

Kirchman, D., K'nees, E., & Hodson, R. (1985). Leucine incorporation and its potential as a measure of protein synthesis by bacteria in natural aquatic systems. *Applied and Environmental Microbiology*, *49*(3), 599–607. https://aem.asm.org/content/49/3/599

Kwon, E. Y., Primeau, F., & Sarmiento, J. L. (2009). The impact of remineralization depth on the air–sea carbon balance. *Nature Geoscience*, *2*(9), 630–635. https://doi.org/10.1038/ngeo612

La Cono, V., Smedile, F., La Spada, G., Arcadi, E., Genovese, M., Ruggeri, G., Genovese, L., Giuliano, L., & Yakimov, M. M. (2015). Shifts in the meso- and bathypelagic archaea communities composition during recovery and short-term handling of decompressed deep-sea samples. *Environmental Microbiology Reports*, *7*(3), 450–459. https://doi.org/https://doi.org/10.1111/1758-2229.12272

La Ferla, R., Maimone, G., Lo Giudice, A., Azzaro, F., Cosenza, A., & Azzaro, M. (2015). Cell size and other phenotypic traits of prokaryotic cells in pelagic areas of the Ross Sea (Antarctica). *Hydrobiologia*, *761*(1), 181–194. https://doi.org/10.1007/s10750-015-2426-7

Landa, M., Blain, S., Christaki, U., Monchy, S., & Obernosterer, I. (2016). Shifts in bacterial community composition associated with increased carbon cycling in a mosaic of phytoplankton blooms. *The ISME Journal*, *10*(1), 39–50. https://doi.org/10.1038/ismej.2015.105

Landa, M., Blain, S., Harmand, J., Monchy, S., Rapaport, A., & Obernosterer, I. (2018). Major changes in the composition of a Southern Ocean bacterial community in response to diatom-derived dissolved organic matter. *FEMS Microbiology Ecology*, *94*(4). https://doi.org/10.1093/femsec/fiy034

LeCleir, G. R., DeBruyn, J. M., Maas, E. W., Boyd, P. W., & Wilhelm, S. W. (2014). Temporal changes in particle-associated microbial communities after interception by nonlethal sediment traps. *FEMS Microbiology Ecology*, *87*(1), 153–163. https://doi.org/10.1111/1574-6941.12213

Liu, S., Wawrik, B., & Liu, Z. (2017). Different Bacterial Communities Involved in Peptide Decomposition between Normoxic and Hypoxic Coastal Waters. *Frontiers in Microbiology*, *8*, 353. https://doi.org/10.3389/fmicb.2017.00353

Lorenzen, C., & Jeffrey, S. (1980). Determination of chlorophyll in seawater. *Unesco technical papers in marine sciences*, *35*(1), 1–20.

Luria, C. M., Amaral-Zettler, L. A., Ducklow, H. W., Repeta, D. J., Rhyne, A. L., & Rich, J. J. (2017). Seasonal Shifts in Bacterial Community Responses to Phytoplankton-Derived Dissolved Organic Matter in the Western Antarctic Peninsula. *Frontiers in Microbiology*, *8*, 2117. https://doi.org/10.3389/fmicb.2017.02117

Marie, D., Brussaard, C. P. D., Thyrhaug, R., Bratbak, G., & Vaulot, D. (1999). Enumeration of Marine Viruses in Culture and Natural Samples by Flow Cytometry. *Applied and Environmental Microbiology*, *65*(1), 45–52. https://doi.org/10.1128/AEM.65.1.45-52.1999

Martinez, J., Smith, D. C., Steward, G. F., & Azam, F. (1996). Variability in ectohydrolytic enzyme activities of pelagic marine bacteria and its significance for substrate processing in the sea. *Aquatic Microbial Ecology*, *10*(3), 223–230. https://doi.org/10.3354/ame010223

Mathot, S., Smith Jr., W. O., Carlson, C. A., Garrison, D. L., Gowing, M. M., & Vickers, C. L. (2000). CARBON PARTITIONING WITHIN PHAEOCYSTIS ANTARCTICA (PRYMNESIOPHYCEAE) COLONIES IN THE ROSS SEA, ANTARCTICA. *Journal of Phycology*, *36*(6), 1049–1056. https://doi.org/https://doi.org/10.1046/j.1529-8817.2000.99078.x

Nielsen, E. S. (1952). The Use of Radio-active Carbon (C14) for Measuring Organic Production in the Sea. *ICES Journal of Marine Science*, *18*(2), 117–140. https://doi.org/10.1093/icesjms/18.2.117

Oksanen, J., Blanchet, F. G., Friendly, M., Kindt, R., Legendre, P., McGlinn, D., Minchin, P. R., O'Hara, R. B., Simpson, G. L., Solymos, P., Stevens, M. H. H., Szoecs, E., & Wagner, H. (2019). *Vegan: Community Ecology Package*. https://CRAN.R-project.org/package=vegan

Orsi, W. D., Smith, J. M., Wilcox, H. M., Swalwell, J. E., Carini, P., Worden, A. Z., & Santoro, A. E. (2015). Ecophysiology of uncultivated marine euryarchaea is linked to particulate organic matter. *The ISME Journal*, *9*(8), 1747–1763. https://doi.org/10.1038/ismej.2014.260

Parada, A. E., Needham, D. M., & Fuhrman, J. A. (2016). Every base matters: Assessing small subunit rRNA primers for marine microbiomes with mock communities, time series and global field samples. *Environmental Microbiology*, *18*(5), 1403–1414. https://doi.org/https://doi.org/10.1111/1462-2920.13023

Passow, U., & Carlson, C. A. (2012). The biological pump in a high CO2 world. *Marine Ecology Progress Series*, *470*, 249–271. https://www.int-res.com/abstracts/meps/v470/p249-271/

Pedler, B. E., Aluwihare, L. I., & Azam, F. (2014). Single bacterial strain capable of significant contribution to carbon cycling in the surface ocean. *Proceedings of the National Academy of Sciences*, *111*(20), 7202–7207. https://doi.org/10.1073/pnas.1401887111

Pelve, E. A., Fontanez, K. M., & DeLong, E. F. (2017). Bacterial Succession on Sinking Particles in the Ocean's Interior. *Frontiers in Microbiology*, *8*, 2269. https://doi.org/10.3389/fmicb.2017.02269

Porter, K. G., & Feig, Y. S. (1980). The use of DAPI for identifying and counting aquatic microflora1. *Limnology and Oceanography*, *25*(5), 943–948. https://doi.org/https://doi.org/10.4319/lo.1980.25.5.0943

Price, M. N., Dehal, P. S., & Arkin, A. P. (2010). FastTree 2 – Approximately Maximum-Likelihood Trees for Large Alignments. *PLOS ONE*, *5*(3), e9490. https://doi.org/10.1371/journal.pone.0009490

Quast, C., Pruesse, E., Yilmaz, P., Gerken, J., Schweer, T., Yarza, P., Peplies, J., & Glöckner, F. O. (2013). The SILVA ribosomal RNA gene database project: Improved data processing and web-based tools. *Nucleic acids research*, *41*(Database issue), D590–D596. https://doi.org/10.1093/nar/gks1219

Quero, G. M., Celussi, M., Relitti, F., Kovačević, V., Del Negro, P., & Luna, G. M. (2020). Inorganic and Organic Carbon Uptake Processes and Their Connection to Microbial Diversity in Meso- and Bathypelagic Arctic Waters (Eastern Fram Strait). *Microbial Ecology*, *79*(4), 823–839. https://doi.org/10.1007/s00248-019-01451-2

R Core Team. (2019). *R: A Language and Environment for Statistical Computing*. R Foundation for Statistical Computing. https://www.R-project.org/

Reintjes, G., Arnosti, C., Fuchs, B., & Amann, R. (2019). Selfish, sharing and scavenging bacteria in the Atlantic Ocean: A biogeographical study of bacterial substrate utilisation. *The ISME Journal*, *13*(5), 1119–1132. https://doi.org/10.1038/s41396-018-0326-3

Reintjes, G., Arnosti, C., Fuchs, B. M., & Amann, R. (2017). An alternative polysaccharide uptake mechanism of marine bacteria. *The ISME Journal*, *11*(7), 1640–1650. https://doi.org/10.1038/ismej.2017.26

Rembauville, M., Salter, I., Leblond, N., Gueneugues, A., & Blain, S. (2015). Export fluxes in a naturally iron-fertilized area of the Southern Ocean – Part 1: Seasonal dynamics of particulate organic carbon export from a moored sediment trap. *Biogeosciences*, *12*(11), 3153–3170. https://doi.org/10.5194/bg-12-3153-2015

Riemann, L., & Grossart, H.-P. (2008). Elevated Lytic Phage Production as a Consequence of Particle Colonization by a Marine Flavobacterium (Cellulophaga sp.) *Microbial Ecology*, *56*(3), 505–512. https://doi.org/10.1007/s00248-008-9369-8

Rivaro, P., Ardini, F., Grotti, M., Aulicino, G., Cotroneo, Y., Fusco, G., Mangoni, O., Bolinesi, F., Saggiomo, M., & Celussi, M. (2019). Mesoscale variability related to iron speciation in a coastal Ross Sea area (Antarctica) during summer 2014. *Chemistry and Ecology*, *35*(1), 1–19. https://doi.org/10.1080/02757540.2018.1531987

Rocha, C. L. D. L., & Passow, U. (2007). Factors influencing the sinking of POC and the efficiency of the biological carbon pump. *Deep Sea Research Part II: Topical Studies in Oceanography*, *54*(5), 639–658. https://doi.org/https://doi.org/10.1016/j.dsr2.2007.01.004

Rogers, A., Frinault, B., Barnes, D., Bindoff, N., Downie, R., Ducklow, H., Friedlaender, A., Hart, T., Hill, S., Hofmann, E., Linse, K., McMahon, C., Murphy, E., Pakhomov, E., Reygondeau, G., Staniland, I., Wolf-Gladrow, D., & Wright, R. (2020). Antarctic Futures: An Assessment of Climate-Driven Changes in Ecosystem Structure, Function, and Service Provisioning in the Southern Ocean. *Annual Review of Marine Science*, *12*(1), 87–120. https://doi.org/10.1146/annurev-marine-010419-011028

Sabine, C. L., Feely, R. A., Gruber, N., Key, R. M., Lee, K., Bullister, J. L., Wanninkhof, R., Wong, C. S., Wallace, D. W. R., Tilbrook, B., Millero, F. J., Peng, T.-H., Kozyr, A., Ono, T., & Rios, A. F. (2004). The Oceanic Sink for Anthropogenic CO2. *Science*, *305*(5682), 367–371. https://doi.org/10.1126/science.1097403

Schine, C. M. S., van Dijken, G., & Arrigo, K. R. (2016). Spatial analysis of trends in primary production and relationship with large-scale climate variability in the Ross Sea, Antarctica (1997–2013). *Journal of Geophysical Research: Oceans*, *121*(1), 368–386. https://doi.org/https://doi.org/10.1002/2015JC011014

Smetacek, V., & Nicol, S. (2005). Polar ocean ecosystems in a changing world. *Nature*, *437*(7057), 362–368. https://doi.org/10.1038/nature04161

Smith, D. C., Simon, M., Alldredge, A. L., & Azam, F. (1992). Intense hydrolytic enzyme activity on marine aggregates and implications for rapid particle dissolution. *Nature*, *359*(6391), 139–142. https://doi.org/10.1038/359139a0

Smith, W. O., Ainley, D. G., Arrigo, K. R., & Dinniman, M. S. (2014). The Oceanography and Ecology of the Ross Sea. *Annual Review of Marine Science*, *6*(1), 469–487. https://doi.org/10.1146/annurev-marine-010213-135114

Sowell, S. M., Wilhelm, L. J., Norbeck, A. D., Lipton, M. S., Nicora, C. D., Barofsky, D. F., Carlson, C. A., Smith, R. D., & Giovanonni, S. J. (2009). Transport functions dominate the SAR11 metaproteome at low-nutrient extremes in the Sargasso Sea. *The ISME Journal*, *3*(1), 93–105. https://doi.org/10.1038/ismej.2008.83

Sperling, M., Piontek, J., Engel, A., Wiltshire, K. H., Niggemann, J., Gerdts, G., & Wichels, A. (2017). Combined Carbohydrates Support Rich Communities of Particle-

Associated Marine Bacterioplankton. *Frontiers in Microbiology*, *8*, 65. https://doi.org/10.3389/fmicb.2017.00065

Strzepek, R. F., Maldonado, M. T., Hunter, K. A., Frew, R. D., & Boyd, P. W. (2011). Adaptive strategies by Southern Ocean phytoplankton to lessen iron limitation: Uptake of organically complexed iron and reduced cellular iron requirements. *Limnology and Oceanography*, *56*(6), 1983–2002. https://doi.org/10.4319/lo.2011.56.6.1983

Tamburini, C., Boutrif, M., Garel, M., Colwell, R. R., & Deming, J. W. (2013). Prokaryotic responses to hydrostatic pressure in the ocean – a review. *Environmental Microbiology*, *15*(5), 1262–1274. https://doi.org/10.1111/1462-2920.12084

Teeling, H., Fuchs, B. M., Becher, D., Klockow, C., Gardebrecht, A., Bennke, C. M., Kassabgy, M., Huang, S., Mann, A. J., Waldmann, J., Weber, M., Klindworth, A., Otto, A., Lange, J., Bernhardt, J., Reinsch, C., Hecker, M., Peplies, J., Bockelmann, F. D., … Amann, R. (2012). Substrate-controlled succession of marine bacterioplankton populations induced by a phytoplankton bloom. *Science*, *336*(6081), 608–611. https://doi.org/10.1126/science.1218344

Teeling, H., Fuchs, B. M., Bennke, C. M., Krüger, K., Chafee, M., Kappelmann, L., Reintjes, G., Waldmann, J., Quast, C., Glöckner, F. O., Lucas, J., Wichels, A., Gerdts, G., Wiltshire, K. H., & Amann, R. I. (2016). Recurring patterns in bacterioplankton dynamics during coastal spring algae blooms. *eLife*, *5*(APRIL2016), 1–31. https://doi.org/10.7554/eLife.11888

Thompson, L. R., Field, C., Romanuk, T., Kamanda Ngugi, D., Siam, R., El Dorry, H., & Stingl, U. (2013). Patterns of ecological specialization among microbial populations in the Red Sea and diverse oligotrophic marine environments. *Ecology and Evolution*, *3*(6), 1780–1797. https://doi.org/10.1002/ece3.593

Throndsen, J. (1978). Preservation and storage. *Phytoplankton manual* (pp. 69–74). Unesco.

Tripp, H. J. (2013). The unique metabolism of SAR11 aquatic bacteria. *Journal of Microbiology*, *51*(2), 147–153. https://doi.org/10.1007/s12275-013-2671-2

Turner, J., Comiso, J. C., Marshall, G. J., Lachlan-Cope, T. A., Bracegirdle, T., Maksym, T., Meredith, M. P., Wang, Z., & Orr, A. (2009). Non-annular atmospheric circulation change induced by stratospheric ozone depletion and its role in the recent increase of Antarctic sea ice extent. *Geophysical Research Letters*, *36*(8). https://doi.org/10.1029/2009GL037524

Utermöhl, H. (1958). Zur vervollkommnung der quantitativen phytoplankton-methodik: Mit 1 Tabelle und 15 abbildungen im Text und auf 1 Tafel. *Internationale Vereinigung für theoretische und angewandte Limnologie: Mitteilungen*, *9*(1), 1–38.

Venables, W. N., & Ripley, B. D. (2013). *Modern applied statistics with S-PLUS*. Springer Science & Business Media.

Wickham, H. (2016). *Ggplot2: Elegant Graphics for Data Analysis*. Springer-Verlag New York. https://ggplot2.tidyverse.org

Wietz, M., Wemheuer, B., Simon, H., Giebel, H.-A., Seibt, M. A., Daniel, R., Brinkhoff, T., & Simon, M. (2015). Bacterial community dynamics during polysaccharide degradation at contrasting sites in the Southern and Atlantic Oceans. *Environmental Microbiology*, *17*(10), 3822–3831. https://doi.org/10.1111/1462-2920.12842

Williams, T. J., Wilkins, D., Long, E., Evans, F., DeMaere, M. Z., Raftery, M. J., & Cavicchioli, R. (2013). The role of planktonic Flavobacteria in processing algal organic matter in coastal East Antarctica revealed using metagenomics and metaproteomics. *Environmental Microbiology*, *15*(5), 1302–1317. https://doi.org/10.1111/1462-2920.12017

Yakimov, M. M., Cono, V. L., Smedile, F., DeLuca, T. H., Juárez, S., Ciordia, S., Fernández, M., Albar, J. P., Ferrer, M., Golyshin, P. N., & Giuliano, L. (2011). Contribution of crenarchaeal autotrophic ammonia oxidizers to the dark primary production in Tyrrhenian deep waters (Central Mediterranean Sea). *The ISME Journal*, *5*(6), 945–961. https://doi.org/10.1038/ismej.2010.197

Zeng, Y. (2019). Phylogenetic diversity of dimethylsulfoniopropionatedependent demethylase gene dmdA in distantly related bacteria isolated from Arctic and Antarctic marine environments. *Acta Oceanologica Sinica*, *38*(8), 64–71. https://doi.org/10.1007/s13131-019-1393-7

Zetsche, E.-M., Larsson, A. I., Iversen, M. H., & Ploug, H. (2020). Flow and diffusion around and within diatom aggregates: Effects of aggregate composition and shape. *Limnology and Oceanography*, *65*(8), 1818–1833. https://doi.org/10.1002/lno.11420

Zhang, C. L., Xie, W., Martin-Cuadrado, A.-B., & Rodriguez-Valera, F. (2015). Marine Group II Archaea, potentially important players in the global ocean carbon cycle. *Frontiers in Microbiology*, *6*, 1108. https://doi.org/10.3389/fmicb.2015.01108

Zoccarato, L., Pallavicini, A., Cerino, F., Fonda Umani, S., & Celussi, M. (2016). Water mass dynamics shape Ross Sea protist communities in mesopelagic and bathypelagic layers. *Progress in Oceanography*, *149*, 16–26. https://doi.org/10.1016/j.pocean.2016.10.003

5

Modulation of hydrolytic profiles of cell-bound and cell-free exoenzymes in Antarctic marine bacterial isolates

This Chapter is adapted from: Manna, V., Del Negro, P., Celussi, M., 2019. Modulation of hydrolytic profiles of cell-bound and cell-free exoenzymes in Antarctic marine bacterial isolates. Advances in Oceanography and Limnology, 10, 32–43. https://doi.org/10.4081/aiol.2019.8240

5.1. Introduction

Microorganisms play a pivotal role in the marine carbon cycle (Azam and Malfatti, 2007), by producing, processing and utilizing one of the largest pool of active C-containing molecules on Earth (Hansell et al., 2009). In order to obtain the energy and carbon source required for growth, microbes utilize preferentially high-molecular weight substrates, as they are more bioavailable, according to the size-reactivity model (Benner and Amon, 2015). However, only small molecules can be taken up by the cells and therefore extracellular hydrolysis is a vital process for prokaryotic heterotrophs (reviewed by Arnosti, 2011). In fact, measurable organic matter degradation rates have been found in all marine environments where life is possible, from deep subsurface sediments (Hoarfrost et al., 2017) through the water column (e.g. Celussi et al., 2018; Hoppe and Ullrich, 1999), to sea spray aerosol particles ejected to the atmosphere (Malfatti et al., 2019), form the equator to the poles (Celussi et al., 2009; Misic et al., 2006). Due to the wide array of environmental conditions (e.g. temperature, salinity, pH, pressure) where microorganisms thrive and produce active hydrolytic enzymes, such proteins harbor the potential for extensive utilization in biotechnological and industrial applications (Nigam, 2013).

Specialized prokaryotes invest their energy efforts into the degradation of specific complex substrates (e.g. hydrocarbons, plastics; Hassanshahian et al., 2014; Yoshida et al., 2016) whereas generalists harbor the potential for hydrolyzing a wide array of macromolecules (Martinez et al., 1996). Another strategy is dependent on the location of exoenzymes with respect to the producing cell. In fact, exoenzymes can be cell-associated (i.e. attached to the cell wall or in the periplasmic space) or released (i.e. cell-free) in the surrounding waters (Hoppe et al., 2002), thus identifying selfish vs. 'social' foragers (Traving et al., 2015. In the former case, after the uptake of large oligomers, further degradation occurs in the protected periplasmic space, avoiding diffusive loss of target monomers and enzymes (Reintjes et al., 2017). In the latter case the release of enzymes is thought to be beneficial for microorganisms living attached to particles or colloids, where different cells can take advantage of specific degradation products made available by other consortium members in diffusionally constrained microenvironments (Vetter et al., 1998). Within this scheme Reintjes et al., 2019 recently included the category of 'scavengers', defined as microbes that do not produce specific exoenzymes and take advantage of the 'public goods' made available by other cells. Much attention has lately been addressed to cell-free enzymes, since they may not be strictly dependent on the metabolism of microbes, but their presence could also be a consequence of the history and dynamics of the water masses, due to their potential long-term persistence in the environment (Baltar, 2018). Within this framework we aimed at characterizing the degradative potential of several bacterial isolates and, by utilizing one of these model organisms, providing a proof of concept on the differential production of cell-free enzymes by particle-attached microbes, if compared to their free-living counterparts.

We chose a set of bacteria isolated from several locations and depth in the Ross Sea (Antarctica) for two main reasons. The first, of ecological nature, is related to the high summer productivity of the Ross Sea. Indeed, in this system the export of particulate organic carbon (POC) to the mesopelagic is approximately 40-50% of the sur-

face primary production (Catalano et al., 2010), compared to a global estimate ranging from 1 to 40% (Ducklow et al., 2001). Since the fate of sinking POC is highly dependent on its mineralization by prokaryotes (>70% of the total loss during export – Giering et al., 2014) we envisioned to obtain model organisms (bacterial isolates) and model particles (Antarctic phytodetritus) to deepen the current knowledge on POC degradation and POC-bacteria interactions. The second reason is to be related to the biotechnological potential of bacteria isolated in extreme environments. Due to the limited accessibility of these systems, the current knowledge on the bioactive molecules and secondary metabolites produced by extremophiles is extremely limited (e.g. Lo Giudice and Fani, 2015), opening inestimable chances for novel discoveries.

5.2. Materials and methods

5.2.1. Bacteria isolation

The bacterial strains used for the experimental activities were isolated from water samples collected in austral summer 2006 and 2017. Seawater was sampled at several locations and depths in the Ross Sea (Table 5.1) by means of 12-L Niskin bottles mounted on an SBE 32 carousel sampler. Seawater aliquots were collected in sterile 50-mL tubes, plated onto ZoBell 2216 agar plates and kept at 4°C. Bacterial colonies with different morphologies were selected and purified by serial streaking on the same medium for a minimum of four times. A total of 22 isolates (4 from 2006 and 18 from 2017 cruises) were maintained both in solid ZoBell 2216 agar plates and liquid ZoBell Marine Broth in the dark at 4 and 10°C, respectively. All the experimental activities described in this study were carried out between October and November 2018.

5.2.2. Bacteria identification

From each isolate DNA was extracted by means of the DNeasy Tissue Kit (Qiagen) according to the supplier's instruction. The amplification of the 16S rRNA gene was performed utilizing the universal primer 27F and the Eubacterial primer 1492R as detailed in Celussi et al., 2008. PCR products were purified using the QIAquick PCR purification kit (Qiagen) according to the supplier 's instruction and amplicons were sequenced using ABI Prism Big Dye-terminator chemistry at the 'BMR Genomics' facility at the University of Padova (www.bmr-genomics.it). Sequences were aligned to known sequences in the GenBank database using BLAST (Altschul et al., 1990). Multiple sequence alignment was performed using the SINA aligner (http://www.arb-silva.de/aligner/) and compared to the SILVA reference database release 111 (Quast et al., 2013). Phylogenetic tree was built using the Phylogeny.fr (Dereeper et al., 2008; https://www.phylogeny.fr/) tool, visualized and annotated with Interactive Tree Of Life (iTOL, v3, Letunic and Bork, 2016). The identical nucleotide sequence of several bacterial isolates led us to select 7 of them, out of the original 22, for the subsequent activities. The nucleotide sequences obtained in this study are deposited in GenBank under the accession numbers MK780011-MK780031.

Table 5.1: Details of sampling stations (coordinates, depth and location) in the Ross Sea and identifier of the strain isolated from each sample. Isolates used for experimental activities are highlighted in bold.

Isolate ID	Latitude (°S)	Longitude (°E)	Depth (m)	Date	Location
AF	**74.9400**	**-176.2432**	**400**	**23/01/2006**	**Glomar Challenge Basin core of Circumpolar Deep Water**
AG	**74.9400**	**-176.2432**	**400**	**23/01/2006**	**Glomar Challenge Basin core of Circumpolar Deep Water**
AK	**74.9400**	**-176.2432**	**400**	**23/01/2006**	**Glomar Challenge Basin core of Circumpolar Deep Water**
9	74.752	166.8105	910	23/01/2017	Drygalki Basin Bottom layer
9_1	74.752	166.8105	910	23/01/2017	Drygalki Basin Bottom layer
9_2	**74.752**	**166.8105**	**910**	**23/01/2017**	**Drygalki Basin Bottom layer**
14_1	74.752	166.8105	30	23/01/2017	Drygalki Basin Deep Chlorophyll Maximum
14_2	74.752	166.8105	30	23/01/2017	Drygalki Basin Deep Chlorophyll Maximum
14_3	74.752	166.8105	30	23/01/2017	Drygalki Basin Deep Chlorophyll Maximum
15	74.752	166.8105	5	23/01/2017	Drygalki Basin Surface Layer
16_1	74.0000	175.089	572	17/01/2017	Joides Basin Bottom Layer
16_1_1	**74.0000**	**175.089**	**572**	**17/01/2017**	**Joides Basin Bottom Layer**
16_1_2	74.0000	175.089	572	17/01/2017	Joides Basin Bottom Layer
16_1_3	74.0000	175.089	572	17/01/2017	Joides Basin Bottom Layer
16_1_4	74.0000	175.089	572	17/01/2017	Joides Basin Bottom Layer
16_1_5	74.0000	175.089	572	17/01/2017	Joides Basin Bottom Layer
16_2	74.0000	175.089	572	17/01/2017	Joides Basin Bottom Layer
20_1	**74.0000**	**175.089**	**40**	**17/01/2017**	**Joides Basin Deep Chlorophyll Maximum**
20_2	74.0000	175.089	40	17/01/2017	Joides Basin Deep Chlorophyll Maximum
20_3	74.0000	175.089	40	17/01/2017	Joides Basin Deep Chlorophyll Maximum
21	**74.0000**	**175.089**	**5**	**17/01/2017**	**Joides Basin Surface Layer**

5.2.3. Exoenzymatic fingerprinting

The The selected isolates were transferred in a ZoBell Marine Broth diluted 5 times (ZB/5) in 0.2 µm-filtered and autoclaved (121°C for 15 min) seawater (FASW) collected in the northern Adriatic Sea, and incubated at 0°C. After 2 days of acclimation at the experimental temperature, the isolates were inoculated in duplicate 100 mL aliquots of ZB/5 at a starting abundance of 10^8 Cells L^{-1} (d0). Cell numbers were determined by flow cytometry according to the method described by Marie et al., 1999. A FACSCanto II (Becton Dickinson) instrument was used, equipped with an air-cooled laser at 488 nm and standard filter setup. Samples (0.5 mL) were ultrasonicated (10 cycles of 30 sec on-off) and fixed with 0.5% (final concentration) glutaraldehyde (Grade I for EM analyses, Sigma Aldrich). Fixed samples were kept at 4°C for 15 minutes and diluted 1:10 with 0.2 µm-filtered Tris-EDTA buffer 1× (Sigma Aldrich). Samples were then stained with SYBR Green I nucleic acid dye (Life Technologies) at 1× 10^{-4} dilution of the commercial stock and incubated for 10 minutes in the dark at room temperature. Data were acquired using green fluorescence as trigger and processed with the FACSDiva software (Becton Dickinson). The flow rate was calibrated daily, by running distilled water and weighing it before and after the run (at least 5 replicates). Abundances were then calculated using the acquired cell counts and the respective flow rates. Bacterial abundance was estimated every 2 days by means of flow cytometry, as described above. When the growth curves evidenced the exponential growth phase, 50 mL of the cultures were washed twice in FASW by centrifuging at 3,200 × g for 10 min at 0°C. This procedure was aimed at transferring the isolates in a 'poorer' medium (1.48 mg L^{-1} of dissolved organic carbon, F. Relitti pers. comm.) and allowed the removal of hydrolytic enzymes in the dissolved phase.

Immediately after the washing with FASW, exoenzymatic activities (EEAs) were measured (d_{exp}). The activities of beta-glucosidase (BGLU), alkaline phosphatase (AP), lipase (LIP), chitinase (CHIT) and leucine aminopeptidase (AMA) were estimated by the artificial fluorogenic substrate analogue method (Hoppe, 1993). Artificial substrates were added to 2 mL of the isolates in FASW in triplicate, at saturating concentrations. BGLU, AP, LIP, CHIT and AMA were determined after the addition of 4-methylumbelliferone-β-D-glucoside (200 µM), 4-methylumbelliferone-phosphate (50 µM), 4-methylumbelliferone-oleate (100 µM), 4-methylumbelliferone N-acetyl-β-D glucosaminide (200 µM) and leucine-7-amino-methyl-coumarine (200 µM), respectively. All samples were incubated in the dark at 0°C for 3 h. Enzyme activities were derived from the increase in fluorescence due to the cleavage of the artificial substrate, measured with a Shimadzu RF1501 fluorometer at 365 nm excitation / 455 emission for BGLU, AP, LIP and CHIT and 380 nm excitation / 440 emission for AMA. Calibration curves were performed at each working session utilizing FASW and standard fluorochrome solutions (5 µM). The substrates and the standards were purchased from Sigma-Aldrich. The same procedure was performed on 0.2-µm-filtered subsamples to measure the activity of dissolved exoenzymes, that, as expected, was not detectable at this stage. The remaining volume of the cultures in FASW was incubated at 0°C for a number of days equal to the one necessary for bacteria to grow exponentially, as observed earlier during the experiment (i.e. from d0 to d_{exp}, between 4 and 8 days, depending on the isolate). At the end of this incubation (d_{fin}) EEA measurements and

cell counts were performed a second time.

The hydrolysis rates (normalised per cell numbers) measured in the two time points (d_{exp} and d_{fin}) were then analysed with an nMDS. The simultaneous analysis of several metabolic features (e.g. the degradation and/or utilization of specific substrates) provides useful information on the functional changes that microbes undergo in different culturing conditions and allows to visualize changes in the enzymatic profiles (Celussi et al., 2008; Del Negro et al., 2018). The nMDS was performed using a Bray-Curtis dissimilarity matrix, built with log-transformed ($ln(x+1)$) Isolates' hydrolysis rates. Analysis of similarity (ANOSIM, Clarke and Warwick, 1994) was used to test the significance of samples grouping on the nMDS plot. nMDS and ANOSIM were carried out using the R package vegan (Oksanen et al., 2019), under R version 3.5.1 (R Core Team, 2019).

5.2.4. Exoenzymatic activities on phytodetrital particles

In order to test whether bacteria growing on particles are more prone to produce cell-free (dissolved) exoenzymes, a second experiment was set up. The phytodetritus (particles) was generated from a microplankton net sample (20 µm mesh-size) collected in the Ross Sea (74.7572°S; 166.8105°E) on January 23rd, 2017 in the upper 100m of the water column. Chlorophyll a concentration in the net sample was measured by the standard fluorometric procedure (Lorenzen and Jeffrey, 1980). The identification of microplanktonic organisms in the sample was carried out on a fixed aliquot (formaldehyde solution, 4% f.c.) at the inverted microscope (Labovert FS Leitz) equipped with phase contrast at a magnification of 400× and 630×, according to the Utermöhl method (Utermöhl, 1958). The net sample was subjected to 7 cycles of freeze-thawing (-80°C / +80°C, Bidle and Azam, 1999) after which cells were pelleted (20,000 × g, 10 min, room temperature) and the supernatant (organic carbon in the dissolved phase) removed. Cells were then resuspended in an equal volume of FASW.

Four 50-mL tubes containing FASW with 10^8 Cells L^{-1} of the fast-growing isolate AG were amended with a volume of detritus to yield a concentration of 10 µg of Chlorophyll *a* L^{-1}, so as to simulate the particulate organic matter content during a phytoplankton bloom. The tubes were kept in a temperature-controlled circulating-water-bath at 10°C for 24 h to promote the colonization of particles by bacteria. After this step, the tubes were kept standing at the same temperature for additional 24 h to allow the settlement of particles at the bottom (Martinez et al., 1996). Afterwards, the upper 47 mL within the tubes, potentially bearing only free-living bacteria and dissolved exoenzymes, were carefully transferred to a new sterile 50-mL tube and the remaining 3 mL (potentially bearing only particles and particle-attached bacteria) were added with FASW to a final volume of 50 mL. So, at the end of this process, 4 tubes contained particles + attached bacteria (PART) and 4 tubes contained free-living bacteria and the dissolved fraction of exoenzymes that have been produced in the previous 48h (SUR). Half of the tubes were used for testing β-glucosidase activity and the other half for testing leucine aminopeptidase activity, in experimental duplicates. EEAs were measured after 3 and 6 h (t3 and t6) from the splitting of particles and free-living bacteria, in order to allow the production of cell-free enzymes by particle-attached bacteria. EEAs were analysed as described above on the total and < 0.2 µm fractions. At t3

and t6, samples for the enumeration of bacterial cells were collected and fixed with 0.2-µm filtered dolomite-buffered formalin (2% f.c.). In this experiment bacteria were counted at the epifluorescence microscope after DAPI staining (as detailed in Celussi et al., 2008) in order to discriminate between free-living and particle-attached cells. In this latter case, the number of cells were multiplied by a factor of 2 to compensate for the non-visible cells attached in the lower side of particles.

5.3. Results

5.3.1. Identification

Phylogenetic analysis of 16S rRNA sequences identified the 22 bacterial isolates as members of the classes *Flavobacteriia* and *γ-Proteobacteria* (Fig. 5.1). The identical nucleotide sequence of several bacterial isolates led us to select 7 of them (AG, 20_1, 16_1_1, 21, 9_2, AK and AF), out of the original 22, for the subsequent experimental activities.

5.3.2. Exoenzymatic fingerprinting of bacterial isolates

All the 7 selected isolates were able to produce the assayed exoenzymes (i.e., BGLU, AP, LIP, CHIT and AMA) both at d_{exp} and d_{fin}, with the cell-specific activities of each enzyme varying up to 1 order of magnitude among different isolates in (Fig. 5.2). The enzymatic fingerprints of different isolates were quite variable, both in terms of degradative profiles and of relative contribution of cell-free and cell-bound exoenzymes to the total cell-specific activity.

On the nMDS plot (Fig. 5.3), bacterial isolates were separated into three groups (ANOSIM R=0.95, p=0.001), according to their prevalent exoenzymatic activity. Isolates 21 and 16_1_1 were identified as mostly glycolytic strains (Fig. 5.3), both at d_{exp} and d_{fin} (see Section 5.2.3). At d_{fin} these isolates showed the highest glycolytic activity among the selected bacterial strains, coupled with an increased contribution of the dissolved exoenzymatic fraction to the total specific activity (up to 100%, Fig. 5.2). Four out of the seven tested strains were identified as harbouring a high proteolytic potential (20_1, AF, AK, AG, Fig. 5.3), showing the highest AMA specific hydrolysis rates, between 237.34 ± 1.5 and 427.29 ± 16.29 amol cell^{-1} h^{-1} (Fig. 5.2). The contribution of the dissolved exoenzymatic fraction to the total specific AMA activity was low for all the four 'proteolytic' strains (between 0 and 6%, Fig. 5.2). While at d_{fin} these strains were all identified as highly proteolytic, AK and AG were characterized by high production of lipases and alkaline phosphatases at the beginning of the experiment (d_{exp}, Fig. 5.3). This pattern was partly retained also in the at d_{fin} as AK and AG were the only strains, among the proteolytic ones, to show a relatively higher specific alkaline-phosphatase and lipase activities (Fig. 5.2). All the strongly proteolytic isolates showed extremely low values of BGLU and CHIT specific activities (<2 and <1 amol cell^{-1} h^{-1}, respectively, Fig. 5.2).

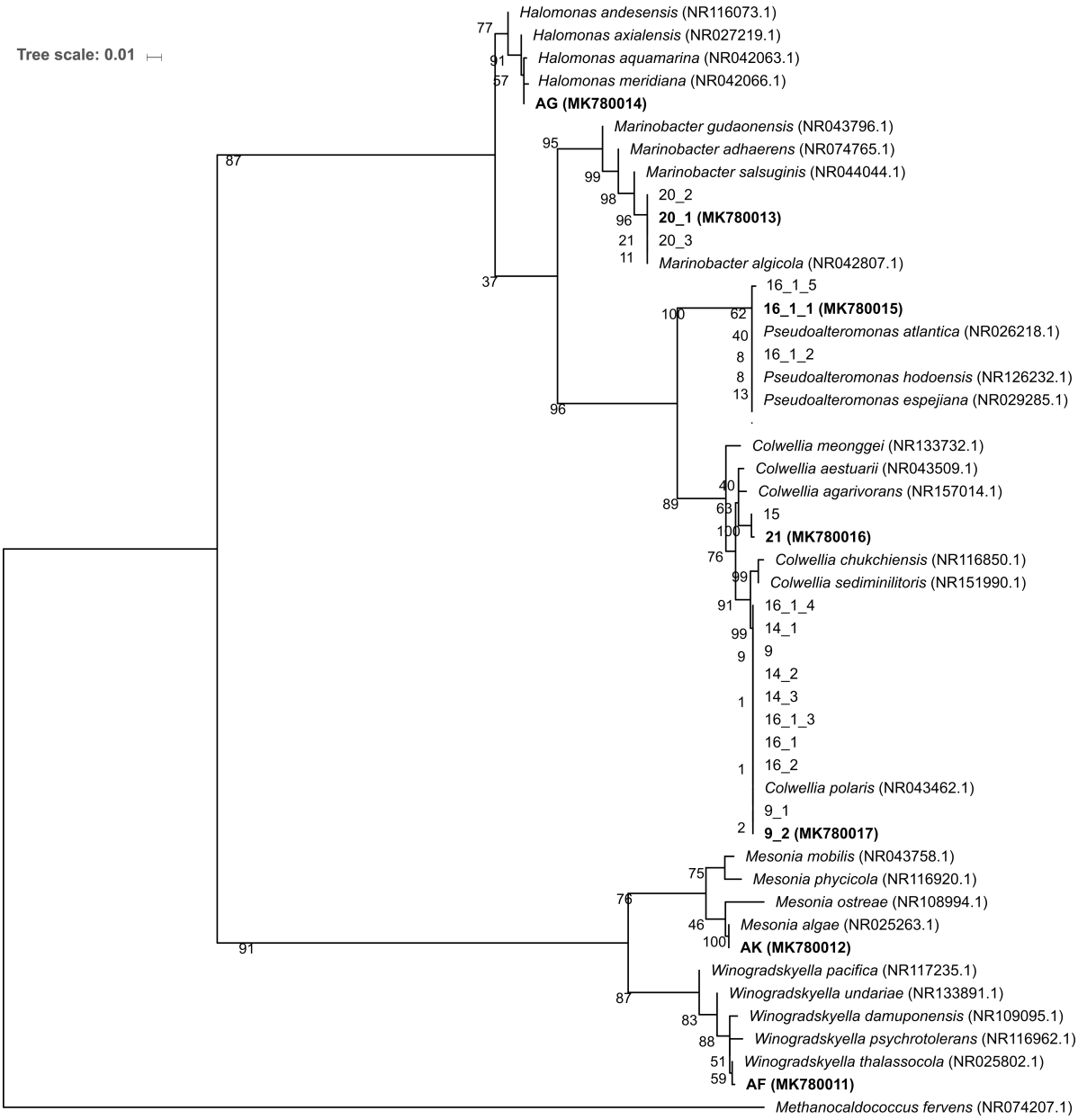

Figure 5.1: Neighbour-joining tree based on 16S rRNA gene phylogeny of the 22 bacterial isolates, with *Methanocaldococcus fervens* as outgroup. GenBank accession numbers are given in parenthesis. Isolates further used for experimental activities are highlighted in bold. The numbers above nodes denote bootstrap values; the scale bar indicates 0.01 changes per nucleotide.

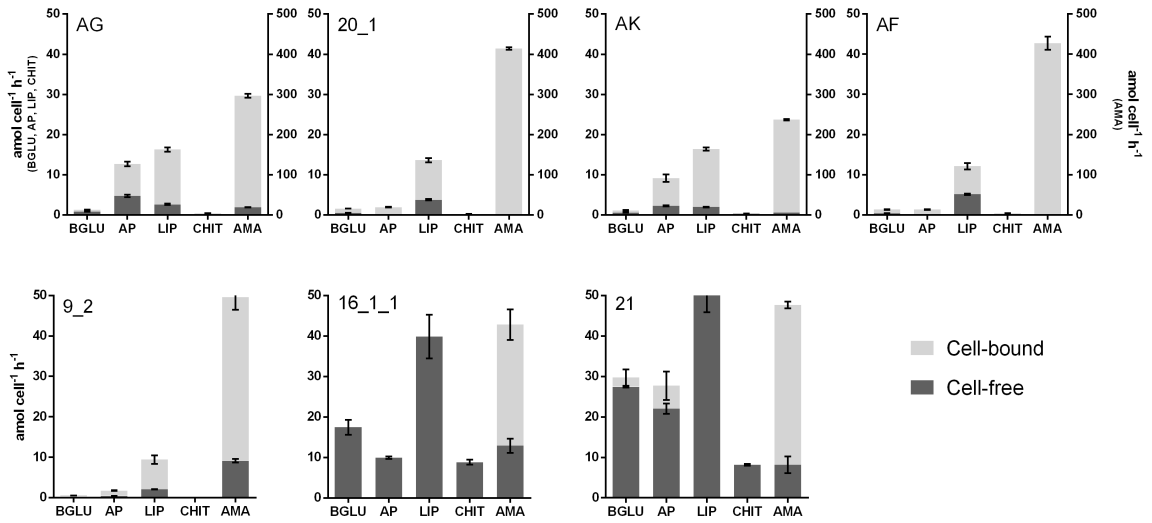

Figure 5.2: Cell-specific enzyme activities at d_{fin} of 5 exoenzyme obtained from 7 marine bacteria isolates. On the top row, AMA values are plotted on the right Y-axis. Error bars represent the standard deviation of three analytical replicates. BGLU= β-glucosidase, AP= alkaline phosphatase, LIP= lipase, CHIT= chitinase, AMA= leucine amino-peptidase.

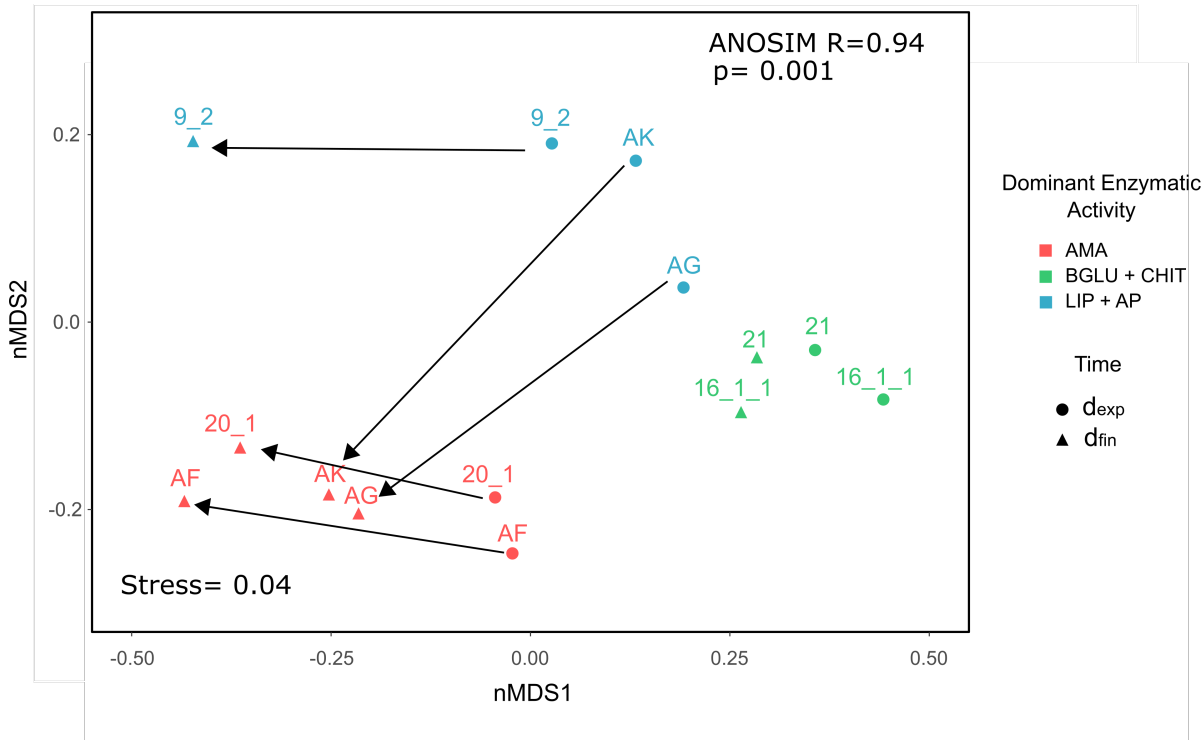

Figure 5.3: Non-metric multidimensional scaling (nMDS – 2 dimensional) plot of the selected isolates enzymatic profiles at d_{exp} and d_{fin}. Arrows highlight the path of the samples between the two experimental conditions. The stress value and the ANOSIM statistics are presented in the lower left and upper right corners, respectively. BGLU= β-glucosidase, AP= alkaline phosphatase, LIP= lipase, CHIT= chitinase, AMA= leucine amino-peptidase.

5.3.3. Exoenzymatic activities on phytodetrital particles

In SUR tubes used to test BGLU activity (see Section 5.2.4), free-living bacterial abundance was $1.40 \times 10^9 \pm 3.21 \times 10^8$ cells L^{-1} at t3, remaining quite constant after 3h (t6, $1.24 \times 10^9 \pm 2.09 \times 10^8$ cells L^{-1}, Fig. 5.4 a). Particle-attached cells abundance was 2 order of magnitude lower, showing rather constant values at both sampling points ($5.58 \times 10^7 \pm 4.60 \times 107$ and $6.07 \times 10^7 \pm 2.42 \times 10^7$ cells L^{-1} at t3 and t6, respectively, Fig. 5.4 a). Tubes bearing particles + attached bacteria (PART) were characterized by a higher abundance of particle-attached cells at both sampling points, showing a decreasing trend over time ($3.70 \times 10^8 \pm 1.82 \times 10^7$ and $2.41 \times 10^8 \pm 7.23 \times 10^7$ cells L^{-1}). Contrariwise, free-living bacteria increased over time in the PART treatment, from $6.37 \times 10^8 \pm 5.92 \times 10^7$ to $9.85 \times 10^8 \pm 1.26 \times 10^7$ cells L^{-1} (Fig. 5.4 a). A similar pattern was noticeable in the tubes used for AMA activity assays (Fig. 5.4). Free-living bacteria in SUR tubes showed constant abundance between t3 and t6 ($1.17 \times 10^9 \pm 1.65 \times 10^8$ and $1.26 \times 10^9 \pm 6.23 \times 10^7$ cells L^{-1}, respectively, Fig. 5.4 b) as well as particle-associated cells ($6.80 \times 10^77 \pm 1.83 \times 10^7$ and $5.12 \times 10^7 \pm 8.9 \times 10^6$ cells L^{-1}, respectively, Fig. 5.4 b). In PART tubes, free-living bacteria increased from 6.08 x $10^8 \pm 2.49$ x 10^7 on t3 to $9.14 \times 10^8 \pm 2.18 \times 10^7$ cells L^{-1} on t6 (Fig. 5.4 b), while particle-attached bacteria abundance declined between sampling times ($4.15 \times 10^8 \pm 1.31 \times 10^8$ and $2.31 \times 10^8 \pm 4.14 \times 10^7$ cells L^{-1}, respectively, Fig. 5.4 b).

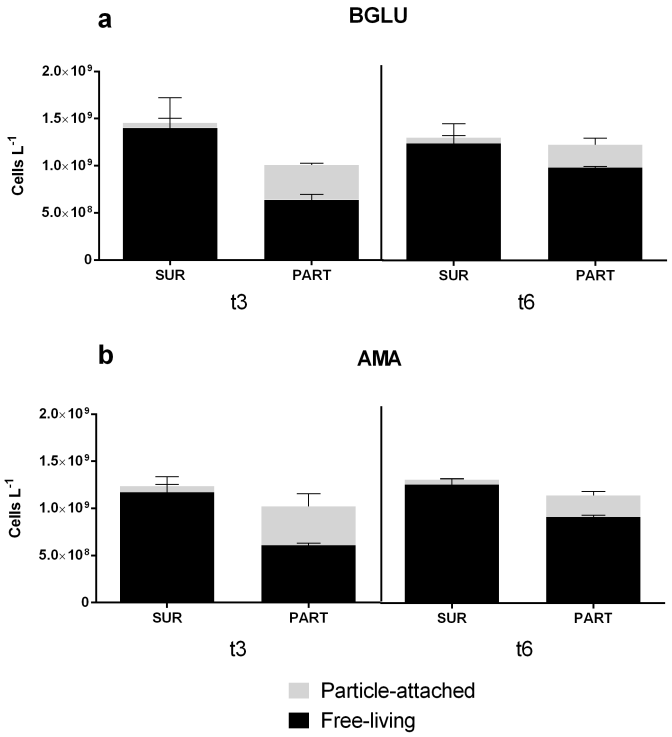

Figure 5.4: Bar plots reporting bacterial abundance in the two experimental conditions (SUR and PART) over time, for tubes used to test a) BGLU and b) AMA activities. Error bars represent the standard deviation from the mean of two experimental replicates. For abbreviations meaning, see Section 5.2.4

Results of BGLU and AMA cell-specific hydrolysis rates are reported in Table 5.2. Overall, the cell-free contribution to the total exoenzymatic activity was higher in tubes

bearing aggregates and associated bacteria (PART) at both sampling times and for both the exoenzymes tested (Table 5.2). In SUR tubes, specific cell-bound glycolytic activity increased by four-fold between t3 and t6 (0.30 ± 0.05 and 1.30 ± 0.47 amol $cell^{-1}$ h^{-1}, respectively, Table 2), while the activity of the dissolved fraction mildly increased over time (Table 5.2). This pattern resulted in diminished relative contribution of the cell-free to the total exoenzymatic activity, which decreased from 60.83 ± 1.77 to 35.32 ± 3.81% between t3 and t6 (Table 5.2). Tubes bearing aggregates and associated bacteria (PART) were characterized by a higher activity of the dissolved exoenzymatic fraction, which remained quite constant over time (1.11 ± 0.20 and 1.01 ± 0.13 amol $cell^{-1}$ h^{-1} at t3 and t6, respectively, Table 5.2). Cell-bound specific activity increased from 0.46 ± 0.08 to 0.85 ± 0.03 amol $cell^{-1}$ h^{-1} during the 3 hours incubation, reducing the cell-free proportion of glycolytic activity from 77.59 ± 27.50% at t3 to 54.71 ± 2.42% at t6 (Table 5.2). Protease specific hydrolysis rates were two order of magnitude greater than BGLU activity both in SUR and PART tubes. In samples potentially bearing only free-living microbes, both cell-bound and cell-free exoenzymatic activity decreased over time (Table 5.2), with a rather constant proportion of dissolved to total AMA between t3 and t6 (16.73 ± 0.77% and 14.43 ± 0.35%, respectively, Table 5.2). Over the 3-hours incubation, cell-specific protease activity showed little variation both for cell-bound (101.32 ± 3.18 and 106.67 ± 5.95 amol $cell^{-1}$ h^{-1} at t3 and t6, respectively) and cell-free enzymes (30.54 ± 1.30 and 31.20 ± 1.26 amol $cell^{-1}$ h^{-1} at t3 and t6, respectively), resulting in a constant contribution of the dissolved fraction over time (Table 5.2).

Table 5.2: Cell-specific hydrolysis rates of β-glucosidase (BGLU) and leucine amino-peptidase (AMA) in amol $cell^{-1}$ h^{-1} assayed during the experiment with phytodetrital particles. Results are given as the mean and standard deviation of two experimental replicates. For abbreviations meaning see Section 5.2.4

	t3			t6		
	Cell-bound	Cell-free	%	Cell-bound	Cell-free	%
BGLU						
SUR	0.30 ± 0.05	0.46 ± 0.02	60.83 ± 1.77	1.30 ± 0.47	0.70 ± 0.09	35.32 ± 3.81
PART	0.46 ± 0.08	1.11 ± 0.20	77.59 ± 7.50	0.85 ± 0.03	1.01 ± 0.13	54.71 ±2.42
AMA						
SUR	206.04 ± 48.83	41.18 ± 6.26	16.73 ± 0.77	192.03 ± 28.12	32.33 ± 3.26	14.43 ± 0.35
PART	101.32 ± 3.18	30.54 ± 1.30	23.18 ± 1.55	106.67 ± 5.95	31.20 ± 1.26	22.67 ± 1.89

Cell-bound = cell-specific hydrolysis rates of cell-attached exoenzymes (total minus cell-free activity); Cell-free: cell specific hydrolysis rates of dissolved exoenzymes (i.e., passing through a 0.2 µm filter); %= relative contribution of cell-free specific hydrolysis rates over the total exoenzymatic activity.

5.4. Discussion

In the ocean, bacteria experience heterogeneous concentrations of organic matter, including hot spot of particulate organic matter (i.e., living and dead phytoplankton cells and marine snow) as well as zones depleted in organic substrates (Stocker, 2012). Therefore, given this extreme variability, the ectohydrolytic profile of a bacterium must reflect a set of strategies to optimize the retrieval of organic substrates from the patchy spatial and temporal distribution of the organic matter in the ocean (Martinez et al., 1996). The enzymatic profile of a single bacterium can thus be viewed as the expression of a peculiar degradative strategy and of its genetic identity, in nature as well as in culture.

The bacterial isolates used in this study were grown in the same culture media, yet, notwithstanding the identical growth condition, they expressed a diverse degradative fingerprint. It is worth to point out that during the first experiment, bacteria were transferred from a rich (ZB/5) to a poor medium (FASW), and since the enzymatic profiles were tested immediately after the washing of the cultures (d_{exp}), it is very likely that the cells expressed enzymatic fingerprints adapted to high organic carbon concentrations. Protease activity varied over 1 order of magnitude (between 42.65 ± 3.79 and 427. 29 ± 16.29 amol cell^{-1} h^{-1}, Fig. 5.2), although specific activity of bacteria that used to grow in a rich medium (d_{exp}) was lower than the one tested after several days of growth in a poor one (d_{fin}) (122.00 ± 132.33 and 219.11 ± 168.95 amol cell^{-1} h^{-1}, respectively). Since protease activity is inhibited or unaffected by the presence of low molecular weight substrate (Donachie et al., 2001), is likely that the high concentration of readily accessible peptides in the rich medium (ZB/5) suppressed the cell-specific protease expression. On the other hand, the complexity of organic matter in the 'poor' medium (i.e., natural DOC), enhanced the proteolytic activity. The shift of the degradative fingerprint of 3 out of the 7 tested isolates between the two time points (Fig. 5.3), partly confirm this hypothesis. Indeed, the nMDS plot highlighted a consistent change in the degradation pattern of isolates AG and AK, which were identified as strongly proteolytic in the 'poor' medium (Fig. 5.2 and 5.3) whereas in the rich medium their specific proteolytic activity was ten-fold lower (44.78 ± 1.49 and 23.40 ± 1.71 amol cell^{-1} h^{-1}, respectively, Appendix Fig. D.1). The same pattern was evident for isolate 9_2 (Fig. 5.3), which almost doubled its cell-specific AMA activity in the 'poor' medium (27.61 ± 0.40 and 58.42 ± 0.42 amol cell^{-1} h^{-1} for rich and 'poor' media, respectively, Appendix Fig. D.1 and Fig. 5.2). These results agree with those reported by Baltar et al., 2017, which found a tight coupling between AMA activity and the complexity of organic matter supplied to the microbial community. While highlighting a certain degree of phenotypic plasticity for a subset of the tested isolates, the pattern showed by the nMDS plot (Fig. 5.3) also suggests that some of the bacterial isolates (i.e., 20_1, AF, 16_1_1 and 21) are genetically 'constrained' to express a specific set of exoenzymes. It has been hypothesized that members of peculiar environments, like the high-latitude pelagic microbial community, may have streamlined their hydrolytic machinery, specializing in the degradation of those substrate that they are more likely to encounter (Arnosti, 2014). This could be the case of isolates 16_1_1 and 21, which expressed the same hydrolytic pattern growing in both culture media (Fig. 5.3). Noteworthy, these two isolates expressed the highest

cell-specific glycolytic activity, 1 order of magnitude higher than the other bacterial isolates (Fig. 5.2). Looking at the two growth conditions, glycolytic activity was, on average, faster in the rich medium relative to the 'poor' one (22.43 ± 20.74 and 10.24 ± 15.30 amol cell^{-1} h^{-1}, respectively) as a consequence of the different concentration of substrates in the two media. In fact, polysaccharide hydrolysis is generally reported as substrate-inducible (Sinsabaugh and Follstad Shah, 2012) and the ZoBell medium is richer in organic carbon (an in this case in polysaccharides, derived by the yeast extract -Sommer, 1998) than natural seawater.

These two strains showed the highest contribution of dissolved extracellular enzymes to the total specific hydrolytic activity, among the tested isolates (up to 100%, Fig. 5.2). The active release of cell-free extracellular enzymes has been linked, among several other factors, to the response of marine bacteria to starvation (Albertson et al., 1990). However, bacteria growing in the 'poor' medium experienced natural DOC concentration (1.48 mg L^{-1}), thus cell starvation was unlikely to occur. More likely, the enhanced contribution of the dissolved exoenzymatic fraction to the total cell-specific activity might be linked to the lifestyle of the tested bacterial isolates. Indeed, the phylogenetic analysis identified the selected bacteria as members of the classes *Flavobacteriia* and *γ-Proteobacteria* (Fig. 5.1), which are often found associated with particles (Crespo et al., 2013; DeLong et al., 1993; Teeling et al., 2012). Modelling, experimental and field studies suggest that the production of dissolved exoenzymes could be advantageous to particle-attached bacteria (Vetter and Deming, 1999; Vetter et al., 1998; Ziervogel and Arnosti, 2008). All our isolates expressed cell-free hydrolytic activity at d_{fin} (Fig. 5.2), although the contribution to total cell-specific activity varied greatly (0-100%, Fig. 5.2). This pattern may derive from the appropriate substrate stimulation exerted by the natural DOC supplied with the 'poor' medium (Alderkamp et al., 2007). Another possible explanation is that the isolates expressing the highest cell-free enzymatic activity (i.e., AG, 16_1_1 and 21, Fig. 5.2), have the genetic potential to produce dissolved extracellular enzymes even when not attached to detrital particles. There are indications that the fate of an extracellular enzyme (i.e., to be cell-bound or cell-free) could be genetically predetermined (Nguyen et al., 2019); thus, isolates expressing high cell-free exoenzymatic activity without the presence of particles could be viewed as 'climax' colonizers, extremely streamlined to take advantage of organic matter hot spots.

Given the expression of a conspicuous amount of cell-free extracellular enzymes in these isolates, we tested the hypothesis that the dissolved exoenzymatic activity may be enhanced by the presence of phytodetrital particles. For this test, one fast-growing bacterium, AG, identified as *Halomonas meridiana* (Fig. 5.1), was chosen. *Halomonas meridiana* is a halotolerant, mesophilic, Gram-negative bacterium, first isolated from Antarctic hypersaline lakes (James et al., 1990). This species shows some adaptation to exploit particles as organic matter hotspots, such as flagellar motility, and the ability to produce metalloproteases, required for the functioning of adhesion or detachment mechanisms (Anithajothi et al., 2014). Our results show that the contribution of the dissolved fraction to the total specific activity was always higher in tubes bearing particles and attached bacteria (PART, Table 5.2), confirming our initial hypothesis. The difference between SUR and PART tubes was already evident after 3h from the

tubes splitting for both BGLU and AMA (Table 5.2), albeit reducing over time. The reduced contribution of cell-free exoenzymes to total activity at t6 may be the result of the degradation of already present cell-free enzymes (i.e., produced during the colonization ad settling phases, see Section 5.2.4), as these are themselves subjected to proteolytic hydrolysis (Ziervogel and Arnosti, 2008). The phytodetritus used for the experimental amendment was mainly composed of diatoms species (80% of total microplankton on the net sample, F. Cerino, personal communication), an important source of polysaccharides in the marine environment (Alldredge et al., 1993; Ziervogel and Arnosti, 2008). Nevertheless, glycolytic activity was extremely low (<2 amol $cell^{-1}$ h^{-1}, Table 5.2) during our experiment, with values very similar to those measured during the first experiment (Fig. 5.2).

Recent studies highlight the existence of an alternative uptake mechanism of polysaccharides in marine bacteria (Reintjes et al., 2019; Reintjes et al., 2017), suggesting that the use of simple model substrates (such as the one utilized in fluorometric assays) to assess glycolytic rates may be partially ineffective, especially when dealing with algal-derived, complex polysaccharides. The tested isolate, AG, also showed similar pattern of AMA activity in SUR tubes and when cultured in the 'poor' media, remarkably modulating proteolytic activity when exposed to phytodetrital particles. Indeed, cell-specific hydrolysis rates in PART tubes were 50% lower than the rates measured both in SUR tubes and expressed in its enzymatic profiles, with an enhanced contribution of cell-free AMA activity in particle-enriched treatments (up to 23%), suggesting a fine regulation of the degradative machinery according to the environmental conditions.

5.5. Conclusions

The results here presented showed that even closely-related bacterial isolates express different exoenzymatic profiles, and that the enzymatic fingerprint of an isolate may vary consistently according to the quality and quantity of the organic matter supplied as substrate for growth. Moreover, we added a piece of evidence on the mechanisms regulating cell-free exoenzymatic activity, demonstrating that bacteria growing associated with phytodetrital particles are more prone to actively release dissolved extracellular enzymes. By investigating the 'mise en place' of the microbial hydrolytic machinery under different environmental stimuli, this work deepens the current knowledge of the factors driving the organic matter hydrolysis in the ocean, the rate-limiting step of the marine carbon cycle. The continuation of these experimental activities, testing the response of different bacterial isolates to different substrates, will help to determine the conditions under which different hydrolysis patterns develop, deepening the current knowledge on the organic matter cycling in the ocean.

Acknowledgements

This study was carried out as part of the Italian Program for Research in Antarctica (PNRA) with funds from the project PRIAMO (PRokaryotes Interactions with Antarctic phytodetritus: a Micro- to macroscale voyage from the surface to the deep Ocean), PNRA16_00103.

References

Albertson, N. H., Nyström, T., & Kjelleberg, S. (1990). Exoprotease activity of two marine bacteria during starvation. *Applied and Environmental Microbiology*, *56*(1), 218–223. https://aem.asm.org/content/56/1/218

Alderkamp, A.-C., Buma, A. G. J., & van Rijssel, M. (2007). The carbohydrates of Phaeocystis and their degradation in the microbial food web. In M. A. van Leeuwe, J. Stefels, S. Belviso, C. Lancelot, P. G. Verity, & W. W. C. Gieskes (Eds.), *Phaeocystis, major link in the biogeochemical cycling of climate-relevant elements* (pp. 99–118). Springer Netherlands. https://doi.org/10.1007/978-1-4020-6214-8_9

Alldredge, A. L., Passow, U., & Logan, B. E. (1993). The abundance and significance of a class of large, transparent organic particles in the ocean. *Deep Sea Research Part I: Oceanographic Research Papers*, *40*(6), 1131–1140. https://doi.org/https://doi.org/10.1016/0967-0637(93)90129-Q

Altschul, S. F., Gish, W., Miller, W., Myers, E. W., & Lipman, D. J. (1990). Basic local alignment search tool. *Journal of Molecular Biology*, *215*(3), 403–410. https://doi.org/https://doi.org/10.1016/S0022-2836(05)80360-2

Anithajothi, R., Nagarani, N., Umagowsalya, G., Duraikannu, K., & Ramakritinan, C. (2014). Screening, isolation and characterization of protease producing moderately halophilic microorganism halomonas meridiana associated with coral mucus. *Toxicological & Environmental Chemistry*, *96*(2), 296–306. https://doi.org/10.1080/02772248.2014.925182

Arnosti, C. (2011). Microbial Extracellular Enzymes and the Marine Carbon Cycle. *Annual Review of Marine Science*, *3*(1), 401–425. https://doi.org/10.1146/annurev-marine-120709-142731

Arnosti, C. (2014). Patterns of Microbially Driven Carbon Cycling in the Ocean: Links between Extracellular Enzymes and Microbial Communities (C. Panagiotopoulos, Ed.). *Advances in Oceanography*, *2014*, 706082. https://doi.org/10.1155/2014/706082

Azam, F., & Malfatti, F. (2007). Microbial structuring of marine ecosystems. *Nature Reviews Microbiology*, *5*(10), 782–791. https://doi.org/10.1038/nrmicro1747

Baltar, F. (2018). Watch out for the "living dead
: Cell-free enzymes and their fate. *Frontiers in Microbiology*, *8*(JAN), 2438. https://doi.org/10.3389/fmicb.2017.02438

Baltar, F., Morán, X. A. G., & Lønborg, C. (2017). Warming and organic matter sources impact the proportion of dissolved to total activities in marine extracellular enzymatic rates. *Biogeochemistry*, *133*(3), 307–316. https://doi.org/10.1007/s10533-017-0334-9

Benner, R., & Amon, R. M. (2015). The size-reactivity continuum of major bioelements in the Ocean. *Annual Review of Marine Science*, *7*(1), 185–205. https://doi.org/10.1146/annurev-marine-010213-135126

Bidle, K. D., & Azam, F. (1999). Accelerated dissolution of diatom silica by marine bacterial assemblages. *Nature*, *397*(6719), 508–512. https://doi.org/10.1038/17351

Catalano, G., Budillon, G., La Ferla, R., Povero, P., Ravaioli, M., Saggiomo, V., Accornero, A., Azzaro, M., Carrada, G., Giglio, F., Langone, L., Mangoni, O., Misic, C., & Modigh, M. (2010). The Ross Sea. In L. Liu, K.-K. Atkinson, L. Quinones, & R. Talaue-McManus (Eds.), *Carbon and nutrient fluxes in continental margins: A global synthesis* (pp. 303–318). Springer.

Celussi, M., Balestra, C., Fabbro, C., Crevatin, E., Cataletto, B., Fonda Umani, S., & Del Negro, P. (2008). Organic-matter degradative potential of Halomonas glaciei isolated from frazil ice in the Ross Sea (Antarctica). *FEMS Microbiology Ecology*, *65*(3), 504–512. https://doi.org/10.1111/j.1574-6941.2008.00551.x

Celussi, M., Cataletto, B., Fonda Umani, S., & Del Negro, P. (2009). Depth profiles of bacterioplankton assemblages and their activities in the Ross Sea. *Deep Sea Research Part I: Oceanographic Research Papers*, *56*(12), 2193–2205. https://doi.org/10.1016/j.dsr.2009.09.001

Celussi, M., Quero, G. M., Zoccarato, L., Franzo, A., Corinaldesi, C., Rastelli, E., Lo Martire, M., Galand, P. E., Ghiglione, J.-F., Chiggiato, J., Coluccelli, A., Russo, A., Pallavicini, A., Fonda Umani, S., Del Negro, P., & Luna, G. M. (2018). Planktonic prokaryote and protist communities in a submarine canyon system in the ligurian sea (nw mediterranean). *Progress in Oceanography*, *168*, 210–221. https://doi.org/https://doi.org/10.1016/j.pocean.2018.10.002

Clarke, K. R., & Warwick, R. M. (1994). Similarity-based testing for community pattern: The two-way layout with no replication. *Marine Biology*, *118*(1), 167–176. https://doi.org/10.1007/BF00699231

Crespo, B. G., Pommier, T., Fernández-Gómez, B., & Pedrós-Alió, C. (2013). Taxonomic composition of the particle-attached and free-living bacterial assemblages in the Northwest Mediterranean Sea analyzed by pyrosequencing of the 16S rRNA. *MicrobiologyOpen*, *2*(4), 541–552. https://doi.org/10.1002/mbo3.92

Del Negro, P., Celussi, M., De Vittor, C., & Fonda Umani, S. (2018). Rapid acclimation of microbes to changing substrate pools in epipelagic waters of an Antarctic polynya during austral summer 2003. *Polar Biology*, *41*(1), 1–10. https://doi.org/10.1007/s00300-017-2165-5

DeLong, E. F., Franks, D. G., & Alldredge, A. L. (1993). Phylogenetic diversity of aggregate-attached vs. free-living marine bacterial assemblages. *Limnology and Oceanography*, *38*(5), 924–934. https://doi.org/https://doi.org/10.4319/lo.1993.38.5.0924

Dereeper, A., Guignon, V., Blanc, G., Audic, S., Buffet, S., Chevenet, F., Dufayard, J.-F., Guindon, S., Lefort, V., Lescot, M., Claverie, J.-M., & Gascuel, O. (2008). Phylogeny.fr: Robust phylogenetic analysis for the non-specialist. *Nucleic Acids Research*, *36*(suppl_2), W465–W469. https://doi.org/10.1093/nar/gkn180

Donachie, S. P., Christian, J. R., & Karl, D. M. (2001). Nutrient regulation of bacterial production and ectoenzyme activities in the subtropical north pacific ocean. *Deep Sea Research Part II: Topical Studies in Oceanography*, *48*(8), 1719–1732. https://doi.org/https://doi.org/10.1016/S0967-0645(00)00158-2

Ducklow, H. W., Steinberg, D. K., & Buesseler, K. O. (2001). Upper ocean carbon export and the biological pump. *Oceanography*, *14*(SPL.ISS. 4), 50–58. https://doi.org/10.5670/oceanog.2001.06

Giering, S. L. C., Sanders, R., Lampitt, R. S., Anderson, T. R., Tamburini, C., Boutrif, M., Zubkov, M. V., Marsay, C. M., Henson, S. A., Saw, K., Cook, K., & Mayor, D. J. (2014). Reconciliation of the carbon budget in the ocean's twilight zone. *Nature*, *507*(7493), 480–483. https://doi.org/10.1038/nature13123

Hansell, D. A., Carlson, C. A., Repeta, D. J., & Schlitzer, R. (2009). Dissolved organic matter in the ocean a controversy stim ulates new insights. *Oceanography*, *22*(SPL.ISS. 4), 202–211. https://doi.org/10.5670/oceanog.2009.109

Hassanshahian, M., Zeynalipour, M. S., & Musa, F. H. (2014). Isolation and characterization of crude oil degrading bacteria from the persian gulf (khorramshahr provenance). *Marine Pollution Bulletin*, *82*(1), 39–44. https://doi.org/https://doi.org/10.1016/j.marpolbul.2014.03.027

Hoarfrost, A., Snider, R., & Arnosti, C. (2017). Improved measurement of extracellular enzymatic activities in subsurface sediments using competitive desorption treatment. *Frontiers in Earth Science*, *5*, 13. https://doi.org/10.3389/feart.2017.00013

Hoppe, H.-G. (1993). Use of Fluorogenic Model Substrates for Extracellular Enzyme Activity (EEA) Measurement of Bacteria. In P. F. Kemp, B. F. Sherr, E. B. Sherr, & J. J. Cole (Eds.), *Handbook of Methods in Aquatic Microbial Ecology* (1st ed., pp. 423–431). Routledge. https://doi.org/10.1201/9780203752746-49

Hoppe, H.-G., Arnosti, C., & Herndl, G. (2002). Ecological Significance of Bacterial Enzymes in the Marine Environment. In R. Burns & R. Dick (Eds.), *Enzymes in the Environment. Activity, ecology, and applications* (pp. 73–107). Marcel Dekker. https://doi.org/10.1201/9780203904039.ch3

Hoppe, H.-G., & Ullrich, S. (1999). Profiles of ectoenzymes in the Indian Ocean: Phenomena of phosphatase activity in the mesopelagic zone. *Aquatic Microbial Ecology*, *19*(2), 139–148. https://www.int-res.com/abstracts/ame/v19/n2/p139-148/

James, S., Dobson, S., Franzmann, P., & McMeekin, T. (1990). Halomonas meridiana, a new species of extremely halotolerant bacteria isolated from antarctic saline lakes. *Systematic and Applied Microbiology*, *13*(3), 270–278. https://doi.org/https://doi.org/10.1016/S0723-2020(11)80198-0

Letunic, I., & Bork, P. (2016). Interactive tree of life (iTOL) v3: An online tool for the display and annotation of phylogenetic and other trees. *Nucleic Acids Research*, *44*(W1), W242–W245. https://doi.org/10.1093/nar/gkw290

Lo Giudice, A., & Fani, R. (2015). Cold-adapted bacteria from a coastal area of the Ross Sea (Terra Nova Bay, Antarctica): Linking microbial ecology to biotechnology. *Hydrobiologia*, *761*(1), 417–441. https://doi.org/10.1007/s10750-015-2497-5

Lorenzen, C., & Jeffrey, S. (1980). Determination of chlorophyll in seawater. *Unesco technical papers in marine sciences*, *35*(1), 1–20.

Malfatti, F., Lee, C., Tinta, T., Pendergraft, M. A., Celussi, M., Zhou, Y., Sultana, C. M., Rotter, A., Axson, J. L., Collins, D. B., Santander, M. V., Anides Morales, A. L., Aluwihare, L. I., Riemer, N., Grassian, V. H., Azam, F., & Prather, K. A. (2019). Detection of Active Microbial Enzymes in Nascent Sea Spray Aerosol: Implications for Atmospheric Chemistry and Climate. *Environmental Science & Technology Letters*, *6*(3), 171–177. https://doi.org/10.1021/acs.estlett.8b00699

Marie, D., Brussaard, C. P. D., Thyrhaug, R., Bratbak, G., & Vaulot, D. (1999). Enumeration of Marine Viruses in Culture and Natural Samples by Flow Cytometry. *Applied and Environmental Microbiology*, *65*(1), 45–52. https://doi.org/10.1128/AEM.65.1.45-52.1999

Martinez, J., Smith, D. C., Steward, G. F., & Azam, F. (1996). Variability in ectohydrolytic enzyme activities of pelagic marine bacteria and its significance for substrate processing in the sea. *Aquatic Microbial Ecology*, *10*(3), 223–230. https://doi.org/10.3354/ame010223

Misic, C., Castellano, M., Fabiano, M., Ruggieri, N., Saggiomo, V., & Povero, P. (2006). Ectoenzymatic activity in surface waters: A transect from the Mediterranean Sea across the Indian Ocean to Australia. *Deep Sea Research Part I: Oceanographic Research Papers*, *53*(9), 1517–1532. https://doi.org/10.1016/j.dsr.2006.07.001

Nguyen, T. T. H., Myrold, D. D., & Mueller, R. S. (2019). Distributions of extracellular peptidases across prokaryotic genomes reflect phylogeny and habitat. *Frontiers in Microbiology*, *10*, 413. https://doi.org/10.3389/fmicb.2019.00413

Nigam, P. S. (2013). Microbial enzymes with special characteristics for biotechnological applications. *Biomolecules*, *3*(3), 597–611. https://doi.org/10.3390/biom3030597

Oksanen, J., Blanchet, F. G., Friendly, M., Kindt, R., Legendre, P., McGlinn, D., Minchin, P. R., O'Hara, R. B., Simpson, G. L., Solymos, P., Stevens, M. H. H., Szoecs, E., & Wagner, H. (2019). *Vegan: Community Ecology Package*. https://CRAN.R-project.org/package=vegan

Quast, C., Pruesse, E., Yilmaz, P., Gerken, J., Schweer, T., Yarza, P., Peplies, J., & Glöckner, F. O. (2013). The SILVA ribosomal RNA gene database project: Improved data processing and web-based tools. *Nucleic acids research*, *41*(Database issue), D590–D596. https://doi.org/10.1093/nar/gks1219

R Core Team. (2019). *R: A Language and Environment for Statistical Computing*. R Foundation for Statistical Computing. https://www.R-project.org/

Reintjes, G., Arnosti, C., Fuchs, B., & Amann, R. (2019). Selfish, sharing and scavenging bacteria in the Atlantic Ocean: A biogeographical study of bacterial substrate utilisation. *The ISME Journal*, *13*(5), 1119–1132. https://doi.org/10.1038/s41396-018-0326-3

Reintjes, G., Arnosti, C., Fuchs, B. M., & Amann, R. (2017). An alternative polysaccharide uptake mechanism of marine bacteria. *The ISME Journal*, *11*(7), 1640–1650. https://doi.org/10.1038/ismej.2017.26

Sinsabaugh, R. L., & Follstad Shah, J. J. (2012). Ecoenzymatic Stoichiometry and Ecological Theory. *Annual Review of Ecology, Evolution, and Systematics*, *43*(1), 313–343. https://doi.org/10.1146/annurev-ecolsys-071112-124414

Sommer, R. (1998). Yeast extracts : Production, properties and components. *9th International Symposium on Yeast*.

Stocker, R. (2012). Marine microbes see a sea of gradients. *Science*, *338*(6107), 628–633. https://doi.org/10.1126/science.1208929

Teeling, H., Fuchs, B. M., Becher, D., Klockow, C., Gardebrecht, A., Bennke, C. M., Kassabgy, M., Huang, S., Mann, A. J., Waldmann, J., Weber, M., Klindworth, A., Otto, A., Lange, J., Bernhardt, J., Reinsch, C., Hecker, M., Peplies, J., Bockelmann,

F. D., … Amann, R. (2012). Substrate-controlled succession of marine bacterioplankton populations induced by a phytoplankton bloom. *Science*, *336*(6081), 608–611. https://doi.org/10.1126/science.1218344

Traving, S. J., Thygesen, U. H., Riemann, L., & Stedmon, C. A. (2015). A model of extracellular enzymes in free-living microbes: Which strategy pays off? *Applied and Environmental Microbiology*, *81*(21), 7385–7393. https://doi.org/10.1128/AEM.02070-15

Utermöhl, H. (1958). Zur vervollkommnung der quantitativen phytoplankton-methodik: Mit 1 Tabelle und 15 abbildungen im Text und auf 1 Tafel. *Internationale Vereinigung für theoretische und angewandte Limnologie: Mitteilungen*, *9*(1), 1–38.

Vetter, Y. A., & Deming, J. W. (1999). Growth rates of marine bacterial isolates on particulate organic substrates solubilized by freely released extracellular enzymes. *Microbial Ecology*, *37*(2), 86–94. https://doi.org/10.1007/s002489900133

Vetter, Y. A., Deming, J. W., Jumars, P. A., & Krieger-Brockett, B. B. (1998). A predictive model of bacterial foraging by means of freely released extracellular enzymes. *Microbial Ecology*, *36*(1), 75–92. https://doi.org/10.1007/s002489900095

Yoshida, S., Hiraga, K., Takehana, T., Taniguchi, I., Yamaji, H., Maeda, Y., Toyohara, K., Miyamoto, K., Kimura, Y., & Oda, K. (2016). A bacterium that degrades and assimilates poly(ethylene terephthalate). *Science*, *351*(6278), 1196–1199. https://doi.org/10.1126/science.aad6359

Ziervogel, K., & Arnosti, C. (2008). Polysaccharide hydrolysis in aggregates and free enzyme activity in aggregate-free seawater from the north-eastern gulf of mexico. *Environmental Microbiology*, *10*(2), 289–299. https://doi.org/https://doi.org/10.1111/j.1462-2920.2007.01451.x

6

Concluding Remarks and Future Outlooks

The research effort developed in this thesis was aimed at linking microscale interactions between microbes and organic matter with local, as well as global, biogeochemical dynamics. To pursue this aim, this work has considered time scales from days to decades, investigating the microbe-organic matter interplay both in field and in experimentally controlled conditions.

In Chapters 2 and 3 it has been demonstrated how regional environmental perturbations can impair microbe-mediated OM processing over time scales from days to years. This is a striking result as microbes represent the engine of biogeochemical cycles and a prolonged repression of their metabolic rates may have significant impacts on the planktonic trophic network, possibly impairing the whole ecosystem productivity. Following the events considered in Chapters 2 and 3, both primary (i.e., phytoplankton) and secondary (i.e., bacterial) production were exceptionally constrained. Although not investigated, a likely consequence of this impairment would be a reduction of carbon and energy fluxes channelled to higher trophic levels (i.e., zooplankton and fishes) through grazing or bacterivorous activity. Therefore, the ultimate effect of these regional environmental perturbations may also affect pivotal ecosystem services of economic interest, like fisheries and mussel farms. For example, the northern Adriatic Sea is one of the most relevant fishing grounds of the Mediterranean Sea (Fortibuoni et al., 2010; Lotze et al., 2011). By impairing the microbial processes underlining OM fluxes, these events may contribute to accelerate the already ongoing decline of northern Adriatic fisheries (Giani et al., 2012 and references therein).

The frequency and intensity of environmental perturbations, like prolonged high salinity anomalies as well as extreme meteorological events, is predicted to increase as a consequence of the ongoing climate change (Denamiel et al., 2020; Döll and Schmied, 2012). Therefore, investigating the effects of these phenomena is crucial for the assessment of ongoing changes, as well as a useful tool to predict consequences of future changes on marine ecosystems. In this regard, long-term ecological research (LTER) programs are a crucial tool to interpret current observation in an organic context, allowing to distinguish between transient disturbances and the background ecosystem functioning. In the next few years, a conspicuous effort should be put in integrating "-omics" approaches into ongoing LTER programs. As demonstrated in Chapter 2, the extent of regional environmental perturbations is often underestimated or even ignored until all the biogeochemical data are integrated and analysed together. On the other hand, changes in microbial community composition and/or functionality may show earlier and more evident signals of change in response to episodic disturbances, making easier the early detection of significant biogeochemical perturbations. Finally, an effort should be made towards the developing of an integrated approach to analyse the data collected in LTER programs. While fundamental research will certainly benefit from the development of an integrated knowledge on the temporal evolution of planktonic trophic networks, this holistic approach may aid stakeholders in decision-making processes.

The research presented in Chapter 4 aimed to investigate microbial community dynamics following colonization of detrital particles. Most of the current research on particle-associated communities is focused on natural or artificial aggregates resembling marine snow. These amorphous OM particles are probably the most widespread

sinking aggregates in the ocean, contributing to the organic carbon export from the surface to the deep ocean (Boyd et al., 2019). However, cumulative evidence showed that the POM pool in the ocean interior may be substantially made up by healthy or at least intact phytoplankton cells (Agusti et al., 2015; DiTullio et al., 2000; Zoccarato et al., 2016). The results presented in this Chapter demonstrated that the composition of the detrital pool (i.e., the taxonomic identity of microplankton assemblages) selected specific microbial assemblages from the bulk community. These results point out that POM composition inherently determines its export modes and efficiency through the selection of peculiar microbial assemblages. In a context where current global climate change will result in an increased retention time of particles in the surface layers of water bodies (Legendre et al., 2015), these results suggest changes in the efficiency of the biological carbon pump in the Ross Sea. Following diatom blooms, the amount of carbon exported from surface at depth may be greatly reduced as diatom-rich POM is rapidly colonized and processed by both surface and mesopelagic communities. On the other hand, *Phaeocystis* sp. POM may become a more important channel of carbon export to the seabed, unless specific prokaryotic assemblages (i.e., Flavobacteria-dominated) are encountered on the particles' path towards the ocean interior.

With the advent of global ocean sampling expeditions and the increasing accessibility of "-omics" data, the worldwide microbial community identity and functional patterns become everyday more detailed. At the same time, impressive methodological advancements are improving our understanding of the organic matter chemical landscape in the ocean (Riedel and Dittmar, 2014). Controlled experimental manipulations like the microcosms experiment carried out in Chapter 4 allow to link specific organic matter features with changes in structure and functions of natural microbial communities. Linking all these data, the efficiency and modes with which POM is processed as it sinks trough the water column can be estimated on global scales. While a significant effort has been put in the last decade in increasing metagenomic and metatranscriptomic surveys of the ocean, "classical" incubation experiments are losing their appeal. This research shows instead that an effort should be made in the next years to couple canonical experimental approaches with high-throughput methods, like barcoding, transcriptomic and proteomic. Such data are pivotal to the understanding of the fine-scale dynamics that regulate organic matter cycling in the ocean and will be of paramount importance for the development of accurate biogeochemical models.

Most of the reactive OM pool in the ocean is composed by HMW molecules (Benner and Amon, 2015). To access this reservoir, marine microbes need a suite of ectohydrolytic enzymes in order to chop down these molecules to a manageable size to be taken up into the cells and further processed. The spatial displacement of these exoenzymes defines the wide-accepted paradigm that cell-bound enzymes are mostly used by free-living microbes, whereas particle-associated ones mostly rely on cell-free exoenzymes (Vetter et al., 1998). Within this framework, the research presented in 5 was aimed to provide a proof of concept on the differential production of cell-free exoenzymes by particle-associated microbes.

The results presented in Chapter 5 demonstrated that some bacterial isolates may produce copious amounts of cell-free exoenzymes even when grown in particle-free media, suggesting that some bacterioplankton members may be extremely streamlined for POM degradation. Notwithstanding this, when exposed to particles, one of the tested bacterial isolates showed an enhanced production of cell-free exoenzymes when compared to particle-free growing conditions. Although further experimental work is needed in this direction, the preliminary proof of concept provided by this work brings forward our knowledge on the rate-limiting step of the marine carbon cycle (Arnosti, 2011). These data on degradation rates of cell-bound vs. cell-free exoenzymes have the potential to be used to setup numerical organic matter degradation model with a dramatic level of detail. Further research in this direction requires testing of different isolates, widening the spectre of assayed exoenzymes and of the substrate supplied for growth. Moreover, a significant effort should be made in characterizing the biochemical pathways as well as the genes responsible for production of cell-bound and cell-free exoenzymes. Given the impressive amount of metagenomic and metatranscriptomic data available from all around the world, with detailed information about the molecular mechanisms involved in exoenzymes production global patterns of organic matter degradation can be extracted. Continuing this research effort would not only improve our fundamental knowledge on the organic matter biogeochemistry but also has a great applied biotechnological potential. The engineering of bacterial enzymes indeed is one of the main focuses of marine biotechnologies and the search for enzyme production mechanisms may lead, with good chances, to the discovery of enzymes and other compounds useful for industrial and biotechnological applications.

References

Agusti, S., González-Gordillo, J. I., Vaqué, D., Estrada, M., Cerezo, M. I., Salazar, G., Gasol, J. M., & Duarte, C. M. (2015). Ubiquitous healthy diatoms in the deep sea confirm deep carbon injection by the biological pump. *Nature Communications*, *6*(1), 7608. https://doi.org/10.1038/ncomms8608

Arnosti, C. (2011). Microbial Extracellular Enzymes and the Marine Carbon Cycle. *Annual Review of Marine Science*, *3*(1), 401–425. https://doi.org/10.1146/annurev-marine-120709-142731

Benner, R., & Amon, R. M. (2015). The size-reactivity continuum of major bioelements in the Ocean. *Annual Review of Marine Science*, *7*(1), 185–205. https://doi.org/10.1146/annurev-marine-010213-135126

Boyd, P. W., Claustre, H., Levy, M., Siegel, D. A., & Weber, T. (2019). Multi-faceted particle pumps drive carbon sequestration in the ocean. *Nature*, *568*(7752), 327–335. https://doi.org/10.1038/s41586-019-1098-2

Denamiel, C., Pranić, P., Quentin, F., Mihanović, H., & Vilibić, I. (2020). Pseudo-global warming projections of extreme wave storms in complex coastal regions: The case of the Adriatic Sea. *Climate Dynamics*, *55*(9-10), 2483–2509. https://doi.org/10.1007/s00382-020-05397-x

DiTullio, G. R., Grebmeier, J. M., Arrigo, K. R., Lizotte, M. P., Robinson, D. H., Leventer, A., Barry, J. P., VanWoert, M. L., & Dunbar, R. B. (2000). Rapid and early export of Phaeocystis antarctica blooms in the Ross Sea, Antarctica. *Nature*, *404*(6778), 595–598. https://doi.org/10.1038/35007061

Döll, P., & Schmied, H. M. (2012). How is the impact of climate change on river flow regimes related to the impact on mean annual runoff? A global-scale analysis. *Environmental Research Letters*, *7*(1), 014037. https://doi.org/10.1088/1748-9326/7/1/014037

Fortibuoni, T., Libralato, S., Raicevich, S., Giovanardi, O., & Solidoro, C. (2010). Coding early naturalists' accounts into long-term fish community changes in the adriatic sea (1800-2000) (S. Thrush, Ed.). *PLoS ONE*, *5*(11), e15502. https://doi.org/10.1371/journal.pone.0015502

Giani, M., Djakovac, T., Degobbis, D., Cozzi, S., Solidoro, C., & Fonda Umani, S. (2012). Recent changes in the marine ecosystems of the northern Adriatic Sea. *Estuarine, Coastal and Shelf Science*, *115*, 1–13. https://doi.org/10.1016/j.ecss.2012.08.023

Legendre, L., Rivkin, R. B., Weinbauer, M. G., Guidi, L., & Uitz, J. (2015). The microbial carbon pump concept: Potential biogeochemical significance in the globally changing ocean. *Progress in Oceanography*, *134*, 432–450. https://doi.org/10.1016/j.pocean.2015.01.008

Lotze, H. K., Coll, M., & Dunne, J. A. (2011). Historical Changes in Marine Resources, Food-web Structure and Ecosystem Functioning in the Adriatic Sea, Mediterranean. *Ecosystems*, *14*(2), 198–222. https://doi.org/10.1007/s10021-010-9404-8

Riedel, T., & Dittmar, T. (2014). A Method Detection Limit for the Analysis of Natural Organic Matter via Fourier Transform Ion Cyclotron Resonance Mass Spectrometry. *Analytical Chemistry*, *86*(16), 8376–8382. https://doi.org/10.1021/ac501946m

Vetter, Y. A., Deming, J. W., Jumars, P. A., & Krieger-Brockett, B. B. (1998). A predictive model of bacterial foraging by means of freely released extracellular enzymes. *Microbial Ecology*, *36*(1), 75–92. https://doi.org/10.1007/s002489900095

Zoccarato, L., Pallavicini, A., Cerino, F., Fonda Umani, S., & Celussi, M. (2016). Water mass dynamics shape Ross Sea protist communities in mesopelagic and bathypelagic layers. *Progress in Oceanography*, *149*, 16–26. https://doi.org/10.1016/j.pocean.2016.10.003

Acknowledgements

First and foremost I wish to thank my supervisors Dr Paola Del Negro and Dr Mauro Celussi. They have been supportive of me and this work since the beginning, and none of this would have been realized without them. They provided invaluable teaching and guidance trough the complex, and sometimes puzzling, marine microbial world. Thanks to them, I had the very rare opportunity to tailor this PhD project on my curiosity, of course making my own errors. Yet their door was always open for scientific, as well as human, support and advice.

I would like to express my gratitude to all the colleagues that supported, in one way or another, the past three years work. Special thanks goes to Dr Francesca Malfatti for the many profitable discussions and for being first a person and then a scientist. I also warmly thank my office-mate, Cinzia Fabbro, for introducing me to the marvelous world of bacteriology and, most importantly, for relieving the long keyboard-knocking winter afternoons with a laugh.

I also want to thank my friends: Matteo, Federica and Lidia for their warm welcome and sincere friendship, even if they had to change their tag in ”biogeochemical brothers” after my arrival; Martina, for having always something to laugh on; Federica and Larissa for being always so inexplicably cheerful; Tommaso, for sharing long dark hours at the microscope; Federica, for sharing the common expat fate; Daniela, for all the misanthropist good-mornings.

A special mention goes to Matteo and Martina, the S. Croce smokers club, for all the talking about life, universe and everything at the teatime.

I have to thank my mom and dad for being the person I am today. They made everything they could to give me the privilege to pursue my dreams and I will be never grateful enough for that.

Finally, I want to thank Greta for her unconditional love and support throughout this northern adventure and for having the courage to change everything for sharing her everyday life with me.

Appendices

A

Supplementary Material to Chapter 2

Text, tables and figures in this Appendix are adapted from the supplementary material to: Long-term patterns and drivers of microbial organic matter utilization in the northernmost basin of the Mediterranean Sea.Manna, V., De Vittor, C., Giani, M., Del Negro, P., Celussi, M., 2021. Marine Environmental Research, 164, 105245. https://doi.org/10.1016/j.marenvres.2020.105245

A.1. Supplementary Table

Table A.1: Descriptive statistics of biological and chemical variables used for time series analysis.

	Chl *a*	POC	DOC	HP	SYN	HCP
	$\mu g\ L^{-1}$	µM	µM	$10^8 Cells\ L^{-1}$	$10^6 Cells\ L^{-1}$	$\mu gC\ L^{-1} h^{-1}$
Minimum	0.15	4.62	49.77	1.52	0.09	0.04
1st Quartile	0.54	13.01	88.18	6.68	11.51	0.16
Median	0.74	17.52	96.69	9.38	31.09	0.28
Mean	0.88	18.05	100.45	10.21	48.92	0.36
SD	0.52	6.76	19.54	4.93	56.13	0.28
3rd Quartile	1.11	22.61	111.31	13.13	69.12	0.47
Maximum	3.76	43.08	162.3	26.02	422.97	1.66

Chl *a* – Chlorophyll *a* concentration; POC – Particulate Organic Carbon concentration; DOC – Dissolved Organic Carbon concentration; HP – Heterotrophic Prokaryotes abundance; SYN – *Synechococcus* abundance; HCP – Heterotrophic Carbon Production.

A.2. Data sources

Analytical procedures utilized to generate the data used in 2 have been carried out by the following laboratories or people: CTD: R. Auriemma (OGS), P. Berger (OGS), M. Celio (LBM-ARPAFVG), E. Cociancic (OGS), C. Comici (OGS); Particulate organic matter: C. Comici (OGS), F. Relitti (OGS), F. Tamberlich (LBM); Dissolved organic carbon: C. De Vittor (OGS), M. Kralj (OGS), F. Relitti (OGS); Chlorophyll a: M. Bazzaro (OGS), F. De Prà (LBM), C. De Vittor, M. Lipizer (OGS), F. Relitti (OGS); Epifluorescence microscopy: M. Celussi (OGS), M. Borin Dolfin (OGS-UNITS), P. Del Negro (OGS), A.A. Gallina (OGS-UNITS), A. Karuza (OGS), A. Paoli (OGS); Flow cytometry: M. Celussi (OGS), V. Manna (OGS-UNITS); Heterotrophic production: M. Celussi (OGS), E. Crevatin (OGS), P. Del Negro (OGS), C. Larato (OGS), V. Manna (OGS-UNITS), P. Ramani (LBM).

B

Supplementary Material to Chapter 3

Text, tables and figures in this Appendix are adapted from the supplementary material to: Effect of an extreme cold event on the metabolism of planktonic microbes in the northernmost basin of the Mediterranean Sea. Manna, V., Fabbro, C., Cerino, F., Bazzaro, M., Del Negro, P., Celussi, M., 2019. Estuarine, Coastal and Shelf Science, 225, 106252. https://doi.org/10.1016/j.ecss.2019.106252

B.1. Methods

B.1.1. Cell-free extracellular enzymatic activity

Cell-free extracellular enzymatic activities (EEAs) were tested using fluorogenic substrate analogues (Hoppe, 1993) derived from 7-amino-4-methylcoumarin (AMC) and 4-methylumbelliferone (MUF), filtering samples through a 0.2 µm low protein-binding PES membranes (Baltar et al., 2010). Leucine-aminopeptidase activity (AMA) was assayed as the hydrolysis rate of leucine-AMC. Alkaline phosphatase (AP), β-galactosidase (BGAL), β-glucosidase (BGLU), chitinase (CHIT) and lipase (LIP) activities were assayed using MUF-phosphate, MUF-β-D-galactoside, MUF-β-D-glucoside, MUF-N-acetyl-β-D-glucosaminide and MUF-oleate (Sigma Aldrich), respectively. Hydrolysis was measured by incubating 2 mL subsamples with 200 µM leucine-AMC, MUF-β-D-glucoside ,MUF-β-D-galactoside, MUF-N-acetyl-β-D-glucosaminide, 50 µM MUF-phosphate, 100 µM MUF-oleate (saturating final concentrations, Celussi and Del Negro, 2012) for 3 h in the dark at *in situ* temperature. Fluorescence increase due to AMC and MUF hydrolysed from the model substrates was measured using a Shimadzu RF-1501 spectrofluorometer (AMC= 380 nm excitation and 440 nm emission; MUF= 365 nm excitation and 455 nm emission). Triplicate calibration curves were performed daily, using 0.2 µm-filtered seawater and 5 µM standard solutions of AMC and MUF (Sigma Aldrich). Relative contribution of the dissolved fraction to the total exoenzymatic activity was then calculated.

B.1.2. Planktonic respiration

Planktonic respiration was measured as oxygen consumption, using a non-invasive oxygen optode sensor spots and fibre-optic system (FireStingO_2, PyroScience, Germany). The optodes (5 mm tip diameter, with optical isolation and a 90% response time of <15 s) were glued at the inner side of 40 mL clear glass vials. The optodes were connected to a 4-channel O_2 data logger (FireStingO_2, Fiber-Optic Oxygen Meter SPFIB-CL2, PyroScience) provided with submersible temperature sensor (TSUB21, PyroScience) and controlled by the manufacturer's software (FireStingO_2 Logger V 3.213, PyroScience). A Two-point calibration (0 and 100% oxygen saturation) of the optodes was performed using temperature-equilibrated samples (10°C) with experimental salinity = 37. According to the manufacturer's instructions, the solution for the 0% oxygen saturation points was prepared by adding sodium sulphite (Na_2SO_3) to distilled water to a final concentration of 30 g L^{-1}; for 100% oxygen saturation, autoclaved and subsequently 0.22 µm-filtered seawater, was bubbled with 0.22 µm-filtered air (SterivexTM filter unit, Millipore) for 15 min. Each vial, provided with a HCl-washed stirring magnet, was carefully closed with gas-tight lid, and incubated in the darkness in a thermo-regulated bath (RE 415, Lauda, Germany) at the *in situ* temperature (± 0.1°C). Oxygen concentration was measured every 5 minutes for 6 hours. Every experiment was run in triplicate. Oxygen decreasing rates were calculated as the slope of linear regression of oxygen concentration (after a thermal equilibration period of 20 min) vs time. Measurements on sterilized seawater in at least 3 vials served as controls (system drift) and were performed before the analyses. Planktonic respiration rates were then calculated by subtracting the average system drift.

B.1.3. Cytometric fingerprinting

Raw cytometric data retrieved from FACSDiva software (Becton Dickinson) were analysed with the R package flowDiv (Wanderley et al., 2019), following the protocol described by Quiroga et al., 2017. Gated prokaryotic cells were classified according to their relative size (side scatter, SSC) and to nucleic acids content (green fluorescence, FL1). Detection channels were clustered into 16 bins each, resulting in 256 (16 × 16) cytometric categories. For each sample, a fingerprint of the cytometric assemblage was obtained based on the number of cells in each cytometric category. Then samples were pairwise compared applying Bray–Curtis index, to build a dissimilarity matrix based on their cytometric fingerprint. Samples were clustered applying the Ward's minimum variance method (Murtagh and Legendre, 2014) and aggregated, according to their optimal cutting level, to form three clusters. Clustering method choice and optimal number of clusters were identified using the R package clValid (Brock et al., 2008). Cytometric fingerprinting and cluster analysis were performed with R version 3.5.0 (R Core Team, 2019).

B.2. Results

B.2.1. Cell-free extracellular enzymatic activity

The time courses of the proportion of cell-free over total hydrolysis rates reported in Fig. B.1 showed a general decreasing trend throughout the sampling period. Cell-free β-glucosidase contribution (BGLU, Fig. B.1 a) ranged between 38.57 ± 1.90 and 100.00 ± 0.00% of the total EEA, with minimum and maximum values found on 2nd and 15th March, respectively. The trend was rather variable during the sampling period, increasing steadily from 28th February to 8th March to near-maximum value (96.91 ± 5.34%). After dropping on 13th March (37.43 ± 2.58%), cell-free BGLU contribution peaked on 15th March to its maximum and decreased on the last sampling day. Cell-free β-galactosidase (BGAL, Fig. B.1 a) proportion to total EEAs presented the lowest variability among the tested hydrolysis rates, ranging between 70.33 ± 6.83 and 100.00 ± 0.00%. Higher and constant values were found between 28th February and 12th March (99.06 ± 1.43%, on average), mildly dropping on 13th March to the minimum value, staying then constant until the end of the sampling period. The proportion of cell-free to total chitinase activity (CHIT, Fig. B.1 a) showed a highly variable trend, with the highest value measured on 28th February (100.00 ± 0.00%), dropping to its minimum on 3rd March (43.72 ± 3.09%). The proportion of dissolved to total CHIT activity peaked near maximum values between 5th and 13th March (91.06 ± 7.46%, on average), dropped on 14th March (50.34 ±4.29%) and steeply increased up to 100.00 ± 0.00%, finally declining to 57.10 ± 6.95% o the last sampling day. Cell-free contribution to the activity of Leucine-aminopeptidase (AMA, Fig. B.1 b) showed the highest variability among the tested activities, ranging from 12.78 ± 0.94 to 100.00 ± 0.00%, with maximum and minimum values found on 28th February and 12th March, respectively. A steep decline was evident on 2nd March (19.49 ± 2.91%), then the trend remained constant, with minor oscillations, throughout the sampling period. Cell-free proportion to total lipase activity (LIP, Fig. B.1 b) ranged between 100.00 ± 0.00 and 36.32 ± 3.04%. The highest and lowest values were measured on 28th February and 13th

March, respectively. Over time, the trend showed wide oscillations, with values dropping to near minimum values between 2nd and 3rd March (38.37 ± 4.01 and 39.41 ± 9.35%, respectively), peaking on 5th March (92.43 ± 13.10%), then decreasing until 15th March, with a small peak on the last sampling day. The proportion of dissolved to total AP (Fig. B.1 b) steeply declined between 28th February and 3rd March (100.00 ± 0.00 and 48.59 ± 3.77%, respectively). Then, higher and constant values were measured between 5th and 12th March (72.55 ± 1.51%), mildly declining until the end of the sampling window, when the lowest value was found (30.17 ± 1.99%).

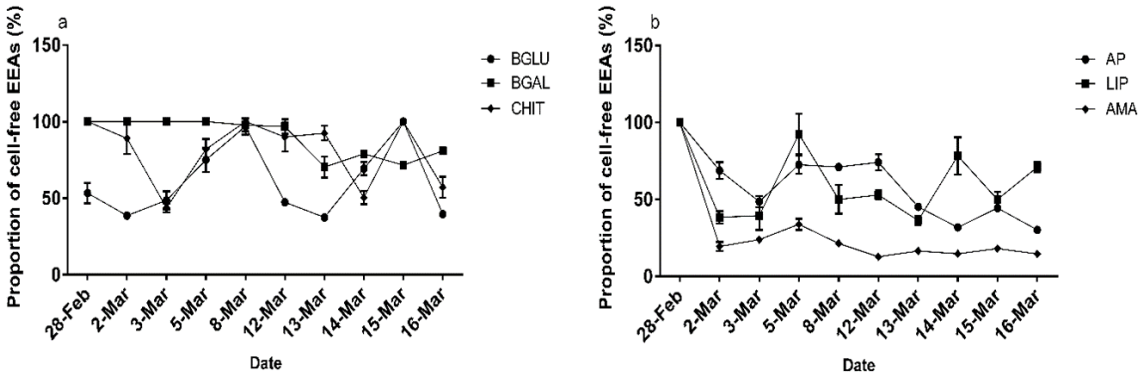

Figure B.1: Time series of cell-free exoenzymatic activities (expressed in nM h^{-1}); a) β-glucosidase (BGLU), β-galactosidase (BGAL) and chitinase (CHIT); b) leucine-aminopeptidase (AMA), alkaline-phosphatase (AP) and lipase (LIP). Note that X axes are not linear. Error bars represent the standard deviation of three analytical replicates.

B.2.2. Planktonic respiration

Planktonic respiration (Fig. B.2) ranged between 5.73 ± 18.82 and 109.98 ± 7.67 nmol O_2 L^{-1} h^{-1}, steadily decreasing from 1st to 5th March, when values fell below the detection limit. A steep increase took place between 8th and 13th March, when the maximum rate was measured, dropping to 33.66 ± 4.39 nmol O_2 L^{-1} h^{-1} at the end of the sampling period.

B.2.3. Cytometric fingerprinting

The cytometric fingerprinting analysis gathered prokaryotic assemblages in three distinct groups (Fig. B.3): 26th – 28th February; 1st – 5th March and 8th – 12th March. The first cluster included cytometric assemblages characterized by an equal contribution of the two NA fraction (i.e., HNA and LNA) and by the highest cell abundance, while the second cluster gathered together samples showing a slightly increased contribution of LNA cells, coupled with the lowest heterotrophic prokaryote abundance measured during the sampling period. Finally, the third cluster included assemblages with the highest HNA cell abundance.

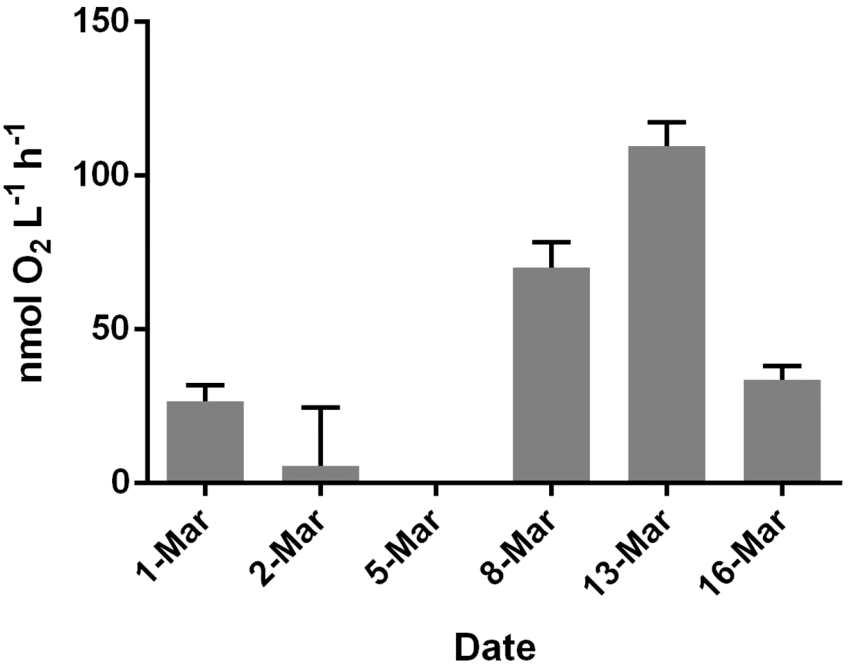

Figure B.2: Time series of planktonic respiration expressed as consumed nmol O_2 L^{-1} h^{-1}. Note that X axis is not linear. Error bars represent the standard deviation of three analytical replicates.

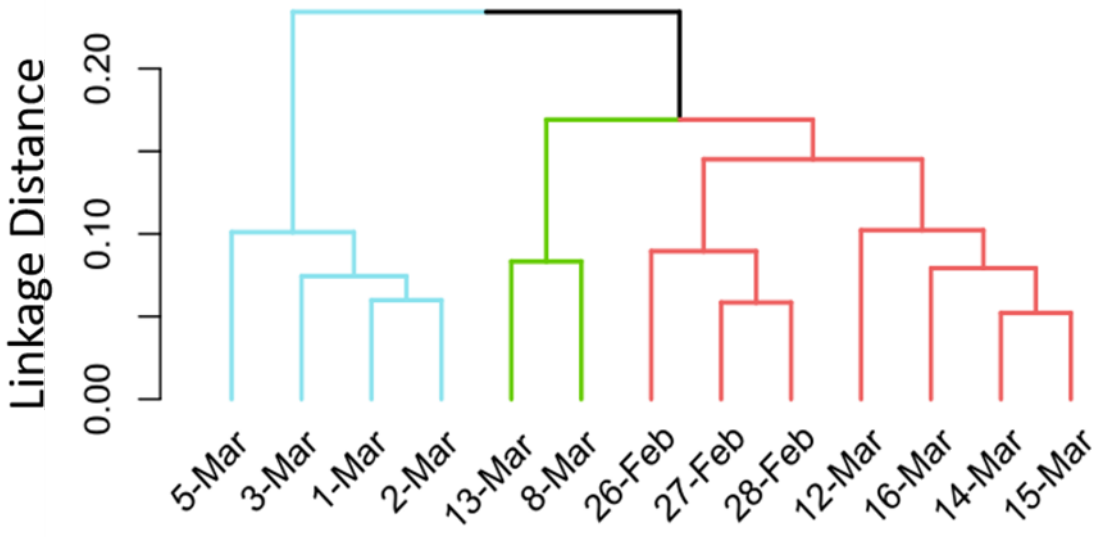

Figure B.3: Cluster analysis dendrogram of cytometric assemblages built using Bray-Curtis dissimilarity matrix calculated between cytometric assemblages. Ward's minimum variance was used a clustering method.

B.3. Supplementary figures

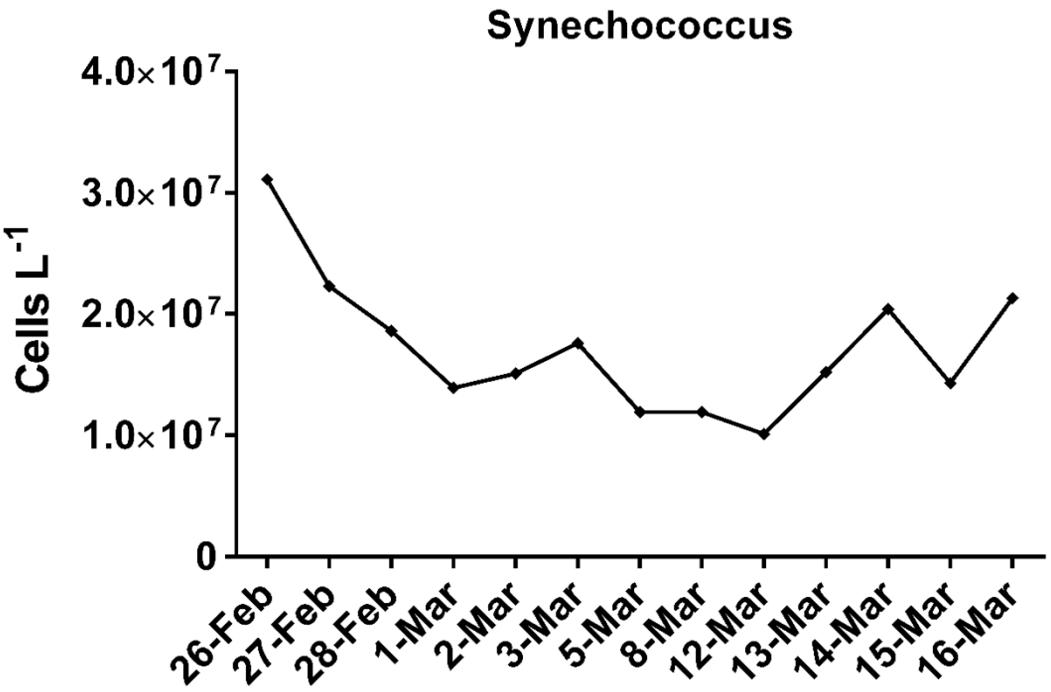

Figure B.4: Time series of *Synechococcus* abundance during the sampling period. Note that X axis is not linear.

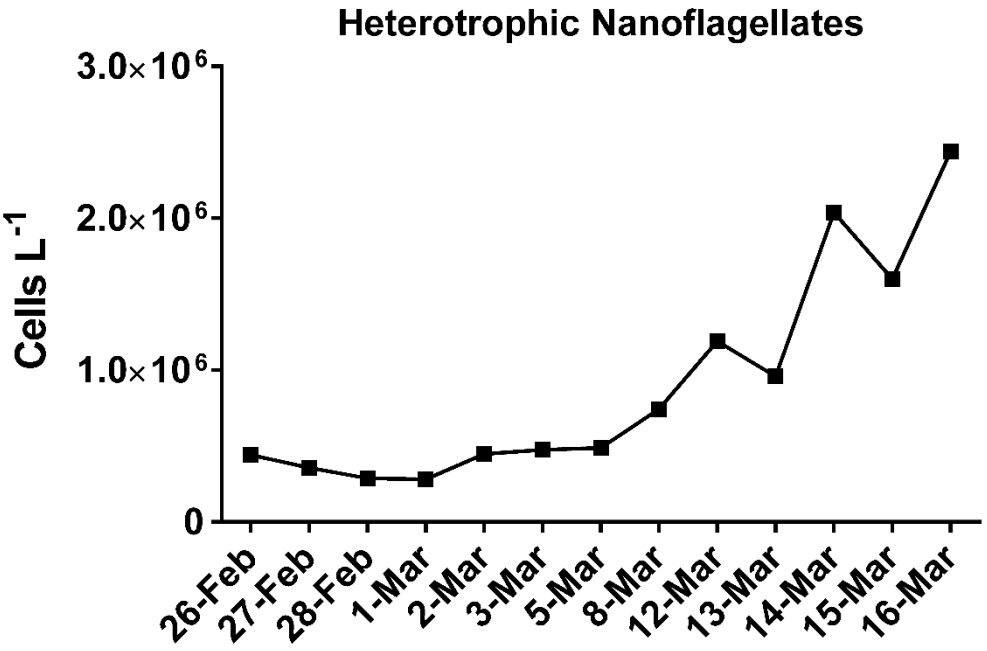

Figure B.5: Time series of heterotrophic nanoflagellates abundance during the sampling period. Note that X axis is not linear.

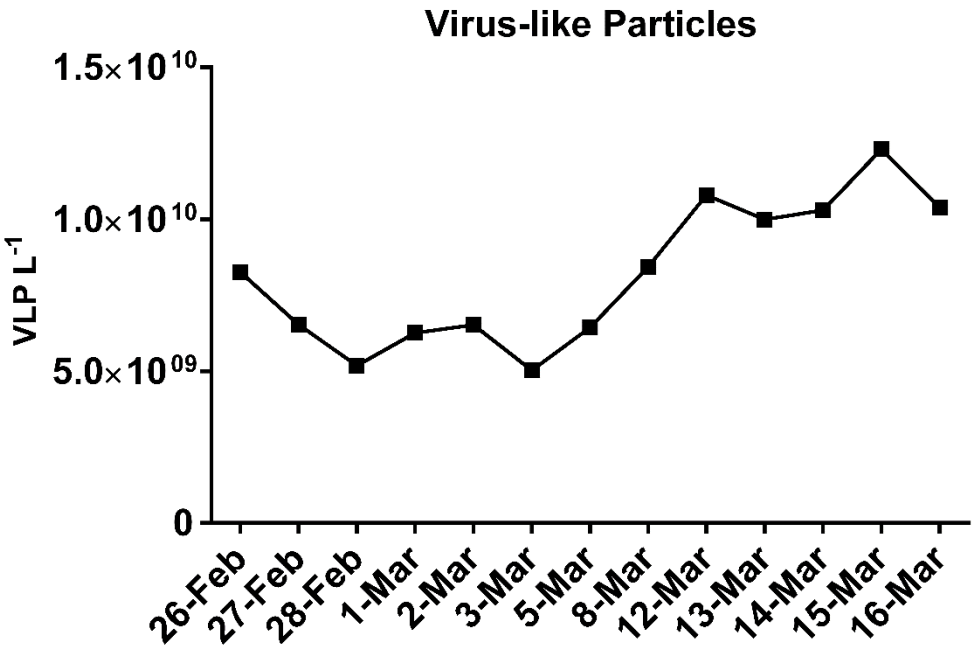

Figure B.6: Time series of virus-like particles (VLP) abundance during the sampling period. Note that X axis is not linear.

B.4. Data sources

Analytical procedures utilized to generate the data used in 3 have been carried out by the following laboratories or people: Exoenzymatic essays, heterotrophic production, flow cytometry: V. Manna (OGS-UNITS); Salinity: OGS-CTO, service; Particulate organic matter: F. Relitti (OGS); Inorganic nutrients: L. Urbini (OGS); Chlorophyll a: M. Bazzaro (OGS); Respiration rates: C. Fabbro (OGS); Phytoplankton: F. Cerino (OGS).

References

Baltar, F., Arístegui, J., Gasol, J. M., Sintes, E., Van Aken, H. M., & Herndl, G. J. (2010). High dissolved extracellular enzymatic activity in the deep central Atlantic ocean. *Aquatic Microbial Ecology*, *58*(3), 287–302. https://doi.org/10.3354/ame01377

Brock, G., Pihur, V., Datta, S., & Datta, S. (2008). clValid: An R Package for Cluster Validation. *Journal of Statistical Software; Vol 1, Issue 4 (2008)*. https://www.jstatsoft.org/v025/i04

Celussi, M., & Del Negro, P. (2012). Microbial degradation at a shallow coastal site: Long-term spectra and rates of exoenzymatic activities in the NE Adriatic Sea. *Estuarine, Coastal and Shelf Science*, *115*, 75–86. https://doi.org/10.1016/j.ecss.2012.02.002

Hoppe, H.-G. (1993). Use of Fluorogenic Model Substrates for Extracellular Enzyme Activity (EEA) Measurement of Bacteria. In P. F. Kemp, B. F. Sherr, E. B. Sherr, & J. J. Cole (Eds.), *Handbook of Methods in Aquatic Microbial Ecology* (1st ed., pp. 423–431). Routledge. https://doi.org/10.1201/9780203752746-49

Murtagh, F., & Legendre, P. (2014). Ward's Hierarchical Agglomerative Clustering Method: Which Algorithms Implement Ward's Criterion? *Journal of Classification*, *31*(3), 274–295. https://doi.org/10.1007/s00357-014-9161-z

Quiroga, M. V., Mataloni, G., Wanderley, B. M. S., Amado, A. M., & Unrein, F. (2017). Bacterioplankton morphotypes structure and cytometric fingerprint rely on environmental conditions in a sub-Antarctic peatland. *Hydrobiologia*, *787*(1), 255–268. https://doi.org/10.1007/s10750-016-2969-2

R Core Team. (2019). *R: A Language and Environment for Statistical Computing*. R Foundation for Statistical Computing. https://www.R-project.org/

Wanderley, B. M. S., A. Araújo, D. S., Quiroga, M. V., Amado, A. M., Neto, A. D. D., Sarmento, H., Metz, S. D., & Unrein, F. (2019). flowDiv: A new pipeline for analyzing flow cytometric diversity. *BMC Bioinformatics*, *20*(1), 274. https://doi.org/10.1186/s12859-019-2787-4

C

Supplementary Material to Chapter 4

Text, tables and figures in this Appendix are adapted from the supplementary material to: Prokaryotic Response to Phytodetritus-Derived Organic Material in Epi- and Mesopelagic Antarctic Waters. Manna V., Malfatti F., Banchi E., Cerino F., De Pascale .F, Franzo A., Schiavon R., Vezzi A., Del Negro, P. and Celussi, M., 2020. Frontiers in Microbiology, 11:1242. https://doi.org/10.3389/fmicb.2020.01242

C.1. Methods

Particulate Organic Carbon (POC) concentrations in plankton samples were measured using an elemental analyzer CHNO-S Costech mod. ECS 4010 applying the method by Pella and Colombo, 1973. Three replicates of 3 mL were used for the analysis in each of the four plankton samples. POC was collected onto precombusted GF/F filters and stored frozen at -20°C. Before the analyses, the filters were treated with the addition of 200 µL 1 N HCl to remove the carbonates (Lorrain et al., 2003) and then dried in oven at 60°C for about 1 h. Subsequently, sample and blank filters were folded and put on a 9×10 mm tin capsule. Known amounts of standard Acetanilide (C_8H_9NO – Carlo Erba; Assay ≥99.5 %) were used to calibrate the instrument.

Samples for dissolved organic carbon (DOC) concentrations in plankton samples were obtained by filtering 3 mL aliquots (in 3 replicates) through GF/F membranes and by collecting the filtrate in 20 mL glass vials, subsequently stored at -20°C. The membranes, the vials and the glassware used for the filtration had been precombusted at 480°C for 4h. Before the analyses, samples were diluted 20 times with MilliQ water, automatically acidified to pH < 2 using 6 N HCl solution (1% v/v) and sparged (150 mL min^{-1}) with high-purity oxygen for 8 min.

DOC analyses were performed by the high temperature catalytic oxidation method using a Shimadzu TOC-V CSH (Cauwet, 1994), injecting 100 µL of sample. Carbon concentration was determined by automatic comparison with four-point calibration curves. Standardization was carried out using potassium hydrogen phthalate. Each value was determined from a minimum of three injections, with a coefficient of variation < 2%.

For phytoplankton *in situ* analysis, samples were collected by Niskin bottles at discrete depths (surface and bottom) and fixed with pre-filtered and neutralized formaldehyde (1.6% f.c., Throndsen, 1978). Depending on phytoplankton densities, a variable volume of seawater (10–100 mL) was allowed to settle in an Utermöhl chamber and examined following the Utermöhl method (Utermöhl, 1958). Cell counts were performed using an inverted light microscope (LEICA DMi8) equipped with phase contrast along transects (1–4) at a magnification of 400× counting a minimum of 200 cells. Half or the whole Utermöhl chamber was further examined at a magnification of 200×, to obtain a more correct evaluation of less abundant microphytoplankton (>20 µm) taxa.

C.2. Results

C.2.1. Microplankton *in situ* distribution

The surface layer was characterized by high phytoplankton abundances (from 8.4 × 10^5 Cells L^{-1}, at station C1, to 8.1 × 10^6 Cells L^{-1}, at station D). At the bottom, abundances were not higher than 2.0 × 10^3 Cells L^{-1}. In the surface layer of the station D, the phytoplankton community was dominated by diatoms (up to 92.0% of the total abundance), while dinoflagellates and flagellates accounted for 1.2 and 7.0% of the total, respectively. Among diatoms, species belonging to the genera *Pseudo-nitzschia* and *Fragilariopsis* were the most abundant (4.9 and 2.0 × 10^6 Cells L^{-1}, respectively). Sta-

tions C2 and C1 were characterized by similar percentages of diatoms and flagellated forms. At the station B, a different phytoplankton community was present, being dominated by flagellated forms (92.3% of the total), among which the haptophyte *Phaeocystis antarctica* was the most abundant taxon (4.1×10^6 Cells L^{-1}). Heterotrophic flagellates belonging to the choanoflagellate group were present in relatively high abundances, up to 4.1×10^5 Cells L^{-1}. Diatoms and dinoflagellates accounted for 5.8 and 2.0% of the total, respectively. In the deep layers, dinoflagellates represented a high percentage (on average, 58.3% of the total abundance and up to 84.8% at the station C1), compared to the surface layer (on average, 2.7%).

C.3. Supplementary figures and tables

C.3.1. Supplementary figures

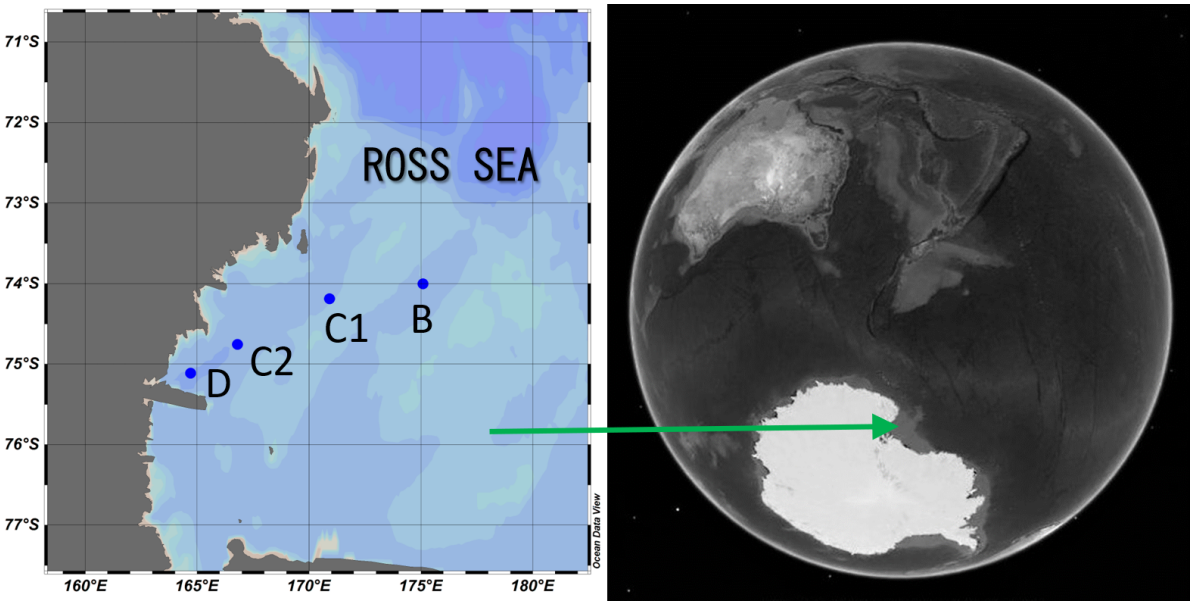

Figure C.1: Map of the sampling stations in the Ross Sea (Southern Ocean). The map was created by means of the ODV (Schlitzer, 2020) and the Google Earth software. Station bottom depths are reported in the Table 4.1

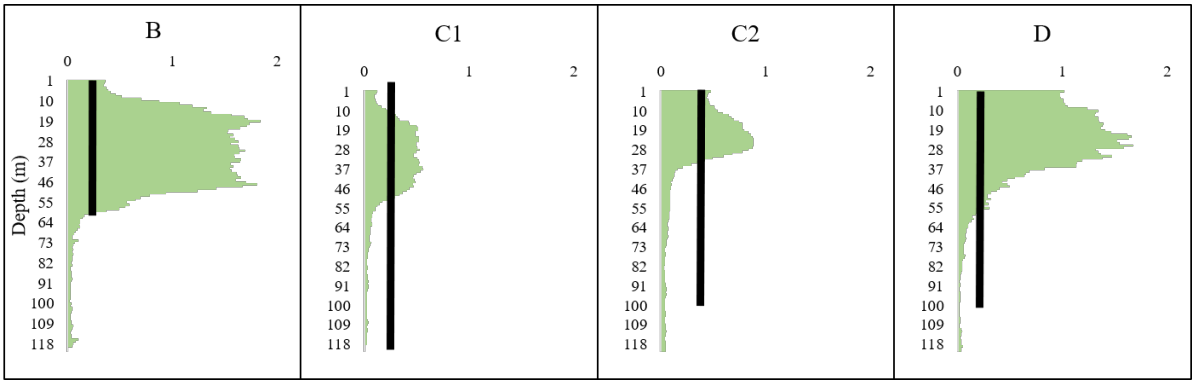

Figure C.2: Chlorophyll *a* fluorescence profiles (CTD) at the four stations. The black bars mark the section of the water column where the plankton net was deployed.

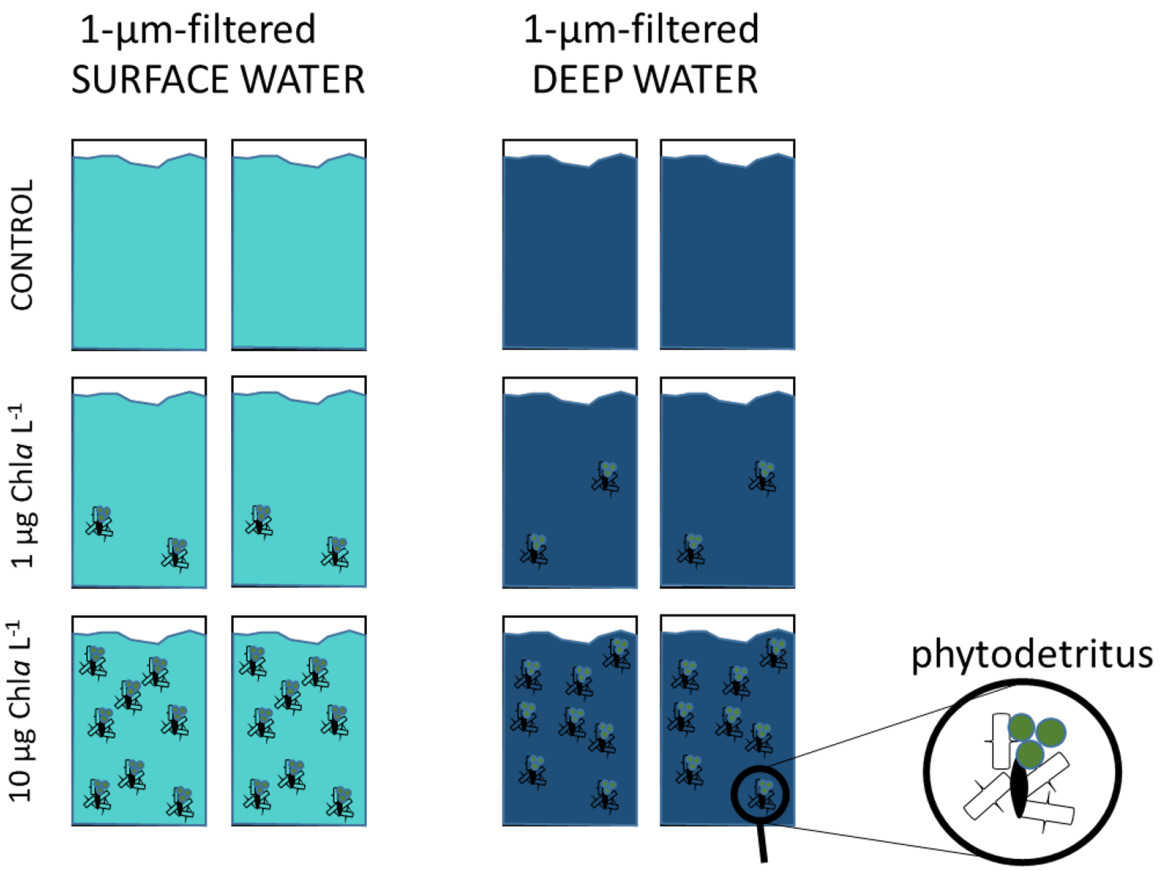

Figure C.3: Conceptual scheme depicting the experimental design of microcosms experiments at each station. Treatment and control microcosms were incubated in the dark, at *in situ* temperature for four days. The detailed experimental design is described in Section 4.2

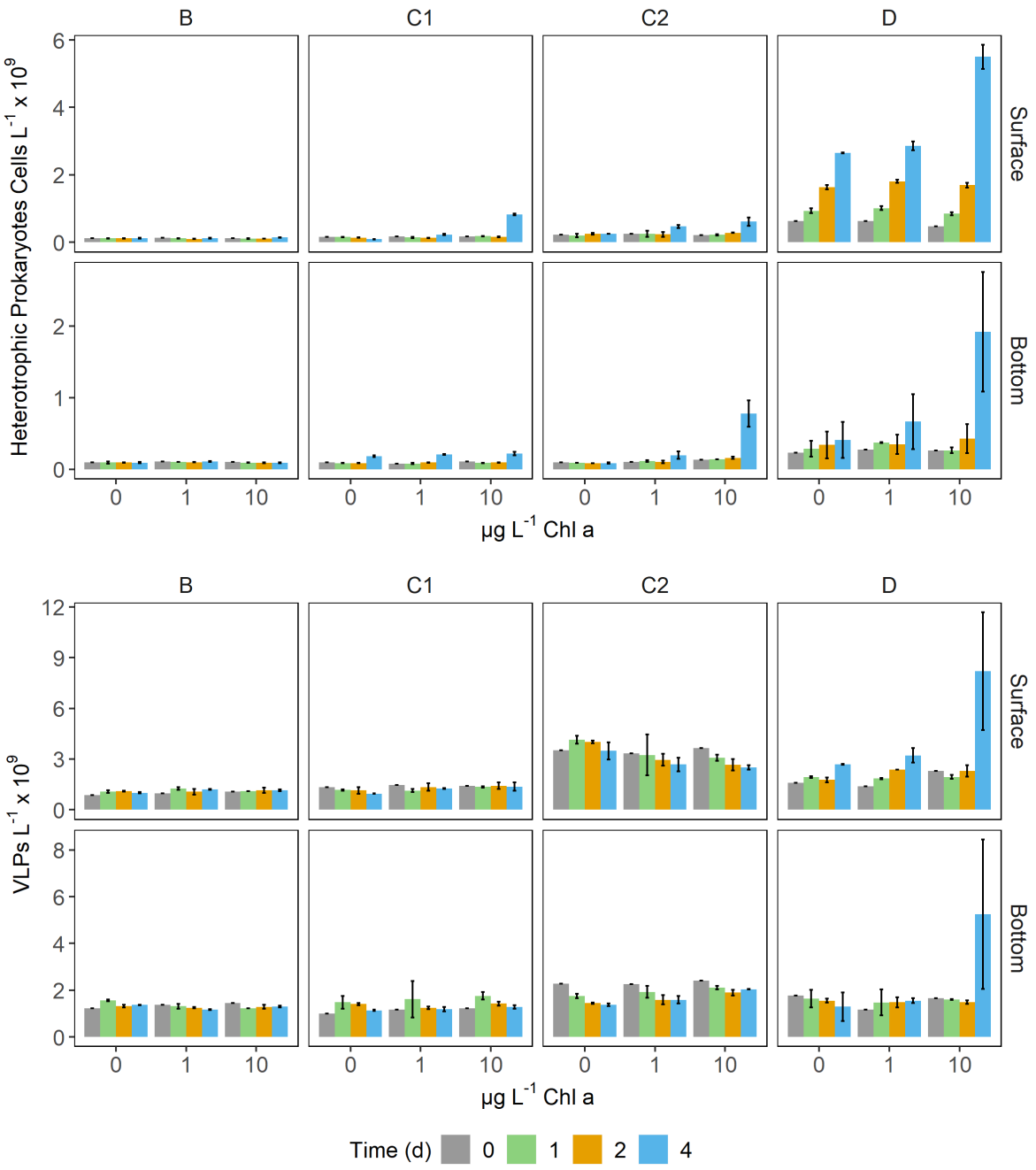

Figure C.4: Bar plots showing the abundance of virus-like particles (VLPs, upper panel) and of free-living heterotrophic prokaryotes (FL-HP, lower panel) over time in control and amended microcosms (0, 1 and 10 µg L^{-1} Chl *a*). Note that Y-axes are differentially scaled. Error bars represent the standard deviation of two experimental replicates.

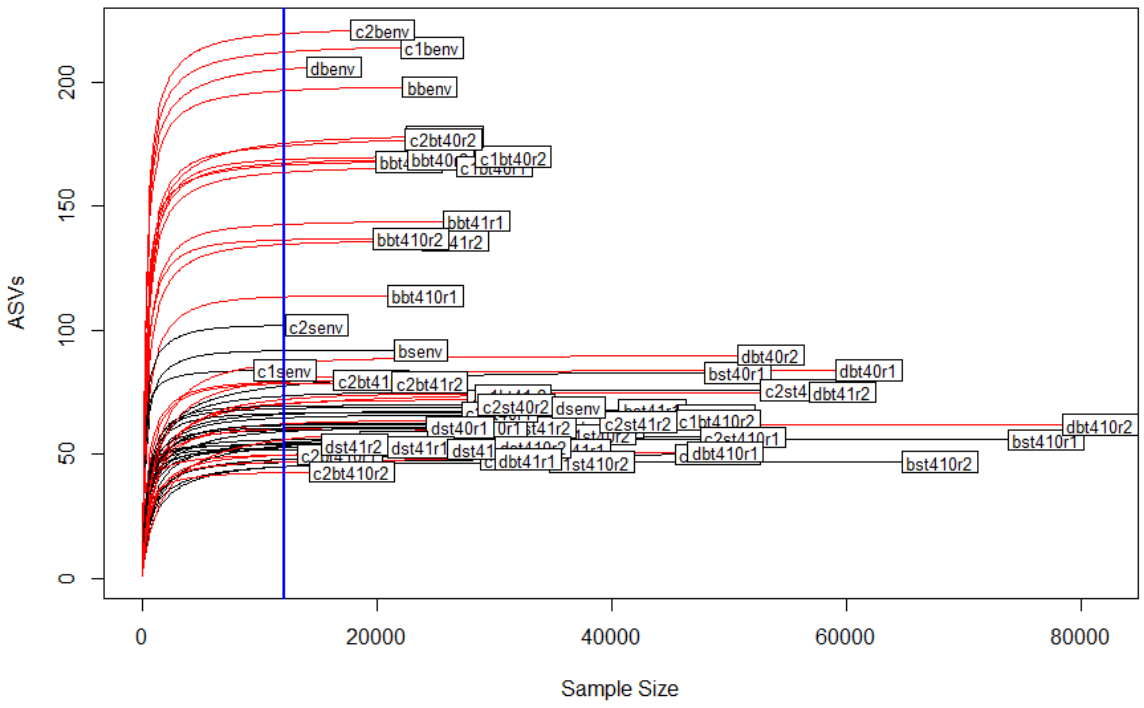

Figure C.5:
Rarefaction curves of observed ASVs calculated on the non-normalized ASV table. The blue line marks the minimum number of reads (12110), retrieved in C2 surface sample on d0 (C2Senv). Surface samples are marked by black lines, bottom samples by red ones.

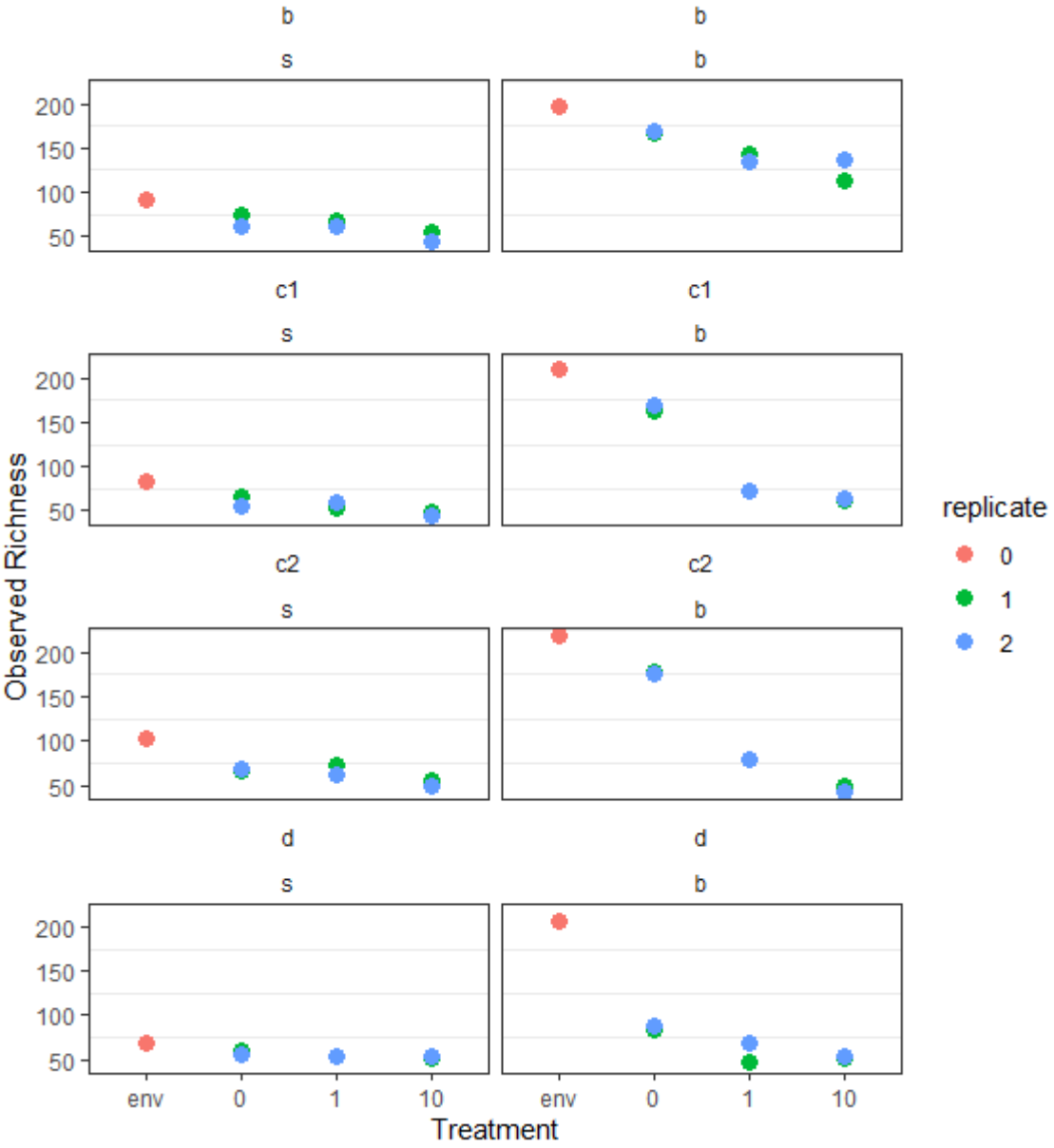

Figure C.6: Observed richness (i.e., number of unique ASVs) in the investigated samples. The x axis maps to different treatments: env= initial community, 0= control bottles, 1= bottles amended with 1 µg L^{-1}, 10= bottles amended with 10 µg L^{-1}. Different colors map to the different experimental replicates [0= initial (t0) community].

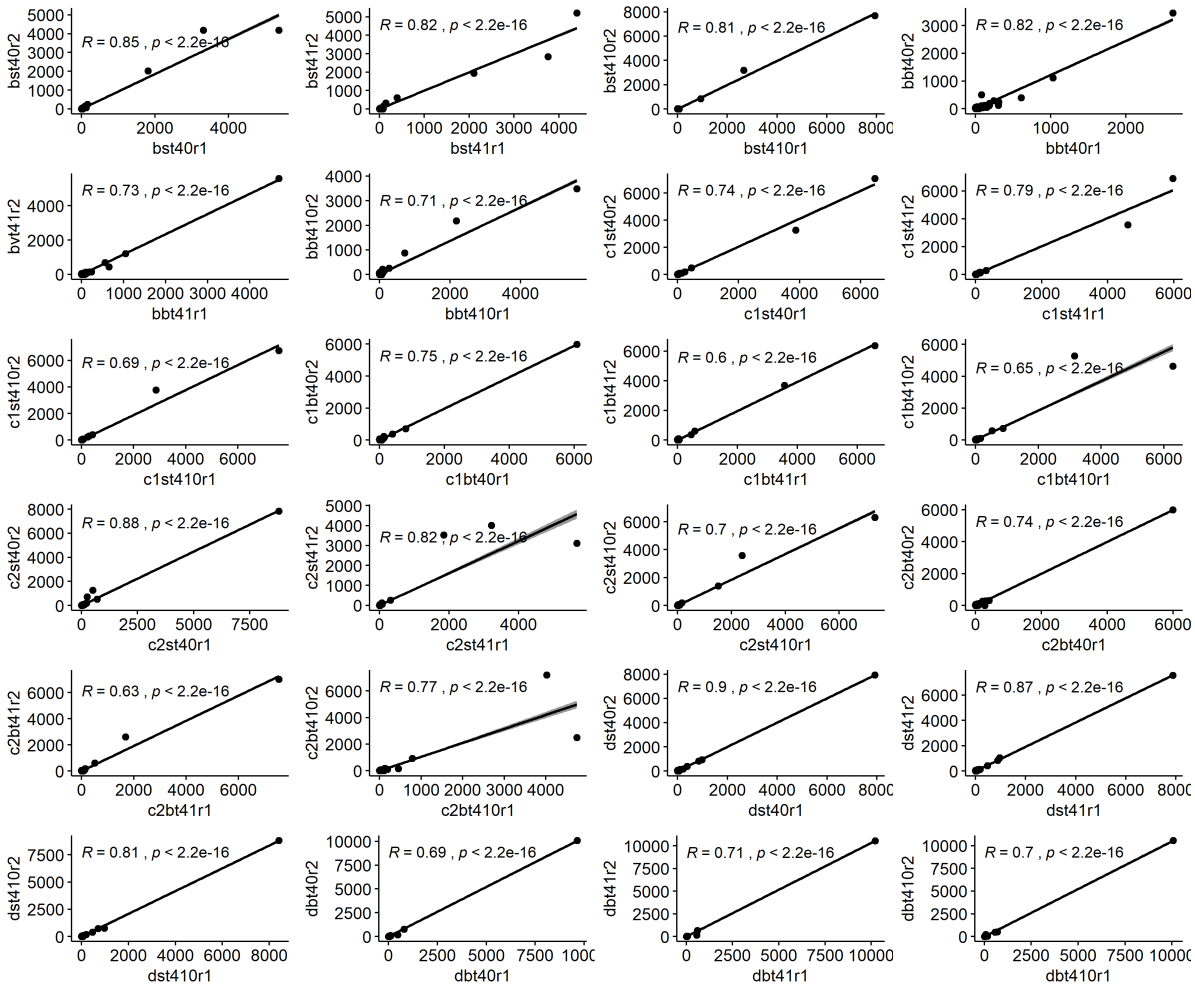

Figure C.7: Scatterplots of Spearman's rank correlations of sequencing duplicates (raw ASVs table). Spearman's rho and p-value are shown in each plot. Samples are identified according to the following code: station_depth_time_treatment_replicate. For example, replicate 1 of surface sample of station B enclosures amended with 1 µg L^{-1} Chl *a* equivalent of detritus would be identified as bst41r1.

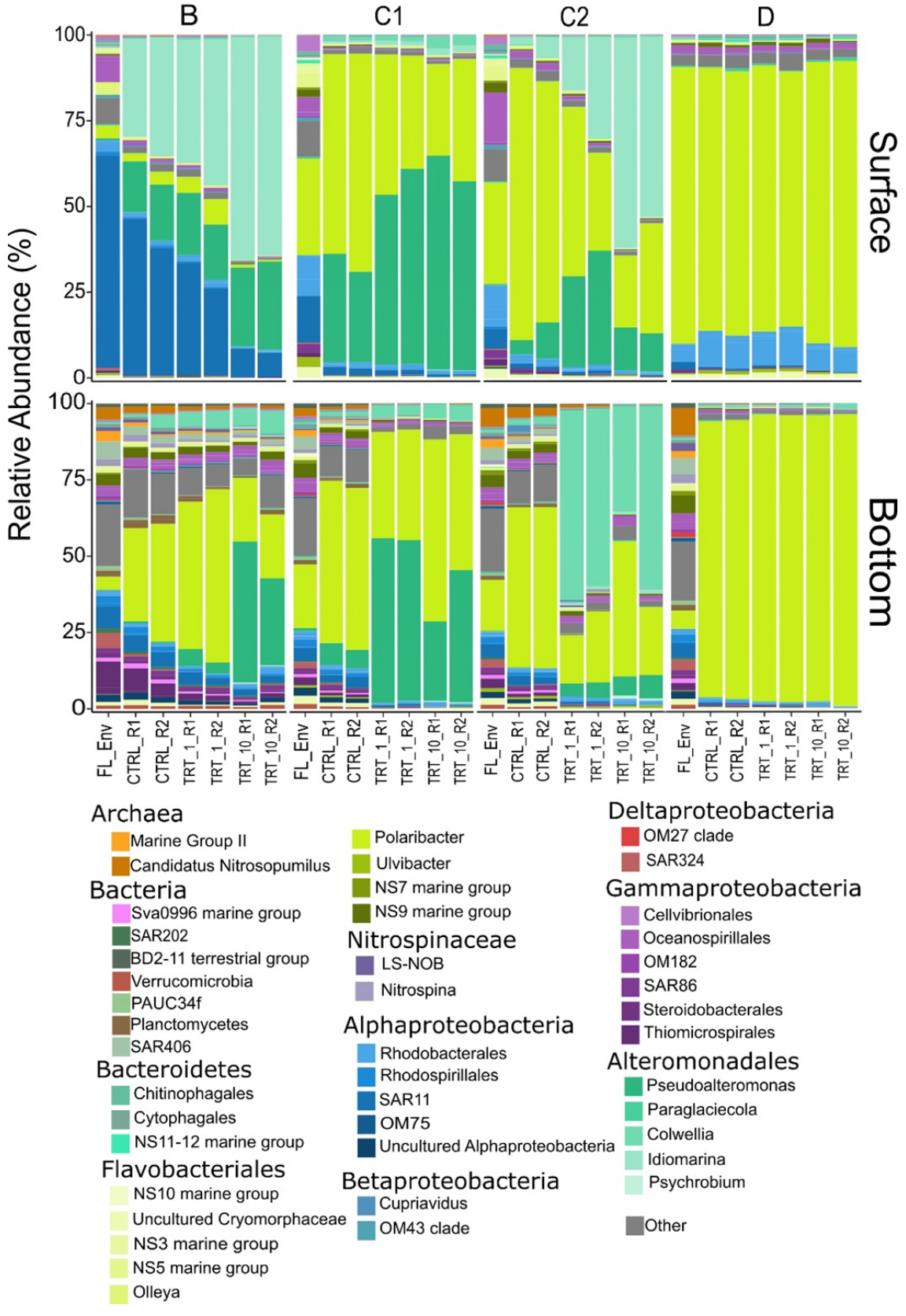

Figure C.8: (Caption on the next page)

Figure C.8: Relative abundance plots of major taxa (>1% in at least one sample). FL_Env: initial free-living (1 µm-filtered) community, CTRL: control samples; TRT_1: amendments at 1 µg L^{-1} Chl *a*; TRT_10: amendments at 10 µg L^{-1} Chl *a*; R1 and R2 identify the two experimental replicates.

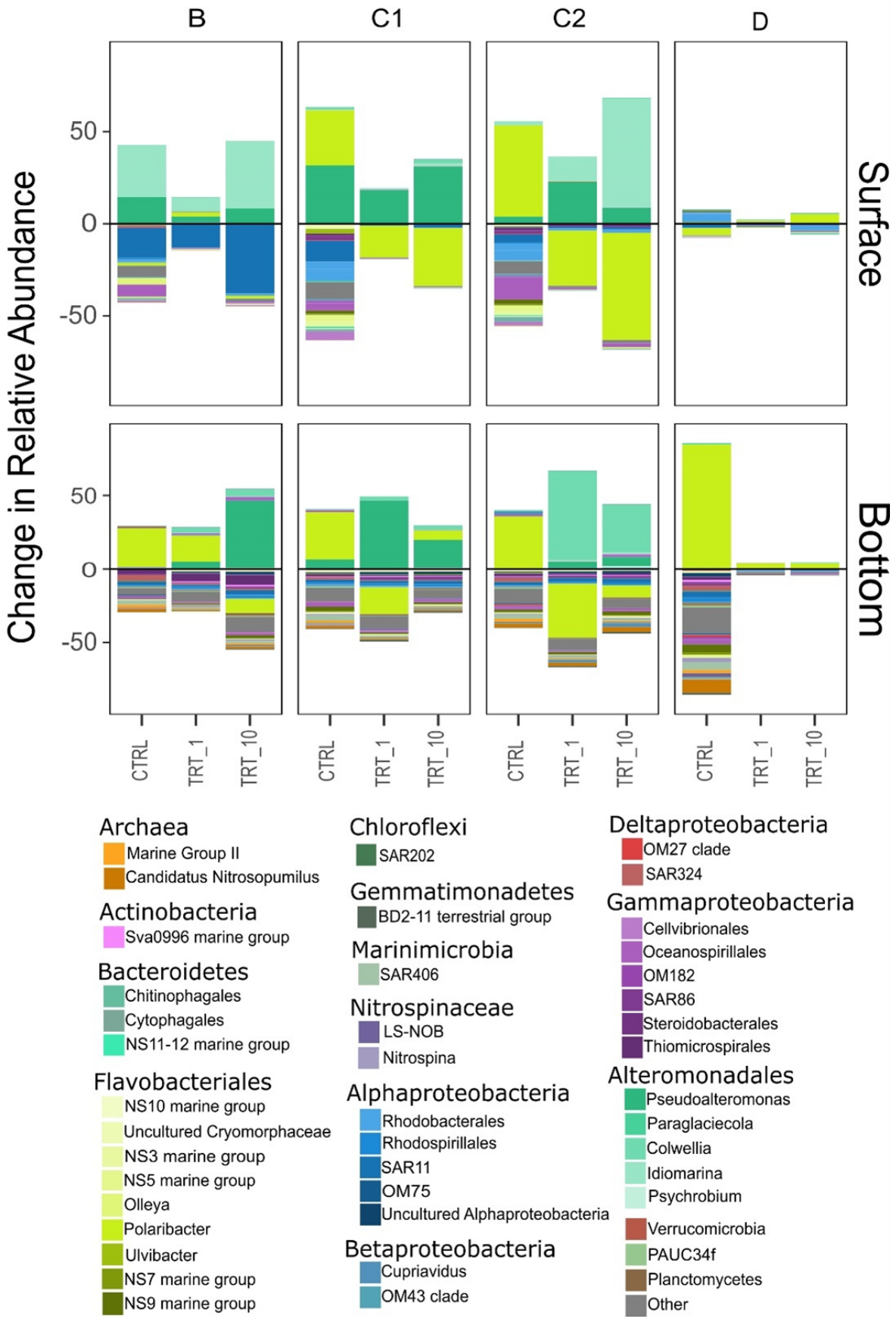

Figure C.9: (Caption on the next page)

Figure C.9: Treatment-related shifts in prokaryotic community. Shifts in controls are compared to the initial (d0, 1 µm-filtered) community, whereas taxa shifts in treatments (i.e., 1 and 10 µg L^{-1}) are compared against the controls (both on d4). CTRL: control samples; TRT_1: amendments at 1 µg L^{-1} Chl *a*; TRT_10: amendments at 10 µg L^{-1} Chl *a*; R1 and R2 identify the two experimental replicates.

C.3.2. Supplementary tables

Table C.1: Results of chemical analysis on phytodetritus samples. The units of measure are reported in parenthesis. DOC and POC are presented as mean ± SD.

Phytodetritus	Chl *a* (mg L^{-1})	DOC (mgC L^{-1})	POC (mgC L^{-1})	POC:Chl *a*
B	2.38	27.41±0.68	52.29±1.63	21.97
C1	0.58	24.43±0.48	49.81±5.84	85.88
C2	0.20	36.52±2.51	41.81±5.89	209.05
D	0.78	27.78±0.61	34.47±0.81	44.192

Table C.2: Concentration of DOC and POC in environmental samples and added with phytodetritus amendments and calculated DOC and POC enrichment factors in the microcosms.

Bottle	Depth		Environmental DOC* (mgC L^{-1})	Added DOC (mgC L^{-1})		Calculated POC** (mgC L^{-1})	Added POC (mgC L^{-1})		EF DOC		EF POC	
		Treatment		1	10		1	10	1	10	1	10
B	Surface		0.76	0.01	0.12	0.002	0.02	0.22	1.00	1.20	14.91	139.74
	Bottom		0.75	0.01	0.12	0.001	0.02	0.22	1.00	1.20	18.52	176.11
C1	Surface		1.19	0.04	0.43	0.002	0.08	0.82	1.00	1.40	40.50	396.22
	Bottom		1.42	0.04	0.43	0.001	0.08	0.82	1.00	1.30	67.72	667.71
C2	Surface		0.83	0.09	0.91	0.003	0.11	1.13	1.10	2.10	40.71	398.22
	Bottom		0.69	0.09	0.91	0.001	0.11	1.13	1.10	2.30	91.52	906.31
D	Surface		0.87	0.04	0.36	0.008	0.04	0.45	1.10	1.30	6.51	56.01
	Bottom		1.16	0.04	0.36	0.003	0.04	0.45	1.10	1.40	15.73	148.22

DOC: dissolved organic carbon; POC: particulate organic carbon; EF: enrichment factor, calculated as (Hardy et al., 1997). *F. Relitti, unpublished data. **POC concentration calculated converting prokaryotic abundance in 1µm-filtered samples assuming 13 fgC $Cell^{-1}$ (Carlson et al., 1999). See main text for details.

Table C.3: Analysis of variance output of the GLM (negative binomial) models indicating the significance of phytodetrital features on the number of attached prokaryotes. As the residuals of the GLM on d1 data showed a non-normal distribution, those data were not further discussed. Significant (<0.05) P-values are highlighted in bold.

Variable	df	Deviance	Residual df	Residual Dev.	P-value	Shapiro test for residuals (P-value)
d0						
NULL	NA	NA	31	41.8	NA	
Pseudo-nitzschia	1	5.59	30	36.21	**0.02**	
Phaeocystis	1	0.62	29	35.6	0.43	0.07
Chaetoceros	1	1.95	28	33.64	0.16	
Choanoflagellates	0	0	28	33.64	NA	
d1						
NULL	NA	NA	31	64.75	NA	
Pseudo-nitzschia	1	29.83	30	34.92	**<0.001**	
Phaeocystis	1	0.64	29	34.28	0.424	**0.03**
Chaetoceros	1	2.23	28	32.06	0.136	
Choanoflagellates	0	0	28	32.06	NA	
d4						
NULL	NA	NA	31	61.85	NA	
Pseudo-nitzschia	1	17.57	30	44.28	**<0.001**	
Phaeocystis	1	6.91	29	37.38	**0.0085**	0.38
Chaetoceros	1	2.91	28	34.47	**0.0088**	
Choanoflagellates	0	0	28	34.47	NA	

C.4. Data sources

Analytical procedures utilized to generate the data used in 4 have been carried out by the following laboratories or people: Exoenzymatic essays: A. Franzo (OGS); Heterotrophic production and DIC fixation: M. Celussi (OGS); Flow cytometry: A. Bariče-vić (IRB), M. Celussi (OGS), M. Smodlaka Tanković (IRB); Epifluorescence microscopy: S. Maggiore (UNITS), V. Manna (OGS-UNITS); Microplankton collection, phytodetritus generation and characterization: F. Cerino (OGS); Chlorophyll a: M. Celussi (OGS); Dissolved and Particulate organic carbon: F. Relitti (OGS); Molecular and bioinformatic analyses: E. Banchi (OGS), F. De Pascale (UNIPD), V. Manna (OGS-UNITS), R. Schiavon (UNIPD), A. Vezzi (UNIPD).

References

Carlson, C. A., Bates, N. R., Ducklow, H. W., & Hansell, D. A. (1999). Estimation of bacterial respiration and growth efficiency in the ross sea, antarctica. *Aquatic Microbial Ecology*, *19*(3), 229–244. https://www.int-res.com/abstracts/ame/v19/n3/p229-244/

Cauwet, G. (1994). Htco method for dissolved organic carbon analysis in seawater: Influence of catalyst on blank estimation. *Marine Chemistry*, *47*(1), 55–64. https://doi.org/https://doi.org/10.1016/0304-4203(94)90013-2

Hardy, J. T., Hunter, K. A., Calmet, D., Cleary, J. J., Duce, R. A., Forbes, T. L., Gladyshev, M. L., Harding, G., Shenker, J. M., Tratnyek, P., & al et, e. (1997). Report Group 2 – Biological effects of chemical and radiative change in the sea surface. In P. S. Liss & R. A. Duce (Eds.), *The Sea Surface and Global Change* (pp. 35–70). Cambridge University Press. https://doi.org/10.1017/CBO9780511525025.003

Lorrain, A., Savoye, N., Chauvaud, L., Paulet, Y.-M., & Naulet, N. (2003). Decarbonation and preservation method for the analysis of organic c and n contents and stable isotope ratios of low-carbonated suspended particulate material. *Analytica Chimica Acta*, *491*(2), 125–133. https://doi.org/https://doi.org/10.1016/S0003-2670(03)00815-8

Pella, E., & Colombo, B. (1973). Study of carbon, hydrogen and nitrogen determination by combustion-gas chromatography. *Mikrochimica Acta*, *61*(5), 697–719. https://doi.org/10.1007/BF01218130

Schlitzer, R. (2020). Ocean data view. https://odv.awi.de/

Throndsen, J. (1978). Preservation and storage. *Phytoplankton manual* (pp. 69–74). Unesco.

Utermöhl, H. (1958). Zur vervollkommnung der quantitativen phytoplankton-methodik: Mit 1 Tabelle und 15 abbildungen im Text und auf 1 Tafel. *Internationale Vereinigung für theoretische und angewandte Limnologie: Mitteilungen*, *9*(1), 1–38.

D

Supplementary Material to Chapter 5

Text, tables and figures in this Appendix are adapted from the supplementary material to: Modulation of hydrolytic profiles of cell-bound and cell-free exoenzymes in Antarctic marine bacterial isolates. Manna, V., Del Negro, P., Celussi, M., 2019. Advances in Oceanography and Limnology, 10, 32–43. https://doi.org/10.4081/aiol.2019.8240

D.1. Supplementary figure

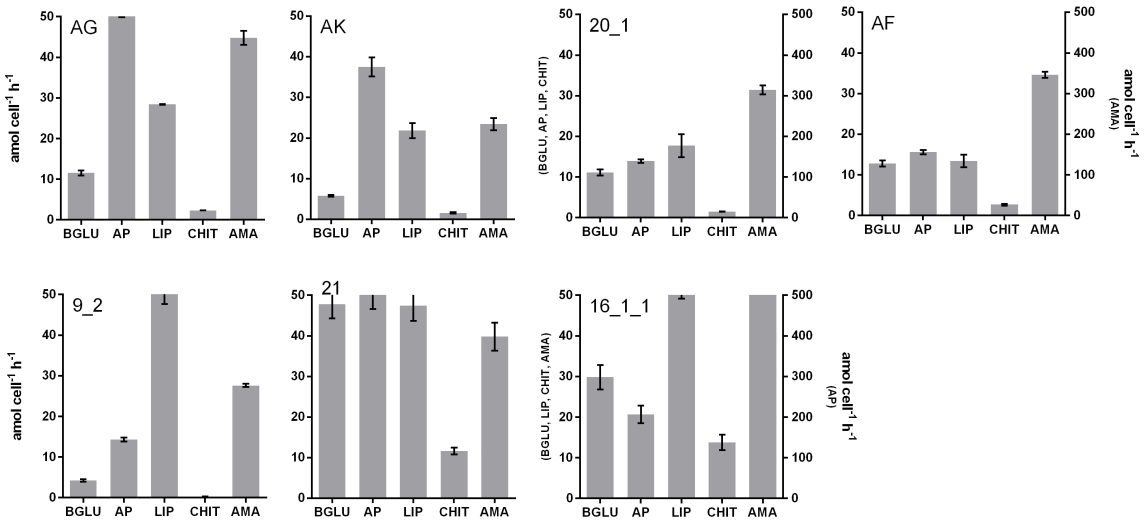

Figure D.1: Cell-specific enzyme activities at d_{exp} of 5 exoenzyme obtained from 7 marine bacteria isolates. Error bars represent the standard deviation of three analytical replicates. BGLU= β-glucosidase, AP= alkaline phosphatase, LIP= lipase, CHIT= chitinase, AMA= leucine amino-peptidase.

D.2. Data sources

Analytical procedures utilized to generate the data used in 5 have been carried out by the following laboratories or people: Bacterial isolation: M. Celussi (OGS), P. Del Negro (OGS), V. Manna (OGS-UNITS). Microplankton collection and phytodetritus generation: F. Cerino (OGS). Molecular analyses: M. Celussi (OGS), V. Manna (OGS-UNITS). Exoenzymatic essays, epifluorescence microscopy, flow cytometry: V. Manna (OGS-UNITS).